

Thesis

1716

THE DEVELOPMENT OF SNOWMELT RUNOFF MODELS IN THE  
SCOTTISH HIGHLANDS

Submitted for the degree of  
Doctor of Philosophy

Anthony Mark Bennett B.Sc. (Hons)



November 1990

Department of Environmental Science

University of Stirling

**PAGE  
NUMBERING  
AS  
ORIGINAL**

## **ABSTRACT**

Detailed snow surveys were carried out in the Allt a Mharcaidh catchment on the western edge of the Cairngorm mountains during the winters of 1985/86, 1986/87 and 1988/89. Snowpack data collected included depth, density, areal extent and water equivalent. From these data it was possible to determine seasonal patterns in snowpack behaviour and relate these to the initial snowpack water equivalent volume and timing of the snow accumulation and ablation.

Using meteorological and flow data collected in the Mharcaidh by the Institute of Hydrology as part of the SWAP project simple linear regression relationships were determined. These indicated that the availability of detailed meteorological data did not improve the ability to simulate observed flow and that a successful regression could be established using simple and readily available data.

Using this data temperature index models were developed and tested on the Mharcaidh. These showed that the mean daily temperature provided a better index of melt than more complex indices and that simple changes regarding the addition of a freezing level hindered the model performance

despite being closer to reality than other assumptions made in the model. This suggested that the degree of complexity in the model has to be similar for all operations to obtain optimum results; having one particularly complex sub-model reduces the performance of the others.

Two other types were tested on the Mharcaidh based on the layered structure developed by Martinec (1975) and Anderson's (1968) method using temperature and windspeed as an index to the energy changes at the snowpack boundary during rain-on-snow events. These again show that simple methods using readily available data can produce acceptable results and that increasing the complexity of the model does not produce a similar increase in performance.

The three different models were then run on different datasets for different catchments and years. The dependence of Anderson's method on good quality data is highlighted suggesting that it is not as widely applicable as the other models. The level of performance for all models is related to the extent and depth of the snowpack indicating that further improvements may be necessary to the hydrological components of the model rather than the melt sub-model itself. The models were tested in simulated real time conditions on one dataset and, following this, guidelines for use in real time to predict snowmelt runoff are given.

## CONTENTS

Abstract	i
Contents	iii
List of Figures	vi
List of Tables	xiii
List of Plates	xvi
Acknowledgements	xvii
<b>1 INTRODUCTION</b>	<b>1</b>
1.1 Why model snowmelt?	1
1.2 Approaches to modelling snowmelt runoff	3
1.3 Previous work	7
1.3.1 The physics based energy balance approach	8
1.3.2 The parametric energy balance approach	18
1.3.3 Temperature index method	21
1.3.3.1 The work of Martinec and Rango	21
1.3.3.2 Other authors	32
1.3.3.3 British work	33
1.4 Aims of the project	43
<b>2 FIELD TECHNIQUES</b>	<b>49</b>
2.1 Introduction	49
2.2 The Allt a Mharcaidh	49
2.3 Instrumentation and secondary data collection in the Mharcaidh	52
2.4 Snowpack data collection	58
2.4.1 Snow depth and water equivalent	59
2.4.2 Areal snowpack data	63
2.5 Snow surveys in the Mharcaidh	66
2.5.1 Site selection	66
2.5.2 Measurement Techniques	75
2.5.3 Sources of error in the snow surveys	84
<b>3 COLLATION OF FIELD DATA</b>	<b>92</b>
3.1 Snow surveys	92
3.1.1 Snow covered area	92
3.1.2 Snowpack volume	100
3.1.3 Water equivalent averaged over snowpack	106
3.2 Relative distribution of snow in the catchment	110
3.2.1 Snowpack water equivalent and volume	110
3.2.2 Implications for generating runoff	121
3.3 Meteorological and flow data	124
3.3.1 Observed patterns	124
3.3.2 Relationships between meteorological variables and observed flow	132
3.3.3 Multiple regression analysis	136
3.4 Comparison of measured inputs and observed outputs	140

<b>4</b>	<b>MODEL DEVELOPMENT USING MHARCAIDH DATA</b>	<b>145</b>
4.1	Introduction	145
4.2	Model structure	147
	4.2.1 Data Input	147
	4.2.2 Meteorological submodel	149
	4.2.3 Snowmelt submodel	152
	4.2.4 Transformation submodel	153
	4.2.5 Depletion submodel	153
	4.2.6 Optimisation	157
	4.2.7 Preliminary analysis of output	163
4.3	Running TINDEK on 1986 and 1987 data	166
	4.3.1 The data sets	166
	4.3.2 Results from the first run of TINDEK	169
	4.3.3 Recommendations following the first runs of TINDEK	176
4.4	Early changes to TINDEK	177
	4.4.1 Addition of the freezing level	177
	4.4.2 Results from FTINDEK	181
	4.4.3 Addition of non-linear routing	185
	4.4.4 Results from adding non-linear routing	188
	4.4.5 Discussion of early changes to TINDEK	191
4.5	Further developments to TINDEK	193
	4.5.1 Alteration of time interval	193
	4.5.2 Results	194
	4.5.3 Results from using average temperature over a daily time scale	203
	4.5.4 Comparison of results so far	204
4.6	Final stages of TINDEK development	209
	4.6.1 Correction of over-prediction in the early stages of the model runs	209
	4.6.2 Results	215
4.7	Conclusion	222
<b>5</b>	<b>OTHER MODEL TYPES</b>	<b>225</b>
5.1	Introduction	225
5.2	Parametric energy balance approach	225
	5.2.1 Introduction	225
	5.2.2 Model structure	227
	5.2.3 Results and further modification	229
	5.2.4 Conclusions	237
5.3	Layered temperature index	238
	5.3.1 Introduction	238
	5.3.2 Model structure	238
	5.3.3 Initial parameter/data input and modelling of the snowpack	239
	5.3.4 Meteorological submodel	244
	5.3.5 Snowmelt submodel	248
	5.3.6 Transformation submodel	249
	5.3.7 Depletion submodel	250
	5.3.8 Results from the layered model	254
5.4	Further developments to MART	262

5.4.1	Snowpack distribution	262
5.5	Conclusion	283
<b>6</b>	<b>APPLYING THE MODEL TO OTHER CATCHMENTS</b>	<b>285</b>
6.1	Introduction	285
6.2	TINDEX	285
6.2.1	Running TINDEX on the Dee datasets	285
6.2.2	Running TINDEX on the Gairn datasets	296
6.2.3	Running TINDEX on the Feshie datasets	308
6.2.4	Summary of TINDEX results	317
6.3	MART	319
6.3.1	Running MART on the Dee datasets	320
6.3.2	Running MART on the Gairn datasets	325
6.3.3	Running MART on the Feshie datasets	331
6.3.4	Summary of MART results	336
6.4	ANDERS	339
6.5	Conclusion	341
<b>7</b>	<b>TOWARDS A UNIVERSALLY APPLICABLE MODEL</b>	<b>343</b>
7.1	Comparison of different models	343
7.2	The application of models in real time	348
7.2.1	Introduction	348
7.3	Sensitivity analysis	364
7.4	Conclusions and guidelines for use in real time	372
<b>8</b>	<b>CONCLUSION AND FURTHER WORK</b>	<b>377</b>
8.1	Summary of results	377
8.2	Further work	381
	Bibliography	383
	Appendix A	395
	Appendix B	414
	Appendix C	426
	Appendix D	433

## LIST OF FIGURES

<u>Figure 1.1</u>	The main components of a snowmelt runoff model.	4
<u>Figure 1.2</u>	Goodness of fit of alternative methods of predicting point snowmelt in Corrie Cas, February 1979; sensitivity of distributed energy balance method is shown. From Ferguson and Morris (1987).	14
<u>Figure 1.3</u>	Cumulative snow surface lowering at a site in Ciste Mhearad. Upper plot is predicted for 7-14 June 1983 using spatially-averaged best fit parameters; lower plot is for 7-14 June 1984 using the 1983 parameters. After Ferguson and Morris (1987).	15
<u>Figure 1.4</u>	Cumulative depletion curves using accumulated degree-days. Upper plot shows observed depletion curves for 1976, 1977 and 1979; the lower plot shows the family of curves created for different initial snowpack water equivalents. After Martinec and Rango (1982, 1983).	28
<u>Figure 1.5</u>	Diagrammatic representation of the method used to determine degree-days by Ferguson (1984). The shaded area represents the number of degree-days at the snowline.	37
<u>Figure 1.6</u>	Different methods of representing the initial snowpack and applying melt. After Ferguson (1984).	38
<u>Figure 1.7</u>	The effects of Ferguson's 1986 exponent $c$ on controlling the shape of the snowpack distribution.	41
<u>Figure 1.8</u>	Main gauged catchments and meteorological stations in the Cairngorms. From Ferguson and Morris (1987).	45
<u>Figure 1.9</u>	Hypsometric curves for the Allt a Mharcaidh, Feshie, Gairn and Dee catchments.	46
<u>Figure 2.1</u>	Instrumentation in the Allt a Mharcaidh experimental catchment. Contour intervals are 62.5m.	54
<u>Figure 2.2</u>	Snow survey sites used by M Birch for the 1986 melt season.	74
<u>Figure 2.3</u>	Snow survey sites and the areas they represent used for the 1987 and 1988 melt seasons.	76
<u>Figure 2.4</u>	Sampling strategies used by Ferguson (1985) in the Feshie catchment (top), and for the 1987 and 1988 snow surveys in the Allt a Mharcaidh (bottom).	78

<u>Figure 2.5</u> Snow courses used for the detailed snowpack study during the 1987 melt season. Day 1 was 23 February and Day 2 was 24 February.	86
<u>Figure 3.1</u> Snow covered area depletion curves for the 1986-1988 melt seasons.	96
<u>Figure 3.2</u> Changing snowpack volume for the 1986-1988 melt seasons.	101
<u>Figure 3.3</u> Changing catchment water equivalent (CWE) for the 1986-1988 melt seasons.	105
<u>Figure 3.4</u> Changing snowpack water equivalent (SWE) for the 1986-1988 melt seasons.	107
<u>Figure 3.5</u> Histograms showing relative snowpack water equivalents for the three elevation zones. Zone 1 = the lowest, zone 3 = the highest. Numbers adjacent to histograms indicate the snow survey in Tables 3.1 - 3.3 that the data was derived from. All horizontal axes represent the three zones.	111
<u>Figure 3.6</u> Simplistic representation of the changing snowpack water equivalent for the three elevation zones.	115
<u>Figure 3.7</u> Histograms showing the snowpack volume held in each of the three elevation zones. Zone 1 = the lowest, zone 3 = the highest. Numbers adjacent to histograms indicate the snow survey in Tables 3.1 - 3.3 that the data was derived from. All horizontal axes represent the three zones.	116
<u>Figure 3.8</u> Time series plots of the 1986 hydrometeorological data.	125
<u>Figure 3.9</u> Time series plots of the 1987 hydrometeorological data.	126
<u>Figure 3.10</u> Daily weather summaries produced by the London Weather Centre for 3 and 11 April 1986, illustrating the dominant high pressure system.	129
<u>Figure 4.1</u> Flowchart summarising the main steps in the temperature index model TINDEX.	146
<u>Figure 4.2</u> Diagrammatic representation of the hypsometric curve used to apply the meteorological data to the Mharcaidh catchment by TINDEX.	151
<u>Figure 4.3</u> The three different snowpack structures and methods of applying melt considered for use in TINDEX.	154

Figure 4.4 Summarised step by step calculations used in the main TINDEX model for one day. Fictitious data are used. 158

Figure 4.5 Pictorial representation of the problems associated with using a statistical index when optimising. If the index is to be optimised on a maximising function then value 4 provides the true optimum; value 2 is a false pinnacle that may be given as the optimum solution by some optimising routines. Similarly, if a minimising function is used value 3 is the optimum parameter value and value 1 is a trough in the response surface that gives a false value 160

Figure 4.6 A sample MINITAB output illustrating the low resolution of the time series plots and the method used to calculate the  $R^2$  value for each model run. 165

Figure 4.7 Time series plots produced from the first TINDEX model runs on the Mharcaidh. The upper plot is for 1987 and the lower is for 1986. 170

Figure 4.8 The 1986 and 1987 observed flows on the same scale y-axis. It must be noted that the two time scales do not coincide and that the plot is merely an indication of the difference in flow magnitude between the two years. 172

Figure 4.9 Time series plots for the FTINDEX model runs on the Mharcaidh 1986 (upper) and 1987 (lower) data. 182

Figure 4.10 Time series plots for TINDEX and FTINDEX on the Mharcaidh data using non-linear routing. The top plot is for FTINDEX on the 1986 data, the middle is for FTINDEX on 1987 and the bottom is for TINDEX on 1987. 189

Figure 4.11(a) Time series plots for the 1987 FTINDEX6 model run using the combined parameter set and linear routing (top) and the 1986 TINDEX6 model run using optimised parameters and non-linear routing (bottom). (Note: the x-axis is labelled 'run day' but should be 'time interval'; to convert to days divide by four.) 196

Figure 4.11(b) Time series plots for the 1987 FTINDEX6 model run using optimised parameters and nonlinear routing and the 1986 FTINDEX6 model run using optimised parameters and linear routing. (Note: the x-axis is labelled 'run day' but should be 'time interval'; to convert to days divide by four.) 196(a)

Figure 4.12 The variation in melt factor determined by Anderson (1978) for North America. No scale for the y-axis is given by Anderson. 211

<u>Figure 4.13</u> The effect of the parameter k on the rate of growth of the gradually increasing melt factor. The maximum value for the melt factor in all cases is three.	216
<u>Figure 4.14a</u> Time series plots from running TINDEK with a gradually increasing melt factor on the 1986 Mharcaidh data. The upper plot used linear routing and the lower used non-linear routing.	217
<u>Figure 4.14b</u> Time series plots from running TINDEK with a gradually increasing melt factor on the 1987 Mharcaidh data. The upper plot used linear routing and the lower used non-linear routing.	217(a)
<u>Figure 4.15</u> Modelled and observed snow cover depletion curves for the 1986 and 1987 TINDEK model runs using the gradually increasing melt factor and non-linear routing. It is interesting to note that there is very little difference between the model runs using optimised and combined parameter sets.	221
<u>Figure 5.1</u> Time series plots from running ANDERS on the Mharcaidh 1986 data. The upper plot shows the model using a rainfall threshold of 1mm and non-linear routing; the middle plot used a 10mm threshold and non-linear routing; the lower plot also used a 10mm threshold and non-linear routing but used the combined parameter set.	233
<u>Figure 5.2</u> Time series plots from running ANDERS on the Mharcaidh 1987 data. The upper plot shows the model using a rainfall threshold of 1mm and non-linear routing; the middle plot used a 10mm threshold and non-linear routing; the lower plot also used a 10mm threshold and non-linear routing but used the combined parameter set.	234
<u>Figure 5.3</u> Diagram to show the elevation zones used by MART for the Allt a Mharcaidh catchment.	240
<u>Figure 5.4</u> Diagrammatic representation of the three different snow distribution scenarios catered for in MART.	245
<u>Figure 5.5</u> Diagram to show how melt or fresh snow was applied to the snowpack within each elevation zone.	251
<u>Figure 5.6</u> Time series plots from running MART on the 1986 Mharcaidh data using combined parameter sets, The upper plot uses linear routing and the lower uses non-linear routing.	256

<u>Figure 5.7</u> Time series plots from running MART on the 1987 Mharcaidh data using combined parameter sets, The upper plot uses linear routing and the lower uses non-linear routing.	257
<u>Figure 5.8</u> A graph to show the statistical superiority of non-linear routing when using MART.	260
<u>Figure 5.9</u> The four snowpack distributions S1 (top) - S4 (bottom) that were used in MART.	263
<u>Figure 5.10</u> Time series plots from running MART with a combined parameter set, non-linear routing and structure S1. 1986 = upper plot; 1987 = lower plot.	266
<u>Figure 5.11</u> Time series plots from running MART with a combined parameter set, non-linear routing and structure S2. 1986 = upper plot; 1987 = lower plot.	267
<u>Figure 5.12</u> Time series plots from running MART with a combined parameter set, non-linear routing and structure S3. 1986 = upper plot; 1987 = lower plot.	268
<u>Figure 5.13</u> Time series plots from running MART with a combined parameter set, non-linear routing and structure S4. 1986 = upper plot; 1987 = lower plot.	269
<u>Figure 5.14</u> Time series plots of TINDEK (upper) and MART (lower) running on the Mharcaidh 1986 data.	273
<u>Figure 5.15</u> Time series plots of TINDEK (upper) and MART (lower) running on the Mharcaidh 1987 data.	274
<u>Figure 5.16</u> Snow covered area depletion curves from the MART model run on the Mharcaidh 1986 data using optimised (upper) and combined (lower) parameters.	279
<u>Figure 5.17</u> Snow covered area depletion curves from the MART model run on the Mharcaidh 1987 data using optimised (upper) and combined (lower) parameters.	280
<u>Figure 6.1</u> Time series plots from TINDEK running on the DEE 1984 data with linear (upper) and non-linear (lower) routing.	289
<u>Figure 6.2</u> Time series plots from running TINDEK on the DEE 1986 data with non-linear (upper) and linear (lower) routing.	290
<u>Figure 6.3</u> Time series plots from running TINDEK on the DEE 1987 data with non-linear (upper) and linear (lower) routing.	291

<u>Figure 6.4</u> Time series plots from running TINDE	299
INDEX on the Gairn data; upper plot is for 1979 with linear routing, middle plot is for 1980 with linear routing and the lower plot is for 1982 with non-linear routing.	
<u>Figure 6.5</u> Time series plots from running TINDE	300
INDEX on the Gairn 1984 data with non-linear (upper) and linear (lower) routing.	
<u>Figure 6.6</u> Time series plots from running TINDE	301
INDEX on the Gairn 1986 data with linear (upper) and non-linear (lower) routing.	
<u>Figure 6.7</u> Time series plots from running TINDE	302
INDEX on the Gairn 1986 data with linear (upper) and non-linear (lower) routing.	
<u>Figure 6.8</u> Time series plots from running TINDE	310
INDEX on the Feshie 1979 data with linear (upper) and non-linear (lower) routing.	
<u>Figure 6.9</u> Time series plots from running TINDE	311
INDEX on the Feshie 1980 data with linear routing (lower) and on the 1981 complete data set with non-linear routing.	
<u>Figure 6.10</u> Time series plots from running TINDE	312
INDEX on the Feshie 1981 data with the first day's values missing using linear (upper) and non-linear (lower) routing.	
<u>Figure 6.11</u> Time series plots from running MART	322
on the Dee 1984 (upper), 1986 (middle) and 1987 (lower) data, all with non-linear routing.	
<u>Figure 6.12</u> Time series plots from running MART	327
on the Gairn 1979 (upper), 1980 (middle) and 1981 (lower) data, all with non-linear routing.	
<u>Figure 6.13</u> Time series plots from running MART	328
on the Gairn 1984 (upper), 1986 (middle) and 1987 (lower) data, all with non-linear routing.	
<u>Figure 6.14</u> Time series plots from running MART	333
on the Feshie 1979 (upper) and 1980 (lower) data, both with non-linear routing.	
<u>Figure 6.15</u> Time series plots from running MART	334
on the Feshie 1981 complete dataset (upper) and with the first day's data removed (lower), both with non-linear routing.	
<u>Figure 6.16</u> Time series plots from running ANDERS	340
on the Dee (upper) and Gairn (lower) datasets. Both model runs used linear routing a rainfall threshold of 10mm	

Figure 7.1 Time series plots from running TINDEX on the Dee 1984 dataset under different conditions. The simulated plot had the environmental lapse rate, recession and melt coefficients set as constants and optimised the snowpack and gradually increasing melt factor parameters from the whole dataset; the predicted plot optimised the same parameters at two day increments, the plot being derived by appending the two day flow preictions as explained in the text. Both model runs used non-linear routing.

356

Figure 7.2 Time series plots from running MART on the Dee 1984 dataset under different conditions. The simulated plot had the environmental lapse rate, recession and melt coefficients set as constants and optimised the snowpack and gradually increasing melt factor parameters from the whole dataset; the predicted plot optimised the same parameters at two day increments, the plot being derived by appending the two day flow preictions as explained in the text. Both model runs used non-linear routing.

360

Figure 7.3 Plots of the response surface of the TINDEX simulated model run varying one of the three optimised parameters at a time and holding the other two at the optimised value.

366

Figure 7.4 Two-dimensional slices through the three-dimensional response surface of the TINDEX simulated model run, the slice being taken through the optimised value of the third parameter.

370

## LIST OF TABLES

<u>Table 2.1</u>	Results from the detailed snow survey carried out on 23 and 24 February 1987.	85
<u>Table 3.1</u>	Summary results from the 1986 snow surveys.	93
<u>Table 3.2</u>	Summary results from the 1987 snow surveys.	94
<u>Table 3.3</u>	Summary results from the 1988 snow surveys.	95
<u>Table 3.4</u>	Snow covered area depletion rates from the 1986 and 1988 snow surveys.	98
<u>Table 3.5</u>	Pearson's correlation coefficients between observed flow and meteorological data for the Allt a Mharcaidh catchment during the 1986 and 1987 melt seasons.	133
<u>Table 3.6</u>	$R^2$ results from the multiple regression analysis on the Mharcaidh 1986 and 1987 data.	137
<u>Table 3.7</u>	$R^2$ results from the multiple regression analysis on the combined Mharcaidh 1986 and 1987 data	139
<u>Table 4.1</u>	Timing of minimum daily flows, February to May, from the 1986 and 1987 flow records. Times are GMT.	148
<u>Table 4.2</u>	Results from applying TINDEX to the Mharcaidh 1986 and 1987 data.	169
<u>Table 4.3</u>	Results from applying FTINDEX to the Mharcaidh 1986 and 1987 data.	181
<u>Table 4.4</u>	Results from applying FTINDEX and TINDEX to the Mharcaidh 1986 and 1987 data using non-linear routing.	188
<u>Table 4.5</u>	Calculated recession coefficients for minimum and maximum observed flows during the 1986 and 1987 melt seasons.	190
<u>Table 4.6</u>	Statistical results from the early model runs of TINDEX and FTINDEX.	192(a)
<u>Table 4.7</u>	Results from running the six-hourly time step models on the 1986 and 1987 data.	197

<u>Table 4.8</u> Comparison of the range and standard deviation of the optimised parameter sets using the two different time intervals.	200
<u>Table 4.9</u> Pearson's correlation coefficients between different temperature indices and observed flow values.	201
<u>Table 4.10</u> Results from applying TINDE <sub>X</sub> and FTINDE <sub>X</sub> on the Mharcaidh data using average daily temperature to determine the degree days.	203(a)
<u>Table 4.11</u> Summarised SE and R <sup>2</sup> values for all model runs using both combined and optimised parameter sets.	205
<u>Table 4.12</u> Summary SE and R <sup>2</sup> resultd for all parameter sets using modelling approaches (a) - (d).	206
<u>Table 4.13</u> Summary SE and R <sup>2</sup> results from all parameter sets using model approaches (a) - (d) on model type (1) only.	208
<u>Table 4.14</u> Results from running TINDE <sub>X</sub> with the melt factor increasing in two stages.	213(a)
<u>Table 4.15</u> Results from using a gradually increasing melt factor (K) when applying TINDE <sub>X</sub> to the Mharcaidh datasets.	218
<u>Table 5.1</u> Results from applying the parametric energy balance model, ANDERS, to the Mharcaidh 1986 and 1987 datasets.	230
<u>Table 5.2</u> Results from applying ANDERS to the Mharcaidh 1986 and 1987 datasets using rainfall thresholds of 5 and 10mm.	235
<u>Table 5.3</u> Mean temperature differences and lapse rates calculated from Lagganlia (265m amsl) and Cairngorm (1245m amsl); temperature data from the 1979, 1980 and 1981 melt seasons.	246
<u>Table 5.4</u> Results from the first runs of MART using linear and non-linear routing on optimised and combined parameter sets.	258
<u>Table 5.5</u> Comparison of TINDE <sub>X</sub> and MART R <sup>2</sup> values	261
<u>Table 5.6</u> Results from running MART with the five different snowpack structures.	265
<u>Table 5.7</u> Snowpack volumes modelled by the optimised and combined MART model runs for the different snowpack structures.	276

<u>Table 6.1</u> Datasets used to apply TINDEK and MART to the Dee, Gairn and Feshie catchments.	286
<u>Table 6.2</u> Results from applying TINDEK to the Dee datasets.	288
<u>Table 6.3</u> Results from applying TINDEK to the Gairn datasets.	298
<u>Table 6.4</u> Results from applying TINDEK to the Feshie datasets.	309
<u>Table 6.5</u> The optimised initial snowpack volumes for both the Feshie and Gairn model runs.	315
<u>Table 6.8</u> The optimised initial snowpack volumes for the Dee and Gairn 1984, 1986 and 1987 TINDEK model runs.	317
<u>Table 6.7</u> Results from applying MART to the DEE datasets.	321
<u>Table 6.8</u> Results from applying MART to the Gairn datasets.	326
<u>Table 6.9</u> Results from applying MART to the Feshie 1979, 1980 and 1981 datasets.	332
<u>Table 7.1</u> Values of the environmental lapse rate, recession and melt coefficients set as constants for the TINDEK and MART simulated real time models.	351
<u>Table 7.2</u> Parameter sets obtained from applying TINDEK in simulated real time to the Dee 1984 dataset.	355
<u>Table 7.3</u> Parameter sets obtained from applying MART in simulated real time to the Dee 1984 dataset.	359

## LIST OF PLATES

- Plate 2.1 The Allt a Mharcaidh catchment viewed from the A9 two miles south of Aviemore. 50
- Plate 2.2 Gauge Site 1 at 320m in the Allt a Mharcaidh catchment. 55
- Plate 2.3 The Mountain Weather Station located at 1000m, on the south-west slopes of Sgoran Dubh Mor. Rime can be seen on the main body of the MWS but the sensors are relatively ice-free. 57
- Plate 2.4 The effect of elevation and aspect on snow distribution. West facing slopes have less snow than those with an easterly aspect; little snow is present on the lower slopes of the catchment. 69
- Plate 2.5 Snowdrift on the south-western slopes of the Allt a Mharcaidh caused by high winds. 71
- Plate 2.6 Melt water flowing under the remains of the snowpack held in the main gully. This illustrates the importance of the gully snow survey site as snow would lie here until late in the year. 72
- Plate 2.7 One of the snow pits dug during the 1987 snow surveys. These were used to examine the variation in snow density and to establish a more accurate idea of the snowpack characteristics. 81
- Plate 3.1 Exposed spurs and ridges in the catchment quickly lost their snow cover. 123

## **ACKNOWLEDGEMENTS**

I would like to begin by thanking my three supervisors, Professor Rob Ferguson, Dr John Harrison and Dr Alan Jenkins for their assistance in the completion of this project. Special thanks are due to Rob for the speedy return of scripts with helpful comments during the later stages, and for the help and advice received throughout. Thanks are due to staff at the Institute of Hydrology for their help with field data, Mike Birch for allowing me to use his 1986 snow survey data and to Joe Porter for assistance with the Mharcaidh fieldwork. Dr Jim Burton of Heriot Watt University provided meteorological data and the North East River Purification Board provided hydrological data. I would like to thank NERC and the Institute of Hydrology for funding the first three years of the project.

In the Environmental Science Department at Stirling I would like to thank Professors Michael Thomas and Keith Smith for allowing me access to Departmental facilities; Des Donnelly, Lyn Napier, Dave Harrison, Chris Anderson, Muriel McLeod, John McArthur, Mary Smith and Bill Jamieson for technical advice on various matters, and Ina Mack for keeping me under control!

I also thank Rob Marshall, Rob Isbister, Dave Farley, Simon

Booth, Anne Bailey and the Operators in the Computer Unit at Stirling for helping to solve the numerous problems that arose during the four years. I would like to thank Lieutenant Commander John Keenan at the Royal Naval Engineering College for helping me get to grips with Fortran 77.

My thanks go to my parents for support, both morally and financially, during my time at Stirling, and to all my friends for providing a lighter side to life. Finally, special thanks go to my wife Jill who, in addition to helping with the Mharcaidh snow surveys, typing and proof reading the thesis, provided me with continual support, encouragement and companionship throughout the project.

## CHAPTER 1 INTRODUCTION

### 1.1 Why model snowmelt?

In addition to providing a valuable economic resource for many countries as a base for winter sports, snow covered areas can also be beneficial in other ways. Snowpacks can be considered as natural reservoirs containing the products of a winter's precipitation which release their contents at predictable times every year, though the timing of this may vary slightly. This natural regulation of the precipitation is exploited in many countries for hydroelectric power generation and in water supply management, the low summer precipitation being supplemented by snowmelt from the higher regions. This is most common in countries containing glacierised areas such as those in the European Alps, North America, Asia, Scandinavia, Australia and New Zealand where the summer snowmelt produces almost uniform flows from year to year. Being able to predict the timing and magnitude of this summer snowmelt allows man to operate these schemes more efficiently and is thus of economic benefit.

At present the spring snowmelt in Britain, more specifically Scotland, is not utilised in this manner as the flow is not as constant from year to year, though there may be scope for use in supplementing reservoir storage at certain times. This does not mean that there is not a need

for being able to predict snowmelt events. A combination of high rainfall, reservoirs at near full status and a period of intense snowmelt from a shallow snow cover in February 1989 brought severe flooding to the northern Highlands, resulting in the main rail bridge in Inverness being washed away and many homes and fields being flooded. More recently, in February 1990 a combination of rainfall and snowmelt again resulted in severe flooding, this time affecting a wider area. The Tay burst its banks at many points and much of Perth was flooded, along with more flooding further north in the Great Glen. Many households were still recovering from the floods the previous year and there was a call for more warning in the future. Archer (1975 and 1986) has identified the importance of snowmelt flood events in Northumberland and other areas in Britain, and Fitzharris and Grimmond (1982) describe snowmelt floods in the Frazer River, New Zealand. The cost of these floods in both economic terms and human distress highlights the importance of being able to accurately predict the resultant runoff from snowmelt over a wide area.

The onset of spring snowmelt is often accompanied by a surge in the dissolved solutes in a stream, especially in areas with thin soils and resistant bedrock (Skartveit and Gjessing, 1979). This is because the impurities in the snowpack (accumulated over many months) are held on the surface of the ice crystals and interstitial water and, when melt starts, are leached out by water percolating

through the snowpack (Morris and Thomas, 1985a). The resultant pulse of pollutants, usually acidic in the Cairngorms (Morris and Thomas, 1985b), is often detrimental to the ecology of the streams, especially fish life. With the recent increase in fish farming in the Highlands it may therefore be of economic benefit to be able to predict these events and to be able to say when it is 'safe' to put fry/smolts into the streams.

## 1.2 Approaches to modelling snowmelt runoff

Snowmelt can be modelled in a number of different ways depending on the detail of data available and the use for which the output is needed. The complexity of the different approaches used to calculate the actual melt varies from simple regression-type models to more complex routines that form a separate module within a fully distributed catchment model such as IHDM (Bevan and O'Connell, 1982; Rogers et al, 1985).

Generally, snowmelt runoff models consist of a number of smaller 'submodels' (Figure 1.1). The World Meteorological Organisation (1986) identifies three submodels which need to know the snow covered area (SCA) during the melt season. This is normally determined by field observations or estimated from known depletion patterns observed over past melt seasons. Ferguson and Morris (1987) describe a fourth submodel which avoids this need for estimated or updated

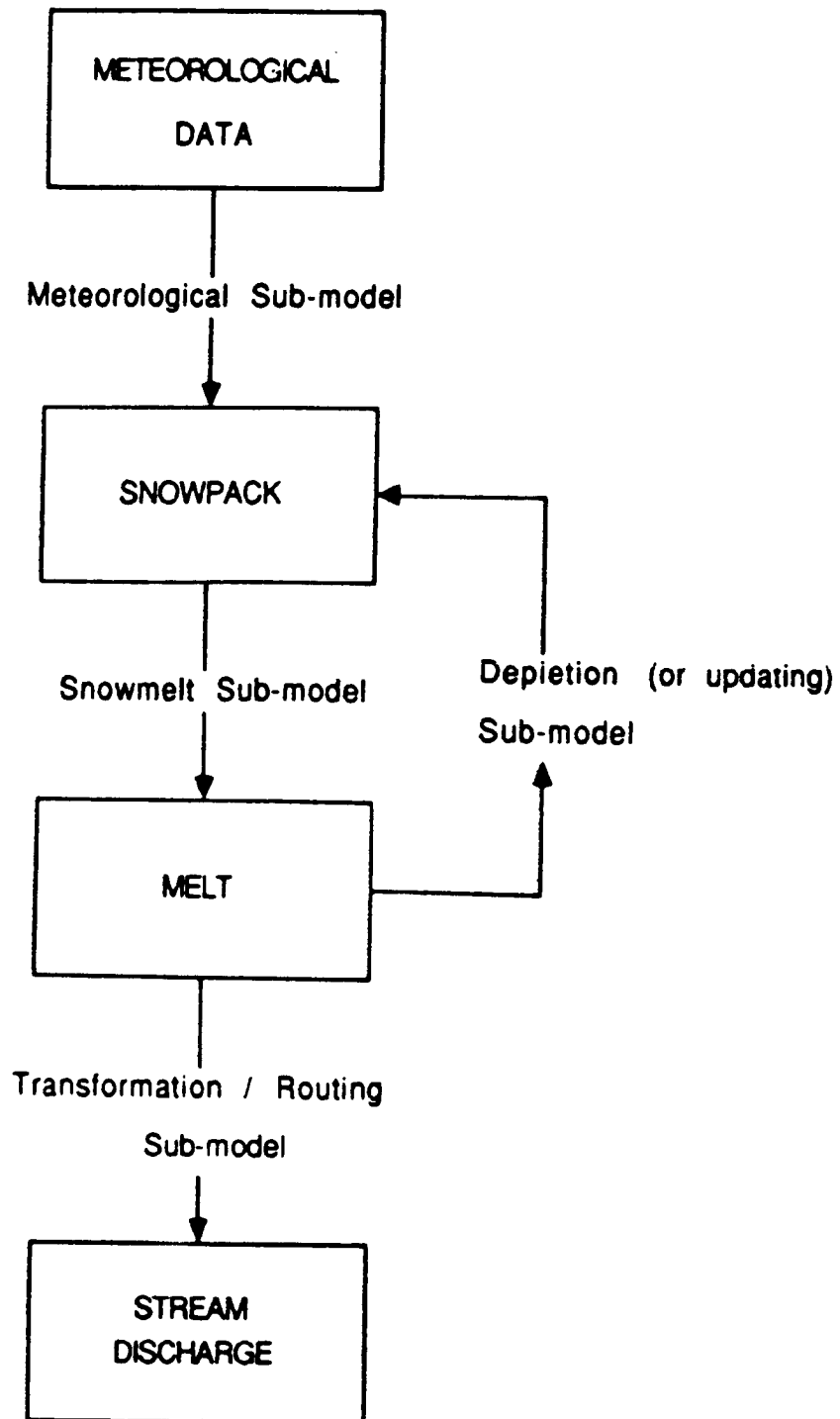


Figure 1.1 The main components of a snowmelt runoff model.

SCA by endogenously modelling the snowpack depletion.

The core of the various snowmelt runoff models is the **snowmelt submodel** which calculates the amount of melt occurring over the snowpack and the resultant meltwater arriving at the snow/ground interface. The three main methods used to do this are described later in the chapter.

The **meteorological submodel** precedes the snowmelt submodel and determines the inputs to the snowpack from meteorological data collected outside or within the catchment. It will often determine whether the precipitation is likely to be in the form of snow, rain or a combination of both, reduce or increase the temperature to take account of altitudinal effects and, depending on the nature of the melt calculation used in the snowmelt submodel, make calculations regarding other meteorological variables. It is of greatest importance in catchments or study areas with high relief where the effects of altitude will be large; if the area has only limited relief then the submodel will often be concerned only with applying point measurements of precipitation to a larger area.

Once the melt has been calculated and the snowpack updated the **transformation submodel** calculates the stream discharge at the output of the drainage basin. This submodel often has to deal with inputs in the form of both snowmelt and

rainfall over the snow-free parts of the catchment and is often similar to the rainfall-runoff component of more conventional hydrological models, the complexity of the routing transformations used again varying from model to model.

The final submodel is the one identified by Ferguson and Morris which they name the **depletion submodel**. As the snow melts the snowpack may decrease in area in addition to total water equivalent diminishing. The rate of change in snow covered area of a catchment will depend on the nature of the snowpack and relief of the catchment. A catchment with a uniform snow cover and little relief will tend to retain 100% SCA until the snowpack water equivalent (SWE) is low and then rapidly decrease to near snow free conditions in a few days whilst a catchment with more relief and less uniform snow cover will show a more uniform decrease in the snow cover over a longer time period. Many models allow the area of the snowpack to be updated when observations permit (from personal observation or remote sensing as proposed by Rango and Martinec, 1982). Where this is not possible the decrease in snowpack area is predicted by the depletion submodel as proposed by Ferguson (1984), applying the melt calculated in the snowmelt submodel to the snowpack and reducing it where necessary. It may sometimes be the case that the meteorological submodel indicates fresh snowfall; if this is so the depletion submodel may temporarily increase the area of the

snowpack.

Attention is usually concentrated on the snowmelt submodel when comparing the performance of different snowmelt runoff models but it must be remembered that all four submodels affect the output. There is little point in having a detailed and complex snowmelt routine when the transformation submodel is inadequate and oversimplifies the processes taking place or the meteorological submodel fails to supply accurate input to the model.

### 1.3 Previous work

Much work has been done on studying the physical processes involved in snowmelt, resultant runoff, the effects of snowmelt and related topics. Where appropriate this is referred to in later chapters; the work described here involved the development and comparison of different snowmelt runoff models.

Snowmelt runoff models generally calculate the amount of melt using one of three methods. The **physics based energy balance** calculates the energy and mass balance transfers at the snowpack and determines the amount of melt from this. As this method requires very detailed meteorological data the **parametric energy balance** approach is often used which attempts to represent the energy balance of the snowpack using only temperature, precipitation and windspeed data

which are more universally available. Finally, the **temperature index** approach identifies temperature as the most important index of melt and calculates the snowmelt from this. Because it is the simplest of the three methods and the data is readily available this is the most commonly used approach.

### 1.3.1 The physics based energy balance approach

It is possible to calculate the actual melt using the physical energy balance method when sufficient data are available. The method is based on the detailed flow of mass and energy within the snowpack and at its boundaries which may be written as:

$$Q_m = Q_{sn} + Q_{ln} + Q_h + Q_e + Q_g + Q_p - dU/dt, \quad (1.1)$$

where

$Q_m$  = energy available for melt,

$Q_{sn}$  = net short wave radiation absorbed by the snow,

$Q_{ln}$  = net long wave radiation at the snow/air boundary,

$Q_h$  = convective/sensible heat from the air at the snow/air interface,

$Q_e$  = latent heat at the snow/air interface (positive for condensation and negative for evaporation and sublimation),

$Q_g$  = conducted heat from the ground at the snow/ground interface,

$Q_p$  = heat gained from rainfall,

$dU/dt$  = rate of change of stored energy per unit area of  
snowcover, (after Male and Gray, 1981).

The ground heat flux  $Q_g$ , which is normally small, may produce small amounts of melt near the snow-ground surface though these are usually insignificant along with the flux of heat from rainfall,  $Q_p$ , which is more uniformly distributed due to the rain infiltrating through the snowpack.  $Q_{sn}$ , the short-wave radiation flux, is usually strongest at the surface although limited amounts do penetrate into the snowpack. The long-wave radiation flux,  $Q_{ln}$ , operates only at the snowpack surface and is always negative for snow-covered areas.

Due to the cloudy conditions often found in the Highlands radiant energy is often not as important as sensible heat, especially when compared to other areas where clear skies are more common. Consequently  $Q_h$ , the convective/sensible heat from the air, is more important but, due to its dependence on airflow, is difficult to accurately calculate as this is so variable over mountainous terrain (Barry, 1981). This is also the case with  $Q_e$ , the latent heat flux, as it is also a turbulent transfer process.

It is possible to calculate snowmelt water equivalent for a given value of  $Q_m$  by knowing the thermal quality of the snow (i.e. the fraction of ice in a unit mass of wet snow, usually in the order of 0.95 as the snowpack generally

retains 3 to 5% water by weight (Male and Gray, 1981)), the latent heat of fusion and the density of water. The latter two are usually considered constant at  $333.5 \text{ kJkg}^{-1}$  and  $1000 \text{ kgm}^{-3}$  respectively. Negative values of  $Q_m$  are used to raise the cold content of the snowpack; following a cold spell or at the start of the melt season the energy available for melt is used to raise the temperature of the snow to the melting point before any actual melt can take place (part of the ripening process).

Many authors have used the energy balance method to produce a model for calculating snowmelt at a point (for example, Colbeck, 1972, 1974, 1975, Oblad and Rosse, 1977, Dunne et al, 1976, Harding, 1986, Kuusisto, 1986). Morris and Godfrey (1978) describe one of the methods used to calculate snowmelt in the European Hydrological System (Systeme Hydrologique Europeen or SHE) developed jointly by SOGREAH (France), the Danish Hydraulics Institute and the Institute of Hydrology (UK). SHE is a physically based deterministic model, developed so that it can be run under a number of different conditions with the detail of calculation being selected in accordance with the quality of data, facilities available and output required. The routine described by Morris and Godfrey is the most detailed and complex of the snowmelt routines in SHE and is intended to be used when changes in structure and temperature of the snowpack will have a major effect on water flow within the pack; in this way it was the first

attempt to model the flux of both energy and mass within the snowpack taking account of the changes taking place as the model runs. The calculation is based on two differential equations that describe the flow of heat and water through the snow; water vapour transfer and movement through the pack are not included directly but are represented by a parameter  $k_{eff}$  which represents the effective thermal conductivity (this method is similar to that used by Obled and Rosse (1977)). Morris (1983) describes in detail the complex equations that are used in the calculations and gives results from applying it to a site near the Corrie Cas carpark at the Cairngorm skiing development, a sub-Arctic site on the northern boundary of the Cairngorms.

Whilst acknowledging that the model could be improved by decreasing the time step and grid spacing over which the calculations are made, and also by studying the stability of the air at the boundary layer through collecting meteorological data at various heights above the snowpack (the model assumes stable conditions), Morris and Godfrey concluded that in the cases they had studied the model produced a good replication of the conservation of mass and energy.

Morris (1982) compared this method of determining snowmelt to the other two alternatives available in the SHE model (degree-day and energy budget at the two snowpack

interfaces, all three being carried out at a point), applying the model at both the Corrie Cas site and to a high Alpine area on the slopes of Riffleberg in the Swiss Alps. The degree-day method was found to be the least satisfactory of the three methods, having a r.m.s. error in the snowmelt rate of  $0.80\text{mm day}^{-1}$  for the Cairngorm data and  $0.72$  for the Riffleberg site. It must be remembered that this is for melt at a point, Morris did not examine the performance at the catchment scale where the degree-day method is thought to perform better.

The simplified energy balance method produced better results, the r.m.s. values (for snowpack depth) being  $0.25$  for Cairngorm and  $0.12$  for Riffleberg (these results are not directly comparable to the degree-day method as different model runs of different length produced the best results). The Alpine data produced better results as the snow was ripe for the whole of the model run and the average temperature of the surface snow was always similar to the air temperature. This was not the case for the Cairngorm site where the snow temperature was variable and often differed from that calculated by the model. However, whilst the model performed better than when using the degree-day approach, Morris noted that the value of one parameter  $z_0$ , the roughness height of the snowpack (mm) differed by a factor of more than 100 between the two data sets. This can be attributed to the importance of the sensible heat component of the energy balance in

determining melt in cloudy conditions described above. Thus, whilst the model performed well for each specific site, the sensitivity of the model to this parameter meant that it was not possible for Morris to use the model in a general form with  $z_0$  decided in advance.

The final method, the full distributed model based on the flow of mass and energy, was tested on two days data at the Cairngorm site. The normalised r.m.s. error was 0.60 for three sets of <sup>independent</sup> data. Whilst this is larger than the value for the simplified energy balance approach Morris argued that it did not mean the method was less successful. The full distributed method produced values for the snowpack temperature and depth that were closer to observed values than those predicted by the energy balance method and Morris hoped that further development of the distributed model would improve its performance.

Ferguson and Morris (1987) discuss in detail the problems caused by the sensitivity of the physics based models to the aerodynamic roughness length parameter,  $z_0$ , illustrated in Figure 1.2. In the case of the simplified energy balance method available in the SHE this may be caused by the value of  $z_0$  not being solely dependent on the aerodynamic roughness length of the snow surface, but also on other factors such as extent, density, depth and average temperature of the snowpack. Morris (1982) reported that data from nine sites in the Cairngorms gave  $z_0$  values

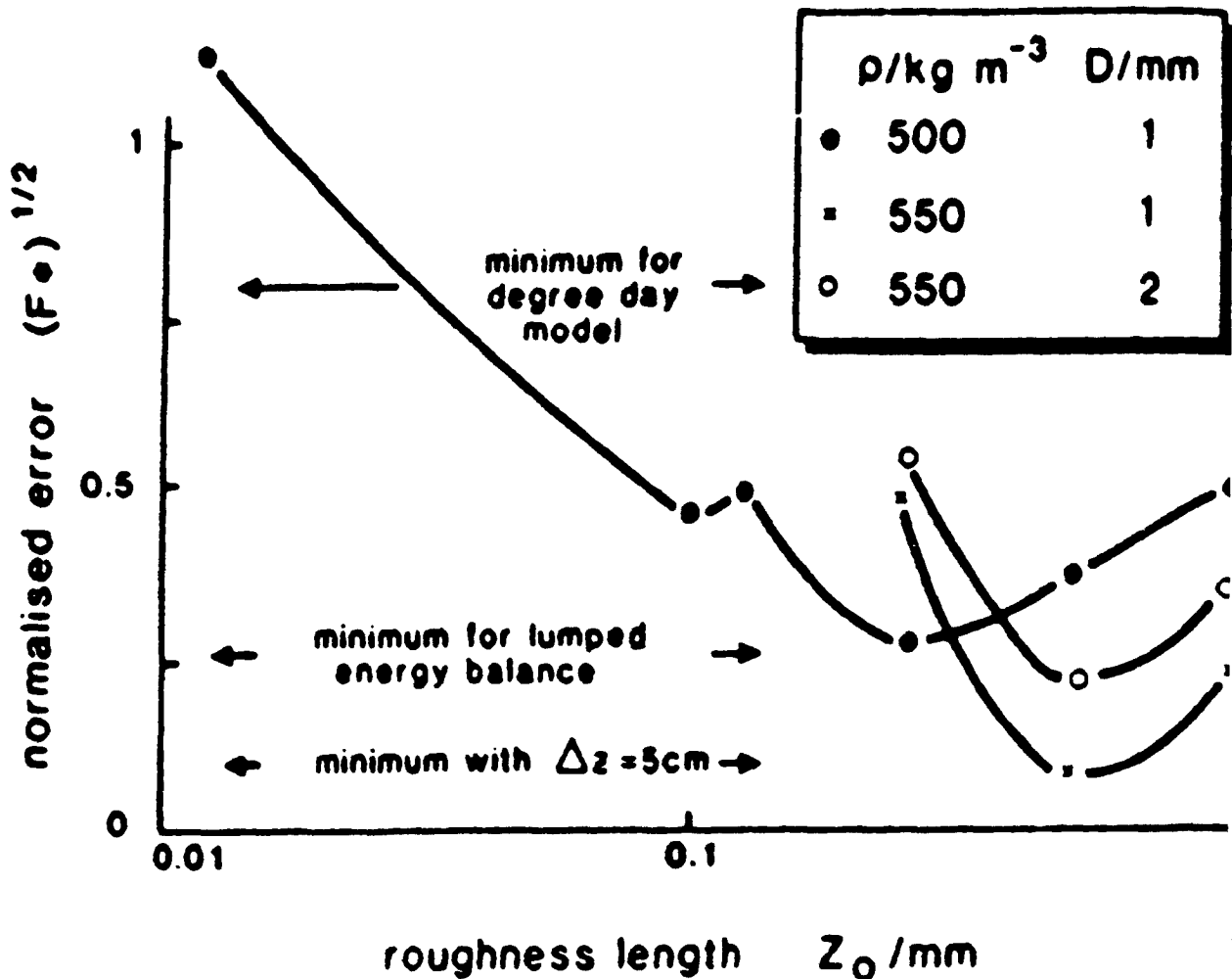


Figure 1.2

Goodness of fit of alternative methods of predicting point snowmelt in Corrie Cas, February 1979; sensitivity of distributed energy balance method is shown. From Ferguson and Morris (1987).

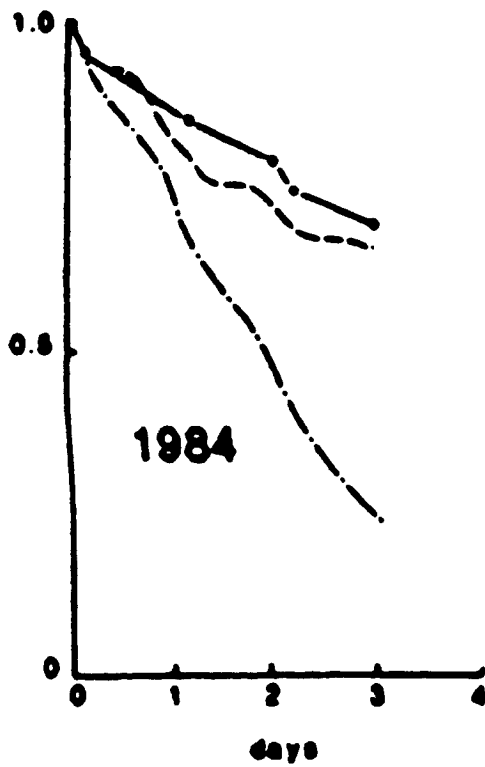
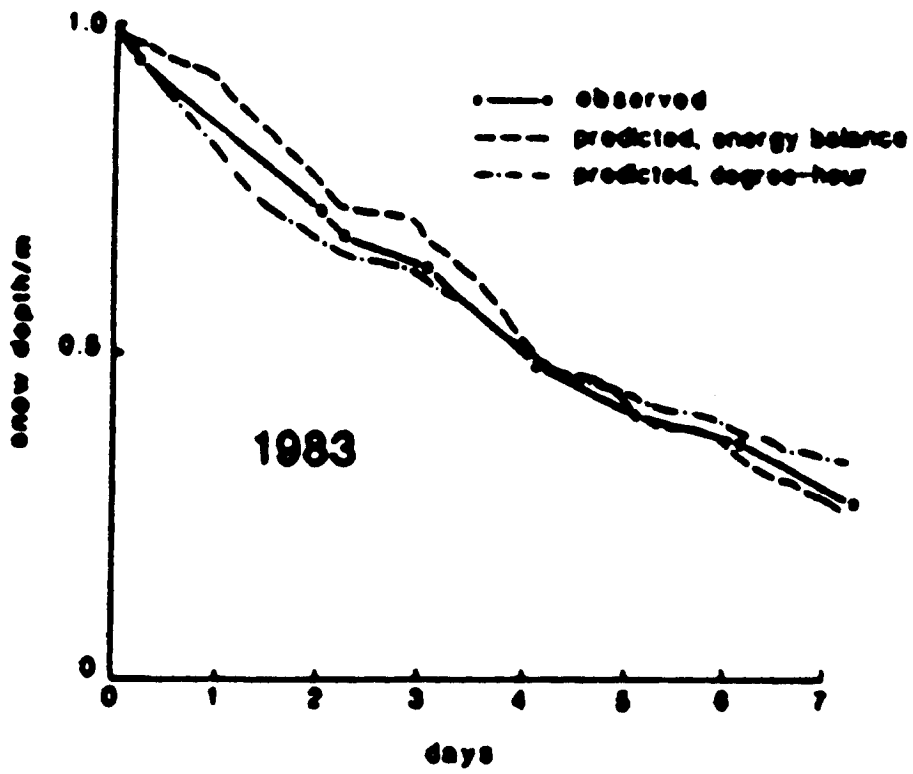


Figure 1.3

Cumulative snow surface lowering at a site in Ciste Mhearad. Upper plot is predicted for 7-14 June 1983 using spatially-averaged best fit parameters; lower plot is for 7-14 June 1984 using the 1983 parameters. After Ferguson and Morris (1987).

ranging from  $0.41 \times 10^{-5} \text{m}$  to  $1.18 \times 10^{-4} \text{m}$  using this method. Harding (1986) found from averaged twenty minute wind profiles taken over a large, snow covered lake in Norway that values ranged from 0.25 to 10mm; the range is likely to be larger in mountain areas where relief and vegetation influence wind flow. Whilst this range in optimised values may be related to the variability of  $z_0$ , in reality it remains a problem in applying the model to predictive uses. Despite this Ferguson and Morris conclude that the energy balance approach is superior to the degree-day method at the point scale. This is illustrated by Figure 1.3 which compares measured snow depth to that predicted by the two methods for two melt events in 1983 and 1984 in the Ciste Mhearad, a small catchment to the north-east of the Cairngorm summit. Rogers and Anderson (1986) found that  $z_0$  ranged from 0.14 to 2mm over a seven day period at nine sites in the catchment, and had a mean value of 0.8mm. This value was used in the model and, whilst neither method appears to perform better for the 1983 event, when the same parameters are used for the four day 1984 event it can be seen that the degree-day method systematically overpredicts the melt rate (due to different weather conditions). The energy balance method, whilst not being as accurate as for the 1983 event, performs better using the same parameters.

Many of the models developed using the energy balance approach have their performance assessed by comparing predicted to observed melt at a point. Whilst this is

useful in examining the predictive ability of the model to calculate actual melt, further work is needed before the model can be used for flood forecasting, i.e. the melt produced has to be converted to runoff via a transformation submodel. Often, in the early stages of model development, this transformation submodel is oversimplified and results in a significant decrease in model performance (Braun and Lang, 1986; Ferguson and Morris, 1987 (Ciste Mheard example)). If the performance of the melt routine is to be preserved in the model it is important that the degree of complexity or simplification is kept as constant as possible through all stages of the model. Models such as the SHE cater for this with melt calculated from the degree-day method being routed using a simple empirical method based on that developed by Anderson (1968) whilst also providing a detailed, grid, physics based method for melt calculated from the energy balance method. This is also the case with the Institute of Hydrology Distributed Model (IHDM) that represents the catchment as a series of channels and hillslopes. Charbonneau et al (1981) applied a number of different snowmelt runoff models to the Durance River basin (548km<sup>2</sup>) in the French Alps. They found that the choice of meteorological or transformation submodel was often more important than the choice of melt routine, largely because they tended to be oversimplified and were able to ensure the accuracy of the detailed melt subroutines.

Morris (1986) and Morris and Thomas (1985) have applied the snowmelt routine developed for the SHE to other uses, namely modelling the preferential elution of pollutants during snowmelt events in the Cairngorms and to assess the potential effects of climatic change arising from increased levels of CO<sub>2</sub> in the atmosphere. The model produced acceptable replications of high conductivity flood events in Highland streams and it is hoped that it and similar models will allow predictions about the effects of hypothetical future climatic changes to be made.

Concluding, it can be seen that whilst the physics based energy balance approach may be the most accurate at calculating melt at a point, the requirement of high quality data and difficulties in applying these data over mountainous areas give the method little potential for use in a general form, especially if prediction is required.

### 1.3.2 The parametric energy balance approach

The WMO (1986), in reviewing snowmelt model development and performance using all methods, found that whilst the energy balance methods usually gave better results than the degree-day models at the point scale, they were rarely used for operational real time forecasting due to lack of sufficient data. This has led to the development of models that are more sophisticated than the simple temperature

temperature index ones but can still operate from widely available data, thus making their use for predictive purposes possible. These models are based on the assumption that the different components of the energy balance are of different significance in determining the total energy available for melt, and that by representing the most important components by simple empirical formulae improvements in model performance can be made.

Anderson (1968, 1973 and 1976) describes the snowmelt routine used by the National Weather Service River Forecast Service in North America. This is a **conceptual** model, i.e. each of the significant physical processes affecting snowmelt is mathematically **represented** in the model through a series of equations and indices. The model separates rain-on-snow events from pure snowmelt events and attempts to take account of the varying sensible heat contribution to melt determined by different wind conditions.

The model separates rain-on-snow events from pure snowmelt because:

- (1) The magnitudes of the various energy transfer approaches tend to be different during the two types of event.
- (2) The dominant energy transfer processes during rain-on-snow events are known and can be simulated using readily available data.
- (3) The seasonal variation in melt rates is generally

quite different for the two different types of event.

By doing this, and making several assumptions about the energy transfer processes during rain-on-snow events, Anderson shows that it is possible to represent the energy balance during these events using only air temperature, precipitation and windspeed data, all of which are readily available. This makes the approach more applicable than the full energy-balance method which, in addition to being so sensitive to model parameters, needs detailed meteorological data that are not readily available.

Braun and Lang (1986) investigated the performance of five different model structures on catchments ranging from 3.2 to 1696km<sup>2</sup>. The different models were based on the following approaches:

- (1) temperature index method (after Bergstrom, 1976);
- (2) temperature and wind index method;
- (3) combination method (after Anderson, 1973);
- (4) extended combination method including water vapour pressure as an input variable;
- (5) full energy balance (after Price and Dunne, 1976).

They concluded that, for catchments <1000km<sup>2</sup>, the combination model according to Anderson (1973) was the most suitable approach as it could operate on readily available data and perform better than the temperature index method.

### 1.3.3 Temperature index method

Air temperature is generally regarded as the best single indicator of the full energy balance at the snow surface (Ferguson and Morris, 1987) and as it is readily available has often been used as an index of snowmelt. Anderson (1973) also states that it is usually used to estimate melt rather than the energy balance as air temperatures can be more accurately forecast and is more widely available, thus allowing it to be used for real time forecasting of runoff.

There is no single, universally applicable temperature index of snowmelt as each index tends to be for a specific catchment or area (Male and Gray, 1981). However, the simplest expression relating snowmelt to air temperature may be written as:

$$M = M_f(T_a - T_b), \quad (1.2)$$

where

M = melt produced in cm water equivalent in unit time,

$M_f$  = melt factor ( $\text{cm}^\circ\text{C}^{-1} \text{ unit time}^{-1}$ ),

$T_a$  = air temperature taken as index (usually mean or maximum daily temperature),

$T_b$  = base temperature for melt to occur, usually  $0^\circ\text{C}$ .

#### 1.3.3.1 The work of Martinec and Rango

Martinec (1960, 1965, 1975) developed a temperature index

model for use in the Swiss Alps in which melt was calculated on a daily basis using the number of degree-days (average of the positive temperatures over a 24 hour period):

$$M = M_f \cdot T_d, \quad (1.3)$$

where

$M_f$  = degree-day factor ( $\text{cm}^\circ\text{C day}^{-1}$ ), the same as the melt factor in (1.2),

$T_d$  = the number of degree-days in  $^\circ\text{C day}^{-1}$ .

Like Male and Gray (1981), Martinec found that due to varying conditions in the snowpack and the fact that the air temperature is not the only source of energy the degree-day factor varies over a wide range. This range is typically between 0.2 and 0.6  $\text{cm}^\circ\text{C}^{-1} \text{day}^{-1}$  for Central Europe (46 - 51°N) but may be lower further north where radiation inputs for a given air temperature will be less. Martinec and Rango (1986) describe the variability of the degree-day factor, giving examples of values ranging from 0.09 to 0.76  $\text{cm}^\circ\text{C}^{-1}\text{day}^{-1}$ , and point out that it varies both spatially and temporally within a catchment as well as from catchment to catchment. (Note: these are optimised values from the model runs and, whilst they indicate variation, as the results are from conceptual, parametric models they should not necessarily be taken as the physical truth.) Martinec (1960) described the relationship between snow density and degree-day factor, stating that as it is not possible to measure the degree-day ratio it can be calculated using the

relationship:

$$M_f = 1.1 \cdot p_s/p_w, \quad (1.4)$$

where

$p_s$  = density of the snow,

$p_w$  = density of water.

Once the melt has been calculated the model developed by Martinec then determines the runoff from the catchment. Due to the snowpack and surface soil retaining some of the melt water there is not a direct correlation between the daily snowmelt and runoff; instead the melt leaves the catchment over a period of days in the form of a gradually receding discharge series. This is based on a linear recession coefficient R:

$$R = RD_{n-1}/R_n, \quad (1.5)$$

where

RD= the daily runoff depth,

$n$  = day number of model run

and corresponds to routing the melt through a linear store.

Assuming that no losses take place Martinec thus calculates runoff on day n from:

$$RD_n = M_n(1-R) + RD_{n-1} \cdot R \quad (1.6)$$

In order to allow for losses a runoff coefficient c is introduced and, from (1.3) and (1.6) Martinec gets:

$$RD_n = c \cdot M_f \cdot T_{dn}(1-R) + RD_{n-1} \cdot R \quad (1.7)$$

Thus, only part of the daily melt appears in the hydrograph

and the remainder forms part of the recession flow.

Martinec (1975) further developed the model to allow for varying snow conditions within a catchment. The Dischma basin in the Swiss Alps was divided into three elevation zones and a curve for the decreasing snow cover in each zone was determined for 1970 and 1972. The degree-days for each zone were determined by lapsing the temperature to the midpoint of each zone using a lapse rate of  $0.65^{\circ}\text{C}$  per 100m and the daily melt was calculated for each zone in turn, being applied only to the area of snow in the zone.

Martinec (1980a) also found that the model was improved when using temperature measurements taken inside the catchment as errors from lapsing the temperature were minimised. The total from the three zones was then added to the rainfall (if any) to determine the daily runoff for the catchment. One point Martinec made about the model was that it could be improved by determining the runoff coefficient from the previous day's discharge rather than keeping it constant (i.e. to introduce non-linear routing of the melt rather than linear). This would result in less melt being stored in the catchment at times of high flow (more realistic as the snowpack and surface soil are likely to be saturated), and a continuation of low flow at times of low melt rates. Other authors have also followed the approach of dividing the catchment into a number of different elevation zones; Bergstrom (1978) describes the

Swedish HBV model that can deal with up to 10 different zones, each with uniform snowpack conditions, and Speers et al (1978) adopted the SSARR (Streamflow Synthesis and Reservoir Regulation) model for snowmelt runoff using up to 20 different zones.

Martinec (1980a) studied the runoff mechanisms in the snowpack by tracing environmental tritium and was then able to incorporate the variable runoff coefficient into the model, finding a narrowing of the degree-day factor range. It was also found that the changing total area of the snowpack in different parts of the basin was more important than the spatial variation of areas contributing to meltwater production, and that the daily melt immediately stimulates the outflow from subsurface storage. From this Martinec concluded that it is possible to simulate the complex snowmelt runoff process with a relatively simple model. However, he also stated whilst the pattern of disappearing snow cover was similar from year to year, there is no direct relationship between snow covered area and the stored volume of water. Instead, the areal extent of the snowcover tends to be related to the ratio of snowpack water equivalent and the maximum value for that year (Martinec, 1980b).

Following the work of Rango and Itten (1976), Rango and Martinec (1979, 1981 and 1982), Martinec (1983) and Rango (1988) incorporated remote sensing data into the models.

They replaced the snowpack depletion curves based on aerial photography and personal observation used in earlier models with curves based on satellite images, allowing the model to be applied to larger basins with no loss of model performance. The snowline was traced from each satellite (Landsat) image and imposed onto each of the elevation zones (four in this case as the Dinwoody Creek catchment is more than five times larger than the Dischma) to create a depletion curve for each zone. The daily snow covered area for each zone was then read off the curve and used for the melt calculation. To improve the model so that it could be used for operational forecasting they suggested that a faster processing of the satellite images was needed. Knowing the typical 'shape' of the depletion curve for a given zone would allow the immediate short-term reduction of snowpack area to be predicted which, combined with temperature and precipitation predictions, would allow streamflow forecasts rather than just simulation (Rango and Martinec, 1979). One further point of interest is that they also concluded that the siting of the meteorological site was more important to model performance than catchment size.

The use of depletion curves is taken further by Martinec (1980b) and Rango and Martinec (1982). Instead of the depletion curve showing decreasing snow covered area in each zone or catchment with time they put forward two alternative methods.

The first of these, shown in Figure 1.4, replaces the time scale with cumulative degree-days. This is designed to remove the 'steps' that may occur on the standard depletion curves due to fresh snowfall (in some cases the snow covered area may increase to 100% but Rango and Martinec do not allow for this). This is taken a stage further by the second alternative which uses cumulative snowmelt depth as the time scale. The argument for using this is that smaller 'steps' may be created by the fresh snow having to be 'ripened' before actual melt can take place. It is intended that in the final example the area under the curve is directly proportional to the volume of meltwater and that its shape is not affected by the frequency of snowfalls during the ablation season, thus ensuring that the curves are applicable to more than one year. In use, Martinec and Rango (1983) recommend that a family of curves are created for different initial snowpack water equivalents as this can affect the gradient of the curve (Figure 1.4). Instead of reading the predicted snow covered area for each day of the model run the area is calculated from the cumulative degree-days, thus ensuring that unusually warm or cold periods of weather are accounted for in the model.

The ability of the model to accurately simulate snowmelt runoff from a number of mountain catchments was also evaluated by Rango and Martinec (1981), applying the model to four catchments ranging in size from 2.65 to 484km<sup>2</sup>.

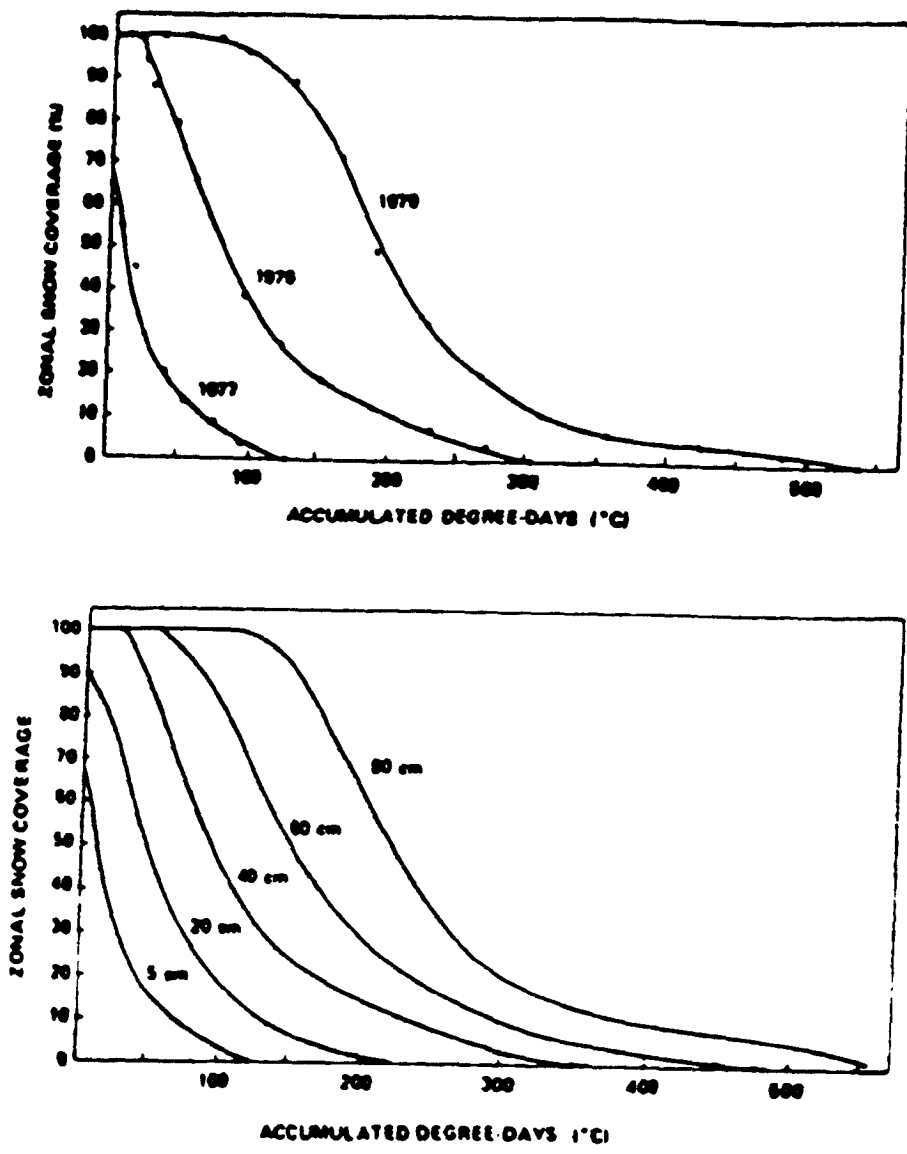


Figure 1.4 Cumulative depletion curves using accumulated degree-days. Upper plot shows observed depletion curves for 1976, 1977 and 1979; the lower plot shows the family of curves created for different initial snowpack water equivalents. After Martinec and Rango (1982, 1983).

Using Nash and Sutcliffe's  $R^2$  as an index of model performance (Nash and Sutcliffe, 1970) they found that the model performed well in all four catchments, the  $R^2$  values ranging from 0.82 to 0.95. Optimum results were obtained under the following conditions:

- (1) Temperature and precipitation recorded at catchment mean elevation.
- (2) Snow cover observations available at weekly intervals.
- (3) Several climatic stations are available for large catchments.
- (4) Previous runoff records exist for recession coefficient determination.

Whilst the performance of the model will decrease as one moves further away from these optimum conditions they found that acceptable results will be obtained provided that:

- (1) Meteorological data is available in the general vicinity of the basin.
- (2) Snow cover observations are available at least two or three times in the season.

Martinec and Rango (1986) again reported on the use of the Snowmelt Runoff Model in 24 different catchments (ranging in area from 0.77 to 4000km<sup>2</sup>) over 78 different snowmelt seasons by various institutions and workers. They produced a set of physically and hydrologically realistic parameter values which can be used as initial estimates under different conditions. From this review of model use and

applicability they found the mean seasonal difference between simulated and observed volume of runoff was 4.4% and the mean  $R^2$  was 0.84.

The work described so far by Martinec and Rango has mainly involved the model simulating the observed flow, i.e. both input and output have been known and optimised parameters used. Whilst using the model to simulate observed and known data is useful, especially in exposing the strengths and weaknesses of the model and allowing further development, if it is to be of real use in predicting snowmelt runoff it has to be tested to see if it can provide a true forecast of runoff, i.e. it must be able to predict the runoff without knowing the actual input or output data. Rango (1988) identified this need to move from simulation to forecasting and ran the model under a number of different circumstances:

- (1) Pure simulation, knowing both input and output data values and optimising parameters as the model ran.
- (2) Simulation with the output data 'unknown'.
- (3) Simulation with estimated/forecast snow cover input.
- (4) Simulation with forecast snow cover input and updating the predicted streamflow with observed values.
- (5) True forecasting on different time scales.

It was found that, operating within the WMO 'Simulated Real time Intercomparison of Hydrological Models' project, merely updating the predicted runoff with the observed

value at seven day intervals the average  $R^2$  was improved from 0.69 to 0.78 for the South Fork of the Rio Grande for 1977. A second set of models were run for the Rio Grande and Illecillewacet catchments for the 1977, 1983, and 1984 melt seasons (both complete and shorter timer intervals) the mean  $R^2$  increased from 0.74 to 0.81.

Rango was and is unable to report any detailed results from using the SRM to provide true forecasts, though reference was made to Jones et al (1984) who used the SRM to forecast snowmelt runoff on the Cache La Poudre River, Colorado, in 1983 for flood potential calculations. Predictions were made over periods of 1-3 days using forecast air temperature and precipitation data and snow cover elevation was obtained from aircraft flights over the catchment. The authors reported that the daily forecast runoff values were within 20% of the actual values, which in this instance was sufficient for their needs. Rango stresses that the performance of the SRM when used for real time forecasting is limited by the accuracy of the temperature predictions and the choice of snow cover depletion curve. Predicted precipitation was of less importance as the catchments generally experienced a 'dry' melt season; this is not so in all areas and must be borne in mind when using the SRM. Rango concluded that 'it may be necessary to provide measures of reliability of SRM forecasts based upon the kind of input data used'.

### 1.3.3.2 Other authors

Many other authors have used the temperature index method to model snowmelt; the WMO (1986) describe the results from an international project undertaken between 1976 and 1983 which involved 11 different operational models from 8 countries. The overall aim of the project was not to find the model that provided the best fit in all cases but to allow users to examine the performance of the models under different conditions. For each data set the models were calibrated using six years' data to determine parameter values for each different catchment and then tested on a further four years' data, the computed output being compared and evaluated by the WMO Secretariat using a number of graphical and numerical methods. As the results are discussed in detail by the WMO (1986) and summarised by Nemec (1986) they are not included here. From them arose a number of points and recommendations:

- (1) All of the models used the temperature index approach as it usually provides a reasonable simulation and detailed energy balance data are often not available.
- (2) The variety in model construction and performance was related to the computing facilities available and the purpose for which the model was developed.
- (3) Most models included a separate sub-routine to reduce runoff during the period the snowpack was ripening, i.e. becoming isothermal and saturated.
- (4) Most models performed better (if they allowed for it)

when meteorological data was available from more than one site for each catchment as it allows cross-checking and gives an idea of the areal variation.

- (5) Sub-dividing the catchment into a number of elevation bands is recommended due to the strong relationships between altitude, temperature and precipitation.
- (6) Some of the models use correction factors to allow for systematic errors in obtaining precipitation data and transforming point to areal data.
- (7) It was important that a number of different criteria be used for evaluating and comparing the performance of the different models. It was suggested that the three graphical and nine numerical methods used for the project be adopted as a basic set for future, large scale, international projects.
- (8) Finally, it was recommended that a further project be initiated looking at the performance of models operating in real time to provide true forecasts. This was to involve both rainfall-runoff and snowmelt-runoff models, and was to allow updating of predicted with observed values where possible.

#### 1.3.3.3 British work

Archer (1981, 1986) reviews post 1960 research on snowmelt flooding and demonstrates how snowmelt has contributed to some of the largest floods experienced in the last two centuries with reference to examples in North East England.

Using the temperature index approach he shows that given a small catchment area (to reduce lag and storage effects) and a temperature of 8°C theoretical snowmelt runoff rates could be in the order of 5mm hr<sup>-1</sup>. On studying the discharge records of some small catchments for the winters of 1978 and 1979 Archer finds peak snowmelt runoff rates of over 4mm hr<sup>-1</sup> to support this. These values differ from the Flood Studies Report published by the N.E.R.C. (1975) which gives an estimate of 42mm day<sup>-1</sup> (1.75mm hr<sup>-1</sup>) as the maximum likely runoff rate from a rare snowmelt event, though it must be stated that this report was based on limited data from lowland catchments and it is not clear to what extent these data can be extrapolated to higher locations. This value of 42mm day<sup>-1</sup> was used in the Institution of Civil Engineers Guide to Floods and Reservoir Safety (1978) to assess the probable maximum winter flood and is used to calculate the capacity of reservoir spillways under the 1975 Reservoirs Safety Act .

Archer (1983) also developed a snowmelt runoff model based on the temperature index method and applied it to three upland tributary catchments of the Tees. Each catchment was divided into ten elevation zones and the melt for each zone was calculated, assuming uniform melt and snow conditions within each zone. Once the melt had been determined it was routed through the catchment using either a lumped (unit hydrograph) or distributed routing routine. The model optimised three snowmelt parameters;

DHF = Melt factor ( $\text{mm}^\circ\text{C hr}^{-1}$ ),  
ALPHA = Liquid water retention coefficient (%),  
LOSS = Input to output losses coefficient (%).

The model was calibrated for five rainfall events (of 1-2 days duration) and then used to simulate five snowmelt events in 1978 and 1979. Archer found that the routing method used had little significance on model performance, (although it must be noted that he was only working on small catchments) the mean Nash and Sutcliffe  $R^2$  for the distributed method being 0.62 (2 s.f.) compared to 0.64 for the unit hydrograph method over 14 different model runs (one set of data was missing for one of the catchments), and the model often optimised LOSS as 0% (75% of events). Maximum hourly point melt was greater than the critical value of 1.75mm stated by the Flood Studies Report mentioned earlier for 64% of the events, the mean value being 2.65mm  $\text{hr}^{-1}$  and the maximum being 6.1mm  $\text{hr}^{-1}$  (this maximum value increases to 11.77mm  $\text{hr}^{-1}$  when water held in the snow was taken into account to determine an hourly yield value), indicating that a review of the methods used to estimate winter probable maximum floods was needed. The model parameters optimised by Archer showed great variation (for example, the melt factor ranged from 0.181 to 3.500mm  $^\circ\text{C hr}^{-1}$ ). Whilst this variation was often only between events, the catchments showing similar values for a particular event, Archer acknowledged that, although the model had potential for future use, considerable errors

were likely if it was used for real time flood forecasting in its present form with constant values for the optimised parameters.

Ferguson (1984, 1986) and Ferguson and Morris (1987) describe a snowmelt runoff developed and tested in the Cairngorms. The model was based on that developed by Martinec (1976) but instead of using the mean daily temperature like most authors, Ferguson determined the degree-day index from the minimum and maximum temperature on the day and the previous day's minimum value (Figure 1.5), assuming equal periods of rise and fall in temperature of 12 hours. This index was used as it gave a non negative degree-day estimate when some or all of the temperatures were below zero.

Another difference was that instead of using snow cover depletion curves the model had a **depletion submodel** that reduced the snowpack at a rate proportional to the daily melt, a simple mass-balance accounting function being used to do this. Temperature was lapsed from the valley meteorological station to the snowline calculated from the previous day's melt, the catchment's hypsometric curve being represented by a series of linear approximations for this purpose. The 1984 model had a choice of methods used to apply the melt, either uniformly over the snowpack, at a variable rate or just at the lower edge depending on the snowpack distribution (Figure 1.6). Precipitation both

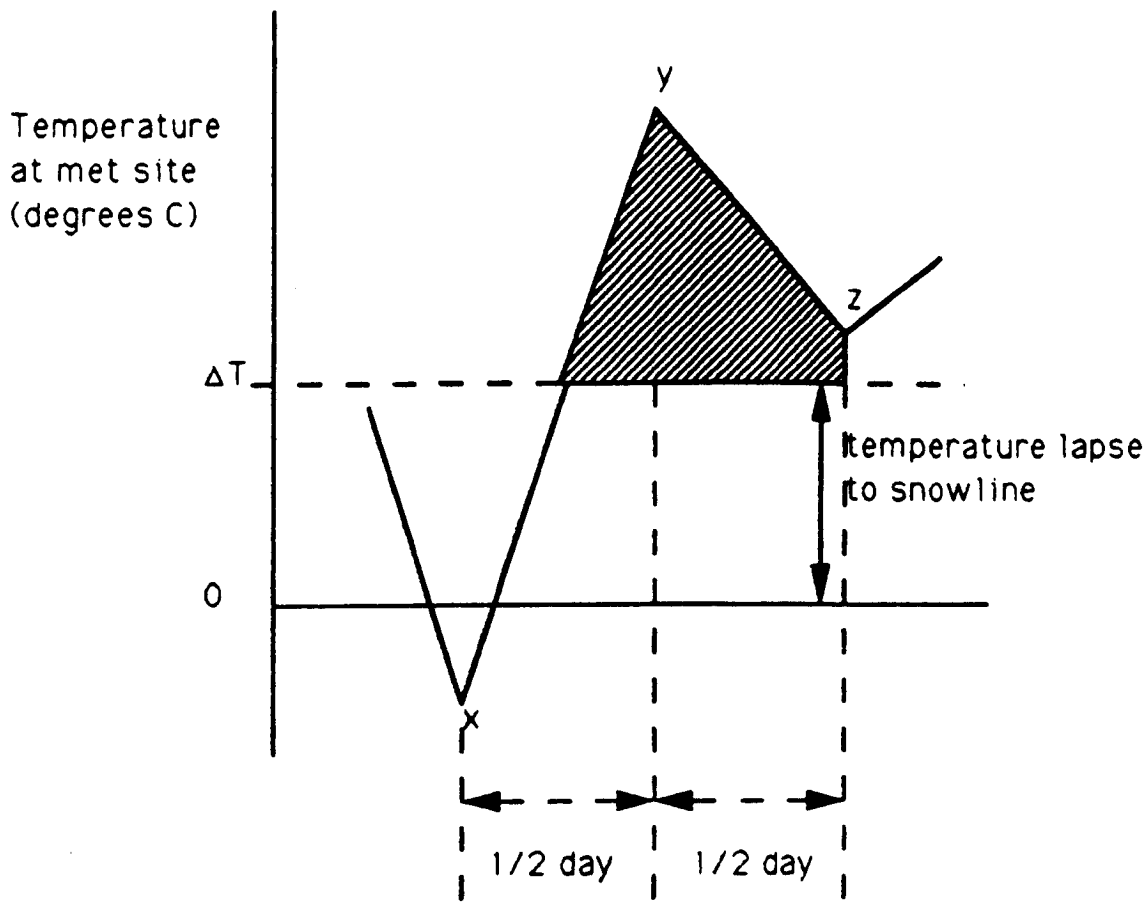


**Figure 1.5**

Diagrammatic representation of the method used to determine degree-days by Ferguson (1984). The shaded area represents the number of degree-days at the snowline.

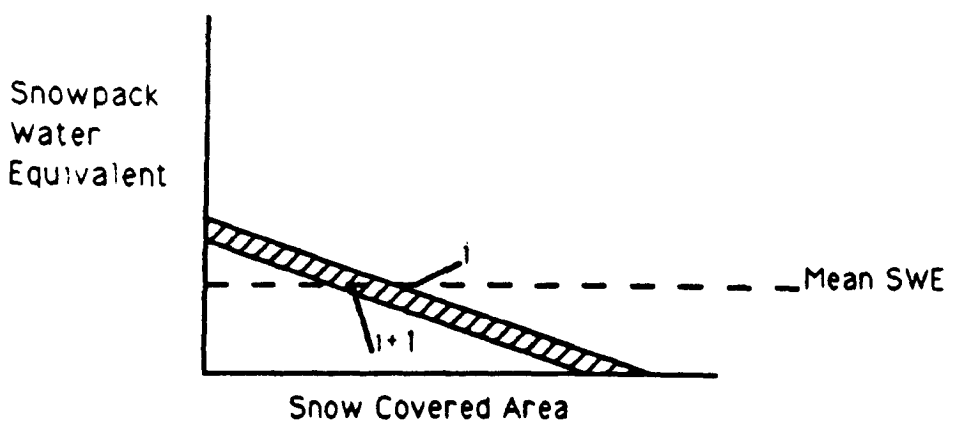
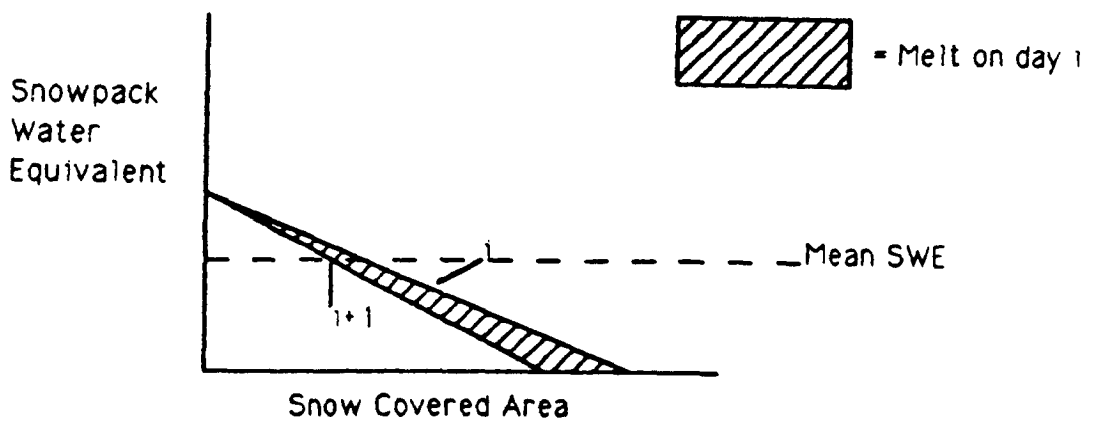
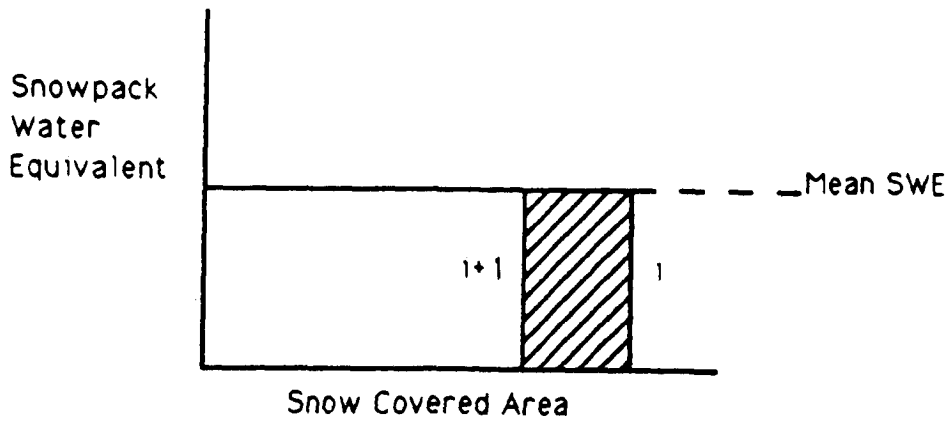


**Figure 1.6** Different methods of representing the initial snowpack and applying melt. After Ferguson (1984).

above and below the snowline was added to the calculated melt and the total was routed using Martinec's (1976) exponential unit hydrograph shown in equation (1.6).

The recession coefficient  $k$  does not affect the total volume of melt produced but controls the time it takes to pass out of the catchment; a high value of  $k$  means the melt takes a long period to leave the catchment and produces a hydrograph with gentle rising and recession limbs whereas a low value of  $k$  gives a 'flashy' hydrograph, there being minimal flow during periods of no or little melt but high flows during significant melt events. Generally, given uniform conditions, one would expect an inverse relationship between catchment area and  $k$ .

The model was used to simulate snowmelt runoff for the 1979 and 1980 melt seasons (both taken as 53 day events) in the 106km<sup>2</sup> Feshie catchment. The model produced a much better fit than multiple regressions on the same data (mean  $R^2$  increased from 0.625 to 0.775, using optimised parameters), and Ferguson concluded that the conceptual basis was sound and the degree of simplification inherent in the model was appropriate given the data available. The three hydrometeorological parameters optimised by the model (melt coefficient, recession coefficient and lapse rate) produced stable values for the two years (i.e., the ranges of each parameter that affected the r.m.s. by no more than 5% overlap were similar for the two years) and the snowpack

parameters optimised to reasonable values, though the model was more sensitive to these. Ferguson argued that the instability of the melt coefficient used by Johnson and Archer (1972) was caused by their model not reducing the area of the snowpack as the melt progressed, and was optimistic about the use of the snowpack depletion submodel, especially where this can be combined with observations in the field or by satellite imagery. The optimised snowpack water equivalents of 450 and 350mm are considerably higher than those predicted as five year maxima by Jackson (1977); Ferguson agrees with Archer (1981) who states that Jackson assumes a very low snow density. One possible weakness of the model is identified, namely its poor performance simulating rain-on-snow events, a pity since these events often produce the highest runoff values.

The 1986 model included an exponent  $c$  that controlled the shape of the snowpack distribution, with  $c = 0$  indicating a uniform snowpack,  $c = 1$  a uniform statistical distribution of the water equivalent (i.e. 0-100mm water equivalent covers the same area as 3-400mm), and  $c > 1$  indicating a non uniform snowpack with high water equivalents covering a low proportion of the snowpack area (Figure 1.7 ). For all cases where  $c > 0$  the snowpack has a point of maximum and minimum water equivalent; this is more realistic in upland environments where drifting and redistribution of the snow is likely. This was also used

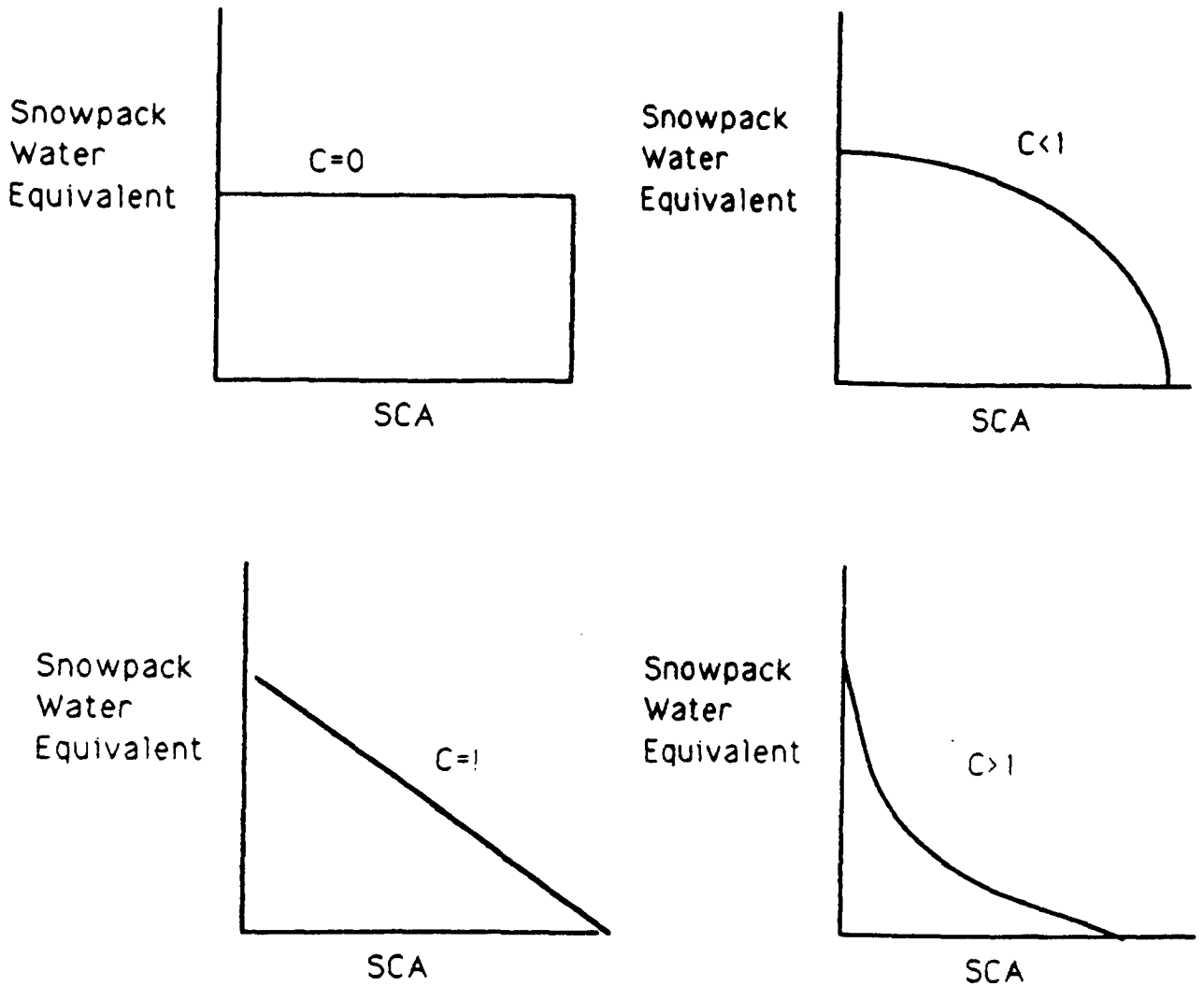


**Figure 1.7**

The effects of Ferguson's 1986 exponent  $c$  on controlling the shape of the snowpack distribution.

to control the distribution of the melt over the snowpack in a similar way, though little benefit was observed to model performance. Ferguson states that the sensitivity of the model to the snowpack parameters can be overcome by adapting the snowpack water equivalent estimate as the model proceeds in a similar way to which Rango and Martinec (1982) change the snowpack depletion curve as their model progresses. For example, should the model be constantly over-predicting runoff the mean snow water equivalent should be reduced, the degree of reduction being proportional to the cumulative error (it should not be necessary to alter the area of the snowpack as this can be accurately estimated by personal observation).

Efforts were also made to evaluate the success of using parameters optimised for the first few days of the model run on observed data for the remainder of the melt event. Results were successful for the 1979 season, near optimal values being found after a period of only a week, though the confidence intervals for estimates were wide. However, for the less snowy season of 1980 the method was less successful, using the first weeks' data gave a mean snowpack water equivalent of 550mm, two weeks gave 220mm and the optimum was 350mm. Thus, whilst early results were promising, especially the use of the depletion submodel, Ferguson concluded that further development and testing were needed before the model could be used for real time forecasting, possible improvements including the

incorporation of a layered catchment structure for larger catchments, different routing methods and updating of mean snowpack water equivalent as the model ran.

Deas (1986) applied the model developed by Ferguson to a number of catchments for a number of events (Feshie 1982/3, Dee 1983/4, Gairn 1979-84). Generally the model performance was not as good as that found by Ferguson (1984), the  $R^2$  ranging from 0.81 to 0.28, median value 0.62, though the optimisation methods used were cruder than those used by Ferguson. The model performance is discussed by Ferguson and Morris (1987) who note that the model performs worst in years of low snowfall, possibly indicating that the transformation/routing submodel is at fault. They also conclude that with suitable model improvements adaptive estimation should be possible, allowing the model to be used for predictive purposes.

#### 1.4 Aims of the project

As the title of this thesis suggests, the main aim of the project was to develop and test snowmelt runoff models for use in Scottish Highland catchments. Ferguson and Morris (1987) state that different models can only be compared and assessed by applying them to a particular region. The region selected for this project was the Cairngorms area of the Highlands, used by many authors for snowmelt research.

This region is suitable because, in addition to being one of the snowiest parts of the United Kingdom, it has had meteorological and hydrological data collected at many sites. The locations of the various meteorological stations and some of the gauging sites are shown in Figure 1.8. A description of these sources of data is given by Ferguson and Morris (1987). Because of this wide range of data it was hoped to develop models with different data requirements and then test these models on other datasets. Having decided on the area from which the hydrometeorological data was to be collated it was then possible to decide on a number of aims for the project. These were as follows:

- (1) To carry out detailed snow surveys in a small experimental catchment where detailed hydrometeorological data were also collected. In addition to allowing the initial snowpack characteristics to be determined this would also enable various modelling approaches to be tested.
- (2) To develop, apply and test various temperature index models using the data collected in this catchment. By using a small catchment it was hoped that any changes would be more easily detected as they are generally more responsive.

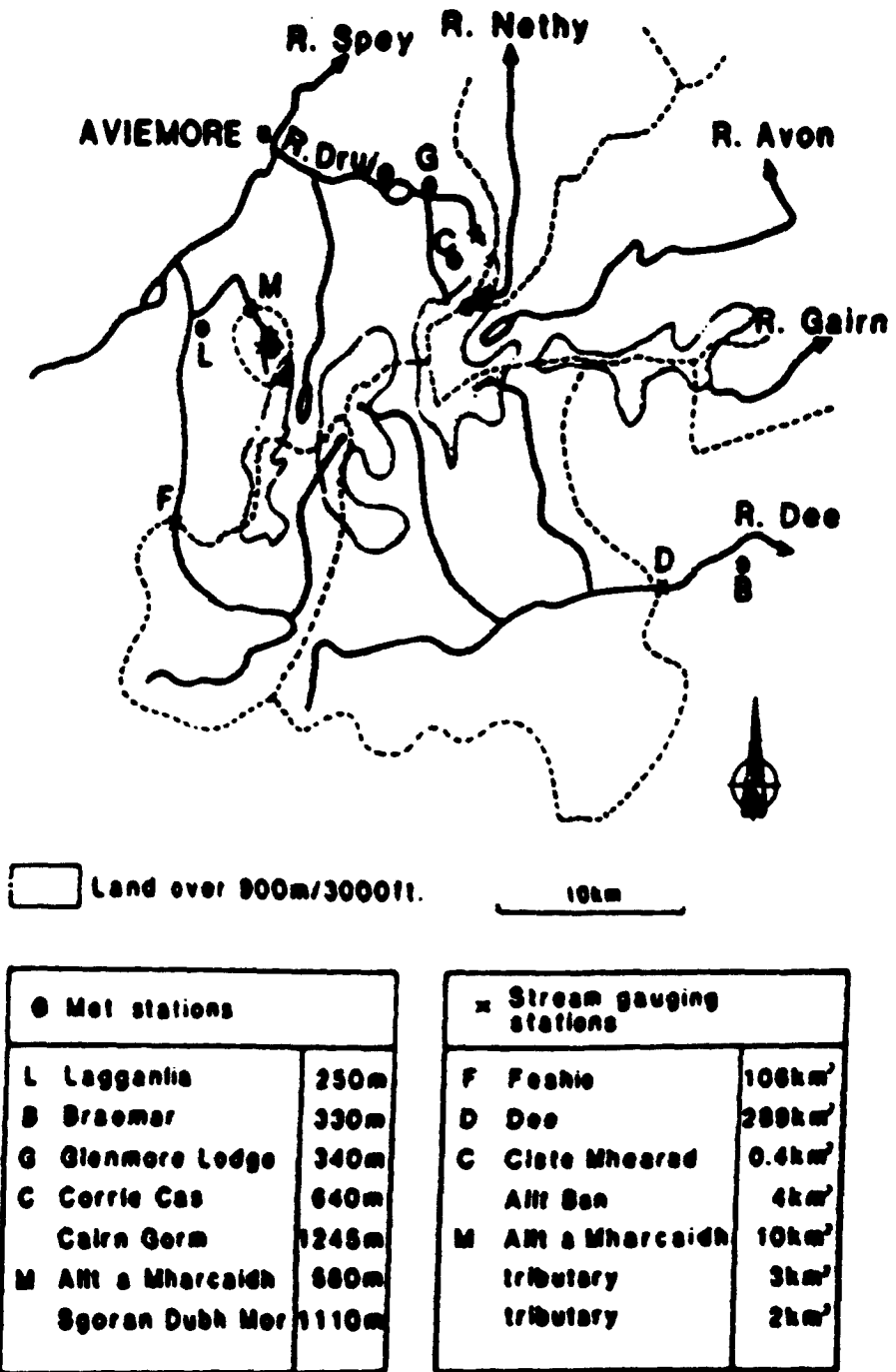


**Figure 1.8** Main gauged catchments and meteorological stations in the Cairngorms. From Ferguson and Morris (1987).

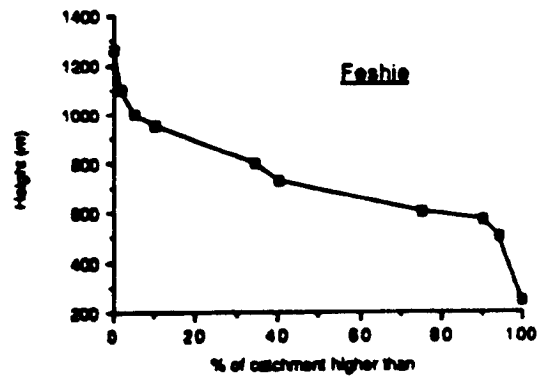
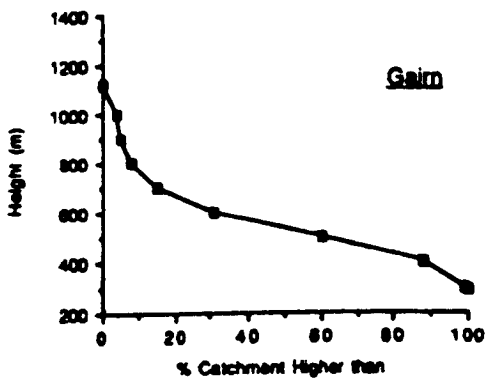
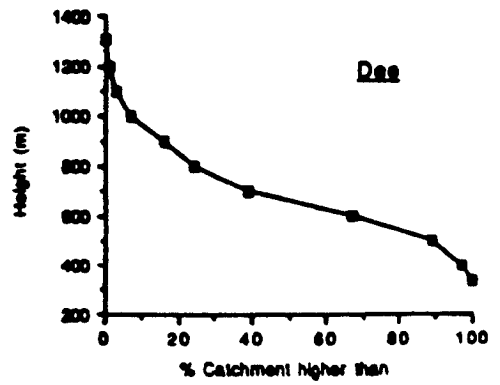
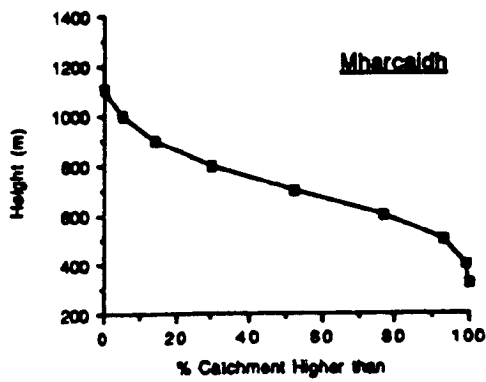


**Figure 1.9**

Hypsometric curves for the Allt a Mharcaidh, Feshie, Gairn and Dee catchments.

- (3) To try other modelling approaches on this data where possible and compare the results to those of the temperature index models.
- (4) To apply the models developed in (2) and (3) to other, larger catchments for the same and additional melt seasons. The models used for this would depend on the results from (2) and (3).
- (5) To decide on universally applicable models and to evaluate these models' potential for use in real time as a means of predicting snowmelt runoff. This was the most important of the five aims and it depended in turn on the results from aims (1) - (4).

Aims (4) and (5) both involved the application of models to large catchments where the effects of snowmelt floods are most noticeable. Three catchments were chosen for this, the Feshie (106km<sup>2</sup>), Gairn (150km<sup>2</sup>) and Dee (106km<sup>2</sup>). Figure 1.9 shows the hypsometric curves of these three catchments along with that of the Allt a Mharcaidh (9.91km<sup>2</sup>), the small experimental catchment used for the snow surveys and early model development. From Figure 1.9 it can be seen that all four catchments have similar hypsometric curves, the main exception being the Gairn which has less high ground.

By developing and testing the different models on these catchments which vary so much in areal extent but have

similar hypsometric curves it was intended to develop a snowmelt runoff model that could be universally applied to Highland catchments.

## CHAPTER 2 FIELD TECHNIQUES

### 2.1 Introduction

As mentioned earlier in 1.4 the Cairngorms is the only area in Britain where it is possible to test various snowmelt models. This is not only because it is the snowiest part of the United Kingdom but also because of the amount of meteorological and hydrological data available.

Meteorological data from the Heriot Watt summit station on Cairngorm and Lagganlia Outward Bound School are used for this study, together with North-East River Purification Board flow data for the Dee and Gairn and University of Stirling flow data for the Feshie. They are shown in Appendix A. These data will be used to test the models; in order to develop them it was necessary to collect data from an experimental catchment where snowpack data could also be collected. The catchment chosen for this was the Allt a Mharcaidh.

### 2.2 The Allt a Mharcaidh

The Allt a Mharcaidh catchment, shown in Plate 2.1, is situated on the northwest edge of the Cairngorm massif above Lagganlia and is part of the Cairngorm National

Nature Reserve (Figure 1.1). It was chosen for study by the Surface Water Acidification Programme (SWAP) that was



at Sgoran Dubh Mor (500m) and the gauging site at  
(NS91045). The Allt a Mharcaidh is a self-contained  
catchment as a self-contained drainage valley and divide it  
into three distinct zones:  
(1) the valley floor  
(2) the valley sides  
(3) the upland plateau.

**Plate 2.1** The Allt a Mharcaidh catchment viewed from the A9 two miles south of Aviemore.

Nature Reserve (Figure 1.8). It was chosen for study by the Surface Water Acidification Programme (SWAP) that was set up in 1985 as a long-term collaborative research project into the cause and effect of acidification in the surface waters of Britain and Scandinavia (Mason and Seip, 1985). The Mharcaidh was chosen as a transitional site, that is, it is not considered to be acidified or receive a particularly high amount of anthropogenic pollutants but may be at risk with regard to future acidification problems due to the slowly weathering biotite-granite bedrock and relatively thin soil/regolith cover (Jenkins, 1989).

The catchment is approximately 9.9km<sup>2</sup> in area and has a vertical relief of almost 800m between the high point of 1111m at Sgoran Dubh Mor (NH905002) and the gauging site at 320m (NH881045). Nolan and Lilly (1985) describe the catchment as a self-contained hanging valley and divide it into three broad zones:

- (1) the valley floor;
- (2) the valley sides;
- (3) the upland plateau.

The valley floor extends from 320m to c.650m and contains the Allt a Mharcaidh, Allt nan Cuileach and other tributary streams. This zone is covered in moraine and deep peat deposits, causing an undulating, hummocky relief and the streams to be deeply incised over much of their length. The lower part of this zone is covered with native Scots

pine, a remnant of the Caledonian Forest, and the higher ground area is covered with lichen-rich heather moor and blanket bog.

The valley sides zone varies in relief within the catchment but generally extends from 650m to 800m, the eastern slopes being steeper than those in the west. The zone is covered by thin alpine podsoles which have formed on the cryic deposits. The zone has a variety of vegetation cover including heather and bog heather moor, alpine azalea-lichen heath and fescue-woolly fringe-moss heath.

The upland plateau zone lies above 800m and whilst the slopes are generally more gentle than in the valley sides zone they are locally steep, notably to the north and west of Sgoran Dubh Mor. The zone is very bouldery and has many terracettes and stone stripes, with bedrock being exposed at a few sites. The soils are generally very thin alpine podsoles and gleyed podsoles with shallow peat deposits also being found in some areas. The vegetation cover is very similar to that in the valley sides zone but also consists of three-leafed rush heath.

### 2.3 Instrumentation and secondary data collection in the Mharcaidh

Since the Mharcaidh was being studied as part of the SWAP project it was well instrumented by the different research

groups working there. Although assistance was given and received from all three groups the instrumentation set up by the Institute of Hydrology was the only source of data used for the purposes of the snowmelt studies and is thus the only instrumentation described. Figure 2.1 shows the location of the instrumentation used in this study.

The Institute set up three stream gauging sites in the catchment. Gauge Site One (GS1) was situated at 320m and gauged the whole study catchment area of c. 9.9km<sup>2</sup> (Plate 2.2). Data loggers recorded the variation in depth detected by two pressure transducers located at stable cross-sections in the river channel. The pressure recordings were then converted to discharge data by means of a rating equation derived by the Institute. Gauge Sites Two and Three (GS2 and GS3) gauged the two upper tributaries of the Mharcaidh, GS2 being sited at c. 570m gauging the south-east basin (c. 1.8km<sup>2</sup>) and GS3 being sited at c.560m and gauging the south-west basin (c. 3.2km<sup>2</sup>). Assistance was given in calibrating GS2 and GS3 by the salt-dilution gauging method described by Elder et al (1990) at times of high flow, and the flow data from all three sites was transferred from the Institute's data-base to the mainframe computer at Stirling.

The Institute also set up two weather stations for recording meteorological data in the catchment. The first of these was a standard Automatic Weather Station (AWS) of

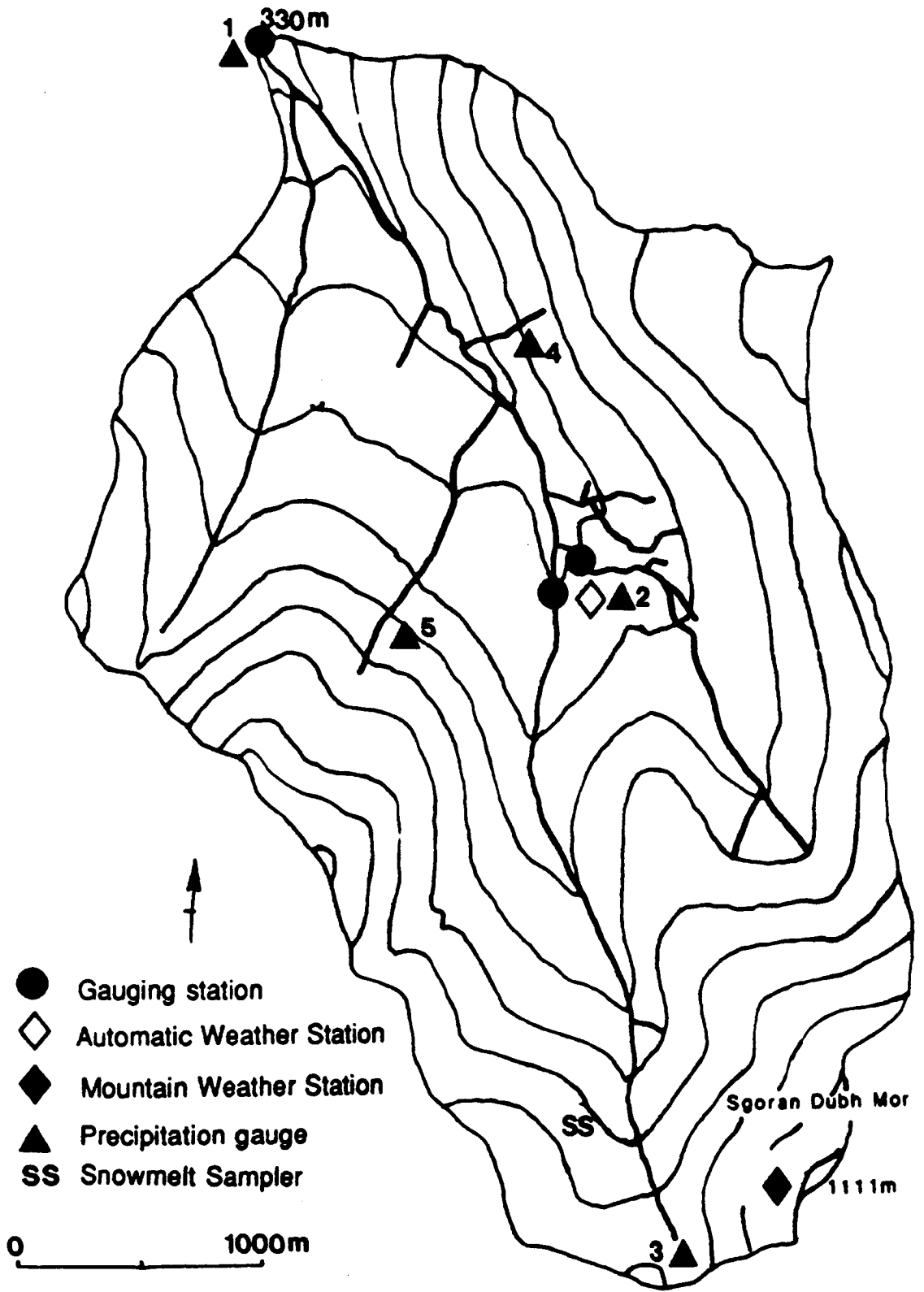


**Figure 2.1** Instrumentation in the Allt a Mharcaidh experimental catchment. Contour intervals are 62.5m.

a type described by Strangeways (1972). This recorded dry and wet bulb temperature, incoming and reflected radiation,

humid  
plat  
stat  
by  
This  
con  
high  
sun  
keep  
pow  
tem  
Whit



from heavy riming on occasion, manual observations were taken by the Institute of Hydrology field workers whenever passing it and showed that the data recorded was reasonably accurate (Jenkins, pers comm). The Institute also had a number of precipitation gauges sited in the catchment (R1-R5), R1 being adjacent to G1, R2 next to the AWS, R3 on the col at the southern extreme of the catchment and R4 and R5 sited on the east and west slopes respectively. When snow-free these recorded rainfall but during the winter months

**Plate 2.2** Gauge Site 1 at 320m in the Allt a Mharcaidh catchment.

to record snowfall. The meteorological data were also recorded by data loggers and transferred to the mainframe computer at Wallingford. This was transferred to the

a type described by Strangeways (1972). This recorded dry and wet bulb temperature, incoming and reflected radiation, humidity, windspeed and direction and was located on a plateau between GS2 and GS3 at c. 575m. The second weather station was a Mountain Weather Station of a type described by Strangeways (1985) and Strangeways and Wyatt (1990). This has been specifically developed for use in cold-region conditions (i.e. very cold temperatures, snow, ice/rime and high wind speeds) and was located a short distance from the summit of Sgoran Dubh Mor. The MWS (Plate 2.3) attempts to keep the sensors free of rime by using compressed air to power a central shock-induction unit, and records temperature, radiation and humidity data.

Whilst Plate 2.3 may show that the MWS did appear to suffer from heavy riming on occasion, manual observations were taken by the Institute of Hydrology field workers whenever passing it and showed that the data recorded was reasonably accurate (Jenkins, pers comm). The Institute also had a number of precipitation gauges sited in the catchment (R1-R5), R1 being adjacent to G1, R2 next to the AWS, R3 on the col at the southern extreme of the catchment and R4 and R5 sited on the east and west slopes respectively. When snow-free these recorded rainfall but during the winter months they were replaced by an artificial grass mat in an attempt to record snowfall. The meteorological data were also recorded by data loggers and transferred to the mainframe computer at Wallingford. This was transferred to the



**Plate 2.3** The Mountain Weather Station located at 1000m, on the south-west slopes of Sgoran Dubh Mor. Rime can be seen on the main body of the MWS but the sensors are relatively ice-free.

computer at Stirling via the JANET electronic mail network.

The final site used by both this study and the Institute in the catchment was what the Institute called the Snow Survey site (SS). Two snowmelt samplers were sited here and, whilst the output from these was not used as it was being used for hydro-chemical studies, the site was used in this study for a number of different reasons.

#### 2.4 Snowpack data collection

Snowmelt models generally need to have details of the snowpack characteristics in order to be able to predict the resultant melt and runoff. If one is merely concerned with the amount of melt taking place at a specific point then only the depth and density are needed (and some temperature index models do not even need these), from which the water equivalent can be calculated and the melt applied to. However, in order to predict runoff from a non-glacierised catchment where the snowpack is a temporary feature, details of the spatial variation of the snowpack are needed, together with the areal extent of the snowcover so that a water equivalent for the whole catchment can be determined and the resultant runoff calculated.

Gillies (1964) says that in addition to snowpack information being useful in assisting with runoff prediction it is also needed to:

- (1) Complete the precipitation record for an area, especially where a high proportion of that area is at high elevations, to allow the water balance to be calculated.
- (2) To allow effective management of the water equivalent held in the snowpack for consumptive use later in the year, be it to top up reservoir levels or to be used for irrigation, hydro-electric power generation etc.
- (3) Standardise experimental catchments so that a full understanding of the hydrological processes taking place can be made, thus allowing effective treatment affecting the precipitation-runoff relationship.

Gillies describes five different methods of quantifying the snowpack characteristics, though Goodison et al (1981) give a more up to date and detailed description. The method(s) used will depend on whether the data is needed for a point source or the whole catchment and can be subdivided into those used to determine snow depth and water equivalent and those dealing with areal extent and variation.

#### 2.4.1 Snow depth and water equivalent

##### (1) Snow ruler and snow board

A board measuring at least 40cm by 40cm is placed on the ground surface and the depth of new snow is recorded with a ruler. The board is then cleared so that the next

snowfall can be read as a direct depth, rather than overlying the old snow which will have compacted.

The method of converting this fresh snow to a water equivalent varies in different countries. The Canadian Atmospheric Environment Service assumes the density of new snow to be  $100\text{kg m}^{-3}$  and thus multiplies the recorded depth by 0.1 to determine the water equivalent at more than 85% of the recording stations; the traditional British method is that 1' of snow = 1" of rain (Jackson 1977). Other countries weigh a known volume of snow and convert the fresh snow depth to a water equivalent as the density of new snow can vary both spatially and temporally.

## (2) Snow gauges

These come in a variety of forms, the three main types being non-recording, weighing and standard precipitation gauges. Many of these are heated to prevent the build-up of ice and snow bridging the orifices and to stop the mechanism from freezing, and the non-recording type often have an anti-freeze mix of ethylene-glycol and oil to prevent evaporation losses (Bailey and Waters, 1986). These gauges are in use worldwide and suffer the same problems as standard precipitation gauges.

The siting of the gauges is important when it is intended to apply the collected data over large areas. Whilst it

may be obvious that the error in extrapolating such data will decrease as the number of gauges used increases, it is surprising that the national average station density for Canada is only 8 gauges per 25,000 km<sup>2</sup> (Goodison et al, 1981).

### (3) Graduated snow stakes

In remote areas graduated snow stakes are often used to allow the snow depth to be observed from afar and have been used by many authors (For example, Bernier, 1986, Gillies, 1964, Kopanev, 1972,). Gillies (1964) states that observations taken from a helicopter of both snow depth and extent may be the optimum but are not financially realistic. More affordable are observations taken from light aircraft but due to the velocity at which these travel the stakes have to be considerable distances apart to avoid the observer suffering from nausea! Also, ground observations indicate that snow tends to build up around the stakes early in the accumulation season and cratering occurs late in the ablation season.

Some workers read the depth at the stakes using binoculars or telescopes from lower down in the catchment (this is done in the Institute of Hydrology experimental catchments at Balquhiddy). As visibility is often very low in the Cairngorms due to low cloud, blizzards or rainfall this method could not be guaranteed, and as snow water

equivalent data was needed for the models and not just snow depth it was decided not to use this method. However, each site visited on the snow surveys (see later) was marked by a survey stake with alternate 50cm red and white bands. It was hoped that when it was not possible to visit all sites due to very deep fresh snow or lack of daylight depths of snow could be observed at some of the more remote sites and converted to a water equivalent using correlation techniques.

#### (4) Snow pillows

Snow pillows are basically large bags containing an antifreeze fluid. The fluid pressure responds to a changing mass of snow on the pillow and is measured with a pressure transducer. By recording the changes in pressure and converting this to a changing water equivalent of the snowpack it is possible to maintain a non-destructive record of the changing snowpack. Beaumont (1965) advises that a 3.66m diameter snow pillow is generally large enough for most snow depths and that a smaller pillow used in deep snow will often over estimate the water equivalent. Bernier (1986) showed that measurements taken over 11 years indicate that snow pillows are less accurate and reliable than personal observation. Because of this and due to the cost, complexity and site requirements for snow pillow use it was decided not to use them in this study.

#### (5) Gamma radiation absorption counters

By burying a geiger counter in the ground prior to winter and then siting a gamma ray emission source above it and the snowpack it is possible to record the changing water content of the snow as a function of the energy absorption by the water layer between the source and counter. Whilst this method may be accurate and reliable at the point it is measured it is difficult to apply to a wider area and is expensive to replicate.

#### 2.4.2 Areal snowpack data

##### (6) Snow surveys

Snow surveys consist of a series of measurements made by an observer at representative sites throughout a study area to establish the snowpack characteristics. These measurements consist primarily of depth and vertically integrated density samples, from which it is possible to calculate the water equivalent of the snow. As this was the primary method of collecting snowpack data in the Mharcaidh it is covered in more detail in the next section.

##### (7) Photographic record of snow cover

This is often regarded as the least accurate and satisfactory method of estimating the water equivalent of

the snowpack (Gillies, 1964) but is often useful as a means of recording snowpack areal extent and, when used along with other methods, can provide an index of changing SWE. By siting cameras such that they have a clear view of the study area and using time lapse photography it is possible to obtain a complete pictorial record of the changing areal extent of the snowpack, both during the accumulation and ablation seasons. Totts (1937) states that if a correlation can be established between areal extent and water content for the study area then the changing water equivalent can be easily monitored. However, each study area is likely to be different and, even if there is a relationship between water equivalent and snow pack area, this will take many years' data to establish. This method alone is thus not suitable for monitoring the changing snowpack characteristics in the Mharcaidh.

The Institute of Hydrology sited a Super 8 cine camera in the catchment at c.500m. This was to assist them in their studies and took a photograph of the catchment above this point every 20 minutes. Unfortunately, it was not possible to evaluate the film as part of this study.

#### (8) Remote sensing of the snowpack

The recent advances in remote sensing technology have resulted in some workers using it to monitor changing snow pack area (for example, Rango and Martinec, 1979,

Lichtenegger et al, 1981, Bagchi, 1983, Rasmussen and Ffolliott, 1979, Shafer et al, 1979). The World Meteorological Organisation (1976) recommended that for operational purposes Landsat data, NOAA-VHRR imagery and NOAA-SR data be applied to basins with areas exceeding 10, 100 and 1000km<sup>2</sup> respectively. Rango and Martinec (1979) modified the model created by Martinec (1975) to incorporate Landsat data and successfully applied it to the 228km<sup>2</sup> Dinwoody Creek in Wyoming, USA. They did note, however, that "certain locations such as the Swiss Alps and northwestern United States have a high frequency of cloudiness which severely hampers the effectiveness of Landsat"; the frequency of cloud cover over the Cairngorms means that this will also be the case in trying to apply the Landsat data to Scotland.

The time period between different passes of the Landsat satellite is also a problem. The current time between two passes over the same area is 18 days. If one of the images is obscured by cloud then the time interval would be 36 days. In the case of many catchments in Scotland this may mean that there are no images of the snowpack whatsoever for a particular season if there was only light or moderate snowfall and a mild spell early in spring.

Meier (1975) reported on the use of passive microwave emission as a means of detecting changing snow depth and wetness but Goodison et al (1981) concluded that this is

still at the research stage and is not reliable enough to use at present. Side-looking airborne radar (SLAR) has been used with success over the Great Lakes and provided resolution down to tens of meters but it was felt that it was beyond the scope of this study to get involved with this.

A further problem in using remote sensing data for snow pack depletion monitoring is the size of the catchment and the resolution to which the images can be studied. The Mharcaidh is less than 10km<sup>2</sup> and the majority of the Scottish catchments to which the models are likely to be applied are in the order of tens or hundreds of km<sup>2</sup>. Whilst Wiesnet (1974) claims an accuracy within 5% for areas greater than 5000km<sup>2</sup> it is unlikely that such accuracy could be determined for Scottish catchments.

## 2.5 Snow surveys in the Mharcaidh

### 2.5.1 Site selection

The conventional method of collecting snowpack data is the use of a snow course. This consists of a series of marked sampling points (survey sites) within the study area where observations are made on the snowpack characteristics. The problems of setting out the locations of the survey sites on a snow course are similar to those in establishing a net of rain gauges within a catchment, with the added

complications imposed by the winter weather and the difficulties of travelling over a snowpack.

Some workers (for example Bernier, 1986, and Dickison and Daugharty, 1978) have sampled over a grid network but usually for short intensive periods, often only once or twice a year, and always in small study basins. Chinn (1969) states that "samples should ideally be taken on a grid pattern over the whole basin but in practise this is quite unfeasible". As a result he recommends that researchers use a single snow course with observations taken along a single elevation transect in the basin, though he acknowledges that more measurements are likely to give a truer representation.

Fitzharris (1978) identifies the presence of a 'snow wedge' distribution in the seasonal snow covers of New Zealand and North America, the snow pack generally increasing in depth and water equivalent with elevation. He states that the changing shape of the snow wedge, both inter- and intraseasonally, renders "unsuitable the traditional snow course where measurements are taken at a single elevation. More reliable indices of snow accumulation will be obtained with a series of snow courses at different elevations on a sample mountain, and with observation of the snow line". Because of this and the extremely variable nature of the Mharcaidh snowpack (Joe Porter, pers comm) it was decided not to sample over a single elevation transect but to try

and establish a snow course that represented the variability of the snowpack in the catchment.

The spatial variation of the snowpack is due to a number of different factors:

(1) Elevation (Plate 2.4)

There is a general increase in snowfall with increasing elevation due to both orographic precipitation and a cooling of the air as it rises. Many authors have identified this and it is perhaps best described by Fitzharris (1978).

(2) Aspect (Plate 2.4)

The aspect of a slope affects the amount of water held in the snowpack. Harrison (1986a) states that "snowpack water equivalents can differ by more than 200% on moderate slopes at the same altitude but varying in aspect". This is due to a number of reasons: in the Mharcaidh in particular the direction of the prevailing wind will combine with aspect to result in the highest snowfall occurring on the lee slopes; once the snow has fallen and the pack stabilised it will melt at different rates depending on the aspect of the slope. Ferguson (1985) has identified this in the Cairngorms and found that north and east facing slopes tend to hold more snow than those on level, west or south facing

ness. Ward (1964) also noted the importance of wind drifting and the high frequency of southerly and south-



those covered by forest and attributes this to drifting.

The Klamath has a number of areas that are affected by this: the Klamath valley floor; the deeply incised gullies of the stream; and the "bowl" found at the head of the two main tributary streams. The deep gully of the main Klamath here between 250 and 300m was thought to be of considerable importance as snow often lies here until mid summer (Plate 2.4) and as mentioned (1966) elsewhere. Deep

**Plate 2.4** The effect of elevation and aspect on snow distribution. West facing slopes have less snow than those with an easterly aspect; little snow is present on the lower slopes of the catchment.

ones. Ward (1984) also noted the importance of wind drifting and the high frequency of southerly and south-westerly winds over the Cairngorms. This is borne out by personal observations in the catchment during the course of the snow surveys (Plate 2.5).

### (3) Topography and vegetation.

The presence of hollows and gullies within a catchment will affect the distribution of the snow. Fresh snow will drift into these hollows as the wind attempts to 'smooth' the landscape and results in a wide variation in the snowpack depth. Kopanev (1972) reports a greater variation and error in observations taken over open, exposed areas than those covered by forest and attributes this to drifting.

The Mharcaidh has a number of areas that are affected by this: the hummocky valley floor; the deeply incised gullies of the streams; and the 'bowls' found at the head of the two main tributary streams. The deep gully of the main Mharcaidh burn between 650 and 900m was thought to be of considerable importance as snow often lies here until mid summer (Plate 2.6) and as Harrison (1986b) observes, deep drifts that are only small in nature may be significant in regulating the baseflow of the stream and extending the recession period. Also, it was thought that the exposed upland plateau was likely to experience a lower snowfall than more sheltered sites at similar elevations due to



Plate 2.5 Snowdrift on the south-western slopes of the Allt a Mharcaidh caused by high winds.



**Plate 2.6** Melt water flowing under the remains of the snowpack held in the main gully. This illustrates the importance of the gully snow survey site as snow would lie here until late in the year.

(2) A redistribution of the survey sites so that more were

drifting and a lack of deep vegetation to 'anchor' the snow.

The project was initially started in December 1985 By Mike Birch who stopped in autumn 1986. The snow course for the first winter was chosen by Mike and Rob Ferguson and is shown in Figure 2.2. This was based on dividing the catchment into five elevation zones, each elevation zone being divided into east, north or west facing. Although this gave a total of 15 different zones, by grouping some together it was possible to minimise the amount of travel and sampling to 10 sites (the distribution of these was altered slightly midway through the winter and the most easterly sites were omitted).

On taking over the project in December 1986 a detailed analysis of the data collected in the previous field season was possible, along with a comparison of the observed changes in distribution of the snowpack shown on the photographs taken by Mike and the data collected. From this it was felt that a number of improvements could be made:

- (1) More data needed to be collected from the eastern sub-catchment (especially as it was then intended to compare the output from the different models on the two sub-catchments).
- (2) A redistribution of the survey sites so that more were

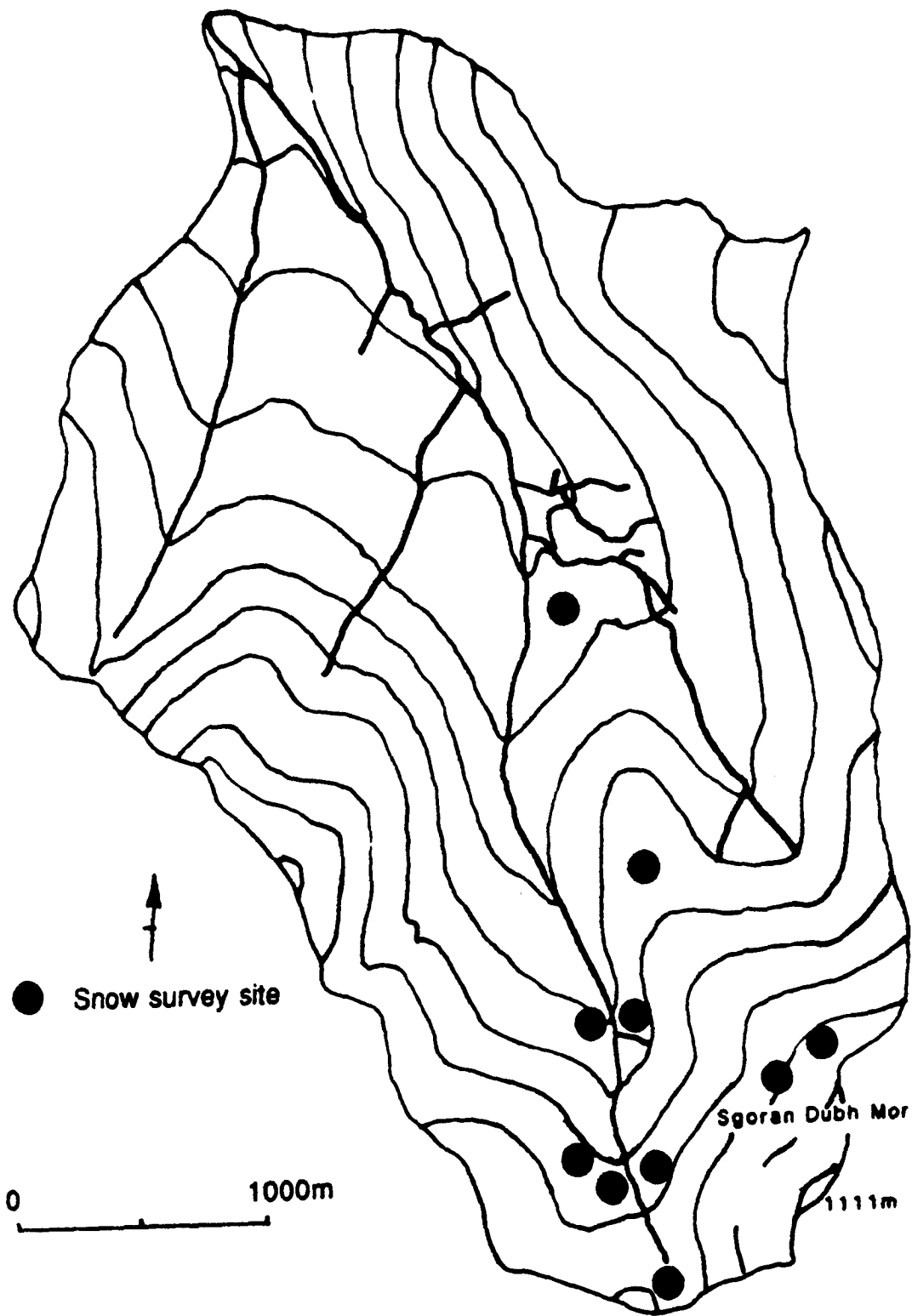


**Figure 2.2** Snow survey sites used by M Birch for the 1986 melt season.

on the open hillsides away from the sheltering and trapping effects of the gullies.

- (3) Sites be located in the lower part of the catchment as, although it received less snow than the higher areas this snow generally melted very quickly, affecting the hydrograph.
- (4) As it was intended to examine the effects of dividing the catchment into different elevation zones on model performance, the siting of the sampling sites had to ensure that samples were taken from each zone.
- (5) The sites be chosen so that on occasions when really bad weather or heavy snowfall made progress into the upper part of the catchment dangerous or difficult, it was possible to complete a considerable portion of the usual snow course and complete the remainder by correlation if needed. The sites chosen meant that seven out of 13 could be safely visited under adverse conditions.

The catchment was visited when it had minimal snow cover and 13 sites were chosen for the snow course, shown in Figure 2.3, together with the area each one represents.

Though the course was almost 14 kilometres long and involved approximately 900m of ascent it could usually be completed within a single day when there was 100% snow cover.

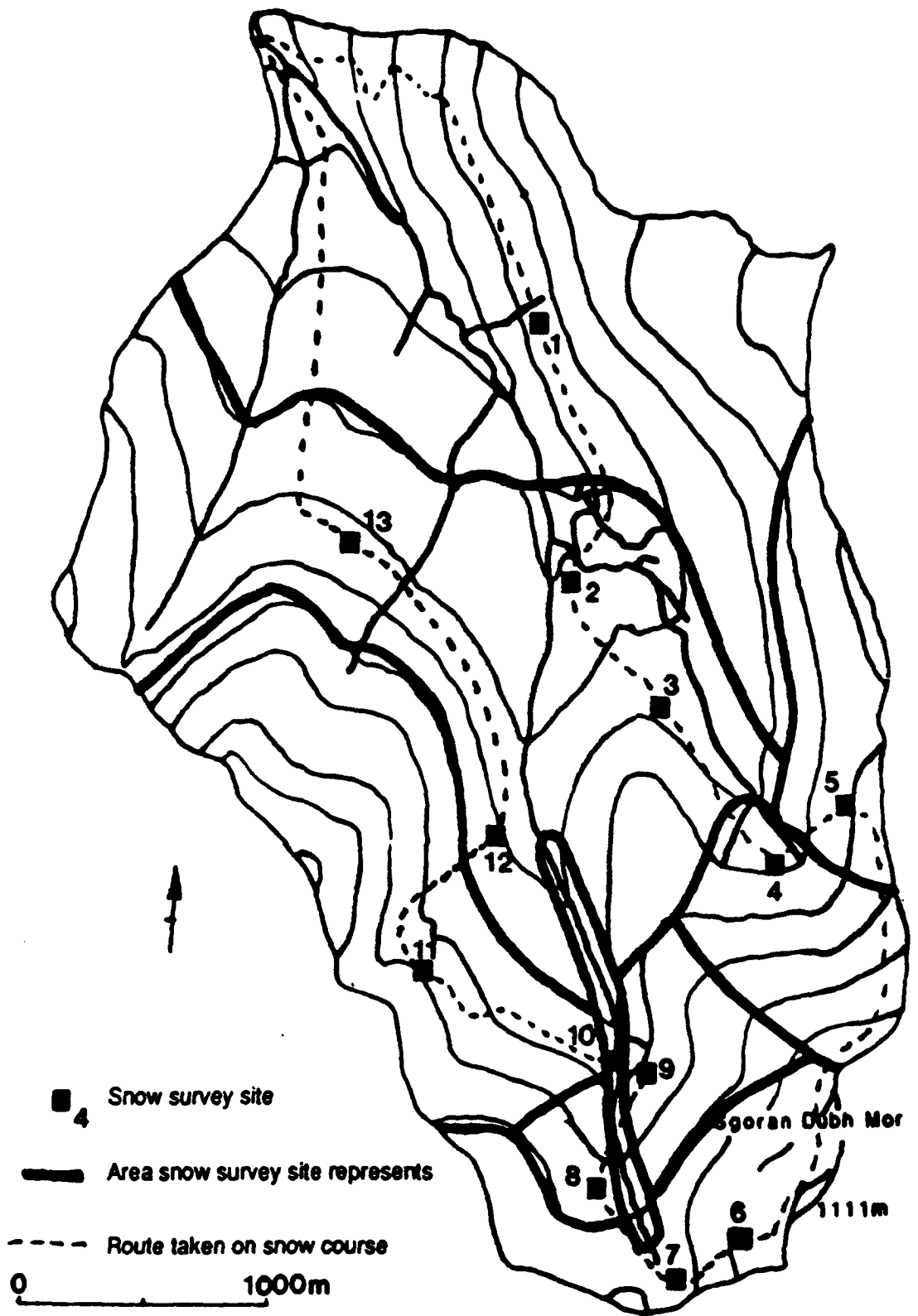


**Figure 2.3** Snow survey sites and the areas they represent used for the 1987 and 1988 melt seasons.

### 2.5.2 Measurement Techniques

Once the location of the sites on the snow course had been decided it was necessary to design a sampling strategy for data collection at each site. Ferguson (1985) carried out snow surveys in the neighbouring Feshie catchment at five sites chosen to represent different combinations of altitude and aspect. At each site 10 snow depth measurements were made at 5m intervals along a transect across the slope and another 10 along a parallel transect 5m upslope (Figure 2.4). As snow density is thought to vary less than snow depth over small distances density measurements were made at a single point where the snow was of intermediate depth.

Chinn (1969) also made a single measurement of snow density after a number of snow depth measurements had been made, but other authors have used different techniques. Gillies (1964) recommends sampling in a grid pattern to investigate the effects of a particular feature such as a snow fence or pylon, and sampling in a cross pattern when studying a wider area. He states that a flexible approach is often needed and a combination of different patterns may be needed on any one snow course. Bernier (1986), working in a similar sized catchment to the Mharcaidh, carried out an intensive 249 point grid sample once a year and a monthly 12 x 10 point grid (all of snow depth), whilst Moore and Owens (1984) sampled snow depth and density at

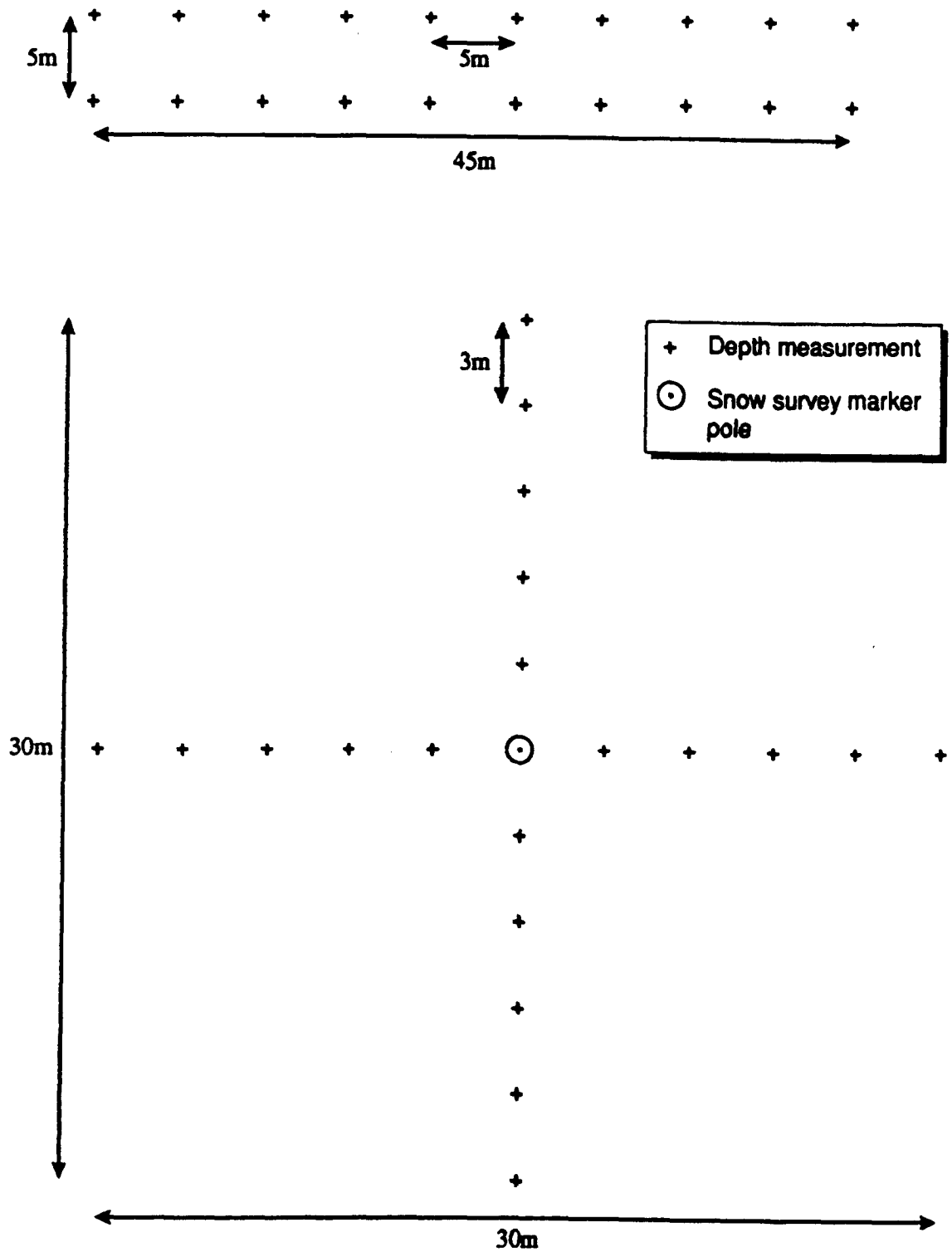


**Figure 2.4** Sampling strategies used by Ferguson (1985) in the Feshie catchment (top), and for the 1987 and 1988 snow surveys in the Allt a Mharcaidh (bottom).

intervals of 900 x 100m for snow depth and the other with sites at 900 x 300m for snow water equivalent (i.e., density as well as depth). At each point five observations were taken at 2m intervals and the mean for each point determined.

It can clearly be seen that there are no set formulae or designs for the sampling strategy in an experimental catchment. One point that must be made is that whilst some of the sampling strategies outlined above may be very detailed, the number of successfully completed surveys in a given study period is often inversely related to the intensity of the sampling network. For example, Dickison and Daugherty (1978) only completed four surveys per year and Gillies (1964) only completed one full survey in the Upper Fraser catchment. With this in mind the sampling strategy for the Mharcaidh was designed as a compromise between what could be realistically completed in a single day and the ideal of a very detailed sampling network.

At each site on the snow course snow depths were measured along four transects running north, south, east and west from each marker stake (Figure 2.4). Five measurements were made at three metre intervals using a graduated metal avalanche probe, measurements being read to the nearest centimetre, and the mean depth of snow calculated. Depending on weather and snow conditions one of two methods was then used to establish the density and water equivalent

Depending on weather and snow conditions one of two methods was then used to establish the density and water equivalent of the pack at the site. If the weather was good and the mean snow depth was less than 1.5m a snow pit was dug, away from the path of the four transects (Plate 2.7). This was used to examine visually the structure of the snowpack and to take density measurements at intervals through the vertical section, especially if fresh snow was lying over older, more compact snow. Density measurements were taken by pushing a plastic measuring cylinder into the wall of the pit and removing a core of snow. The volume of this was read off the cylinder and the weight recorded using a spring balance and heavy gauge polythene bag. From this the density of the snow could be calculated, and applying this to the mean depth of snow allowed the water equivalent of the pack to be determined. When it was not possible to dig a snowpit a number of vertical cores were taken through the snowpack at the site using a snow corer. There are many different types of snow corer based on the same principle of a long hollow tube that is graduated on the side. A summary of some of the more common corers used in North America is given by Goodison et al (1981).

For the first year of the project M Birch used a snow corer made of 4.4cm ID plastic waste pipe, (thought to be suitable because of its very low weight and because snow did not stick to the plastic) and found it satisfactory. However, during the early surveys in the 1986/87 winter it



**Plate 2.7** One of the snow pits dug during the 1987 snow surveys. These were used to examine the variation in snow density and to establish a more accurate idea of the snowpack characteristics.

was observed that the pipe was often distorting when it hit an ice layer and it was not possible to determine how accurate the sample was. Because of this it was decided to design a corer for use specifically in the Mharcaidh under the conditions experienced there. Chinn (1969) states that the Federal sampler with an ID of 3.77cm allows easier and better penetration of ice layers than the Italian CNI (La Commissione Nevi, Italia) sampler used by many authors (For example, Archer, 1970, Moore and Owens, 1984, Gillies, 1964) which has an ID of 7.05cm, though the latter performs better in fresh snow. With this in mind the corer was constructed from a 1.3m length of 4.44cm ID aluminium tubing. The corer was graduated in cm snow depth on one side and cm<sup>3</sup> sampled snow on the other. Four sets of slots were cut in the tube, aiding inspection of the snow core and reducing the weight of the tube to 1.75kg. These slots did not continue right to the base of the tube so that fresh falls of snow could be sampled as accurately as possible by minimising losses of snow through the slots. For deeper samples this was not a problem as the core was less granular/powdery, usually existing as a cohesive cylinder of snow. At the top of the corer two large holes were cut so that the pick of an ice axe could be inserted, allowing more pressure to be applied to push the corer through ice layers and easing the removal of the corer. A set of cutters were also cut into the base of the corer to allow easier penetration through the high density snow.

In use the corer was pushed through the snow until resistance was felt. It was then moved up and down to determine if the resistance was caused by the frozen ground or an ice lens. If it was the latter then more pressure was applied until the corer was through to the ground. It was then removed and the base of the core inspected for traces of vegetation/soil as proof that the full depth of snow had been sampled. The volume and depth of core were read off the scale on the corer and the snow was then transferred into a heavy gauge polythene bag to be weighed. This was often difficult as the snow froze to the aluminium so a plunger (a plastic disc the same size as the ID of the corer on the end of a wooden pole) was made that could be pushed through the corer to remove the snow. The mass of the snow was measured using a spring balance and any observations about the core were noted. From these measurements it was possible to obtain data on the water equivalent of the snow at any one site.

Once the sampling at the site had been completed an estimate was made of the extent of snow cover over the area the site represented before setting off for the next site on the snow course, either by foot or ski. In cases of low visibility a compass bearing was followed and, by knowing how long it typically took to travel from one site to the next, the approximate location of the next site could be located. A more detailed search was then needed to find the marker stake.

In practice most of the snow surveys were successfully completed, there being only one occasion when no measurements were made as it was difficult to stand at GS1 without anything to hold on to! If time was short, weather particularly bad or avalanche risk high, site 11 was missed out and an extra set of measurements were taken to the north of site 8 where the conditions were similar to those at site 11.

### 2.5.3 Sources of error in the snow surveys

Potential errors in the snow survey measurements can be divided into two different types; systematic and random. The largest single error (systematic) is likely to be due to the sites on the snow course not being truly representative of the catchment as a whole. To see if this was the case it was decided to carry out a more detailed survey over the whole catchment early in the study so that any weaknesses could be corrected.

This study was carried out on 23 and 24 February 1987 when the catchment had 100% snow cover and the weather forecast was for stable conditions. The routes taken on the two days are shown in Figure 2.5 and the results are tabulated in Table 2.1. In total, 475 depth measurements and 80 cores were taken over the two days at 31 sites along with three snow pits on the first day. There was not as much data collected on the second day as had been hoped as the

Zone or Sites	Volume from usual route	No. of sites on detailed	Volume from detailed
1	68 420	4	82 415
2,3,12,13	106 029	5	188 892
4	303 480	3	231 263
5	26 000	4	34 666
6,7	58 350	4	57 646
8	16 800	1	16 800
11	141 000	4	141 000
9	37 490	3	41 109
10	140 000	2	84 000
TOTAL	897 569		877 791

Table 2.1 Results from the standard and detailed snow surveys carried out on 23 and 24 February 1987. All volumes are in m3.

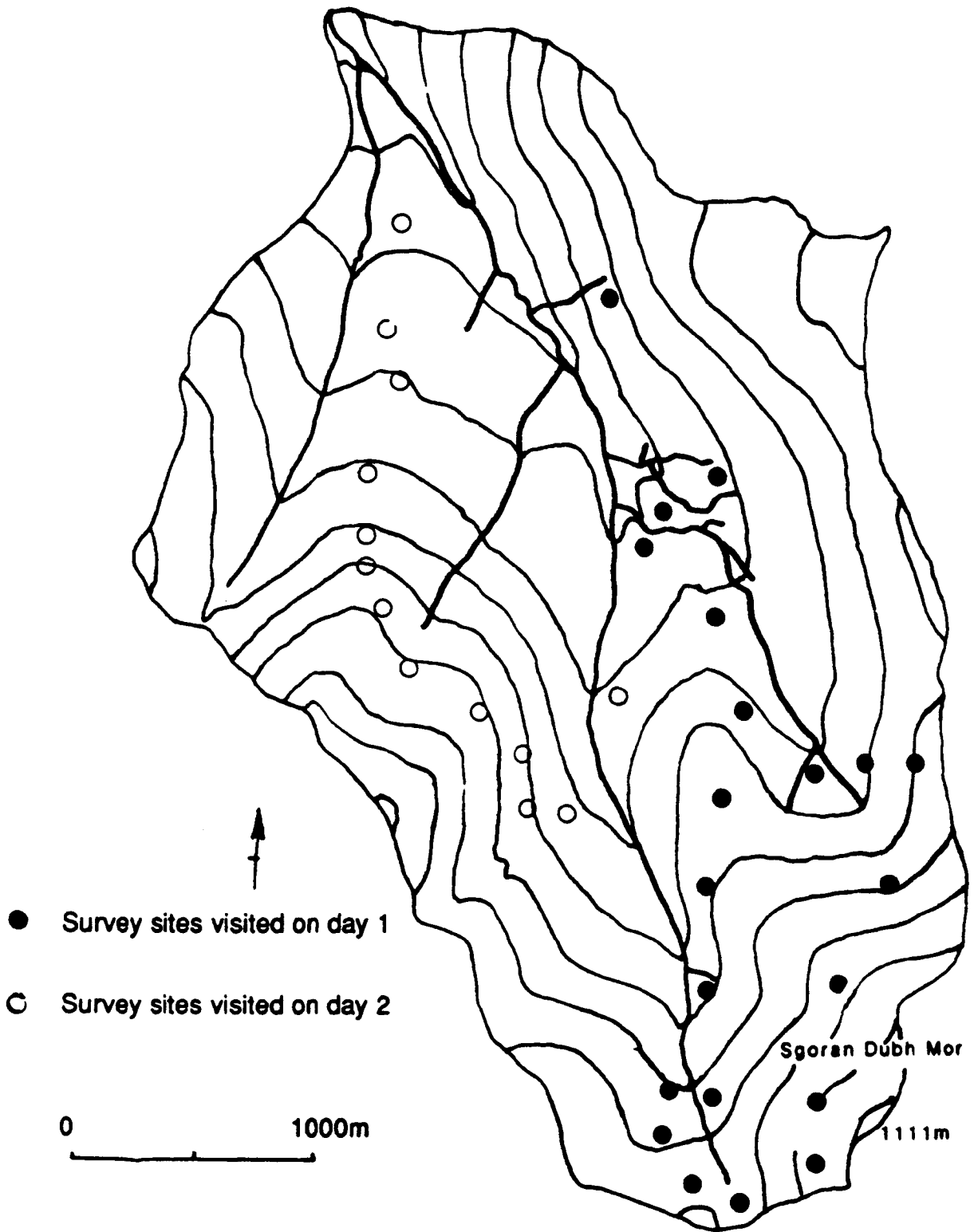


**Figure 2.5** Snow courses used for the detailed snowpack study during the 1987 melt season. Day 1 was 23 February and Day 2 was 24 February.

weather changed and a snow storm developed; rather than continue higher up the southwest area of the catchment as intended it was decided to return early down the northwest slopes. Had the data been collected it would have been of little use as there was drifting fresh snow which would have made comparisons between the standard snow course data and that collected from the detailed study difficult to interpret. Also, the weather was so bad that actually carrying out the sampling higher up would have been very difficult and more errors were likely to be induced than when sampling lower down.

It can be seen from Table 2.1 that the differences between the intensive survey and the standard snow course were very small, the total difference between the two methods being only 19,800m<sup>3</sup> of water equivalent (3 s.f.), representing 2.2% of the total catchment water equivalent determined by the standard snow course. However, when studied closely it can be seen that for three of the areas there were significant differences between the two methods and some explanation is needed.

The first difference is over the area covered by sites 2, 3, 12 and 13 on the snow course. The snow course indicates that 106,000m<sup>3</sup> water equivalent were present whilst the intensive study finds 189,000m<sup>3</sup>, 78% more. This can be explained by one single point on the intensive study, located in the gully above the Macaulay soil sampling

site. Here the water equivalent was measured to be 360mm, almost ten times the value found at the other sites in this area. If this site is removed from the data the new total is 115,500m<sup>3</sup>, which is only 9% more than the snow course value. This can be justified as the gully only represents a small portion of the area, though the fact that there are some gully areas present does indicate that the snow course underestimates the total value for the whole area.

The second difference is in the area covered by site 4 on the standard snow course. Here the values are 303,500m<sup>3</sup> for the snow course data and 231,000m<sup>3</sup> for the intensive study. This difference (72 500m<sup>3</sup> or 24% of the snow course value) may be because the second site in the intensive study was at the top of the zone on top of a ridge in the slope, thus underestimating the snow depth. At other places on the slope the snow was observed to be deeper than that measured at site 4 (usually by falling through a snow drift on the slope!) so it is felt that site 4 does represent the area as a whole.

The final difference to note was in the area represented by site 10, the gully that holds the upper Mharcaidh. Here the difference in the table is 56,000m<sup>3</sup> or 40% of the snow course value. This is because the second site on the intensive study was again at the edge of the zone where the snow was thinner, thus reducing the value for the area. Indeed, it may be argued that it was not within the zone at

all and should have been included with the data from site 9 or 8, in which case it would have increased the snow water equivalent in either of these zones. Also, the value recorded for site 10 itself was '>2000mm water equivalent', the upper limit being determined by the length of the avalanche probe and not the depth of snow in the gully. If it had been possible to measure the true depth of the snow the second value would have had a lesser effect on the total, which might have then been closer to that recorded on the snow course. What can be gained from this is the justification for having the gully zone in the snow course; although it represents only a small percentage of the catchment area the volume of water held in it is significant, especially late in the melt season.

Overall, it can be seen that the snow course does provide a reasonable estimate of the snowpack state in the catchment, and increasing the number of sites from 13 to 30 does not appear to give any significant benefits. It was thus decided to continue with the snow course as it was.

Other errors likely to occur were when actually taking the measurements at each of the sites. The problems with snow sticking in the corer and of the earlier corer distorting and fracturing under pressure have already been mentioned. Care was always taken to ensure that the measurements were taken as carefully and consistently as possible but there will have been obvious random errors induced by wind

blowing snow/ice into/out of the weighing bag, the force of the wind affecting the weighing of the bag and driving snow making the reading of values off the scales on the corer, avalanche probe and spring balance difficult, etc. Chinn (1969) also identifies this, stating that "the more difficult it is to take a sample, the greater may be the error of the results". He also states that under favourable conditions, with snow depth values being read to the nearest centimetre it is normally possible to measure the density of the snow to within  $0.01\text{g cm}^{-3}$  for snow over 50cm deep and to within  $0.05\text{g cm}^{-3}$  for snow less than 20cm.

Of more concern may be the presence of systematic errors caused by using a particular piece of equipment or technique. Chinn claims that snow corers tend to overestimate the water equivalent of the snow by between 7% in shallow, low density fresh snow and 10% in deeper, high density snow. Goodison (1978) and Work et al (1965) have investigated the errors found by using different snow corers and found them to be between -9.1 and +18.5%, the majority tending to overestimate. It is thought that this is due to the teeth at the base of the corers tending to push snow into the tube, i.e. the diameter of the snow from which the snow is sampled is closer to the external diameter of the tube than the internal diameter. As the teeth on the corer used for this study were ground on the outside of the tube and thus tended to push the 'borderline' snow away from the sampled core it is not

thought that this was a problem in the Mharcaidh. As it was not possible to carry out a detailed investigation of the accuracy of the corer used in the Mharcaidh these results must be remembered when comparing the snow survey results to other projects.

When recording the depth of the snow the probe often met no resistance at the base of the snowpack, possibly due to air spaces between the snow and the ground surface being caused by the vegetation. Chinn (1969) and Ferguson (1985) also identify this, the gaps typically being between 1 and 5cm but often up to 10cm. When this happened the probe was pushed through the snow close to the first point, taking great care as it got closer to the approximate base of the snow. As soon as it broke through the base of the snow the depth was recorded, thus doing all that was possible to ensure that measurements were as accurate as possible. This was not a problem with the water equivalent/density measurements taken with the corer as the true volume of the core could be obtained by subtracting the 'empty' volume at the base from the value at the top of the core. There is a risk that the snow within the core could have been compressed as a result of the corer passing through, especially if it went through an ice layer that may have plugged the tube. Whilst this would not have affected the water equivalent measurements it may have caused some of the density values to be increased.

## CHAPTER 3 COLLATION OF FIELD DATA

This chapter describes the results from the snow surveys and puts them into perspective with the observed meteorological and flow data collected in the Mharcaidh. Regression analyses are carried out on the data to determine the potential of different approaches in modelling snowmelt.

### 3.1 Snow surveys

Summarised results of the 1986, 1987 and 1988 snow surveys are shown in Tables 3.1 - 3.3; detailed survey results are given in Appendix B. Figures 3.1 - 3.4 show time series plots of snow covered area, snowpack volume, water equivalent averaged over catchment and water equivalent averaged over snowpack for the three melt seasons.

#### 3.1.1 Snow covered area

Figure 3.1 shows the depletion curves of the snow covered area for the three years. 1986 and 1988 show similar patterns that can be split into four periods:

- (1) Catchment at complete or near complete snow cover. The length of this period is dependant on the water content of the snowpack and the air temperature: a

Date	Julian Day	SCA (km <sup>2</sup> )	Volume (m <sup>3</sup> )	SWE (mm)	CWE (mm)
27 February	58	9.91	1,766,000	178	175
4 March	63	8.51	1,497,000	176	151
5 March	64	9.11	1,481,000	163	149
26 March	85	9.16	857,000	94	86
13 April	103	4.20	986,000	235	99
25 April	115	4.68	1,230,000	263	124
2 May	122	2.43	827,000	340	83
6 May	126	1.00	288,000	288	29
20 May	140	Negligible			

**Table 3.1 Summary of Mharcaidh Snow Survey Results 1986.**

Date	Julian Day	SCA (km <sup>2</sup> )	Volume (m <sup>3</sup> )	SWE (mm)	CWE (mm)
23 January	23	0.73	373,000	511	38
13 February	44	9.91	822,000	83	83
20 February	51	9.91	920,000	93	93
25-26 February	54/57	9.91	891,000	90	90
3 March	62	3.71	525,000	142	53
12 March	71	3.29	386,000	117	39
19 March	78	9.91	437,000	44	44
24 March	83	4.98	426,000	86	43
31 March	90	2.47	439,000	177	44
8 April	98	6.03	367,000	61	37
18 April	108	0.75	250,000	333	25

Table 3.2 Summary of Mharcaidh Snow Survey Results, 1987.

Date	Julian Day	SCA (km <sup>2</sup> )	Volume (m <sup>3</sup> )	SWE (mm)	CWE (mm)
30 January	30	9.91	1,650,000	166	166
3 February	34	9.91	1,454,000	147	147
24 February	55	9.91	665,000	27	67
8/9 March	68/69	4.19	978,000	233	99
29 March	89	4.17	785,000	188	79
13 April	104	2.70	401,000	149	40
5 May	126	Negligible			

**Table 3.3 Summary of Mharcaidh Snow Survey Results, 1988.**

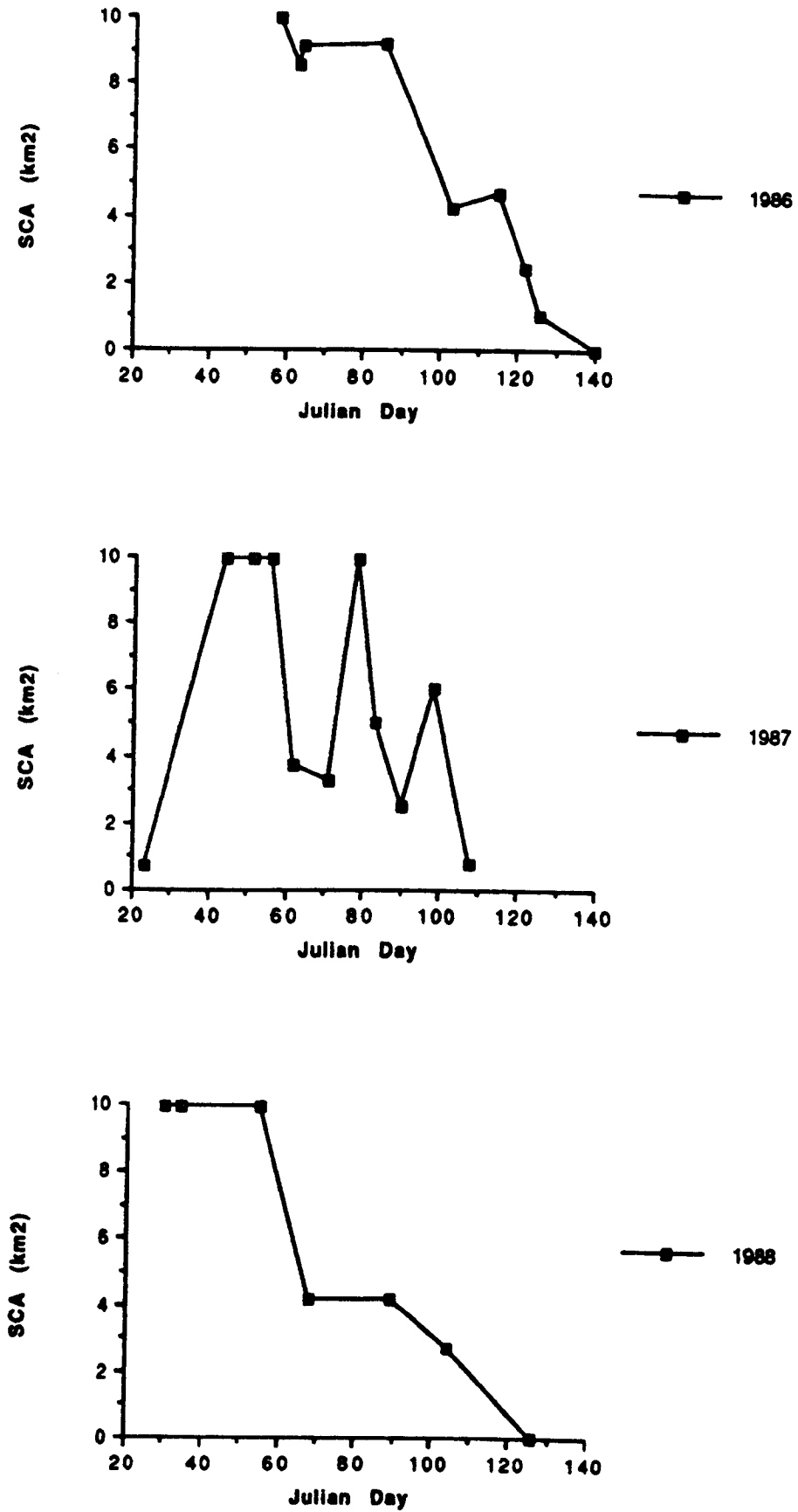


**Figure 3.1** Snow covered area depletion curves for the 1986-1988 melt seasons.

deep snowpack combined with cold weather will result in a long period of complete cover and vice versa. The length of this period can not be accurately taken from the Figure because as mentioned above, the surveys were only carried out when the worst of the winter had passed and the snow conditions were considered stable.

- (2) A period of rapid depletion then follows until SCA is 4.2 - 4.6km<sup>2</sup>. From the hypsometric curve this converts to an altitude of 760 - 775m which corresponds to the top of the 'plateau' in the middle part of the catchment at the base of the steeper headwalls and slopes of the upper catchment.
- (3) Once this area/elevation has been reached (coinciding and relating to the end of the first period of rapid decrease in snowpack volume described later) the SCA stabilises for a short period, thus coinciding with the stable period of the snowpack volume visible in Figure 3.2 which is caused by the snowfall inputs being in equilibrium with the melt outputs from the snowpack.
- (4) Finally the snowpack depletes from near 50% cover to virtually nil, only a few patches in the gullies remaining. The rate of this decrease is related to its timing; in 1986 it commenced after Julian Day 115

and was rapid whilst in 1988 it commenced earlier (Julian Day 90) and was slower.

The depletion rates for the periods (2) and (4) are shown below in Table 3.4.

Year	1986	1988
<u>Period 1</u>		
Decrease in area	5km <sup>2</sup>	5.7km <sup>2</sup>
Duration	18 days	14 days
Rate of decrease	0.27 km <sup>2</sup> day <sup>-1</sup>	0.41 km <sup>2</sup> day <sup>-1</sup>
<u>Period 2</u>		
Decrease in area	4.7km <sup>2</sup>	4.2km <sup>2</sup>
Duration	25 days	37 days
Rate of decrease	0.18 km <sup>2</sup> day <sup>-1</sup>	0.11 km <sup>2</sup> day <sup>-1</sup>

Table 3.4 Snow covered area depletion rates determined from the 1986 and 1988 snow surveys.

From this it can be seen that the rate over period (2) was greater in 1988 than 1986 (due to the snowpack being thinner) and for period (4) was greater in 1986 when it occurred later. Being able to generalise the depletion curves for the 1986 and 1988 melt seasons gives hope that it is possible to model this in the snowmelt models. However, it can be seen from Figure 3.1(b) that the 1987 snowpack does not fit into this generalisation as well as those of 1986 and 1988, suggesting that all is not as simple as might first be thought.

If it is accepted that the initial rise in SCA is due to

the snow surveys starting in the accumulation period it can be seen that periods (1) and (2), i.e. initial 100% SCA followed by rapid decrease to 3.7km<sup>2</sup> SCA, can both be identified for 1987. However, the surveys carried out on Julian Day 78 (19 March) and 98 (8 April) both indicate a rise in SCA that had not previously been identified in the 1986 and 1988 plots/data.

A possible explanation for these anomalies may be attributed to four factors:

- (1) Intensity of snow surveys
- (2) Snowpack volume
- (3) Occurrence of precipitation
- (4) Timing of the period

It can be seen from Figure 3.1 and Tables 3.1 - 3.3 that because the initial volume of the snowpack was less in 1987 than the other two years it completed periods (1) and (2) of the SCA depletion earlier (by JD 62 compared to 103 for 1986 and 69 for 1988). Snow surveys were carried out at 9, 7, 5, 7, 8 and 10 day intervals compared to 20, 15 and 22 for 1988, the most directly comparable year as the dates were similar, which average out to one survey every eight days in 1987 and one every 19 days in 1988.

As 10 and 12.5mm precipitation were recorded at the AWS during the interval preceding the two surveys that

identified an increase in SCA it is possible that, due to the increased intensity of the surveys, a temporary increase in SCA was recorded that may have been missed for the other two years. Cooley (pers comm) working in Idaho, has also identified these temporary increases in SCA and described their importance in accounting for peaks in the runoff that cannot be explained by the simple depletion curve/routine used by many authors.

It can be seen that whilst the SCA depletion curve can be simplified into four phases from the 1986 and 1988 surveys, the 1987 surveys suggest that in reality the situation is more complex. It is possible that the short-term increases in SCA do not have a significant effect in a snowy year, only accounting for a small percentage of the total snowpack water volume over the season, whilst the effect in a low snow year is higher as they account for a higher percentage.

### 3.1.2 Snowpack volume

From Tables 3.1 - 3.3 it can be seen that 1986 and 1988 were much snowier winters than 1987, the maximum surveyed snowpack volume for 1986 being 2.17 times larger than that of 1987 and the 1988 volume being 1.99 times larger. Both R. Ferguson and J. Porter (pers comms) consider the 1986 winter as being especially snowy, 1987 being snow free and 1988 less than or close to the average from their personal

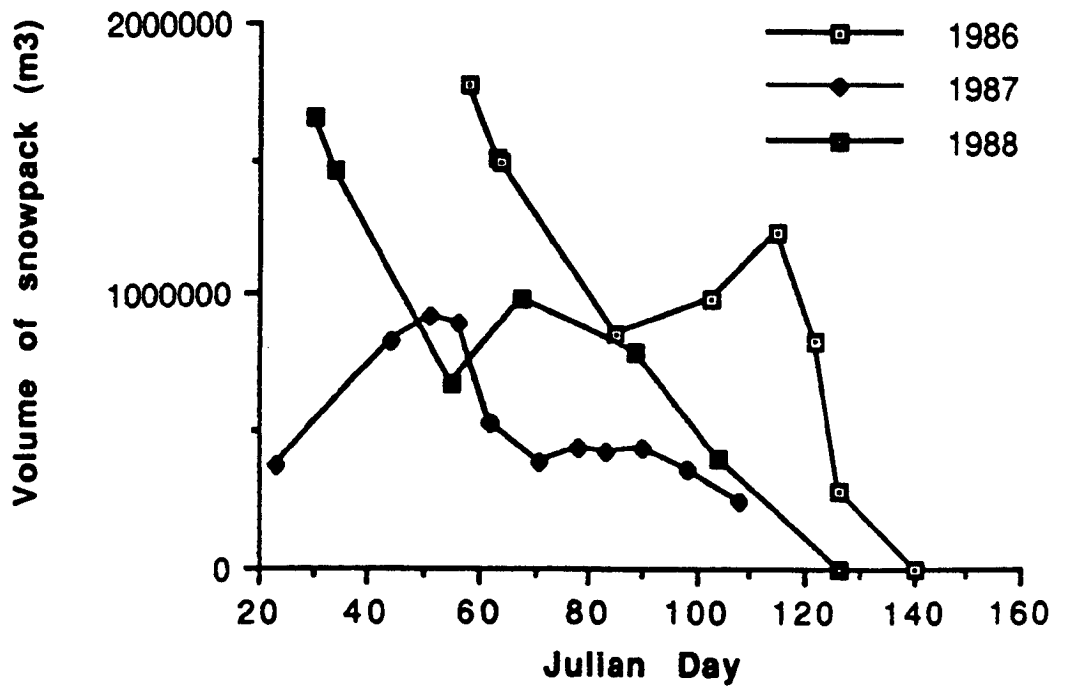


**Figure 3.2** Changing snowpack volume for the 1986-1988 melt seasons.

records. Whilst the data supports them for the 1986 and 1987 winters the total volume measured in the Mharcaidh suggests that 1988 was also a snowy year.

Despite these differences all three years show similar patterns in the reduction of the snowpack volume, though the timing and rate of change is different. From Figure 3.2 three distinct periods can be identified:

- (1) Early in the melt season the volume rapidly decreases by 50-60% (though not for 1987 as the surveys started earlier in the season). This decrease corresponds to early melt in the catchment that occurs over the lower areas during the first warm event of the year.
- (2) Following this period of rapid melt the volume appears to stabilise for 20-30 days. During this period the volume may increase slightly as fresh snowfall accumulates in the higher parts of the catchment. At this stage in the melt season the snowpack volume is in a state of dynamic equilibrium, the melt over lower areas of the catchment being compensated by accumulation higher up.
- (3) Finally, after Julian day 90-100 (late March/early April), there is a period of decrease until the snowpack is completely melted. The duration of this period, along with the rate of decrease, is dependent

upon the volume held in the snowpack and the time of year. Higher volumes take longer to decrease (1988), though if they exist later into the year the rate of decrease increases (1986). These points can be illustrated in detail by referring to the period 8 March - 5 May 1988 (Julian day 68-126). From Figure 3.2 (c) and Table 3.3 it can be seen that the snowpack volume is decreasing throughout this timespan. If it subdivided into three shorter time periods, each period being between two snow surveys, the rate of decrease can be calculated:

(a) 8 March - 29 March (JD 68 - 89)

$$\text{Decrease} = 193,000\text{m}^3 = 9,200\text{m}^3 \text{ day}^{-1}$$

(b) 29 March - 13 April (JD 89 - 104)

$$\text{Decrease} = 384,000\text{m}^3 = 25,600\text{m}^3 \text{ day}^{-1}$$

(c) 13 April - 5 May (JD 104 - 126)

$$\text{Decrease} = 401,000\text{m}^3 = 19,100\text{m}^3 \text{ day}^{-1}$$

(a) relates to the decrease early in the season from a high initial snowpack volume. By period (b) the days are longer and warmer, resulting in a faster decrease. This slows down in (c) as, although it is late in the year, the remaining snow is lying in deep hollows and gullies and is slow to melt.

Whilst (1) to (3) can be seen for all three years there appears to be an anomaly for the 1987 plot (Figure 3.2(b)) which shows a long period of accumulation early in the year (JD 20 - 51). In practice, snow surveys were only carried out after it was perceived that the worst of the winter had passed, usually late January. The snow was late in the 1986/1987 winter and the surveys were then able to record part of the snowpack accumulation in addition to the ablation.

One final point can be made regarding the number of snow surveys carried out each year, i.e. nine in 1986, eleven in 1987 and seven in 1988. Snow surveys were only made when it was safe to go on the mountain and when it was considered that the snowpack characteristics had altered since the previous survey; one further constraint was the availability of a field vehicle to get to the site. It is because of this fact that the 1987 season was the most intensively sampled despite being the least snowy. In hindsight it can be seen from Figure 3.2 (b) that the number of surveys could have been reduced from eleven to five (i.e., surveys 1, 3, 6, 9 and 11) without dramatically altering the snowpack volume plot, though it was shown in 3.1.1 that by sampling at a more regular interval than was needed further characteristics of snowpack behaviour emerged that may be useful in the development of the models.

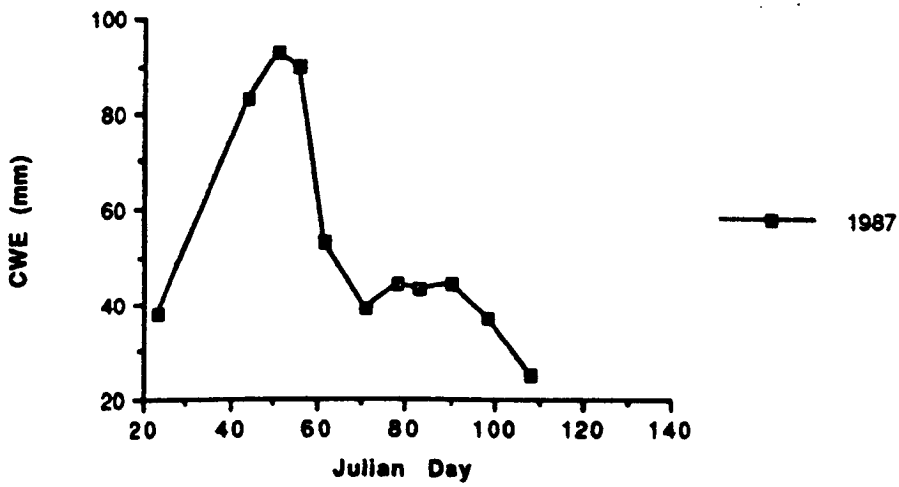
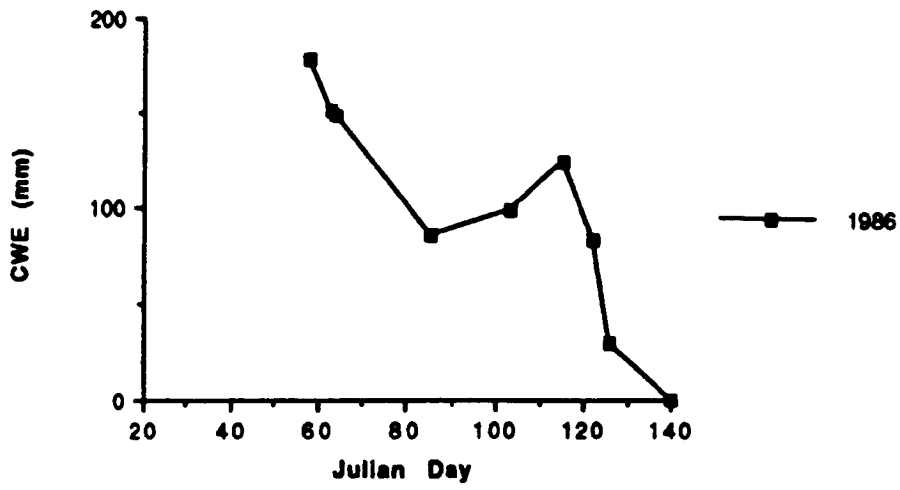


**Figure 3.3** Changing catchment water equivalent (CWE) for the 1986-1988 melt seasons.

It can be seen from Figure 3.3 that the snowpack water equivalent averaged over the catchment (CWE) plots are essentially the same as those of the snowpack volume shown in Figure 3.2. This is because CWE is directly proportional to snowpack volume, the only significant difference being the units used for each index of the snowpack, and because of this no discussion is given.

### 3.1.3 Water equivalent averaged over snowpack

Figure 3.4 shows time series plots of water equivalent averaged over the snowpacks (SWE) for the three years, calculated as volume/area. Again there is a similarity between the 1986 and 1988 plots whilst 1987 appears to be the exception. If the 1986 and 1987 plots are considered first they can be divided into three phases, which link to those identified for the SCA depletion curves and snowpack volume plots:

- (1) A period of initial decrease in the SWE corresponding to period (1) on both the volume and SCA curves, i.e. melt occurs over the lower areas of the catchment, reducing the SWE whilst the SCA is still 100% or at its maximum.
- (2) Once the SCA begins to decrease (period (2) of the SCA) the SWE starts to rapidly **increase**. This is

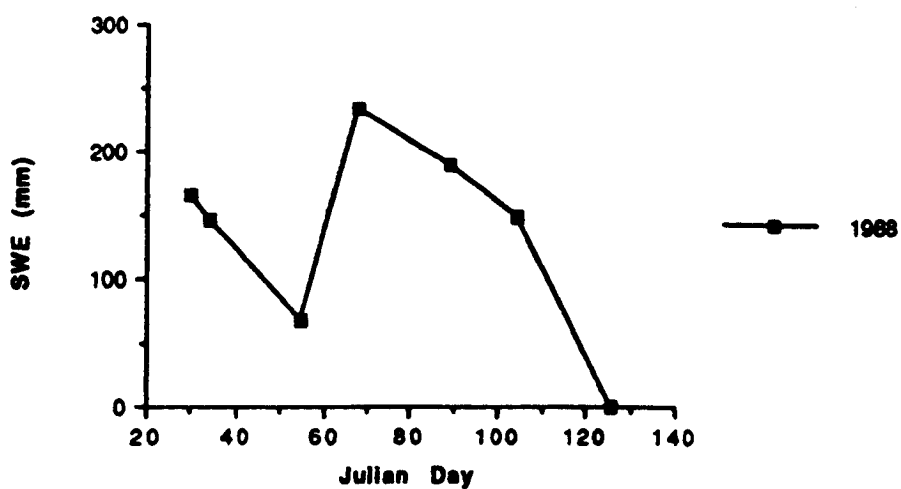
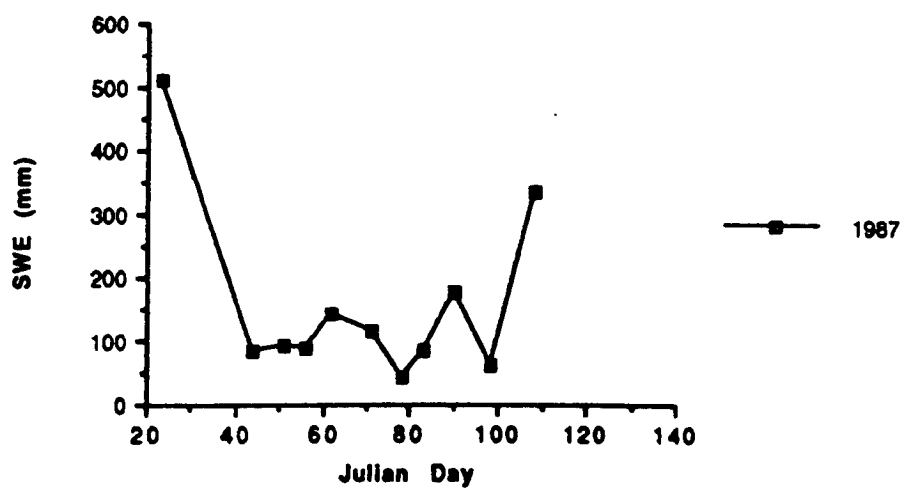
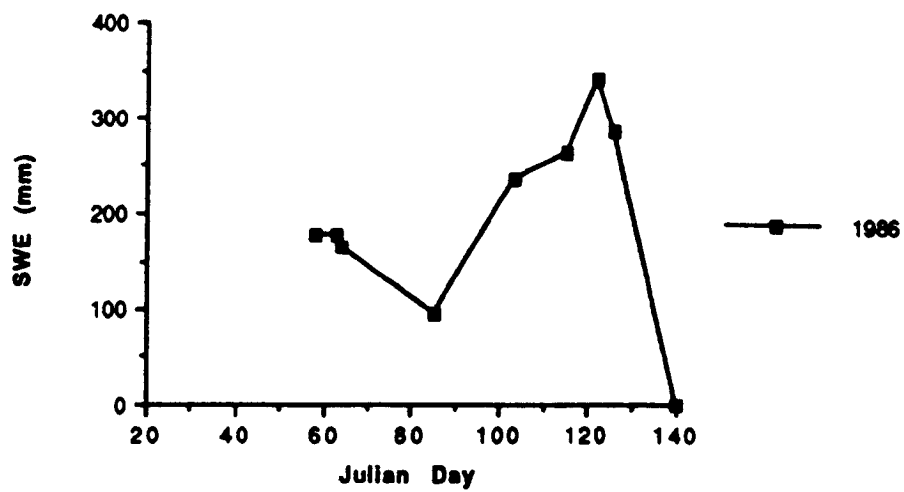


**Figure 3.4** Changing snowpack water equivalent (SWE) for the 1986-1988 melt seasons.

primarily due to the SWE being calculated over a smaller area but can also be attributed to the small increases in snowpack volume associated with fresh snowfall in the higher areas of the catchment (period (2) and (3) of the SCA curves). This ties in with the snow wedge concept identified by Fitzharris (1978) and Ferguson (1984).

(3) Finally the snowpack melt rate is such that the SCA begins to decrease again (period (4) of the SCA curves) and the volume decreases (period (3) of the volume plots) resulting in the SWE decreasing to zero. As with the SCA and volume plots this rate of decrease is dependent on the timing; for 1986 it is rapid (19 mm SWE day<sup>-1</sup>) as it is late in the year whilst for 1988 it is gradual (4mm SWE day<sup>-1</sup>) as it occurs earlier in the year when days are shorter, temperatures colder and fresh snowfall more likely.

It must again be noted that the intensity and timing of the surveys has an effect on the shape of the time series plots. The 1986 season had five surveys carried out at short intervals between 13 April and 6 May (mean interval = 7.67 days), resulting in a clear indication of the snowpack behaviour during the transition from increasing to decreasing SWE (periods (2) to (3)). At the corresponding stage in the 1988 snowpack development/depletion, the surveys were carried out at 17 day intervals, which

suggests that Figure 3.4(c) only provides an indication of the snowpack changes; a higher SWE may have existed before or after survey 4 (8/9 March) but was not detected.

The 1987 plot (Figure 3.4(b)) is again different from that of 1986 and 1988. There is a high initial SWE due to a deep but small snow cover high in the catchment; this rapidly decreases once the SCA increases to 100% of catchment area. The SWE then fluctuates, showing a number of rises and falls for the next eight weeks. If these fluctuations are compared to Figure 3.1(b) and Table 3.2 is studied it can be seen that the rises in SWE are associated with a fall in SCA, and the two rapid falls link with the 'temporary' increases in SCA discussed in 3.1.1. The SWE then increases rapidly as the SCA decreases at the end of the melt season, leaving deep patches of snow in the gullies and hollows. Finally, the melt reduces the SWE to zero.

It can thus be said that whilst the pattern of SWE change is not the same for 1987 as it is for 1986 and 1988, the processes taking place are similar; it is the timing and intensity of survey along with snowpack characteristics that affect the overall pattern. All three years show a general increase in SWE for decreasing SCA and vice versa, a sharp rise in SWE on the SCA depletion from c.50% to cover just the gullies and hollows, and finally a reduction in SWE to zero as these patches melt at the end of the

season. By being able to generalise the snowpack behaviour and link the different properties in this way it is possible that the depletion can be successfully modelled.

### 3.2 Relative distribution of snow in the catchment

#### 3.2.1 Snowpack water equivalent and volume

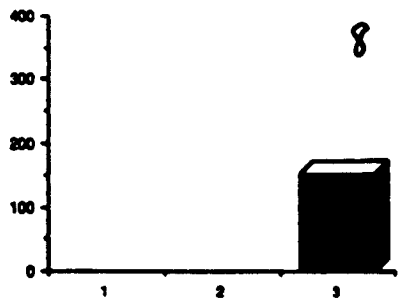
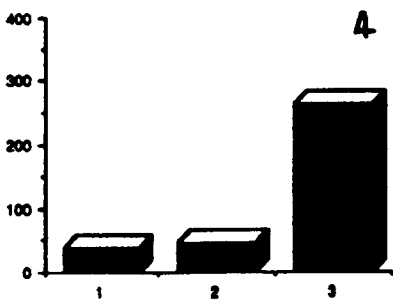
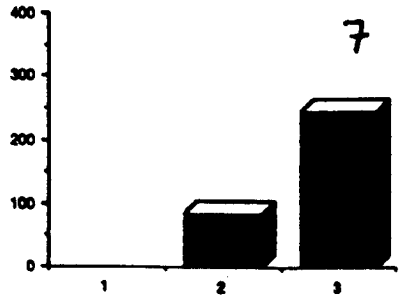
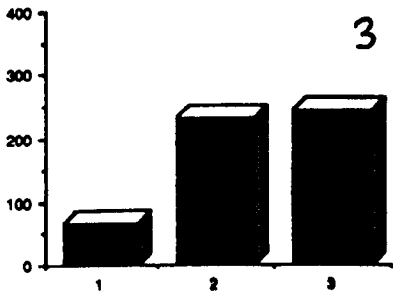
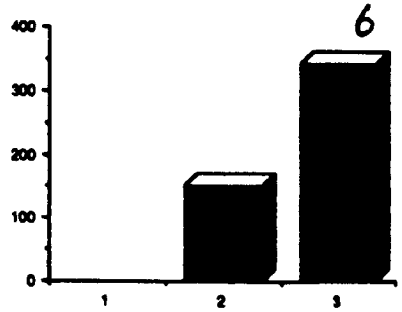
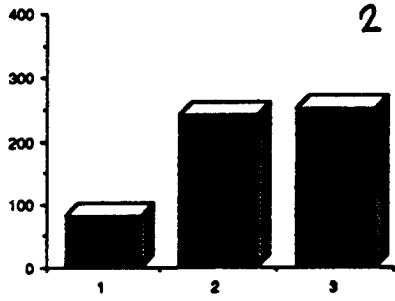
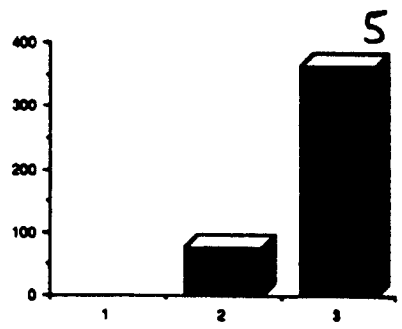
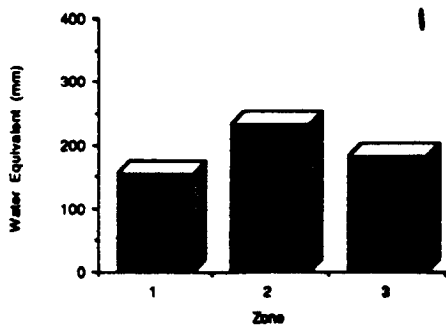
As it was intended to develop/test a layered model on the Mharcaidh data it was decided to examine the distribution of the snow over the three years in relation to the layers. Three elevation bands were chosen:

- (1) All areas below 600m amsl (3.11 km<sup>2</sup>)
- (2) The area between 600 and 800m amsl (4.55 km<sup>2</sup>)
- (3) The area above 800m (2.25 km<sup>2</sup>)

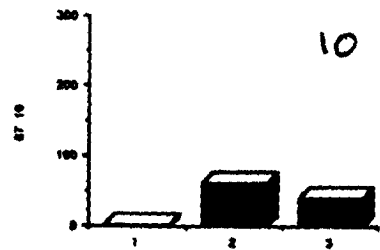
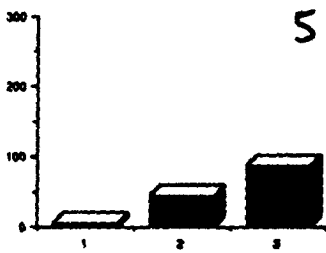
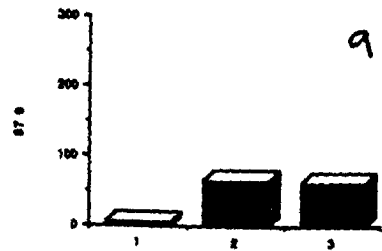
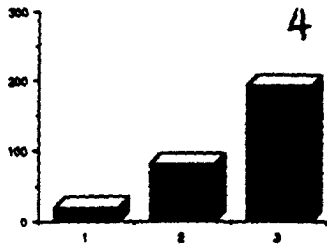
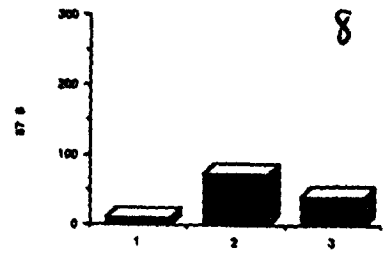
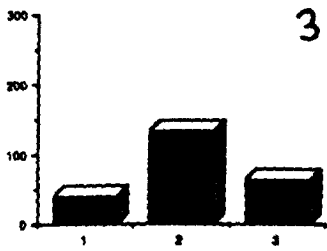
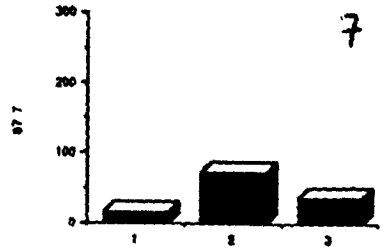
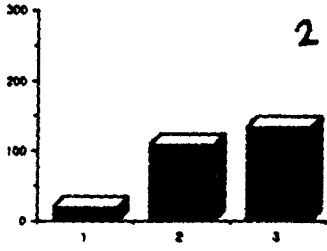
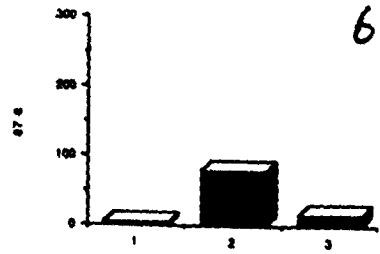
The snow survey data contained in Appendix B was apportioned to each of these elevation bands for the three years' surveys (Figures 3.5 (a) - (c)). From each year's plots the same general pattern in changing SWE (over snow covered area in each zone) can be clearly seen:

- (a) Prior to the start of the melt season each zone has approximately the same mean SWE (this is less clear for 1988).
- (b) During the early stages of the melt season the mean

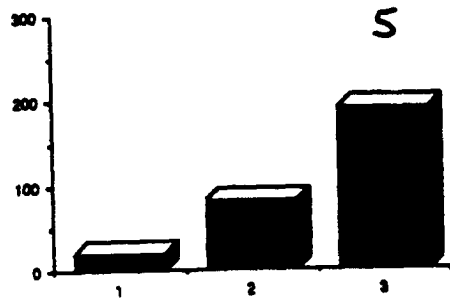
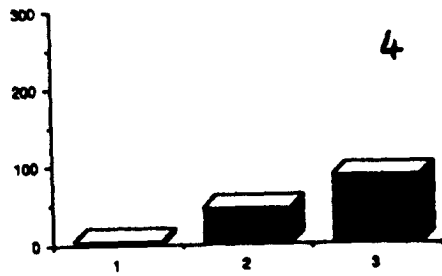
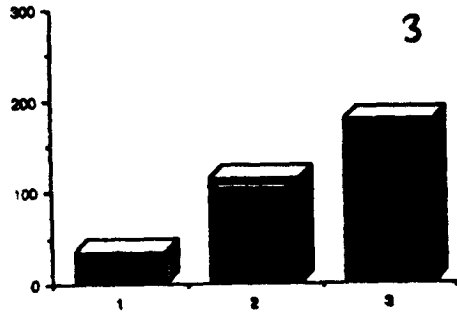
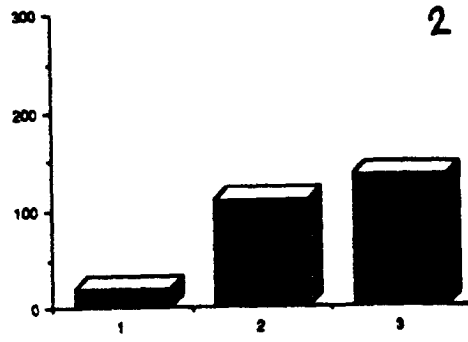
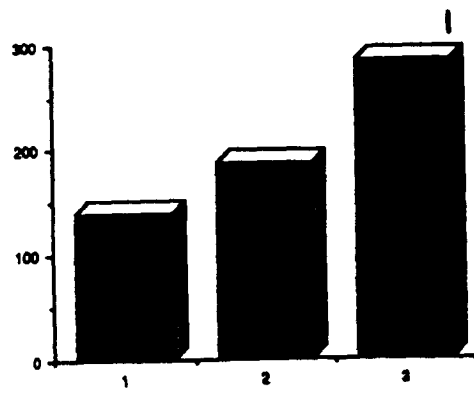
Figure 3.5 Histograms showing relative snowpack water equivalents for the three elevation zones. Zone 1 = the lowest, zone 3 = the highest. Numbers adjacent to histograms indicate the snow survey in Tables 3.1 - 3.3 that the data was derived from. All horizontal axes represent the three zones.



1986



1987



1988

SWE (over SCA in zone) in zone 1 decreases in relation to that in zones 2 and 3, though the actual volume may increase. This corresponds to snow melting over the lower parts of the catchment whilst it is still accumulating higher elevation. (i.e., periods (1) - (2) of the SCA depletion, (2) - (3) of volume and (1) - (2) of SWE behaviour over the whole snowpack).

(c) As the melt season progresses the SWE in zones 1 and 2 decreases so that the zones rank 3, 2 and 1 in SWE. The snow then melts in all three zones resulting in the pack depleting first in zone 1, then zone 2 and finally zone 3.

The three stages (a) - (c) described above can be seen for all three years, though the 1987 plots are complicated by fresh snow accumulating in zones 2 and 3 in the middle of the season. Combined with little increase in SWE in zone 3 due to lack of fresh snow later in the melt season (a) - (c) does not occur over the whole melt season but can still be seen over the first five surveys.

As the pattern in changing SWE is similar for all three years it allows a simplistic representation to be drawn up. One possible version is shown in Figure 3.6. The fact that it is possible to generalise the observed behaviour of SWE in this way means that it is possible to include it in some of the snowmelt models if considered necessary; it may also

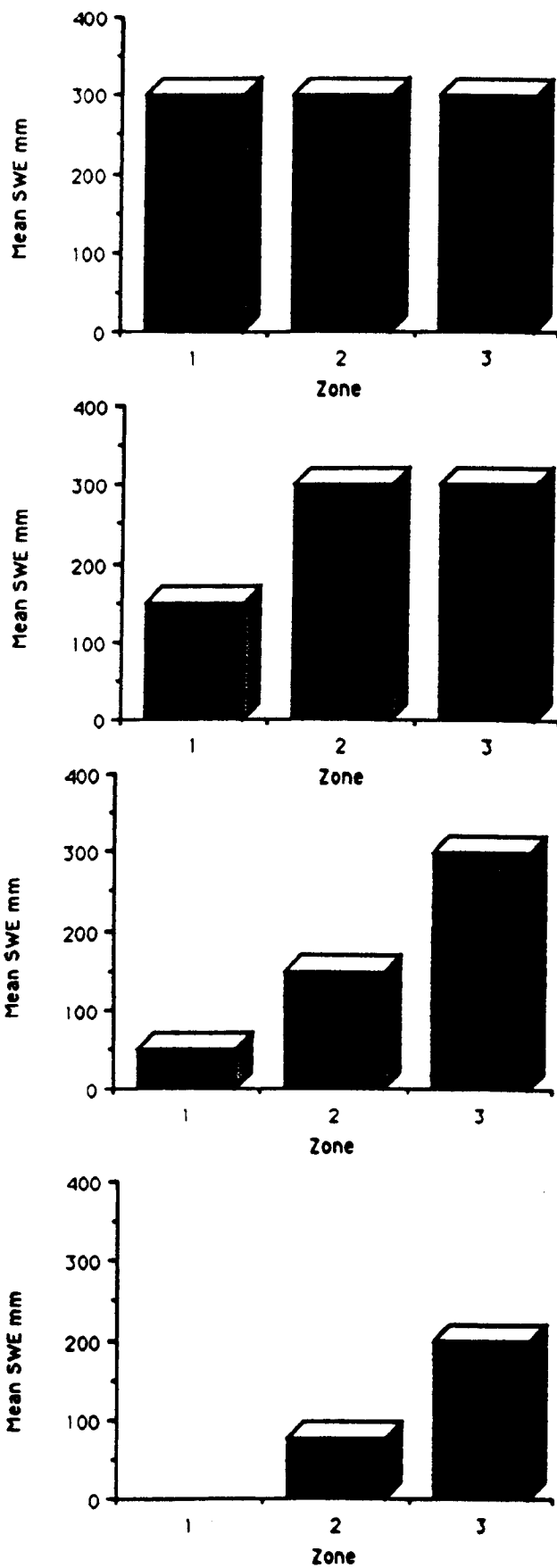
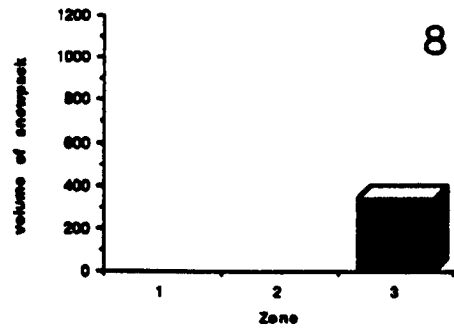
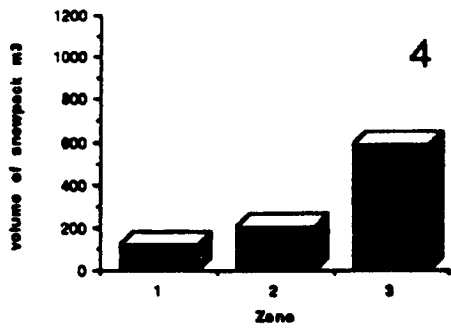
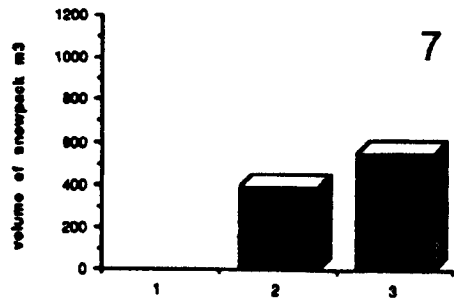
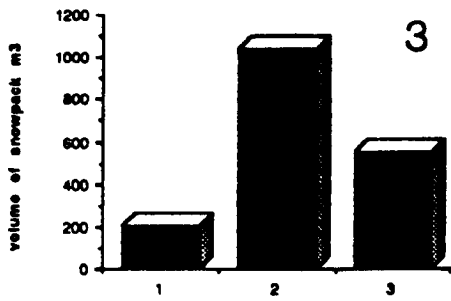
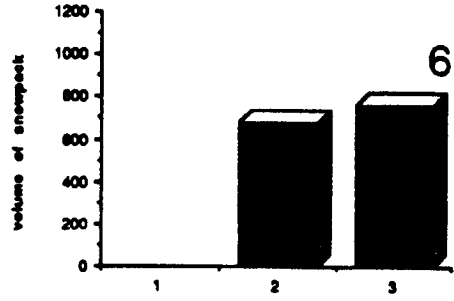
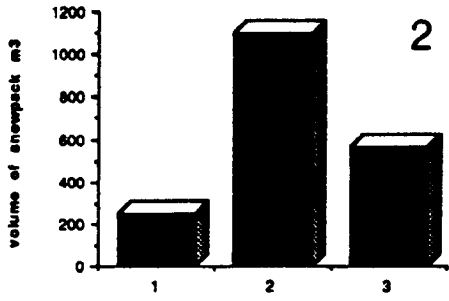
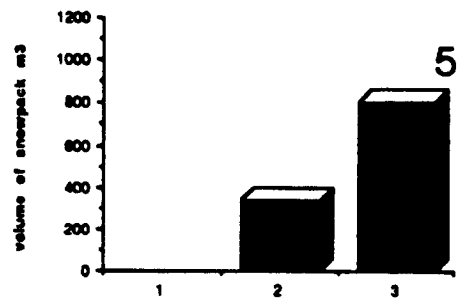
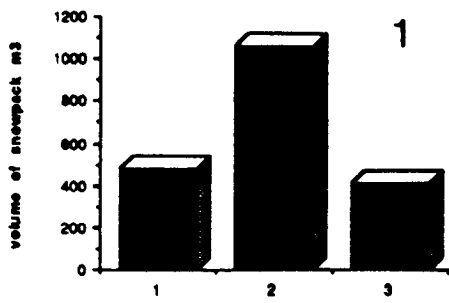
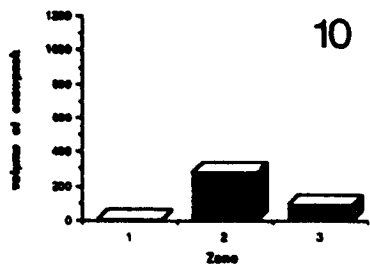
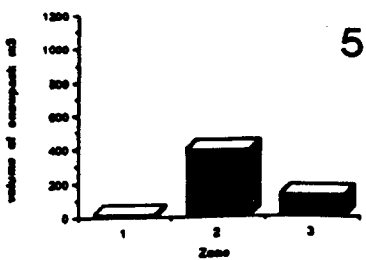
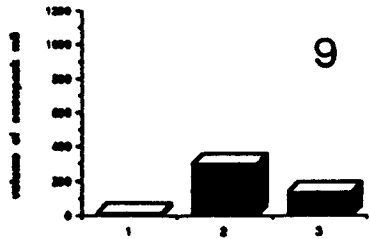
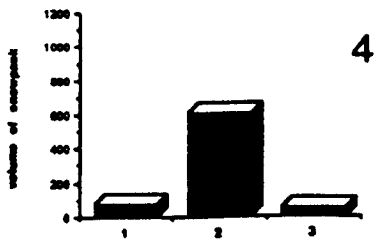
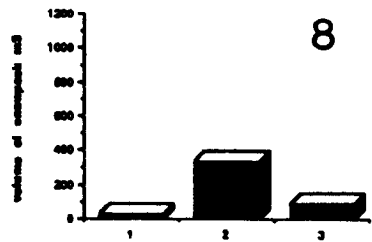
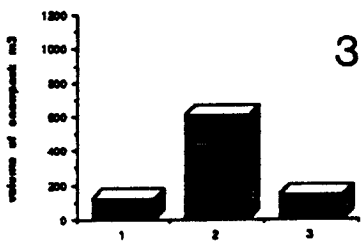
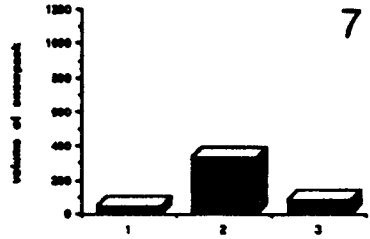
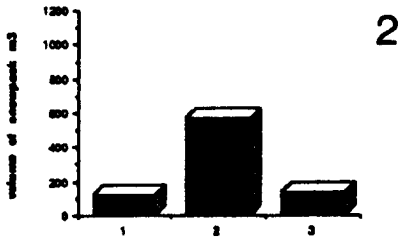
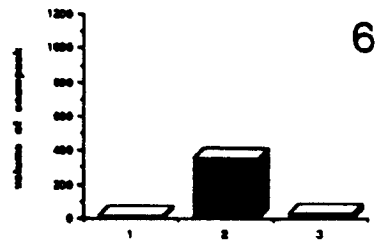
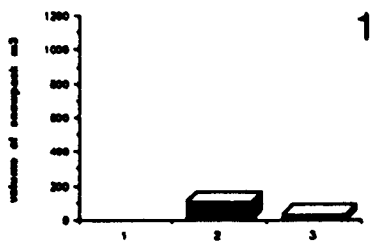


**Figure 3.6** Simplistic representation of the changing snowpack water equivalent for the three elevation zones.

Figure 3.7 Histograms showing the snowpack volume held in each of the three elevation zones. Zone 1 = the lowest, zone 3 = the highest. Numbers adjacent to histograms indicate the snow survey in Tables 3.1 - 3.3 that the data was derived from. All horizontal axes represent the three zones.

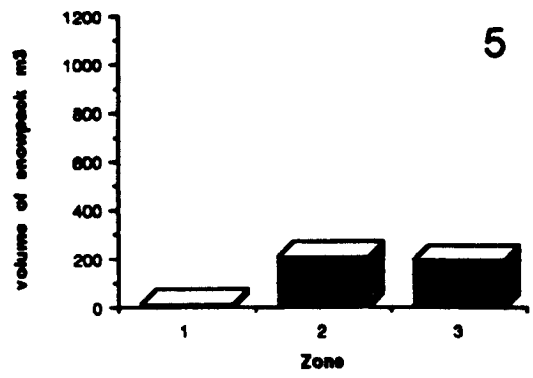
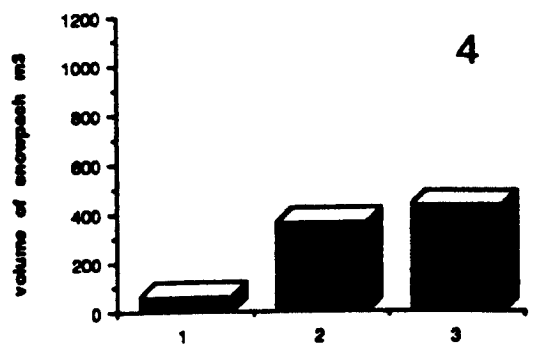
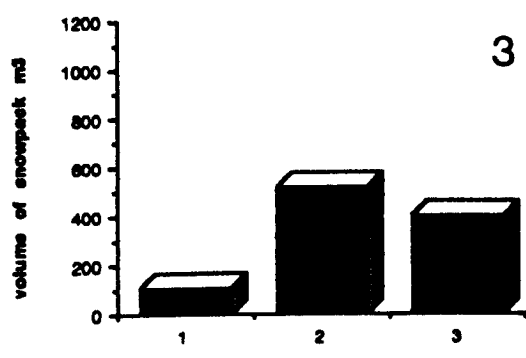
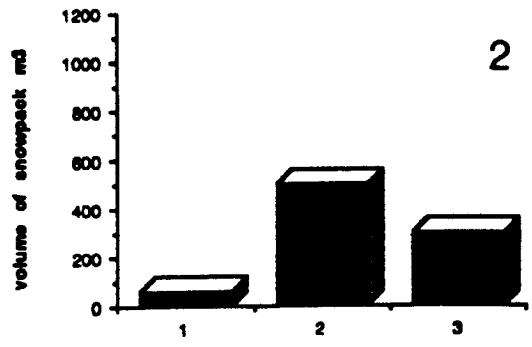
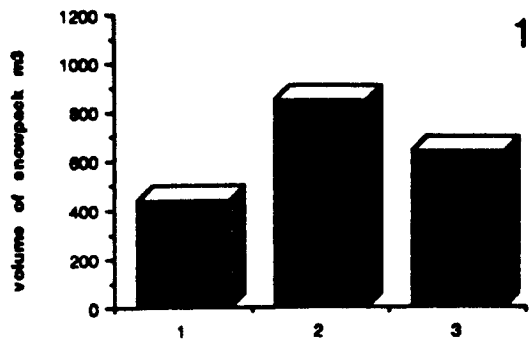


1986



1987

b



1988

be that by using a layered type model with suitable meteorological, melt and depletion submodels it will not be necessary.

Whilst the relative depth of snow in the three zones is shown by using SWE it is also useful to look at the relative volumes of snow in the three zones over the three melt seasons. This is shown in Figure 3.7 and it can be seen that, particularly in the early surveys of 1986 and 1988, the volume in zone 2 is greater than either zone 1 or 3. Whilst it can be argued that this is a function of the Mharcaidh's hypsometric curve, zone 2 having the greatest area, it can also be seen from Figure 1.9 that hypsometric curves for other Highland catchments used in the project are similar to that of the Mharcaidh, i.e. they will also have a greater area in zone 2 than either zone 1 or 3.

It can also be seen from Figure 3.7 that the ratio of volume held in zone 2 to that held in zone 3 decreases as the melt season proceeds. The later and longer the melt season and the higher the initial volumes the more likely it is that zone 3 will eventually hold a higher volume than zone 2. Thus, for 1987 (shortest, earliest season and lowest volume) the volume in zone 2 is always greater than that in zone 3; for 1988 (middle of three years for timing of melt season, duration and initial volume of snowpack) zones 2 and 3 hold similar volumes at the last survey; for 1986 (longest, latest melt season and highest initial

volume) zone 3 has a higher volume than zone 2 for the last five surveys.

### 3.2.2 Implications for generating runoff

What effects do the observed distributions of SWE and volume in the three zones have on the melt/runoff? A number of points can be made:

- (1) Initially zone 1, being the lowest of the three, is the most important in generating runoff as it is below the freezing level for a greater percentage of the time. This causes the SWE and volume of snow to deplete rapidly, thus reducing the SCA and consequential melt generated from the zone later in the melt season.
- (2) As the melt season progresses and the freezing level rises, zone 2 becomes the most important in generating runoff. Due to it covering the largest area it contains the greatest volume of snow, though the SWE may be less than that in zone 3. As more melt occurs this difference increases.
- (3) Finally, melt is potentially available in all three zones in the catchments (only for a short while in zone 1), although the rate varies inversely with altitude. Zones 2 and 3 have the greatest importance

in generating runoff as the only snow (if any) held in zone 1 will be deep patches in hollows and gullies. This is soon the case with zone 2 and eventually zone 3, the thin snow cover on exposed ridges and slopes quickly melting to leave that sheltered in the hollows and basins of the upper catchment (Plates 2.4, 2.6 and 3.1).

- (4) In addition to the general snowpack behaviour there are also temporary increases in the SCA, often to 100% of catchment area, caused by fresh snowfall. These are generally thin and melt quickly, thus only being detected by snow surveys carried out a short time apart. These are possible for any snowpack condition and, if followed by a warm period, can result in melt occurring over the whole catchment and thus generating high runoff values for a short while, there being little storage potential in the shallow snow cover on the lower slopes.

All these points can only be allowed for by dividing the catchment into a number of elevation zones and depleting the snowpack within the individual zones rather than treating the catchment as a whole. The project will investigate if this increases the performance of the models by comparing models with and without a layered structure. It will also investigate the performance of models that treat the catchment as a whole but allow for a freezing

level.

3.3 Metasp...



Plate 3.1 Exposed spurs and ridges within the Mharcaidh catchment often had little or no snow.

level.

### 3.3 Meteorological and flow data

Before commencing model development the 1986 and 1987 meteorological and hydrological data collected in the Mharcaidh by the Institute of Hydrology (contained in Appendix A) were examined. This was to study both the flow/weather patterns through the melt seasons and to see how well discharge can be simulated by meteorological variables using purely empirical relationships rather than conceptual models.

#### 3.3.1 Observed patterns

Plots of runoff, average daily temperature, total daily precipitation, mean daily windspeed, mean daily net radiation and mean daily total radiation for 1986 and 1987 (collected at the AWS at an altitude of 575m amsl (Figure 2.1)) are shown in Figures 3.8 and 3.9 respectively. From these and by studying the Daily Weather Summaries produced by the London Weather Centre (LWC) it is possible to summarise the weather during the two melt seasons:

(a) 1986 1 March - 12 May, 73 days in total

The 1986 melt season was preceded by a month of settled, cold weather. This was caused by an area of high pressure

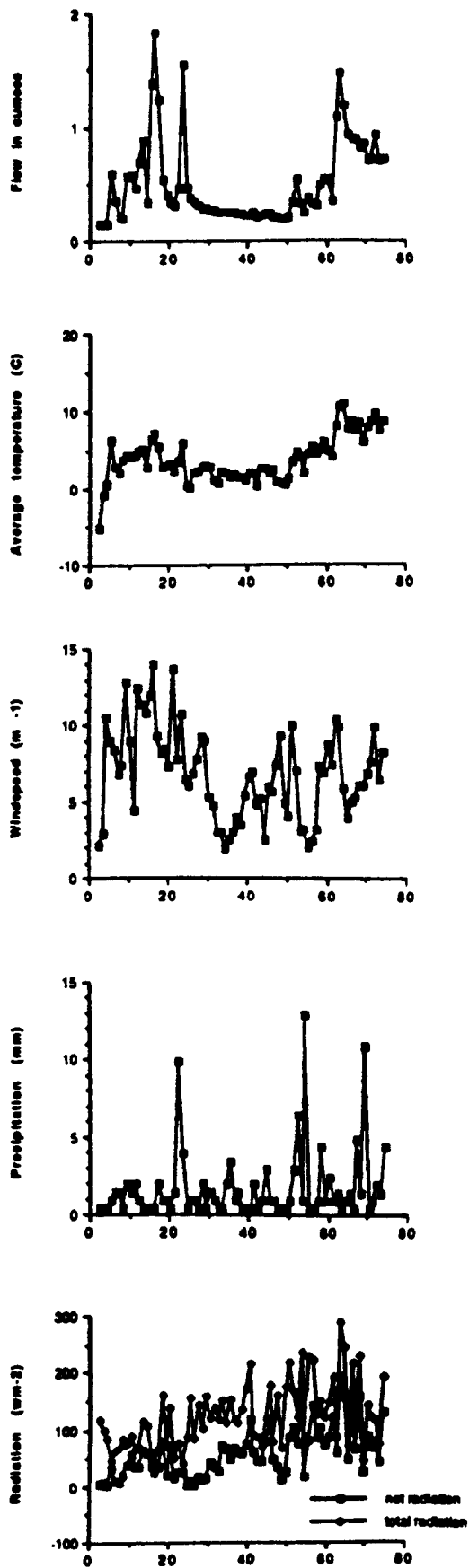


Figure 3.8

Time series plots of the 1986 hydrometeorological data.

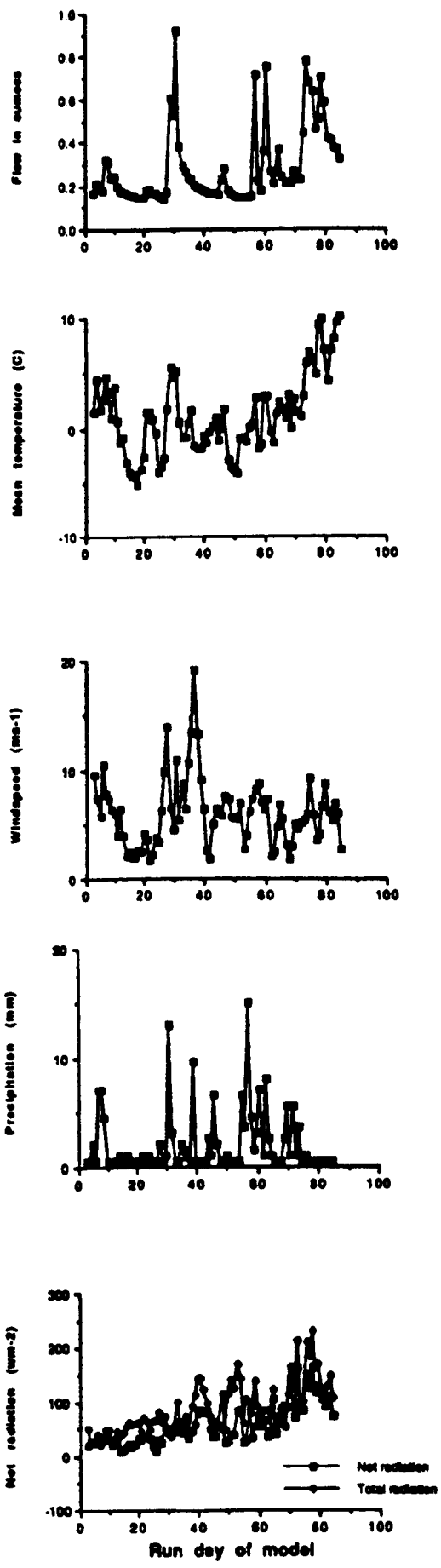


Figure 3.9 Time series plots of the 1987 hydrometeorological data.

building up to the NE of Britain on 2 February and remaining there until 2 March.

On 5 February the LWC noted "temperatures were below normal nearly everywhere, mostly in the rather cold or cold category". By 7 February "it was very cold over much of England and Wales and inland in Scotland, while remaining areas were rather cold." Temperatures remained close to freezing for the remainder of the month, there being many days when frost persisted for the whole day. The high pressure system weakened on 2 March and by 3 March "Scotland had near normal temperatures."

Between 0600 and 1200 on 4 March a warm front crossed Scotland, causing the sharp rise in temperature and fall in total radiation visible in Figure 3.8. This caused "a rapid thaw" and "most of the snow on low ground in the British Isles had thawed away by late evening." There then followed a two-week period of low pressure systems dominating the British weather. During this period temperatures were on the whole at or near to normal.

The most notable event was between 14 and 16 March when the whole of Britain remained in the warm sector of a frontal system. This resulted in the warm temperatures and high windspeeds visible in Figure 3.8 which produced the highest discharge of the two melt seasons ( $1.78\text{m}^3 \text{s}^{-1}$ ). This is equivalent to a melt rate of approximately  $15\text{mm day}^{-1}$  and is

totally due to snowmelt. Gales and persistent rain on 22 March produced the third highest precipitation event of the year (9.5mm), causing another day of high flows.

There then followed another period of settled weather, a high pressure system developing between 1 - 3 April and remaining in position until the 11th (Figure 3.10). This brought the return of cold temperatures and resulted in very low runoff values. It is interesting to note from Figure 3.8 that the difference between total and net radiation is much greater during this period. Due to the cold temperatures the snowpack will have re-frozen, resulting in the formation of ice crystals at the surface. As these are more reflective than wet snow the albedo of the snow will have increased, thus decreasing the net : total radiation ratio.

The cold weather continued for a further ten days until 20/21 April when an occluded front passed over Britain, resulting in the return of warm weather. The increase in temperature was only slight, resulting in low melt and runoff values, but on 30 April a warm front brought very warm and wet weather. This sudden rise in temperature, clearly visible in Figure 3.8, along with high winds and precipitation resulted in the discharge rising from  $0.292$  to  $1.419\text{m}^3 \text{ s}^{-1}$  in less than 48 hours, the third highest daily runoff value for the year. The high temperatures continued until the end of the melt season in a spell of unsettled

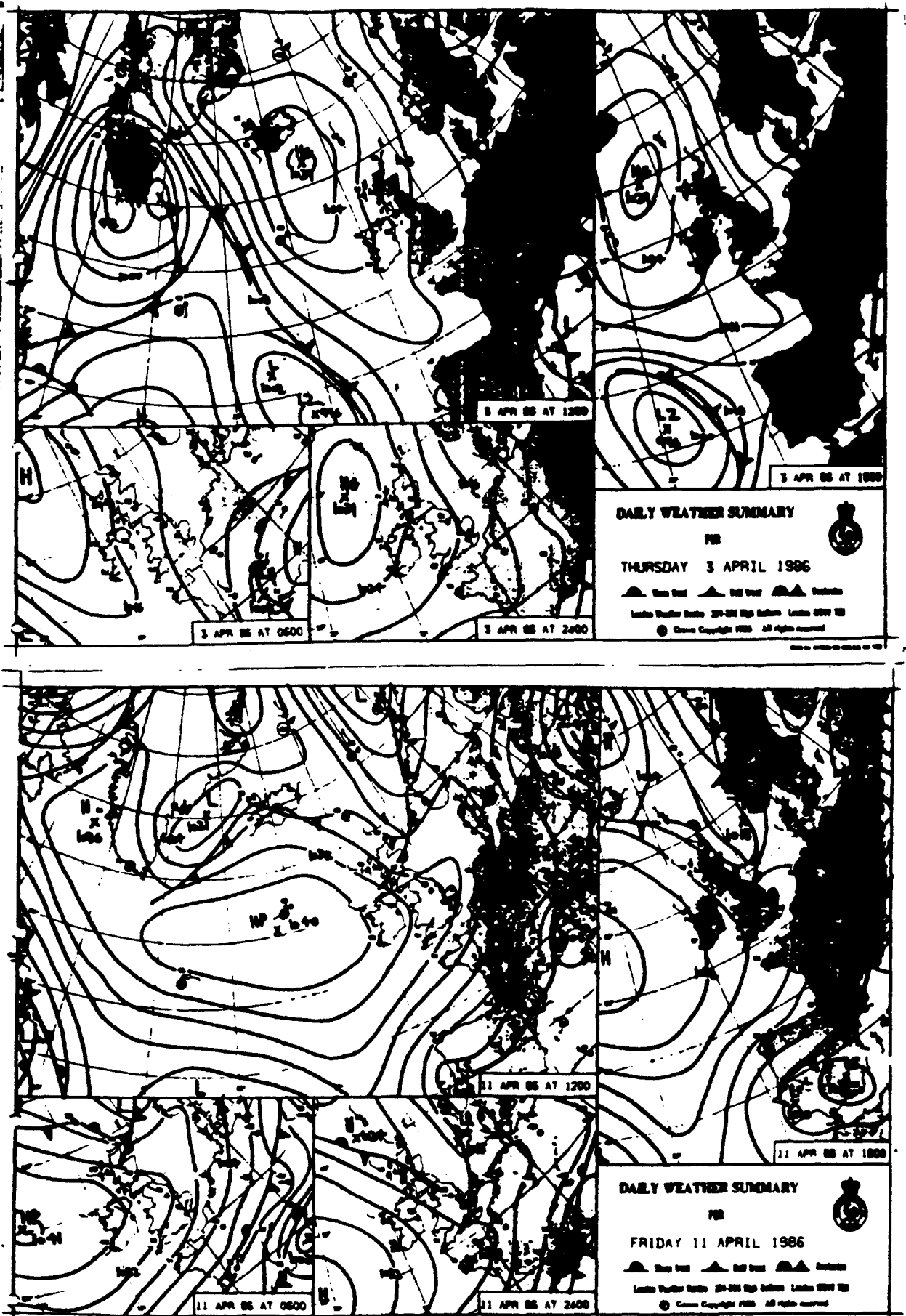


**Figure 3.10** Daily weather summaries produced by the London Weather Centre for 3 and 11 April 1986, illustrating the dominant high pressure system.

weather, high wind and precipitation events being common.

This resulted in a period of sustained melt and high flows until the snowpack was finally depleted.

(b) 1987 1 February - 24 April, 83 days in total

The 1987 melt season was also preceded by a period of stable, cold weather caused by an area of high pressure remaining to the north and east of Britain for most of January. This system weakened in early February, allowing an occluded and warm front to cross Scotland, bringing mild wet conditions on the 5th. This combination produced the first melt event in the Mharcaidh (Figure 3.9).

A new ridge of high pressure developed on 10 February to the north of Britain, this dominating the weather until 26 February. It was characterised by very cold temperatures, the mean daily maximum at the Mharcaidh AWS being  $-1.23^{\circ}\text{C}$  over the whole period, which in turn produced low runoff values. Due to the clear skies the total radiation was high, but, as in 1986, because the snowpack was frozen much of this was reflected resulting in low net radiation values. Windspeeds were low and only 2mm of precipitation was recorded at the AWS.

The high pressure system broke down on 26 February, a series of occluded fronts crossing Scotland between 26 - 28

February. By 1 March Scotland lay in a warm sector of a frontal system, warm south-westerlies from the strengthening Azores high bringing very mild and wet weather (12.5mm precipitation) which resulted in a sudden thaw and the highest runoff value for the season ( $0.892\text{m}^3 \text{s}^{-1}$ ) (as this equates to less than 8mm of runoff it can be mainly attributed to the precipitation).

By 4 March yet another high pressure system, this time over Scandinavia, began to dominate the Scottish weather. Cold winds from the continent brought the return of low flows though the period was not as settled as that earlier in the year or in 1986.

By 27 March the system had moved far enough to the north and east to allow a low pressure system to move across Britain. This produced the highest precipitation event of the season in the Mharcaidh (14.5mm) and a rise in maximum temperature from 0.9 to 5.7°C. The high melt associated with this caused the runoff to rise sharply from 0.125 to  $0.689\text{m}^3 \text{s}^{-1}$ . A further warm and mild event on 31 March/1 April again produced high runoff values.

Temperatures remained normal (-1 to 3°C at AWS) until 12 April when a ridge of high pressure from the Azores high began to extend across Britain, bringing mild and wet weather. This produced a peak in runoff on 13 April in the catchment, and again on the 18th following a day when

temperatures reached 16.1°C. As the SCA was low at this time (0.75km<sup>2</sup>) the runoff was only 0.678m<sup>3</sup> s<sup>-1</sup>; had the SCA been higher then a much higher runoff value is likely to have occurred. The warm weather continued until the end of the melt season, accompanied by high net radiation, resulting in a period of sustained melt and high flows that quickly depleted the remainder of the snowpack.

### 3.3.2 Relationships between meteorological variables and observed flow

The visual similarities between the meteorological variables and observed flow have been discussed in 3.3.1. The strength of all possible relationships between the meteorological variables and observed flow were tested using the MINITAB statistical package. Firstly, Pearson's correlation coefficients were calculated for the two years' data to gain an indication of the strength of the relationships. The results are given in Table 3.5.

From this it can be clearly seen that the strongest relationships are between temperature and flow, the mean daily temperature coefficient being the highest for both years (0.767 and 0.702). Whilst this was expected it does confirm that temperature provides the best single index to melt and resultant runoff. To investigate further, the best-fit regression lines between flow and mean daily

temperature were calculated using the least squares method. From these  $r^2$  values were calculated for 1986 and 1987, indicating that 58.8 and 49.3% of the variability in flow was accounted for by the variability in mean daily temperature.

Meteorological variable	1986	1987
Daily minimum temperature	0.720	0.636
Daily maximum temperature	0.691	0.674
Next minimum temperature	0.600	0.453
Mean daily temperature	0.767	0.702
Net Radiation	0.227	0.515
Total radiation	-0.072	0.259
Total daily precipitation	0.090	0.368
Mean daily windspeed	0.493	0.185

Table 3.5 Pearson's correlation coefficients between observed flow and meteorological data for the Allt a Mharcaidh catchment during the 1986 and 1987 melt seasons.

It can also be observed that the following day's minimum temperature has, not surprisingly, the weakest relationship of the four temperature variables. Whilst this decrease in the strength of the relationship is large for 1987 it is only minor for 1986; this can be accounted for by the period of low and stable flow when there was little difference in daily minimum and maximum temperatures caused by the high pressure system described in 3.3.1.

Of the remaining meteorological variables there does not appear to be much similarity between the two years, though total solar radiation does not have a strong relationship for either year. It thus more useful if the years are considered individually:

(a) 1986

In addition to temperature, mean daily windspeed is the only meteorological variable that shows a strong relationship with flow having a correlation coefficient of 0.493 ( $r^2$  value is 24%). This is due to the major melt events taking place at the beginning and end of the melt season when wind velocities were at their highest; during the period of low melt/flow the wind velocities were low due to the stability of the air mass. This relationship suggests that the approach used by Anderson (1968, 1973, 1976) might be successful in simulating the 1986 flow as it uses wind speed in addition to temperature as an index of melt during rain or snow events.

(b) 1987

Net solar radiation has the second strongest relationship with daily flow for 1987, having a correlation coefficient of 0.515 and computed  $R^2$  of 26.5%. This is due to radiation inputs being one of the strongest factors affecting energy exchange at the snow/air interface (Male and Gray, 1981).

Whilst this accounts for the strong relationship in the 1987 data, it also suggests that stronger relationships might have been expected for 1986. This was not so due to high radiation values occurring during the high pressure period when temperatures were low.

What is perhaps more significant is the strength of the relationship between total daily precipitation and flow for 1987, the correlation coefficient being 0.368 and the  $r^2$  14%, compared to 0.090 and 1% for 1986. This may be largely due to the high precipitation component of the main peak flow of the 1987 melt season identified earlier in 3.3.1(b) and again suggests that the method used by Anderson may have potential for use in the Mharcaidh.

Reference to 3.1.1 and 3.1.2 reveal further explanations for this: the snowpack during the 1987 melt season was very thin and quickly melted over the lower slopes. Snow falling later in the season only provided a thin cover that also quickly melted and offered little storage potential. Thus, for much of the 1987 season, more than 50% of the catchment was snow-free, resulting in a stronger rainfall/runoff relationship compared to years where the snowpack covered a greater extent for a longer period. This suggests that the 1987 flow record will be harder for a snowmelt model to simulate, the snowmelt accounting for a smaller proportion of total runoff.

### 3.3.3 Multiple regression analysis

In order to examine further the ability of the meteorological data to simulate the observed flow it was decided to carry out multiple regressions between the flow and meteorological data. This would also allow the models developed in the project to be compared to linear regressions (again using least-squares method). The MINITAB command BREGRESS was used to extract the best possible regressions using 1-8 meteorological variables. The results are shown in Table 3.6.

From this a number of points can be made:

- (1) When few variables are used the 1986 meteorological data is better at explaining the variation in flow than that of 1987. As the number of variables used increases this superiority decreases until, using all available data, there is only a 0.3% difference in the amount of variation accounted for.
- (2) For both years' data, only three meteorological variables are needed to obtain 90% of the optimum result using all eight variables, i.e. there is little advantage in using all variables. This is especially so for the 1986 dataset which achieves 95% performance using only two variables.

Number of Variables	Year	Meteorological Variables	R <sup>2</sup> (%)	% of best for year
1	1986	Average temperature	58.8	85.5
2		Average temperature and windspeed	65.6	95.3
3		The above and net radiation	67.1	97.5
4		The above and minimum temperature	68.1	99.0
5		The above & next min. temperature	68.7	99.9
6		The above and maximum temperature	68.8	100.0
7		The above and total radiation	68.8	100.0
8		All	68.8	100.0
1	1987	Average temperature	49.3	72.0
2		Average temp. & precipitation	59.0	86.1
3		The above and net radiation	61.7	90.1
4		The above and next minimum temp.	63.8	93.1
5		Average, min, & max temperature precipitation and net radiation	66.1	96.5
6		The above and total radiation	67.2	98.1
7		The above and next minimum temp.	68.1	99.4
8		All	68.5	100.0

Table 3.6 R<sup>2</sup> results from multiple regression analysis on the Mharcaidh 1986 and 1987 meteorological and flow data

- (3) For the 1986 dataset the best solution using two variables is found using those that gave the highest correlation coefficients in 3.3.2, i.e. average temperature and windspeed. However, this is not the case for 1987. Despite net radiation having a stronger individual relationship with observed flow than precipitation, average temperature/precipitation multiple regression out-performs average temperature/net radiation, the corresponding  $R^2$  being 59.0 and 50.5%.
- (4) Even when using detailed meteorological data less than 70% of streamflow variation can be accounted for using linear regression.

This final point was taken further by comparing the regressions obtained for the complete data sets. There was little similarity between the two regression equations (as Ferguson found (1984) for the 1979 and 1980 melt seasons in the Feshie catchment), suggesting that a general equation would not produce satisfactory results. As the overall aim of the project was to develop a model that could be universally applied the BREGRESS command was then applied to the combined 1986 and 1987 data. The results are shown in Table 3.7.

From these results it can be seen that when regressing on the combined data set more than 40% of the variability in

flow is unaccounted for by the eight meteorological variables. It can also be seen that the addition of net or total radiation data into the regression analysis makes no improvement.

Number of Variables	Meteorological variables	R <sup>2</sup> (%)
1	Average temperature	49.8
2	Average temperature and windspeed	54.5
3	The above and next minimum temperature	55.8
4	The above and precipitation	56.4
5	The above and maximum temperature	56.5
6	The above and minimum temperature	57.1
7	The above and net radiation	57.1
8	All (the above and total radiation)	57.1

Table 3.7 R<sup>2</sup> results from multiple regression analysis on the combined 1986 and 1987 meteorological and flow data collected in the Allt a Mharcaidh.

It was felt that this lack of improvement when using additional variables might have been due to the use of four different measures of air temperature. To see if this was the case two further regressions were carried out on the combined dataset, one using average temperature, precipitation and windspeed and the second using these and the two radiation variables. The computed R<sup>2</sup> were 55.3 and 55.4% respectively, confirming that the availability/addition of radiation data makes little difference to the regression.

The regression equation obtained from the combined dataset using all variables was then applied separately to the 1986 and 1987 datasets. The computed  $R^2$  values were 24.3% and 56.0%. Whilst multiple regression is useful as a means of identifying the variables that best account for the variation in streamflow, both individually and in different combinations, it can not be used in a universal form to simulate flow.

### 3.4 Comparison of measured inputs and observed outputs

Finally, before commencing on the actual development and testing of the models it was decided to compare the measured volume of the snowpack and precipitation to the cumulated flow gauged at GS1. The calculations are shown below:

#### 1986

##### Inputs

Volume of snowpack	2 139 000 m <sup>3</sup>
Precipitation = 94 mm over 9.91 km <sup>2</sup>	<u>931 000 m<sup>3</sup></u>
Total	3 070 000 m <sup>3</sup>

##### Outputs

Mean stream discharge @ GS1 = 0.445 m <sup>3</sup> s <sup>-1</sup>	
over 73 days	2 808 000 m <sup>3</sup>
Inputs - Outputs	263 000 m <sup>3</sup>

1987

Inputs

Volume of snowpack	984 000 m <sup>3</sup>
Precipitation = 124.4mm over 9.91 km <sup>2</sup>	<u>1 237 000</u> m <sup>3</sup>
Total	2 221 000 m <sup>3</sup>

Outputs

Mean stream discharge @ GS1 = 0.256 m <sup>3</sup> s <sup>-1</sup> over 83 days	1 836 000 m <sup>3</sup>
Inputs - Outputs	385 000 m <sup>3</sup>

From these results it can be seen that for both years the calculated inputs are greater than the observed outputs for the Mharcaidh and that the difference between the two is similar for both years. This may be due to a number of factors:

- (1) Errors (systematic or random) in the snow surveys over estimating the volume of water held in the snowpack and in measuring the precipitation and discharge.
- (2) Outputs in the form of evaporation/sublimation from the snowpack and transpiration from vegetation not being accounted for.

- (3) Some of the meltwater being used to recharge the soil moisture.
- (4) Meltwater still being in transit through the catchment at the end of the model run period.
- (5) Some of the precipitation being counted twice in determining the total inputs. This is especially likely for 1987 when snow surveys were carried out at intensive intervals, resulting in increases in the snowpack volume being detected late in the season. These increases are due to precipitation, yet the precipitation total was derived simply by multiplying the value recorded at the AWS by the catchment area. A more complex yet realistic calculation would involve multiplying the measured daily precipitation by the non-frozen part of the catchment for each precipitation event, resulting in a decrease in the total inputs.
- (6) Seepage into neighbouring catchments. This is very possible at the southernmost col at the head of the main Mharcaidh burn. The catchment divide is very difficult to define here and snow often accumulated in deep drifts (the location of Snow Survey Site 7).
- (7) Windblow of snow into and out of the catchment. This has been identified by many authors (for example

Davison, 1987, Fohn, 1980, Barry (1981)) and drifting of snow in the Mharcaidh has already been illustrated in Plate 2.5. As the Mharcaidh is situated on the western edge of the Cairngorms it is possible that, under westerly air flows, it is a net exporter of snow into neighbouring easterly catchments as it will receive less from the low lying ground to the west.

- (8) The difference between inputs and outputs may be due to snow still remaining in the catchment in the main gully and sheltered hollows (the importance of late lying snow patches has been identified by Spink, 1980). As the time period chosen for the 1987 melt season finished before that of 1986 this may account for 1987 having the largest difference despite having a smaller total volume.

All factors (1)-(8) are possible and likely, a combination of them all being the most likely explanation for the discrepancies. Whilst the magnitude of the actual differences is not too different for the two years, if it is expressed as a percentage of the calculated total inputs then 1986 is much lower, 8.6% against 17.4%. Factor (5) above would account for this, the precipitation accounting for 55.5% of the total inputs in 1987 and, if counted twice in the calculation, causes the total to be artificially high. Thus, whilst discrepancies do occur between the calculated inputs and observed outputs, the model

development could commence knowing that the snow surveys provided a reasonable estimate of the snowpack accumulation and ablation pattern over the two seasons.

## CHAPTER 4 MODEL DEVELOPMENT USING MHARCAIDH DATA

### 4.1 Introduction

The first model tested was called TINDEX and had the melt calculation based on the parametric temperature index method described by Ferguson (1984, 1986) and outlined in Chapter 1. The program was coded in Fortran 77 and ran on a DEC VAX 11/780 mainframe computer operating under VMS (Versions 5 and 5.1) in interactive mode. Whilst it was possible to run the model in batch mode, allowing a greater number of calculations to be made as CPU (Central Processor Unit) time is not limited, it was felt that the advantages of being able to see the model run and the greater flexibility of interactive mode were more beneficial. The program was structured so that different operations or stages of the model were contained in subroutines, making it easier to examine and alter any specific stage in the model development. These subroutines were accessed from the main core of the program which served as the link between data input and calculated output from the model. The coding of a later version of the model is printed in Appendix C, and a flowchart summarising the main steps in the model is shown in Figure 4.1.

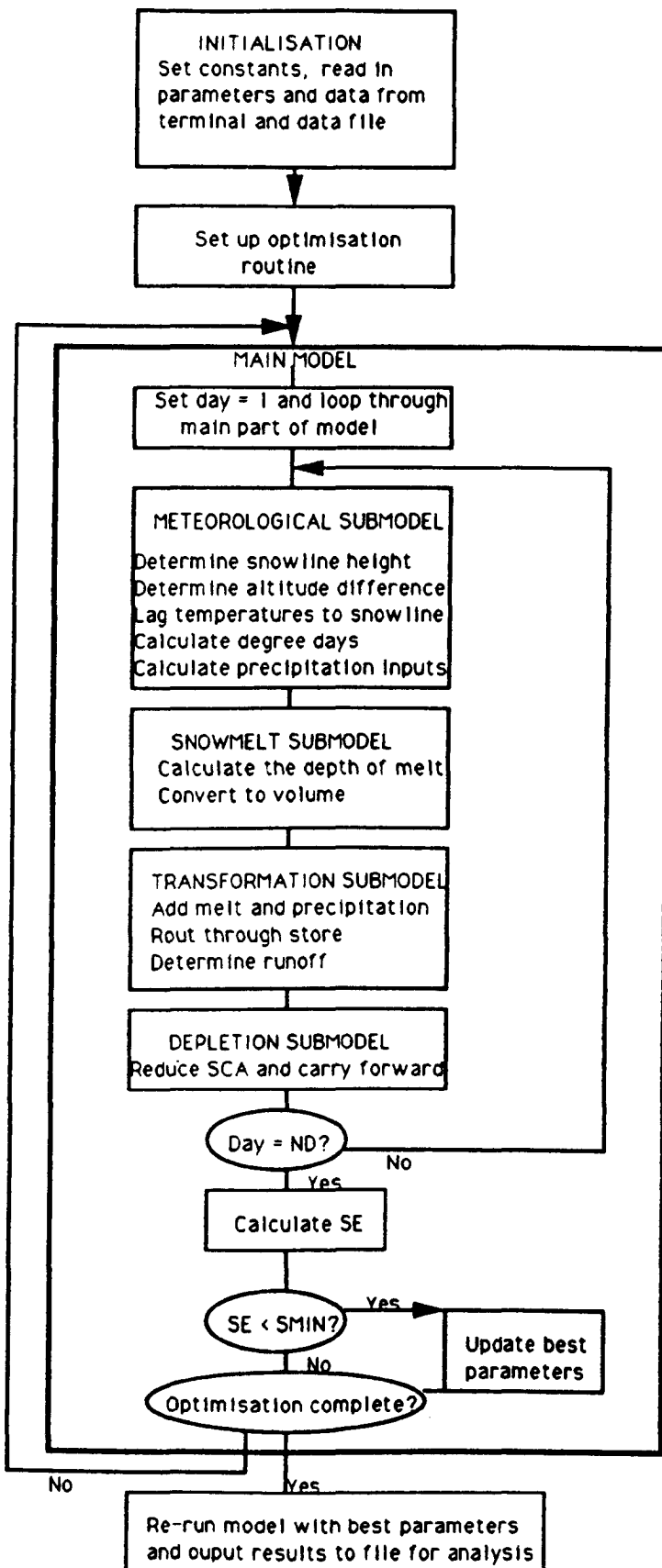


**Figure 4.1** Flowchart summarising the main steps in the temperature index model TINDEX.

## 4.2 Model Structure

### 4.2.1 Data Input

Once the user had typed in the command to run the model, the model prompted the user for a number of parameters:

- QO = Initial discharge at start of model ( $\text{m}^3\text{s}^{-1}$ )
- ND = Number of days over which the model is to be run
- E = Temperature lapse rate ( $^{\circ}\text{C m}^{-1}$ )
- R = Recession coefficient (dimensionless)
- AA = Initial Snow Covered Area ( $\text{km}^2$ )
- M = Melt factor ( $\text{mm}^{\circ}\text{C day}^{-1}$ )
- W = Initial mean Snowpack Water Equivalent over AA (mm)
- AB = Catchment area ( $\text{km}^2$ )

Initially three values of AA, M and W were requested and stored as one-dimensional arrays. The model was later altered so that a number of values of E and R were also requested, and later versions allowed the user to choose how many different values of each parameter he/she wished to input. These parameter arrays were used in the optimisation process which is described later.

Once the parameters and constants had been input, meteorological data and the day's actual discharge were read in from a data file, identified in the command to run the program. The data consisted of the following values:

TMIN = Minimum daily temperature (°C)  
 TMAX = Maximum daily temperature (°C)  
 NTMIN = Following day's minimum temperature (°C)  
 ATEM = Average temperature (°C)  
 PPT = Total daily precipitation (mm)  
 FLOW = Mean daily discharge (m<sup>3</sup>s<sup>-1</sup>)

TMIN, TMAX, NTMIN, ATEM and PPT were all recorded at the AWS in the catchment. FLOW was recorded at GS1 at the catchment outfall. TMIN and TMAX were the minimum and maximum of the 24 hourly values for the day rather than the values at, for instance, 0400 and 1600. NTMIN was obtained in the same way but for the following 24 hour period. ATEM was the arithmetic mean (to one decimal place) of the 24 hourly values. The 24 hour period that served as the 'hydrological day' had to be decided before the mean of the 24 values could be calculated to give the FLOW value. The data for 1986 and 1987 were studied to determine the approximate timing of the daily minimum flow. The values for each month are shown in Table 4.1.

Month	Approximate time of minimum daily flow
February	1000
March	0930
April	0830
May	0730

Table 4.1 Timing of Minimum Daily Flows, February - May, from the 1986 and 1987 flow records. Times are GMT.

Whilst there is an obvious trend for the minimum flow to be earlier in the day as the melt season progresses (due to the rise in radiation associated with longer day-length increasing melt in the early part of the day, thus causing the stage to rise) it was decided to standardise the input data so that the hydrological day started at 0900. In addition to making the coding of the model simpler, this also meant that the comparison between calculated melt and observed flow would be as consistent as possible throughout the melt season. The model then proceeded to calculate the daily melt, resultant runoff and deplete the snowpack using the four submodels as follows:

#### 4.2.2 Meteorological Sub model

The snowline height was calculated from the snow covered area at the start of the day using the hypsometric curve function,  $HT(A)$ . This function represented the hypsometric curve of the Mharcaidh as three straight lines (Figure 4.2). For a given value of  $A$  (snow covered area,  $\text{km}^2$ ) the snowline height was determined in the following way:

If  $A > 8.82$

$$HT = 600 - S2 * (A - 8.82)$$

else if  $8.82 > A > 0.94$

$$HT = 900 - S1 * (A - 0.94)$$

else if  $0.94 > A > 0$

$$HT = 1111 - S0 * A \quad (4.1)$$

where S2, S1 and S0 are the gradients of the three lines shown in Figure 4.2.

For the Mharcaidh,

$$\begin{aligned} S2 &= (600 - 341)/(9.91 - 8.82) \\ &= 233.9 \\ S1 &= (900 - 600)/(8.82 - 0.94) \\ &= 38.1 \\ S0 &= (1111 - 900)/0.94 \\ &= 224.5 \end{aligned} \tag{4.2}$$

Once the snowline height had been calculated the difference in air temperature between it and the AWS was calculated from:

$$DT = E * (HT(A) - 575) \tag{4.3}$$

where

DT = Temperature difference between AWS air temperature observation and that expected at the snowline (°C).

575 = Altitude of AWS in the Mharcaidh (m).

This value of DT, together with TMIN, TMAX and NTMIN were then used to calculate the number of degree-days in the function DD, based on the method used by Ferguson (1984). Figure 1.5 illustrates this method, and the equations used are given below:

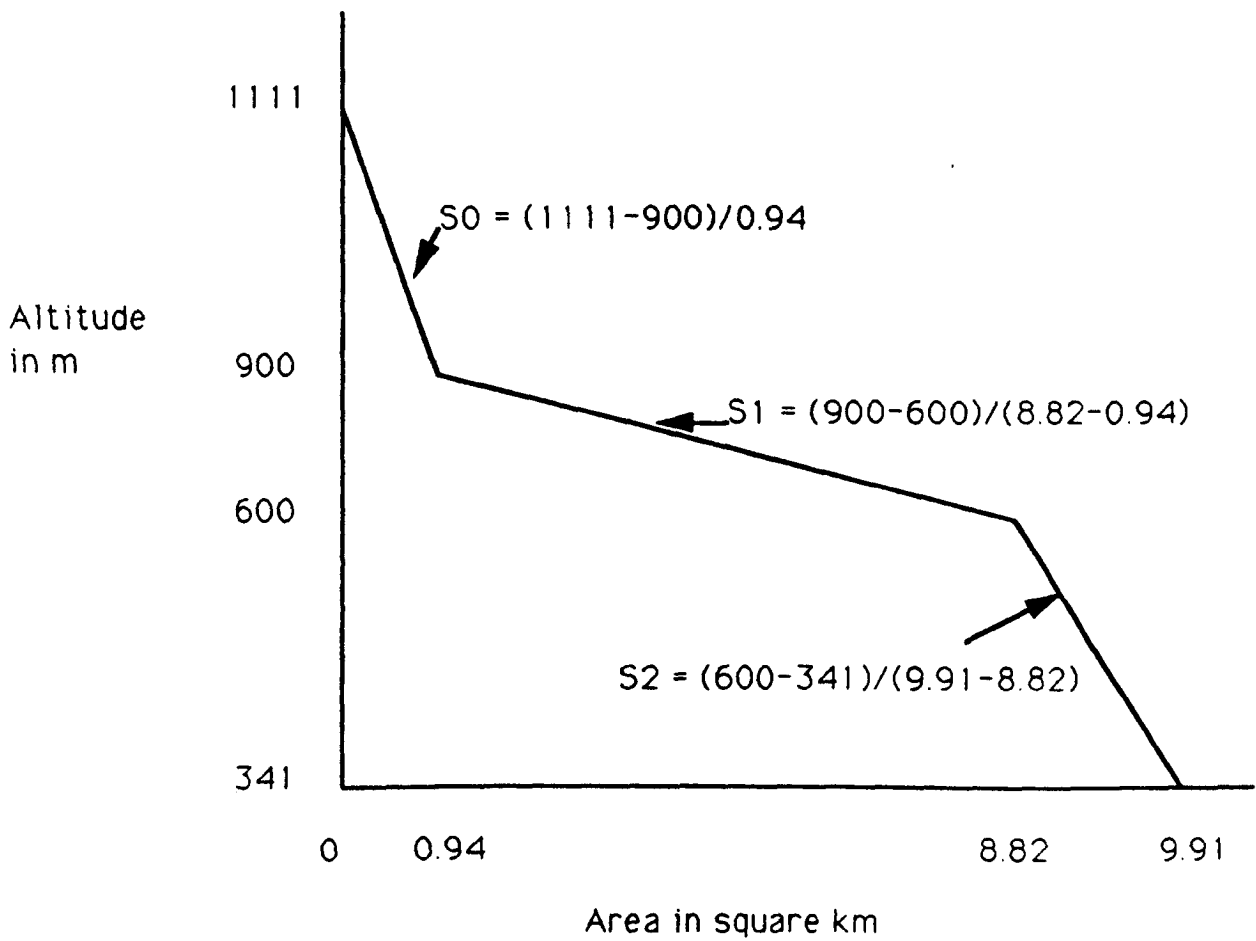


**Figure 4.2** Diagrammatic representation of the hypsometric curve used to apply the meteorological data to the Mharcaidh catchment by TINDEK.

$$\begin{aligned}
L &= \text{MAX} (0, T_{\text{MIN}} - DT)^2 \\
P &= \text{MAX} (0, T_{\text{MAX}} - DT)^2 \\
N &= \text{MAX} (0, N_{\text{TMIN}} - DT)^2 \\
DD &= 0.25 * ((P-L) / (T_{\text{MAX}} - T_{\text{MIN}}) + (P-N) / (T_{\text{MAX}} - N_{\text{TMIN}})) \quad (4.4)
\end{aligned}$$

#### 4.2.3 Snowmelt submodel

Once the number of degree-days had been established, the total volume of melt generated for that day was calculated from:

$$V = M * A * DD \quad (4.5)$$

where

$$V = \text{Total daily melt } (10^3\text{m}^3)$$

The total volume of daily precipitation,  $V_p$  (again in  $10^3\text{m}^3$ ), was then calculated for the snow-free part of the catchment from:

$$V_p = (A_B - A) * PPT \quad (4.6)$$

At this stage in the model development it was decided not to allow for precipitation over the snow-covered part of the catchment, or to differentiate between snow and rain over the snow-free area.

#### 4.2.4 Transformation submodel

Now that the total inputs to the stream were determined, i.e. V and VP, it was then possible to calculate the predicted mean daily discharge Q ( $\text{m}^3\text{s}^{-1}$ ). This was done by routing the combined melt and precipitation (if any) through a simple linear store, described by Martinec (1976) (see 1.3.3.1 equation (1.5)), and used by Ferguson (1984, 1986), in the following way:

$$Q = R * Q_{-1} + (1 - R) * (V + VP)/86.4 \quad (4.7)$$

where

$$Q_{-1} = \text{previous day's discharge, or if first day of model, initial discharge } (Q_0) \text{ } (\text{m}^3\text{s}^{-1})$$

#### 4.2.5 Depletion submodel

In order to reduce the snowpack by the volume of generated daily melt it was necessary to represent both the snowpack structure and simulate the distribution of melt taking place. Three possible alternatives were illustrated in Figure 1.6 after Ferguson (1984). The three considered for TINDEK are illustrated in Figure 4.3 and can be described as follows:

- (1) Uniform depth of snow over whole snow covered area; melt occurring at uniform rate over snowpack.
- (2) Uniform depth of snow over whole snow covered area; melt occurring only at lower boundary of snowpack.

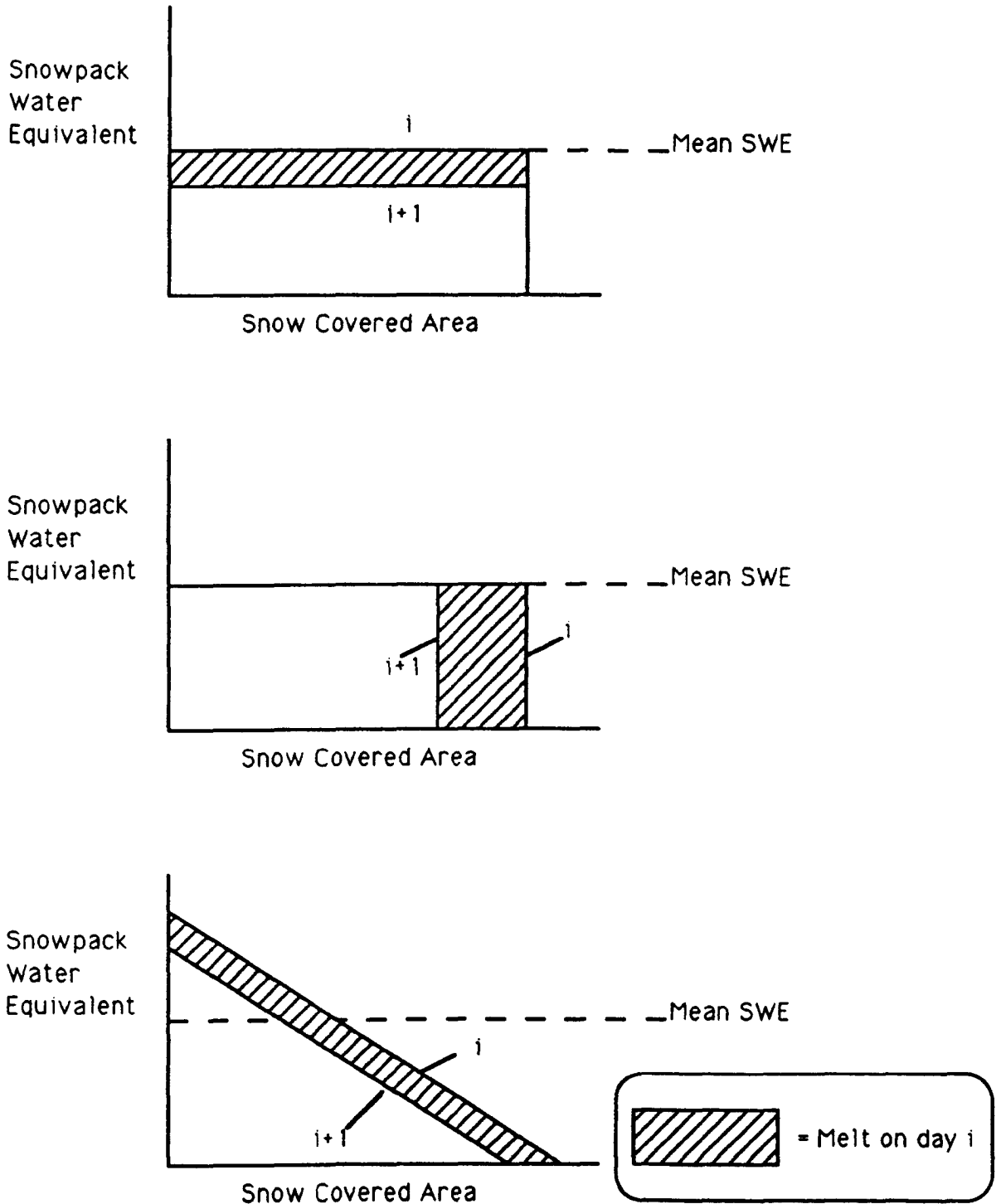


**Figure 4.3** The three different snowpack structures and methods of applying melt considered for use in TINDEK.

- (3) Depth of snow ranging from 0 to twice mean water-equivalent of snowpack; melt occurring at uniform rate over snowpack.

It was decided that neither (1) nor (2) were suitable for the following reasons:

- (a) The snow depth was not uniform over the whole of the snowpack (see 3.1.2 earlier).
- (b) Whilst it is possible that melt occurs over the whole area, option (1) would result in maximum snow covered area until the snowpack was totally depleted, when the cover would be suddenly reduced to 0. Chapter 3 shows that this is not the case and that the areal extent of the snowpack reduces gradually throughout the melt season.
- (c) Whilst (2) does result in a gradual reduction of the snowpack area it does not accurately reflect the distribution of melt over the snowpack. Melt does not occur only at the boundary of the snowpack (though it may be greater there), but over a wider area and, during the middle and later stages of the melt season when days are warmer, melt will be occurring over the whole snowpack.

Having rejected (1) and (2), option (3) was chosen as it offered (i) a range of snow depths over the snowpack; (ii) gradual reduction in snowpack area as the melt season

progressed; (iii) uniform melt over the whole snowpack. It was realised that point (iii), whilst being possible during the middle and later stages of the melt season, was not so early on when those parts of the snowpack at higher altitude might still be below 0°C whilst those lower down would be melting. This problem was investigated in a later version of the model.

Once structure (3) had been selected, the method of depleting the snowpack could then be established. If the slope of the snowpack distribution, SSD, is defined as:

$$SSD = 2 * W/A \quad (4.8)$$

then the depleted area of the snowpack can be calculated by:

$$A_n = (A_{n-1}^2 - 2 * V/SSD)^{0.5} \quad (4.9)$$

where

$A_n$  = Area of snowpack after melt on day n

$V_n$  = Volume of melt produced on day n

This new value of A was then carried forward to the calculations for the following day. It was not necessary to update the value of W as SSD was defined at the start of the model and kept constant throughout, thus ensuring that only A was needed to calculate the daily melt and snowpack.

Once the daily melt, runoff and snowpack depletion had been calculated the model programmed to the next day and repeated the calculations for ND days. Figure 4.4 shows the step-by-step calculations involved for one day, based on fictitious data.

#### 4.2.6 Optimisation

The calculations described so far are for only one value of AA, M and W, yet the model was initially designed to run on three values for each parameter (4.2.1). This was to enable the user to optimise the model, i.e. to find the set of parameters that allowed the model to most accurately simulate the observed flow. The optimisation process used in the model was designed with the following criteria in mind:

- (1) The coding was to be as simple and clear as possible, thus allowing other users to use and change the structure if they so wished, even if coming to the model 'cold'.
- (2) The user was to be kept informed as the optimisation procedure progressed so that the effect of changing parameters could be observed.
- (3) The user was to have full control over the values optimised, i.e. the model would only be optimised for the parameters input by the user. This was to ensure that only physically reasonable solutions were found.

TMIN = 1	E=0.008
TMAX = 5	R=0.6
NTMIN = 2	AA=8
PPT = 1	M=3
FLOW = 0.57	W=200
Q0=0.48	AB=9.91

METEOROLOGICAL SUBMODEL

As 8.82>A>0.94

HT(A)	=	900-(38.1x(8-0.94))	Snowline height
	=	631m	
DT	=	Ex(HT(A)-575)	Temperature difference
	=	0.448 °C	
L	=	(TMIN-DT) <sup>2</sup>	=0.304
P	=	(TMAX-DT) <sup>2</sup>	=20.721
N	=	(NTMIN-DT) <sup>2</sup>	=2.409
DD	=	2.802	Degree days

SNOWMELT SUBMODEL

V	=	MxAxDD	
	=	67.25x10 <sup>6</sup> m <sup>3</sup>	Volume of melt
VP	=	(AB-A)xPPT	
	=	1.91x10 <sup>6</sup> m <sup>3</sup>	Volume of precipitation

TRANSFORMATION SUBMODEL

Q	=	RxQ-1+(1-R)x(V+VP)/86.4	
	=	0.608m <sup>3</sup> s <sup>-1</sup>	Discharge

DEPLETION SUBMODEL

SSD	=	2xW/A	
	=	50	
An	=	((An-1)x(An-1)-(2xv/sdd) <sup>0.5</sup>	
	=	7.830km <sup>2</sup>	Update SCA

Figure 4.4 Summarised step by step calculations used in the main TINDEK model for one day. Fictitious data are used.

(4) The optimisation was to be complete, i.e. the final optimised set of parameters had to produce the peak or sink in the response surface (depending on whether the procedure worked by maximising or minimising a function) and not merely a localised pinnacle or dip (see Figure 4.5).

The optimisation used in the model was based on minimising the standard error (SE) of the predicted values:

$$SE = \frac{1}{n} \sum_{i=1}^n (\text{Observed}^{(i)} - \text{Predicted}^{(i)})^2 \quad (4.10)$$

where

SE = standard error

In the terms used in the model, (4.10) becomes:

$$SE = \frac{1}{ND} \sum_{i=1}^{ND} (\text{FLOW}_{(i)} - Q_{(i)})^2 \quad (4.11)$$

In the actual coding, the daily error, ERR, was calculated and then squared to be added to a cumulating value, SS, the sum of squares:

$$SS_n = SS_{n-1} + \text{ERR}^2 \quad (4.12)$$

where

$$\text{ERR} = \text{FLOW} - Q \quad (4.13)$$

Once the model had been run for ND days, SE was calculated from:

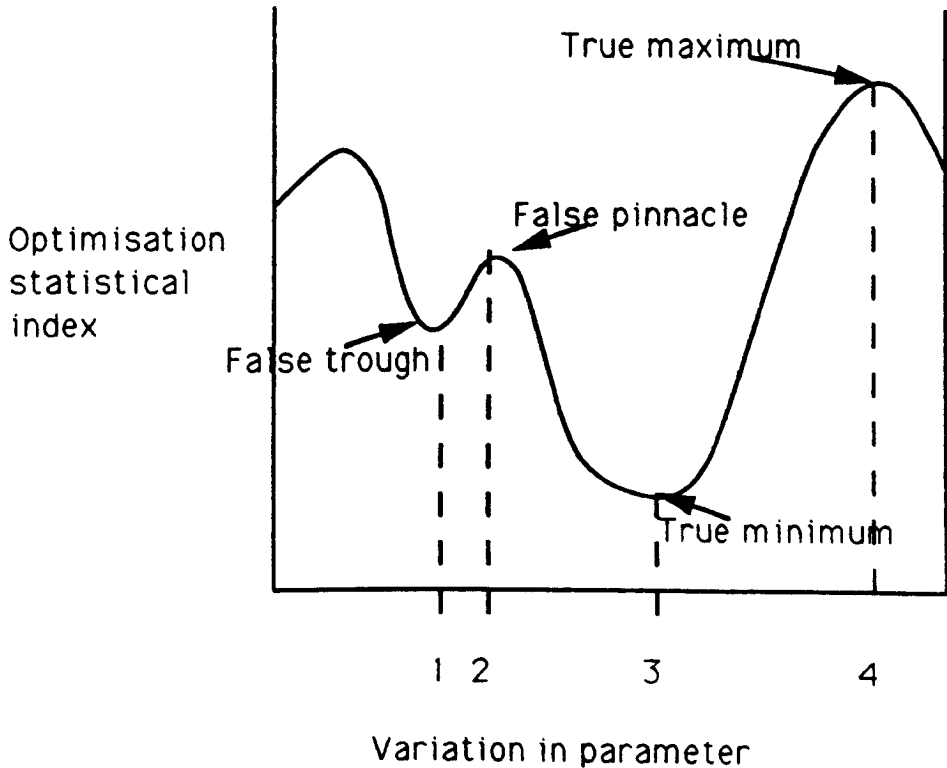


**Figure 4.5** Pictorial representation of the problems associated with using a statistical index when optimising. If the index is to be optimised on a maximising function then value 4 provides the true optimum; value 2 is a false pinnacle that may be given as the optimum solution by some optimising routines. Similarly, if a minimising function is used value 3 is the optimum parameter value and value 1 is a trough in the response surface that gives a false value

The optimisation was carried out using a series of nested Do-loops in the coding for the model. These worked in the following way:

- (1) The model started by using the three initial values of AA, M and W and ran through the data for ND days.
- (2) The value of SE was stored, SMIN, along with AA, M and W which were stored on BA, BM and BW. The model output the value of SE, BA, BM and BW to the terminal to inform the user.
- (3) The initial values of AA and M were then kept constant and the model repeated step (1) with the next value of W.
- (4) If the new value of SE was lower than SMIN, SMIN was updated, along with BA, BM and BW, the user being informed of this via the terminal. If the new value of SE was greater than SMIN then no values were changed.
- (5) Steps (3) and (4) were repeated until all values of W had been used. The model then kept AA constant and repeated steps (3) and (4) with the next value of M and all values of W.
- (6) Step (5) was repeated until all values of M had been used. The model then repeated steps (3), (4) and (5) with the next value of AA and all values of M and W.
- (7) Step (6) was repeated until all possible parameter

combinations had been tried and the optimum solution (from the initial parameter set) stored as BA, BM and BW.

- (8) Finally, the programme re-ran the model with the final values of BA, BM and BW, writing the daily output from the calculation to an external data file for later inspection and analysis.

It can thus be seen that, for the first model tested, a total of 27 ( $3^3$ ) different parameter combinations were used. Models developed later in the project allowed the optimisation of up to seven different parameters, with up to 10 different values for each parameter. This offered a potential of  $10^7$  different parameter combinations; in reality the limitations imposed by the CPU time limit meant that a maximum of approximately  $10^4$  different combinations could be tried, allowing three or four different values if each of the seven parameters were being optimised. If, however, only five parameters were being optimised, then six values of each parameter were possible. When using the model, parameter values to be optimised were initially chosen that spanned the whole range of physically reasonable values. Successive model runs had this range reduced, being centred on the optimised values from the previous run. The increments between values were also reduced, thus allowing the optimisation process to converge on the sink in the response surface that represented the optimum simulation. As the users of the model governed the

increments in the parameter values to be optimised they were also able to decide the sensitivity of the optimised solution.

#### 4.2.7 Preliminary analysis of output

The output data file (usually named LOOK.AT) obtained from the optimal parameter set was read into the MINITAB statistical package. The data file contained daily values of Q, FLOW, A and on some occasions PPT. The user could easily alter the model to output other values such as V, TMIN, TMAX etc. The MINITAB package, being powerful and simple to use, was used to study the output and compare the observed simulated discharges of the Mharcaidh.

Two methods were used to do this, one visual and one statistical:

##### (1) Visual

Using the command MTSLOT both the observed and simulated discharges were plotted as a time series on the same axis. This allowed a visual inspection of the model performance, comparison of peaks and troughs and allowed the user to see if the general pattern of the flow record was replicated. A time series plot of the snow covered area was also produced for some of the data files to allow comparison between the

observed depletion curve (from field observations in 3.1.1) and that from the model run.

(2) Statistical

As the value of SE is directly related to the mean discharge over the model run, a larger value of SE being expected for an event that has higher mean discharges, it is not possible to use this when comparing the model output for different years or for different catchments. Because of this, a value  $R^2$  based on the Nash and Sutcliffe (1970)  $R^2$  coefficient, was calculated using the following equation:

$$R^2 = 1 - (SE/SD)^2 \quad (4.15)$$

where

SD = Standard deviation of observed values

SE = Standard error calculated in (4.14)

Figure 4.6 shows a sample output from the MINITAB analysis, along with the commands used to calculate the  $R^2$  value. It can be seen from the output that the resolution of the MTSLOT produced by MINITAB was very weak - values were rounded up or down to the nearest increment on the y-axis with the result that the plot was very angular. During the later stages of the project the UNIRAS system became available on the VAX, allowing better quality output via either a pen plotter or laser printer using the

```

1
MTB > read 'DB4.1' c1 c2
60 ROWS READ

```

```

ROW      C1      C2
 1      0.051    4.4
 2      0.052    4.7
 3      0.054    4.4
 4      0.036    4.4
. . .

```

```

MTB > exec
MTB > let c4=c2-c1
MTB > let k1=1-stan(c4)**2/stan(c2)**2
MTB > print k1
K1      0.836473
MTB > end
MTB > mtsplot c1 c2

```

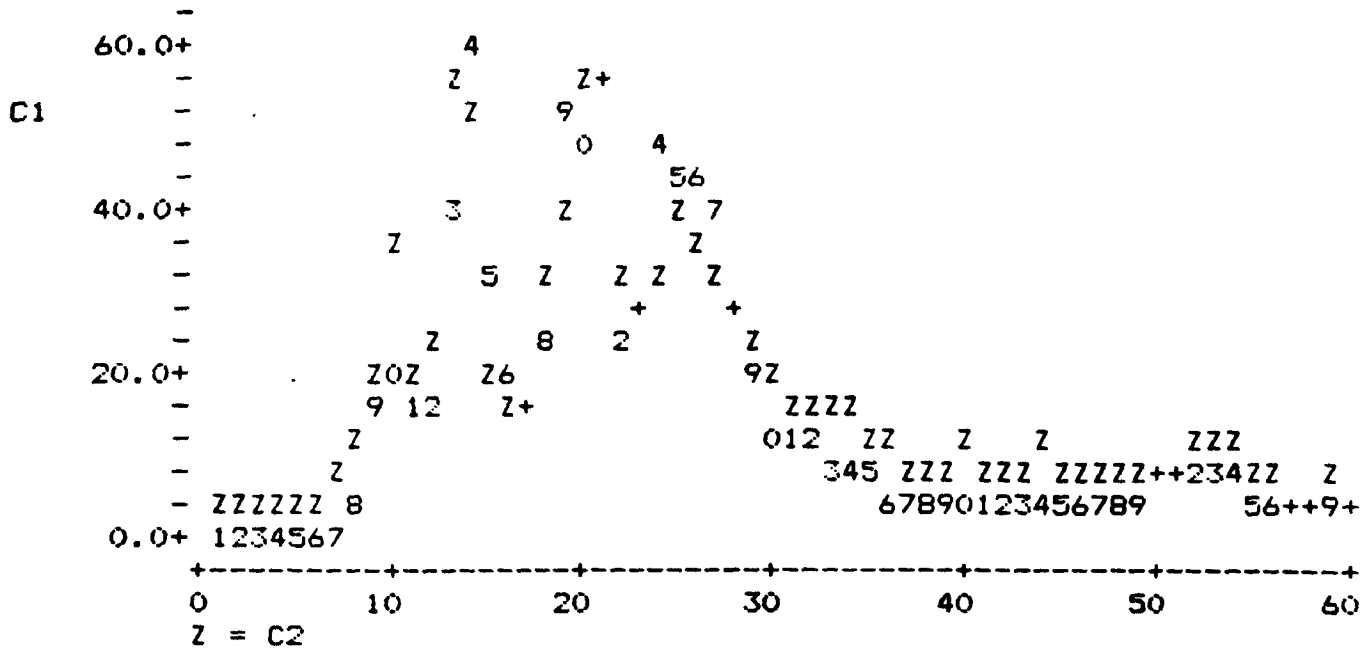


**Figure 4.6** A sample MINITAB output illustrating the low resolution of the time series plots and the method used to calculate the  $R^2$  value for each model run.

UNIGRAPH package. Because of this a 'standard graph' with no data values was created; by reading the Q and FLOW values into this standard graph a plot with high resolution could be quickly generated. The plots that appear later in the thesis were produced in this way.

Once the data file had been analysed in MINITAB, it was renamed and archived on the VAX. In this way it was possible to keep a copy of all optimised model output without using up too much file store.

#### 4.3 Running TINDEK on 1986 and 1987 Data

##### 4.3.1 The data sets

Two data files were created, DAT.DAT and DOT.DAT, containing the meteorological and hydrological data for 1986 and 1987 respectively. The length of the data sets were limited by two factors:

- (1) The length of the melt season - there was no point in testing the model over a period when there was no snow in the catchment as it was not designed to be a rainfall-runoff model.
- (2) The availability of a suitably long and reliable data set. IH reported some problems with GS1 freezing up at some times, battery and data logger failure at the

AWS and data being lost in the transfer process from logger to micro-computer to mainframe. By checking the data set with the observations of Joe Porter (the IH observer who visited the Mharcaidh every two to three days) and the snow survey data the following data sets were created:

DAT.DAT Start 1 March 1986. Finish 12 May 1986. ND = 73  
Initial Q = 0.091. Mean Q = 0.445 m<sup>3</sup>s<sup>-1</sup>

DOT.DAT Start 1 February 1987. Finish 24 April 1987.  
ND = 83 Initial Q = 0.140. Mean Q = 0.256 m<sup>3</sup>s<sup>-1</sup>

Both these data sets, together with those for other catchments and years, are in Appendix A.

Whilst the data sets could have been extended by interpolating between missing values, it was felt that this was likely to produce errors at a later stage. Whether this was likely to improve or worsen the model performance was irrelevant; the fact that it would alter it was enough to mean that extended data sets were not used for model development.

The early model runs using the Mharcaidh data optimised only the parameters AA, M and W (4.2.1). After some three months of model development it was discovered that the meteorological data contained daily average precipitation

data rather than daily totals. Thus, much of the early work had to be re-done. By this point the model was optimising E and T in addition to AA, M and W and it seemed sensible to continue this.

It was decided to impose limits on the range of values the model could optimise for two of the parameters, E and AA. These limits were chosen as the dry and saturated adiabatic lapse rates for E, the maximum and minimum that were realistically likely to occur:

E     Upper limit =  $0.010^{\circ}\text{Cm}^{-1}$  (Dry adiabatic lapse rate)  
       Lower limit =  $0.006^{\circ}\text{Cm}^{-1}$  (saturated adiabatic lapse rate)

For AA the upper limit was determined by the catchment area and the lower from the snow survey data:

AA    Upper limit =  $9.91\text{km}^2$  (Catchment area)  
       Lower limit =  $7\text{km}^2$

The lower limit of AA was chosen as, at the start of both data sets, the catchment had complete or near complete snow cover. Whilst the model might have optimised a lower value of AA in some cases if no limits were imposed, it was decided that, as the ultimate aim of the model development was to create a model that could run on observed data, the limit should be close to the observed value. With hindsight, a better method may have been to let the model

produce two optimised parameter sets, one with limits imposed and one without.

#### 4.3.2 Results from the first run of TINDEX

The optimised parameter sets, together with the SE value,  $R^2$  and the final area of the snowpack (FA) are given below in Table 4.2:

Year	1986	1987
E ( $^{\circ}\text{C m}^{-1}$ )	0.010	0.006
R	0.380	0.540
AA ( $\text{km}^2$ )	7.0	7.0
M ( $\text{mm}^{\circ}\text{C day}^{-1}$ )	3.0	2.0
W (mm)	380	160
SE	0.2245	0.1197
$R^2$	0.628	0.582
FA ( $\text{km}^2$ )	2.280	1.610

Table 4.2 Results from applying TINDEX to the Mharcaidh 1986 and 1987 datasets.

The UNIRAS time series plots of observed and simulated discharge are shown in Figure 4.7. From these plots and the data in Table 4.2 a number of points can be made:

- (1) The optimised E values for the two years are at either end of the permitted range, the higher value for 1986 indicating a greater reduction in air temperature for a given rise in altitude than the 1987 value. This is

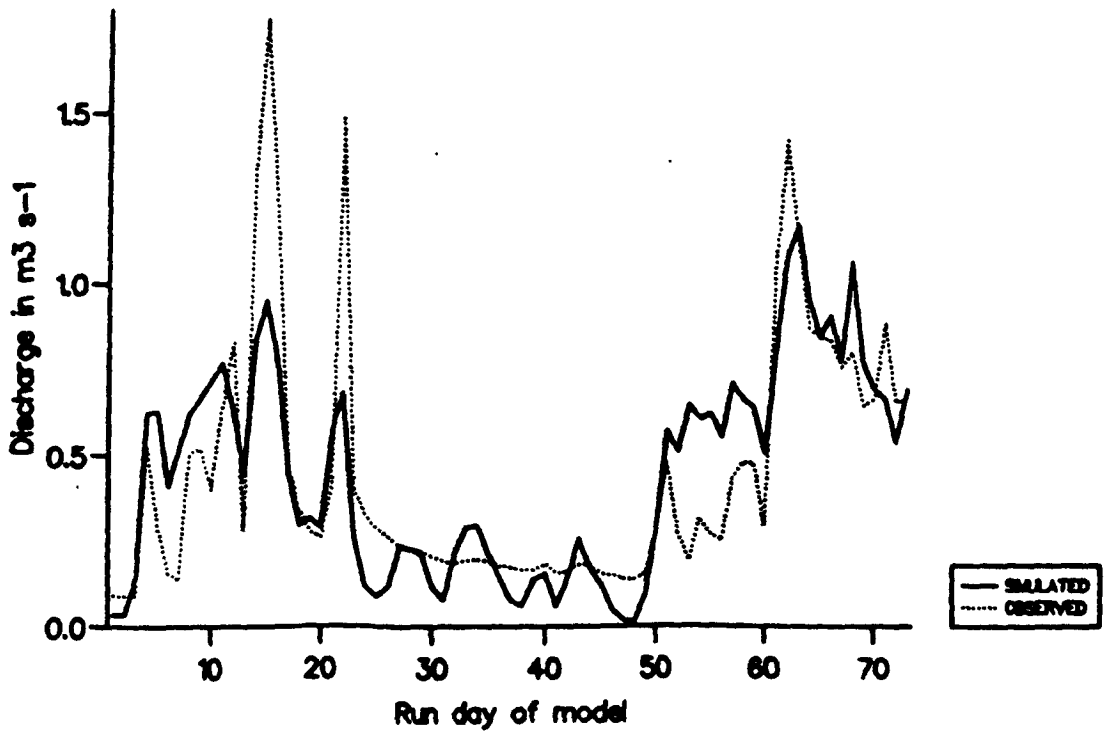
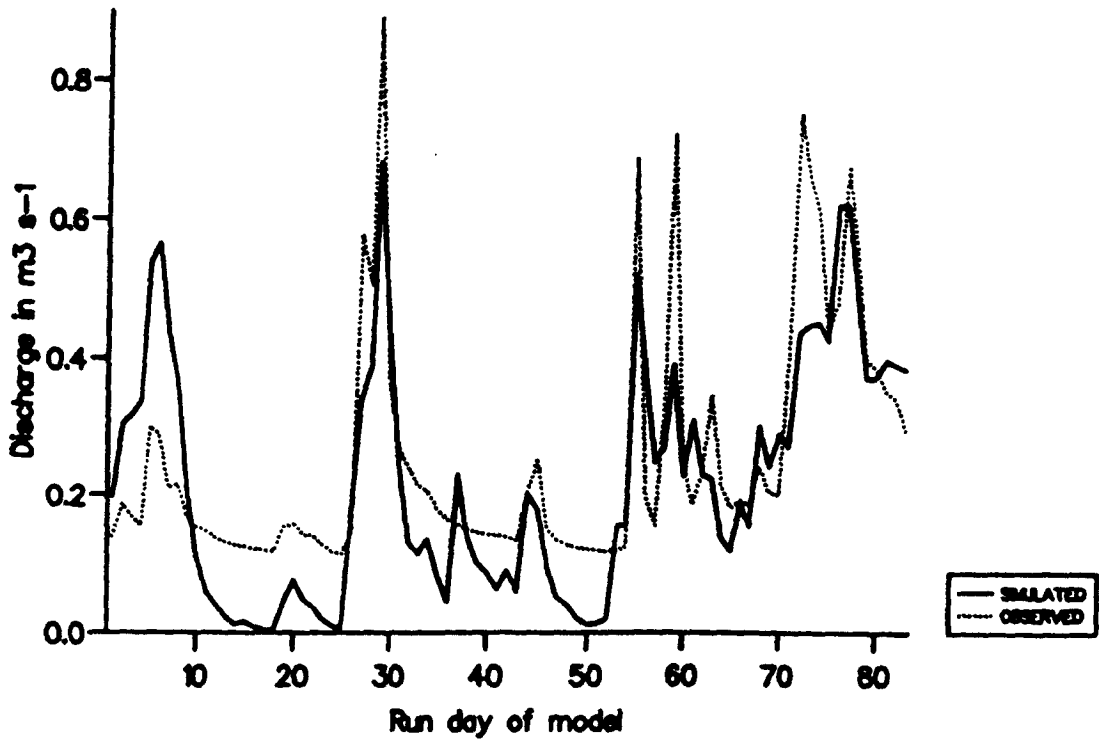
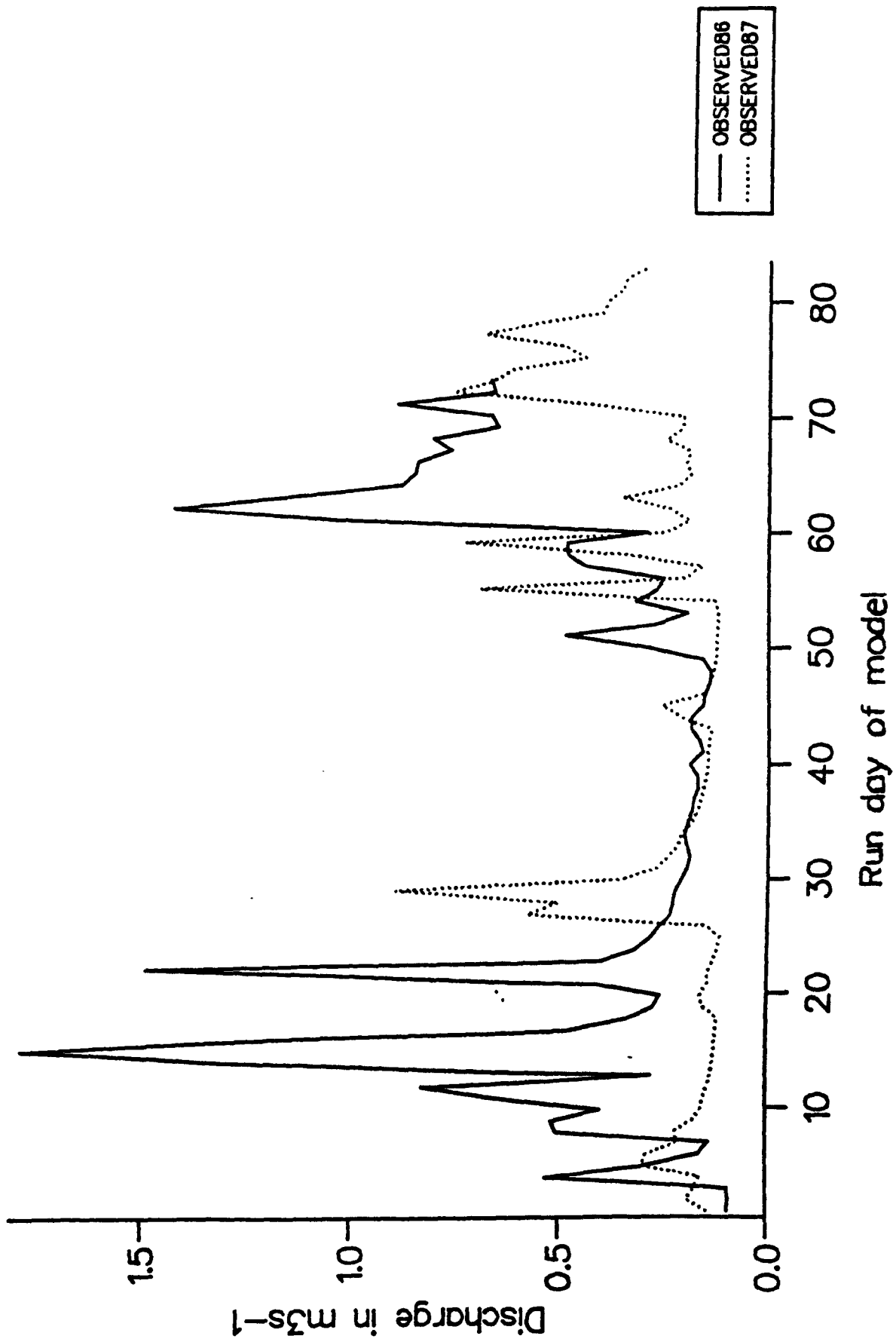


Figure 4.7 Time series plots produced from the first TINDEK model runs on the Mharcaidh. The upper plot is for 1987 and the lower is for 1986.

what would be expected in reality; as 1986 was a snowier year than 1987 (3.1.2) the air mass was likely to be cooled at a greater rate as it was in contact with a greater snowpack surface for a greater length of time.

- (2) The optimised recession coefficient value for 1987 is higher than that for 1986, suggesting that the 1986 flow regime is more flashy than 1987. Comparing the two years' data in Figure 4.7 does not confirm this, but it must be borne in mind that the y-axes have different scales for the two years. Figure 4.8 shows the two years' observed flow plotted on the same axis and clearly illustrates that the 1986 flows are much higher than those of 1987; whilst the rising limbs are steep for both years, the recession limbs are, on the whole, steeper for 1986 than 1987, thus explaining the difference in the optimised R values.

Despite the low value of R for the 1986 data the model is not very successful at reaching the peak flows of the observed data; these are the most important values if the model is to be used for flood-forecasting purposes. The model does match individual peaks well, especially for 1987, indicating that the temperature index method is worth pursuing; attention needs to be concentrated on matching the magnitude of the peaks in addition to the timing. Merely increasing the value



**Figure 4.8** The 1986 and 1987 observed flows on the same scale y-axis. It must be noted that the two time scales do not coincide and that the plot is merely an indication of the difference in flow magnitude between the two years.

of R will not do this; during the period of low flow in 1986 (Days 25-48) the model is already too responsive to inputs, increasing R will only make this worse. What may be needed is a method of varying the magnitude of R so that it is low during peaks of high melt intensities and high during long, cold spells. Martinec (1976, 1980a) did this in some of his models and found that their performance increased.

- (3) The optimised initial SCA value, AA, was the same value for both years ( $7\text{km}^2$ ), the lower of the two limits imposed on the optimisation range. This may reflect a weakness in the model representation of the snowpack and/or other weaknesses that in turn may affect the snowpack distribution.
- (4) The melt coefficients for the two years are different, although they are both physically reasonable values and fall in the range of values found by other authors (for example, Martinec and Rango, 1986). Again this may be due to the model trying to compensate for weaknesses elsewhere in the model or it may reflect a genuine difference in the physical properties of the snowpack and/or the weather patterns over the melt season.
- (5) As expected, given the results in 3.1.3, the mean snowpack water equivalent for 1986 was greater than

that for 1987. However, the difference was greater than expected, the 1986 value being almost 2.4 times larger. This may be compared to the total water content of the two snowpacks shown in Tables 3.1 and 3.2. At the start of the melt season the 1986 snowpack had almost 2.2 times the volume of the 1987 pack ( $1.766 \times 10^6 \text{ m}^3$  compared to  $0.822 \times 10^6 \text{ m}^3$ ). Thus it can be seen that the ratio of the two years' optimal mean snowpack water equivalent is similar to that of the observed initial volumes. However, do the actual volumes of water in the simulated and observed snowpacks agree? At first this would appear not to be the case:

$$\begin{aligned} \text{Volume of 1986 simulated snowpack} &= 7 \text{ km}^2 * 380 \text{ mm} \\ &= 2.660 * 10^6 \text{ m}^3 \end{aligned}$$

$$\text{Volume observed on 04.03.86} = 1.497 * 10^6 \text{ m}^3$$

$$\underline{\text{Difference}} = 1.163 * 10^6 \text{ m}^3$$

$$\begin{aligned} \text{Volume of 1987 simulated snowpack} &= 7 \text{ km}^2 * 160 \text{ mm} \\ &= 1.120 * 10^6 \text{ m}^3 \end{aligned}$$

$$\text{Volume observed on 13.03.91} = 0.822 * 10^6 \text{ m}^3$$

$$\underline{\text{Difference}} = 0.298 * 10^6 \text{ m}^3$$

Some of the discrepancy between the simulated and

observed 1986 volumes can be explained by the fact that the first snow survey for the period (from which the value of  $1.497 \times 10^6 \text{ m}^3$  is taken) is some four days into the melt season; if a value for 1 March is interpolated between the surveys carried out on 27 February and 4 March an extra  $0.161 \times 10^6 \text{ m}^3$  is accounted for, still leaving over a million  $\text{m}^3$  of water discrepancy. If this calculation is repeated for 1987 the volume is reduced by  $0.257 \times 10^6 \text{ m}^3$ , increasing the discrepancy to  $0.555 \times 10^6 \text{ m}^3$ ! However, this is not likely to be the case as, after talking to Joe Porter, it was discovered that the extent of the snowpack was, if anything, greater at the beginning of February than when the second survey was carried out on the 13th.

Even if it is accepted that the initial volume for 1986 can be increased by interpolation, and that this is not valid for 1987, discrepancies of  $1.002 \times 10^6$  and  $0.298 \times 10^6 \text{ m}^3$  still exist. Are these due to the misrepresentation of the snowpack or is the model at fault elsewhere? Reference to Tables 3.1 and 3.2 and Figure 3.2 shows that, for both years, there was not a continual decline in the water equivalent volume of the snowpack as the melt season progressed; the value rose on several occasions after fresh snowfall. If these inputs are added together a further  $0.373 \times 10^6$  and  $0.162 \times 10^6 \text{ m}^3$  and water equivalent is accounted for the two years, further reducing the discrepancies

to  $0.629 \times 10^6$  and  $0.136 \times 10^3 \text{ m}^3$ . The model, disregarding precipitation over the snowpack, does not allow for these inputs once the melt season has started; possibly future versions should deal with precipitation in a different way?

If Figure 4.7 is studied closely it can be seen that for the first few days in both years the model over-predicts the runoff (days 4-12 for 1986, 1-9 for 1987). If the mean daily difference for the two periods is calculated from the data in the output file and converted to total runoff in  $\text{m}^3$  for the two periods, values of  $0.152 \times 10^6$  and  $0.136 \times 10^6 \text{ m}^3$  are obtained, accounting for almost 25% of the unexplained discrepancy for 1986 and all of the 1987 values.

- (6) The final snowpack areas for the two years, whilst both being reasonable values, are larger than expected given the snow survey results shown in Table 3.1 and 3.2.

#### 4.3.3 Recommendations following the first runs of TINDE

From points (1) to (6) it was decided that the following characteristics were the most important and needed to be investigated and improved if possible:

- (1) Over-prediction of melt in the early stages of the model run, resulting in high initial optimised snowpack water equivalent values.
- (2) Under-prediction at times of high flow.
- (3) Ignoring precipitation inputs to the snowpack once the melt season has started.

#### 4.4 Early changes to TINDEX

Following the advice of Nash and Sutcliffe (1970) it was decided to make only one change at a time to TINDEX. In this way it would be possible to investigate the effect of individual changes, thus making the evaluation of their usefulness more straightforward.

##### 4.4.1 Addition of the freezing level

TINDEX calculated melt on the basis that if the air temperature at the AWS was above freezing then melt was occurring over the whole snowpack. Clearly, in reality, this is not the case; on many occasions the snow surveys had started off in rain and warm temperatures, only to later be carried out in sleet and finally snow as one progressed higher up the catchment. In the later part of the melt/survey season it was common for melt to be occurring over the whole snowpack, even if air temperature did vary, but this was often not the case in the early part when air temperatures were colder and thus closer to the

critical 0°C threshold for melt (selected for use in TINDEX - other models use different base values).

It was thus decided to incorporate a freezing level into the model which was renamed FTINDEX. As this was likely to have greatest effect in the early stages of the melt season it was hoped that the over-prediction would be reduced during this stage. Also, by calculating the area of the catchment below the freezing level a more realistic input in the form of precipitation could be included.

The first change to the model was in the hypsometric curve function, HT(A). In TINDEX this had been structured specifically for the Mharcaidh; as the model was to be tested on other catchments later in the project it was decided to make it as universally applicable as possible. The following additional model parameters were read into the model from an external file (HYPSO.DAT):

HMET = Height of meteorological station (m)

HMAX = Maximum altitude of catchment (m)

H1 = Altitude of upper break of slope on hypsometric curve (m)

H2 = Altitude of lower break of slope on hypsometric curve (m)

HMIN = Height of flow data gauging station (m)

A2 = Area of catchment above H2 (km<sup>2</sup>)

A1 = Area of catchment above H1 (km<sup>2</sup>)

The values for the Mharcaidh are as follows:

$$HMET = 575 \text{ m}$$

$$HMAX = 1111 \text{ m}$$

$$H1 = 900 \text{ m}$$

$$H2 = 600 \text{ m}$$

$$HMIN = 345 \text{ m}$$

$$A2 = 8.82 \text{ km}^2$$

$$A1 = 0.94 \text{ km}^2$$

From Figure 4.2, and substituting in equations 4.1 and 4.2 we get:

$$S0 = HMAX - H1 / A1$$

$$S1 = H1 - H2 / (A2 - A1) \text{ and}$$

$$S2 = H2 - HMIN / (AB - A2) \quad (4.16)$$

leading to:

If  $A > A2$

$$HT = H2 - S2 * (A - A2)$$

else if  $A2 > A > A1$

$$HT = H1 - S1 * (A - A1)$$

else if  $A1 > A > 0$

$$HT = HMAX - S0 * A \quad (4.17)$$

The snowline height was calculated in FTINDEX in the same way as TINDEX, using the universal form of  $HT(A)$ . Instead

of calculating DT, i.e. the temperature difference between the AWS and snowline, the altitude difference between the AWS and the predicted altitude of the 0°C isotherm (DALT) was determined from:

$$DALT = ATEM/E \quad (4.18)$$

The freezing level, FL was then calculated from:

$$FL = DALT + HMET \quad (4.19)$$

FL was then used to determine FFA, the area of the catchment above the freezing level. From the hypsometric function HT(A), equation 4.1, substituting FL for HT, and FFA for A,

$$\begin{aligned} FL &= H_1 - S_2 * (FFA - A_2) && \text{becomes} \\ FFA &= A_2 + (H_2 - FL) / S_2 && (4.20) \end{aligned}$$

Similar substitutions were carried out for the other equations in (4.1)

Once FFA had been determined, the area of the snowpack available for melt (MA) was calculated from:

$$MA = A - FFA \quad (4.21)$$

If MA > 0, MA was substituted in equation 4.5 to give

$$V = M * MA * DD \quad (4.22)$$

which was used to calculate the volume of melt.

Precipitation inputs were now added to both the snow-free parts of the catchment (when below the FL) and that part represented by MA:

$$VP = (AB - A + MA) * PPT \text{ which simplifies to}$$

$$VP = (AB - FFA) * PPT \quad (4.23)$$

On occasions when  $FFA > AB$ , i.e. the whole of the catchment was above FL, any precipitation was assumed to be in the form of snow and disregarded (this situation was represented in a later model). The remainder of FTINDEX was the same as TINDEX.

#### 4.4.2 Results from FTINDEX

The optimised parameter sets for 1986 and 1987, along with SE, FA and  $R^2$ , are given below in Table 4.3 along with those of TINDEX for comparison, and the time series plots shown in Figure 4.9.

Year	1986 TINDEX	1987 TINDEX	1986 FTINDEX	1987 FTINDEX
E ( $^{\circ}\text{C m}^{-1}$ )	0.010	0.006	0.010	0.010
R	0.380	0.540	0.710	0.740
AA ( $\text{km}^2$ )	7.0	7.0	7.0	7.0
M ( $\text{mm}^{\circ}\text{C day}^{-1}$ )	3.0	2.0	3.6	1.4
W (mm)	380	160	330	180
SE	0.2245	0.1197	0.2318	0.1302
$R^2$	0.628	0.582	0.610	0.462
FA ( $\text{km}^2$ )	2.28	1.61	1.00	3.95

Table 4.3 Results from applying FTINDEX and TINDEX to the Mharcaidh 1986 and 1987 datasets.

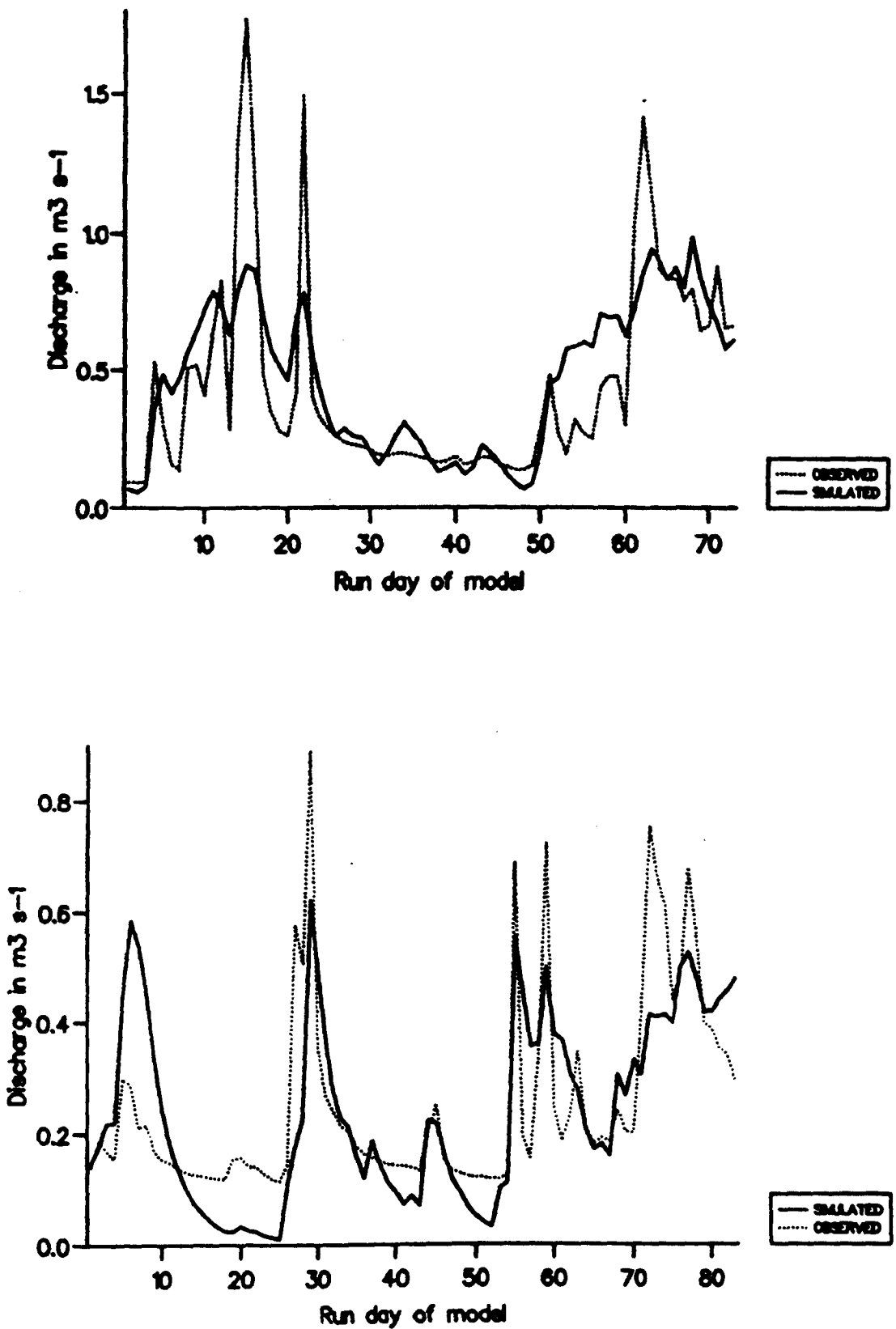


Figure 4.9 Time series plots for the FTINDEX model runs on the Mharcaidh 1986 (upper) and 1987 (lower) data.

From these results it can be seen that the SE and R<sup>2</sup> value for both years indicate that FTINDEX does not perform as well as TINDEX. When the individual optimised parameter values are studied the following points can be seen:

- (1) Whilst the initial SCAs are still 7km<sup>2</sup> and both E values are now the same, the melt coefficients for the two years have moved further apart, making the model less applicable to 'untried' data sets or to forecasting in real time.
- (2) The recession coefficient for both years has optimised to a much higher value, resulting in the simulated peak flows being even lower than those produced by TINDEX. As this was one of the features it was decided to try and correct in 4.3.3(2), it can be seen that in this respect the addition of the freezing level has had a negative effect. The only useful feature about the FTINDEX R values is that they are both very similar for the two years; this is of little benefit if the rest of the model suffers.
- (3) The initial water equivalent value of the snowpack is smaller for 1986 and larger for 1987, resulting in smaller and larger values of FA respectively. Whilst the 1986 values are closer to those found from the snow surveys, the model performance is still worse; when the fact that the 1987 values are much less realistic than the observed values is also considered. Yet again the conclusion must be that the addition of

the freezing level has made the model worse.

- (4) Comparing Figure 4.9 to Figure 4.7 shows that FTINDEX still over-predicts flow in the early part of the melt season. Whilst this over-prediction is lower for the first four days of 1987 it occurs for a longer period (12 days instead of 9); the difference between the flow for this 12 day period equals  $0.128 \times 10^6 \text{ m}^3$  of water, very similar to the  $0.136 \times 10^6 \text{ m}^3$  calculated from TINDEX.

Why is it that the addition of the freezing level makes TINDEX perform worse? It might be that the rest of the model is so simplified that trying to introduce a higher degree of complexity into one of the subroutines that is not matched elsewhere in the model may knock it 'out of balance'. Alternatively, the methods used and reasons for applying the freezing level may be fundamentally incorrect. One of the initial reasons for introducing it into the model was to reduce the over-prediction in the early period of the model run. One possible scenario that may occur is that on occasions when the AWS is marginally above freezing level melt can occur over the lower snowpack below the freezing level; this is not possible in TINDEX, and may explain the over-prediction at the start of FTINDEX. Later in the melt season when the AWS is marginally below the freezing level FTINDEX reduces the area over which melt occurs, thus reducing the total magnitude of melt and the resultant runoff; given the same conditions TINDEX would

produce a higher runoff value.

#### 4.4.3 Addition of non-linear routing

After inspecting Figure 4.7 it was suggested in 4.3.2(2) that the model might be improved by the addition of a variable recession coefficient along the lines of that used by Martinec (1976, 1980a) discussed in 1.3.3.1. A low value of R is needed during high melt events to try and match the observed peak flows; during low flow events a high value of R is needed to smooth out the recession limits of the hydrographs and make the model less responsive to small melt/precipitation inputs. Whilst this is what a visual comparison of the predicted and observed flows may suggest, can it be justified or is it merely a 'fudge factor' to be introduced in the model?

If high magnitude melt events are considered first they can be compared to high intensity rainfall events. With a high volume of meltwater being produced at the surface of the snowpack the pore spaces between the crystals in the snowpack will quickly become saturated as water infiltrates through. This will give rise to saturated 'over-snow' flow, throughflow within the pack and overland flow occurring at the interface between the snowpack and frozen ground. There will then be little scope for the snowpack to store water and travel-times are likely to be rapid. This was studied in the Mharcaidh in the later part of the 1988

melt season using tracing techniques (Appendix D). The results confirm that travel-times are indeed rapid.

During low magnitude flood events the percolation of meltwater from the surface will be less, resulting in a lower saturation of the pore spaces in the snowpack. Saturated 'over-snow' flow is thus less likely to occur and flow is more likely to result from throughflow. As the head of water in the pack will be less the seepage at the base of the snow will be less, resulting in reduced overland flow at the snowpack/ground interface.

It can thus be seen that there is justification for incorporating a variable recession coefficient into the model, both from a modelling viewpoint and when considering the physical processes occurring during different melt events. After studying "A review of British flood forecasting practice" (Reed, 1984) it was decided to introduce a non-linear storage function. The method chosen was similar to that used by the Forth River Purification Board (FRPB) (1977 and also Brunsdon and Sargent, (1982)) which was in turn based on the Isolated Event Model (IEM) (NERC, 1975).

In the standard IEM model the magnitude of the runoff coefficient is related to the pre-event storage within the catchment (taking in surface water, soil moisture and ground water):

$$S = k * Q^{1/2} \quad (4.24)$$

where

S = Water stored in catchment

k = Routing coefficient

Q = Outflow from the catchment

The FRPB modified version of the IEM uses the pre-event runoff rate ( $Q_{-1}$ ) as the index of antecedent catchment wetness. This has the advantage that  $Q_{-1}$  is readily available in real time, whereas the stored water is often difficult to quantify or model. The function used to represent the non-linear store was:

$$R = 1 - kQ_{n-1}^{1/2} \quad (4.25)$$

where

k = is a parameter to be optimised.

It can be seen from Equation 4.25 that as  $Q_{n-1}$  tends to 0, R tends to 1, i.e. at times of low flow the recession coefficient will produce a slow response to inputs in the form of melt or precipitation. Conversely, as  $Q_{n-1}$  tends to  $1/k$  R tends to 0, i.e. at times of high flow the discharge pattern will respond quickly to inputs. As R has upper and lower limits of 1 and 0 respectively, from 4.25 it can be seen that:

$$\begin{aligned} \text{upper limit of } k &= -2/Q_{-1}^{0.5} && \text{and} \\ \text{lower limit of } k &= 1/Q_{-1}^{0.5} && (4.26) \end{aligned}$$

In order to minimise the number of changes in the program the model replaced k with the old R for optimisation purposes and used a value Y instead of the recession coefficient. Q was thus calculated from:

$$Q = Y * Q_{-1} + (1-Y) * (V+VP)/86.4$$

where

$$Y = 1 - R * Q_{-1}^{0.5} \quad (4.27)$$

#### 4.4.4 Results from adding non-linear routing

The results from adding the non-linear routing function to both TINDEX and FTINDEX are shown in Table 4.4. and the time series plots in Figure 4.10. The plot for 1986, TINDEX with non-linear routing, is not shown as the data-file was lost during the transfer of files from the old to the new mainframe later in the project.

Year	1986 TINDEX	1987 TINDEX	1986 FTINDEX	1987 FTINDEX
E (°C m <sup>-1</sup> )	0.010	0.006	0.010	0.006
R	0.390	0.840	0.380	0.590
AA (km <sup>2</sup> )	7.0	7.0	7.0	7.0
M (mm°C day <sup>-1</sup> )	4.1	2.3	4.1	1.4
W (mm)	390	170	350	180
SE	0.2116	0.1302	0.2140	0.1320
R <sup>2</sup>	0.672	0.514	0.668	0.452
FA (km <sup>2</sup> )	1.08	1.19	0.65	3.54

Table 4.4 Results from applying FTINDEX and TINDEX to the Mharcaidh 1986 and 1987 datasets using non-linear routing.

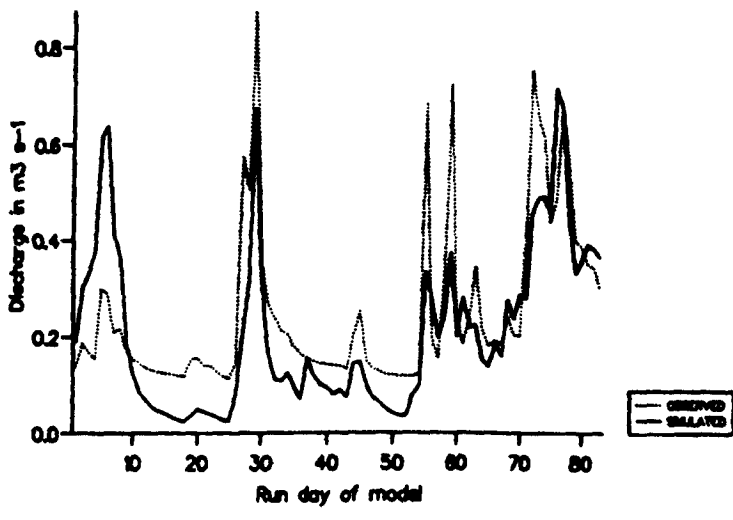
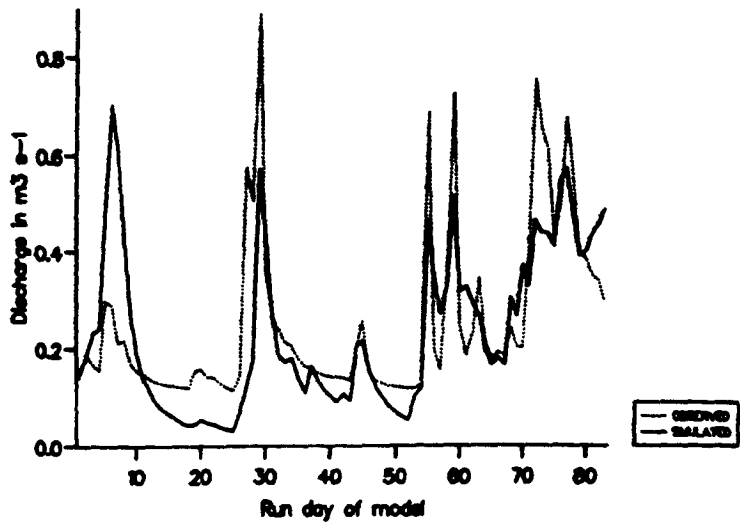
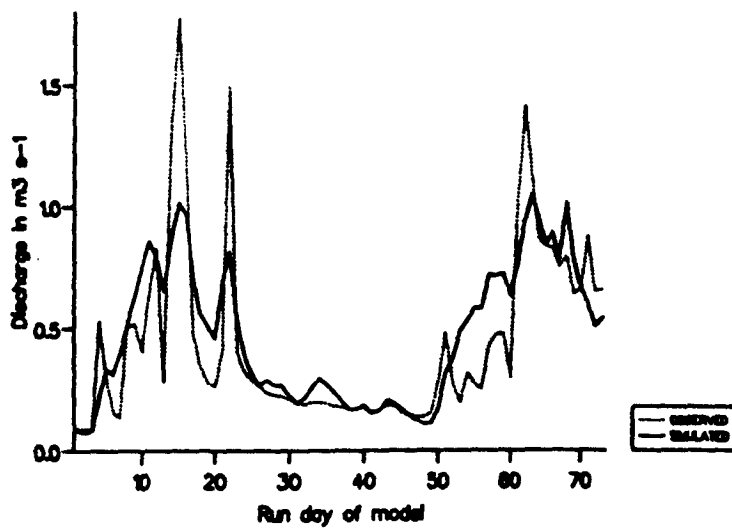


Figure 4.10 Time series plots for TINDEX and FTINDEX on the Mharcaidh data using non-linear routing. The top plot is for FTINDEX on the 1986 data, the middle is for FTINDEX on 1987 and the bottom is for TINDEX on 1987.

If Figure 4.10 is compared to Figures 4.7 and 4.9 it can be seen that the addition of non-linear routing has marginally increased the ability of FTINDEX to reach the peak flows and has made the model less responsive during the periods of low flow. This is not the case for TINDEX; whilst the model is now more stable during low flow events the difference between peak flows during days 55-62 (1987) is increased, though the peak on day 79 is closer to the observed value.

If the optimised R values are studied it can be seen that those for 1986, whilst being lower than 1987, are very similar for the two models (TINDEX = 0.39, FTINDEX = 0.38), an encouraging sign if non-linear routing is to be included in a universally applicable model. If the individual R values are combined with the observed flow datasets to determine the minimum and maximum runoff coefficients for each model and year they yield the results shown below in Table 4.5.

Year	Model	Value of recession coefficient	
		Minimum	Maximum
1986	TINDEX	0.48	0.88
	FTINDEX	0.49	0.89
1987	TINDEX	0.21	0.72
	FTINDEX	0.44	0.80

**Table 4.5** Calculated recession coefficients for minimum and maximum observed flows during the 1986 and 1987 melt seasons. Values are calculated from the optimised R values of TINDEX and FTINDEX, both using non-linear routing.

From these it can be seen that the addition of non-linear routing does provide the variation in the recession coefficient that 4.2.2(2) suggested. To see if it has improved or hindered the performance of the models it is probably best to review the results to date.

#### 4.4.5 Discussion of early changes to TINDEK

Sections 4.3.2, 4.4.2 and 4.4.4 have discussed in various degrees of detail the characteristics of the optimised parameters and the effect that these have on the model and their relation to the snowpack characteristics observed from the snow surveys. It was decided that, at this stage in the model development, the statistical performance of each of the models should be compared to see if any features should be taken further in the model development or removed altogether. Whilst it is valid to compare  $R^2$  values for models of difficult complexity for different years (Nash and Sutcliffe, 1970) this is not so for the SE values as these are dependent on the variation of flow within the observed dataset for each year, i.e. the fact that the SE value for the 1987 run of a model is lower than that of the 1986 run does not mean it is a better fit since the 1987 flows are of lower magnitude and have less variation (Standard deviation of 0.177 compared to 0.371). It was therefore decided to calculate the percentage of the lowest SE for each year for each model and then compare the mean percentage SE value along with the  $R^2$  values. These

values are shown below in Table 4.6, along with the values for a further set of model runs that used the mean of the optimised parameters over the two years for each model combination for re-running the models. The only value that was re-optimised was W as this is dependent on the actual snowpack characteristics for each year. (The optimised value was different from the initial optimised value on only two of the model runs.)

From Table 4.6 it can be seen that when both years' data are considered together none of the changes to the model have improved its performance, TINDEX with linear routing coming out as the best performer when either the optimised or combined data set is used.

If the changes are considered individually it can be seen that the addition of the freezing level has the worst effect on the model. If the mean  $R^2$  of all the model runs without the freezing level is compared to that of those using it we find the value drops from 0.566 to 0.502. The point made in 4.4.2 that given the degree of simplification in TINDEX it may not be appropriate to introduce the freezing level function may be valid; it is interesting to note from Table 4.6 that if the routing/storage function is made more complex the performance of FTINDEX improves. It is therefore concluded that given the current degree of simplification in the model the addition of the freezing level has a detrimental effect.

Model	Routing	Parameters	% of best SE (year)		Mean % of best SE	Rank	Mean R <sup>2</sup>	Rank
			1986	1987				
TINDEX	Linear	Optimised	106	100	103	1	0.605	1
TINDEX	Nonlinear		100	109	104.5	2	0.593	2
FTINDEX	Linear		110	109	109.5	3	0.536	4
FTINDEX	Nonlinear		101	110	105.5	4	0.560	3
TINDEX	Linear	Combined	109	107	108	1	0.546	1
TINDEX	Nonlinear		103	118	110.5	2	0.521	2
FTINDEX	Linear		116	121	118.5	4	0.453	4
FTINDEX	Nonlinear		109	122	115.5	3	0.460	3

Table 4.6 Statistical results from the early versions of TINDEX and FTINDEX model runs using both optimised and combined parameter sets.

The effect of including the non-linear routing function is not so clear, however. If the mean  $R^2$  of the model runs with and without it are also compared we find that the value only drops from 0.535 to 0.534, a fall of 0.2%. Indeed, if the model performance for 1986 only is considered (being a snowier winter (3.1.1) it might be considered a better test of the model) it can be seen that the addition of the non-linear routing function increases the performance of the model. Thus, at this stage of the model development, it is not possible to say if the addition of non-linear routing improves or hinders the model performance.

#### 4.5 Further developments to TINDEX

##### 4.5.1 Alteration of time interval

Before deciding whether or not to continue with the freezing level function, and in order to try and determine if a non-linear or linear routing/storage function gave the best performance, it was decided to alter the time-interval over which the calculations were made. It was felt that operating with daily data in a catchment the size of the Mharcaidh might mask events that would be exposed by a shorter time interval. These events might include short duration, high intensity melt events that would enable the peak flows to be more accurately simulated or conversely even higher flood peaks might be revealed that result in the model's performance deteriorating.

The time interval chosen was six-hourly, i.e. four calculations per day. This was the interval chosen by Anderson (1968, 1973, 1978) and used in the NWSRFS snow accumulation and ablation model. The data sets were recreated to provide six-hourly input data and the model rewritten to allow for the changes. When re-creating the datasets it was decided to use mean temperatures over the six-hour period rather than the method used in TINDEX based on Ferguson's (1984) approach. Whilst the TMIN, TMAX, NTMIN method provides an index that allows for changes in weather patterns, scanning 48 hours data in total in the original model, it was felt that by reducing the time-interval there were unlikely to be any major changes in weather characteristics within the six-hour period. Using mean temperature data not only simplified the coding of the data, it also reduced the number of calculations that had to be made in one complete model run. This was not so important when running earlier versions of TINDEX and FTINDEX but since shortening the time-interval resulted in a four-fold increase in the number of melt periods any improvements that could be made in model efficiency resulted in more options being possible when optimising.

#### 4.5.2 Results

The new models, TINDEX6 and FTINDEX6, were run on the 1986 and 1987 data sets with both linear and non-linear routing. Combined parameter sets from the optimised values (as in

4.4.5) were also used to re-run each model combination. The results from these model runs are shown in Table 4.7.

If the SE values are studied they indicate that for all 16 possible combinations of the model shortening the time interval makes it perform worse (mean SE of 0.1932 compared to 0.1799 for the corresponding daily time step models). However, if the  $R^2$  values are considered, it can be seen that for nine of the 16 combinations shortening the time intervals improves the model performance. The mean  $R^2$  value also indicates this, though the difference is marginal (0.55) compared to 0.547). If comparison of  $R^2$  values are made from subsets of the results shown in Table 4.7 the following points can be made:

- (1) For model runs not using the freezing level a reduction in the interval decreases the performance, the mean  $R^2$  dropping from 0.591 to 0.586.
- (2) For model runs using the combined data sets reducing the time interval decreases the model performance, the mean  $R^2$  dropping from 0.520 to 0.507.
- (3) For model runs using linear routing reducing the time interval worsens the model performance, the mean  $R^2$  value dropping from 0.535 to 0.520.
- (4) For model runs using non-linear routing reducing the time interval improves the model performance, the mean  $R^2$  value rising from 0.559 to 0.586.

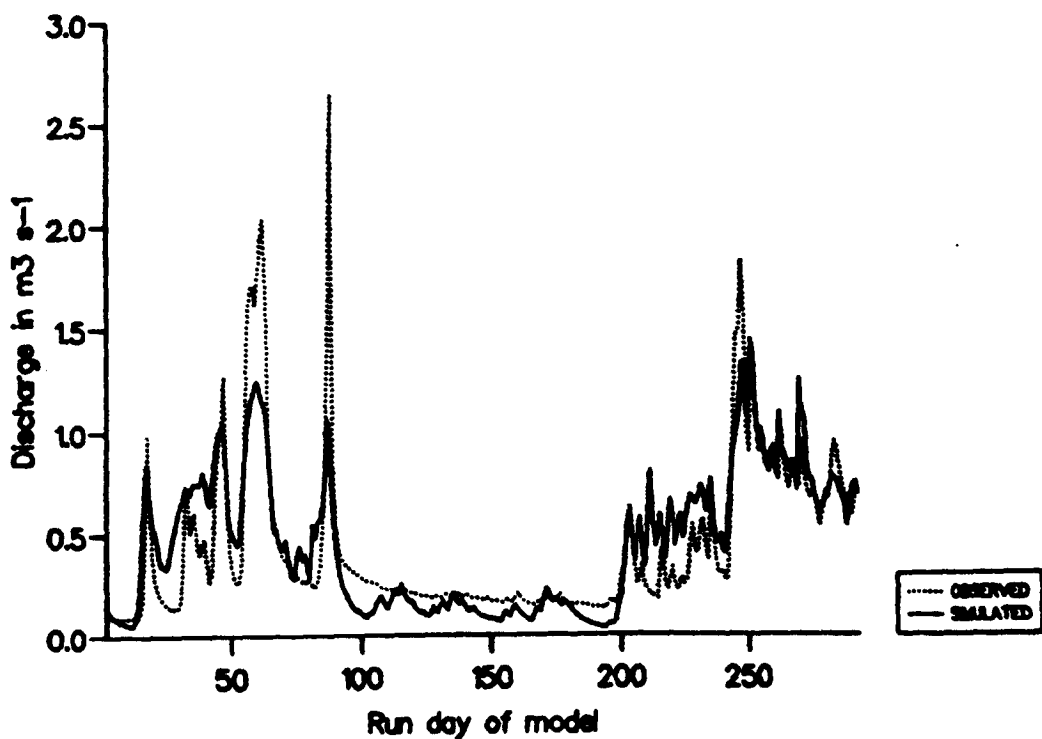
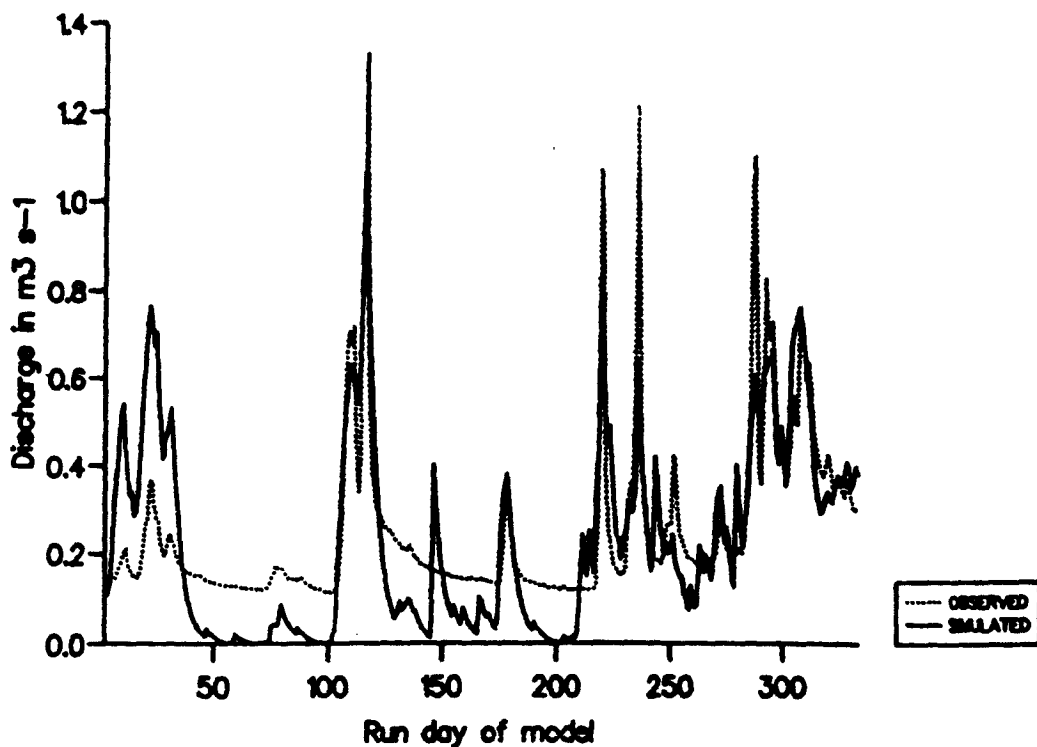


Figure 4.11(a) Time series plots for the 1987 FTINDEX6 model run using the combined parameter set and linear routing (top) and the 1986 TINDEX6 model run using optimised parameters and non-linear routing (bottom). (Note: the x-axis is labelled 'run day' but should be 'time interval'; to convert to days divide by four.)

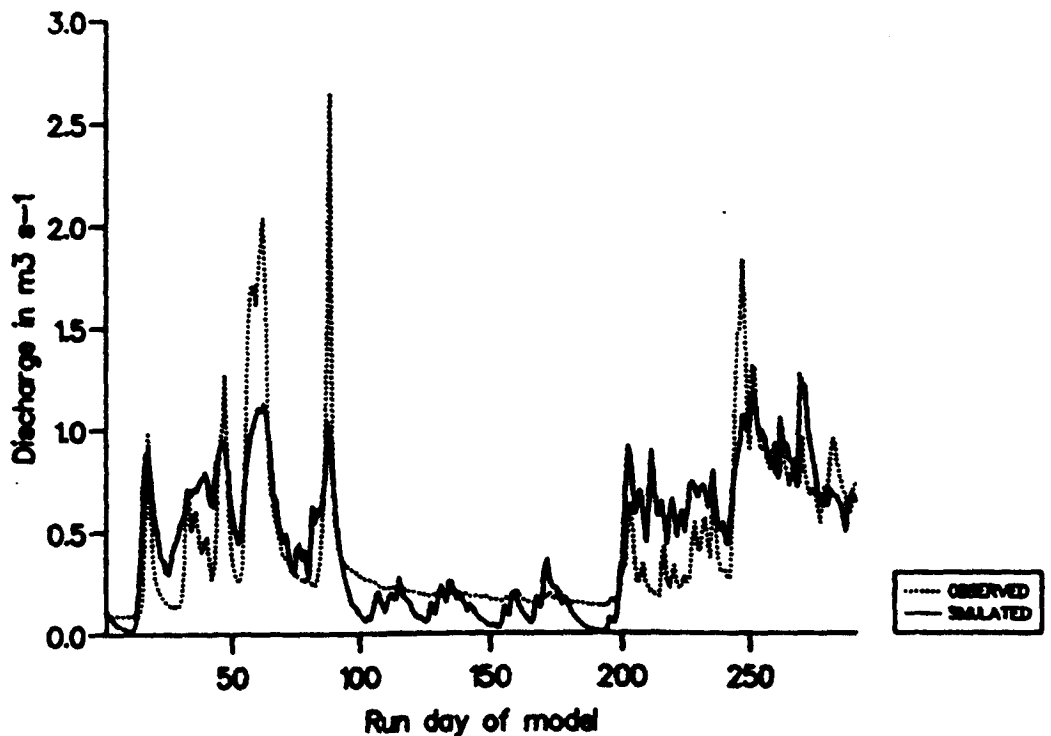
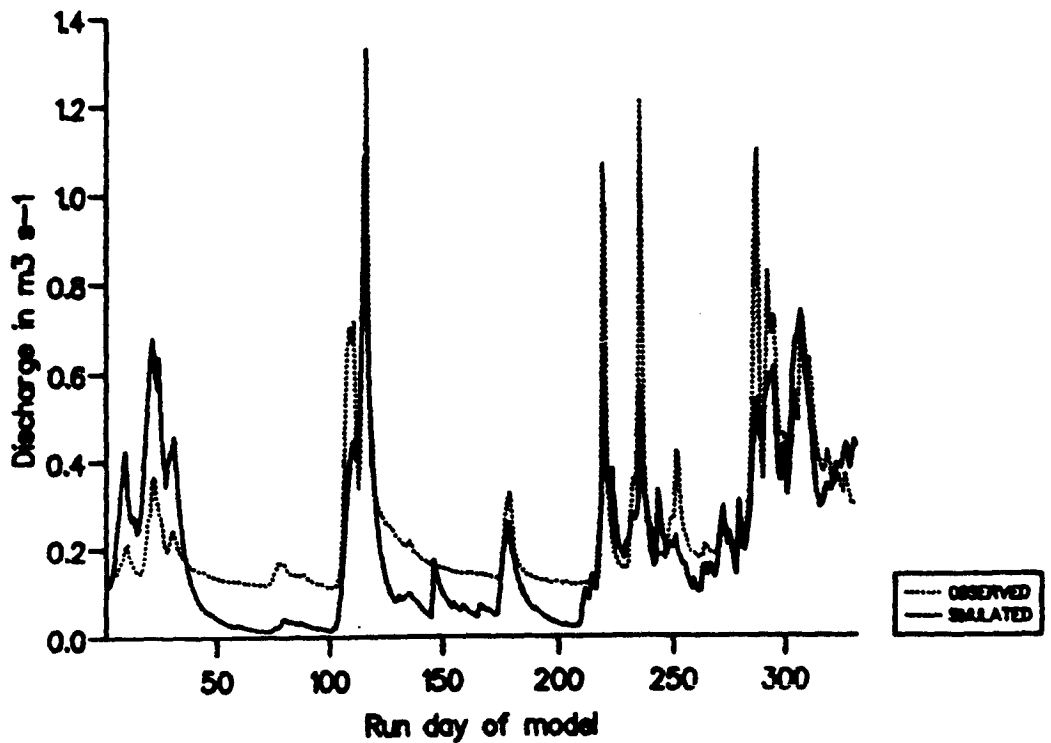


Figure 4.11(b) Time series plots for the 1987 FTINDEX6 model run using optimised parameters and nonlinear routing and the 1986 FTINDEX6 model run using optimised parameters and linear routing. (Note: the x-axis is labelled 'run day' but should be 'time interval'; to convert to days divide by four.)

YEAR	MODEL	ROUTING	PARAMETERS	E	R	A	M	W	SE	R <sup>2</sup>	FA	SE	R <sup>2</sup>
1986	TINDEX 6	Linear	Optimised	0.010	0.75	7.0	3.1	400	0.2246	0.632	2.53	0.2245	0.628
		Non-linear		0.010	0.34	7.0	3.4	400	0.2256	0.687	2.19	0.2116	0.672
	FTINDEX 6	Linear		0.010	0.80	7.0	3.4	330	0.2533	0.607	1.59	0.2318	0.610
		Non-linear		0.010	0.31	7.0	3.6	350	0.2271	0.684	1.60	0.2140	0.668
1987	TINDEX 6	Linear		0.006	0.82	7.1	1.9	170	0.1339	0.563	2.28	0.1197	0.582
		Non-linear		0.006	0.36	7.0	2.0	170	0.1339	0.588	2.05	0.1302	0.514
	FTINDEX 6	Linear		0.010	0.90	7.1	1.4	190	0.1414	0.486	4.21	0.1302	0.462
		Non-linear		0.010	0.23	7.0	1.6	180	0.1358	0.541	3.68	0.1320	0.452
1986	TINDEX 6	Linear	Combined	0.008	0.79	7.0	2.5	400	0.2533	0.605	3.00	0.2318	0.607
		Non-linear		0.008	0.35	7.0	2.7	400	0.2341	0.663	2.73	0.2169	0.653
	FTINDEX 6	Linear		0.010	0.85	7.1	2.4	330	0.2712	0.548	2.9	0.2458	0.556
		Non-linear		0.010	0.27	7.0	2.6	360	0.2479	0.622	2.91	0.2313	0.606
1987	TINDEX 6	Linear		0.008	0.79	7.0	2.5	170	0.1450	0.457	1.43	0.1281	0.485
		Non-linear		0.008	0.35	7.0	2.7	170	0.1431	0.491	1.09	0.1414	0.588
	FTINDEX 6	Linear		0.010	0.85	7.1	2.4	200	0.1703	0.261	2.72	0.1451	0.350
		Non-linear		0.010	0.27	7.0	2.6	150	0.1505	0.410	1.44	0.1441	0.314

Table 4.7

Results from running the six-hourly time-step models on the 1986 and 1987 Mharcaidh data.

The final two columns show the corresponding SE and R<sup>2</sup> values for the daily time-step models.

E = Environmental lapse rate (°C m<sup>-1</sup>), R = Routing coefficient, A = Initial snow covered area (km<sup>2</sup>),

M = Melt coefficient (mm°C day<sup>-1</sup>), W = Initial snowpack water equivalent (mm).

Reference to Figure 4.11 which shows the time series plots for the six-hourly model runs illustrates why points (3) and (4) are so. Shortening the time interval reveals higher observed peak flows for both years. As the non-linear routing function is able to adjust for the increase in range in flow values it is likely to perform better than the linear routing function which is more suited to a stable flow pattern. By decreasing the time interval the number of melt period calculations is increased, resulting in the non-linear routing function being able to adjust from low to high flow values in a series of stages rather than in one or two steps, as would be the case using the daily time interval. It is thus possible that whilst shortening the time interval will make the model more suited to a non-linear routing function, the function itself may be able to perform better over a period of more gradual changes even if the range of flow values is increased.

The fact that the maximum flow values for the two years is increased by shortening the time interval, illustrated in Figure 4.11, explains why for all model combinations the SE value is worse when using the six-hourly melt calculation. Figure 4.11 also shows that during low flow events the six-hourly time step approach produces a pattern of diurnal flow variation as one would expect. The pattern is more extreme than that of the observed values and hinders the model performance, thus increasing the SE value. This

suggests that a more complex routing submodel may be needed when shortening the time interval to deal with the greater flow variation, especially for larger catchments which will tend to smooth the flow more than the Mharcaidh.

Distributed models such as IHDM and SHE (for example Bevan and O'Connell, 1982; Morris, 1980, 1982; Morris et al 1980) cater for this and it may be that they have potential for use in a snowmelt context. Almost six months were spent in the early stages of the project attempting to calibrate and apply the IHDM snowmelt routine GLI to the Mharcaidh. This was unsuccessful for a number of reasons and, following the advice of Alan Jenkins and Rob Ferguson (pers comms) it was decided not to take this any further.

Point (2) (p195) is important if it is remembered that the aim of the model development is to provide a universal model that can be used for different catchments over different years. The fewer parameters that have to be optimised the better and if one model shows superior performance than another when using the combined set of parameters this might be considered more important than the difference in performance for the optimised data sets.

If the results for parameters E, R and M, i.e. those that are not specific to the snow cover characteristics for the year, are studied in Table 4.7, it appears that they are more constant and have less spread than those for the daily

time step models. If so this is a useful characteristic as it may lead to eventually declaring the parameters as constants in the model, thus making it universally applicable. Table 4.8 shows the range and standard deviation of the range of these optimised parameter sets compared to those of the models using the daily time interval.

Time step of model		Daily	6-hourly
E (°C m <sup>-1</sup> )	Range	0.010 - 0.006	0.010 - 0.006
	SD	0.0019	0.0017
R Linear	Range	0.38 - 0.74	0.75 - 0.90
	SD	0.156	0.054
R Non-linear	Range	0.38 - 0.84	0.21 - 0.36
	SD	0.187	0.049
M mm°C day <sup>-1</sup>	Range	1.4 - 4.1	1.4 - 3.6
	SD	1.051	0.851

Table 4.8 Comparison of the range and standard deviation (SD) of the optimised parameter sets using the two different time intervals. (Standard deviations calculated using n as the whole population was used and not a sample)

It can be seen that, with the exception of the range of E values that are the same for both model types, in every case the range and standard deviation of the parameter set optimised on the six-hourly model is smaller. Whilst this decrease is most noticeable for the non-linear models (for the reason outlined earlier), the fact that it is a characteristic common to all three parameters suggests that there is a specific reason for this. In addition to

changing the time step for the model, the method of calculating the degree days was also changed as outlined in 4.5.1. Is this change from the degree-day calculation used by Ferguson (1984) to using average temperature over the time interval responsible for the narrowing of the parameter sets? To investigate this Pearson's correlation coefficients were calculated to determine the strength of the relationship between the observed flow data and TMIN, TMAX, NTMIN, ATEM and the degree-day index used by Ferguson. The results are shown in Table 4.9, along with the correlation coefficients for the daily interval data.

Time interval	Daily		6-hourly	
	1986	1987	1986	1987
Year				
TMIN	0.720	0.636	<u>0.634</u>	0.545
TMAX	0.691	0.674	0.618	0.558
NTMIN	0.600	0.452	0.536	0.548
ATEM	<u>0.767</u>	<u>0.702</u>	0.625	0.559
Ferguson 1984 index	0.718	0.651	0.625	<u>0.564</u>

Table 4.9 Pearson's correlation coefficients between different temperature indices and observed flow values. Underlined values indicate the strongest relationships for each set of temperature indices.

From these results a number of points can be made:

- (1) The weakest correlation for each set is (not surprisingly) between observed flow and the minimum temperature of the following time interval.

- (2) For every pair of coefficients (i.e. daily and six-hourly) the daily time interval gives the higher correlation, indicating that there is in general a stronger relationship between the daily values than the six-hourly. Whilst this helps explain the lower SE values of the daily interval method the fact that there is no clear distinction between the  $R^2$  values using the time interval suggests that further improvements might be made to the daily interval method.
- (3) For the six-hourly method the strongest relationships are not between ATEM and observed flow but TMIN (1986) and Ferguson's index (1987); for the 1986 coefficient set there is no difference in the strength of relationship using either ATEM or Ferguson's index, and for 1987 it is very small (0.9% of the lower value)
- (4) For the daily method the strongest relationships for both years are found using ATEM. The improvement over Ferguson's index is 6.8% (of the lower value) for 1986 and 7.8% for 1987.

Points (2) and (4) suggested that the next stage in the model development was to revert to the daily time interval for the melt calculation and to substitute average daily temperature for Ferguson's index.

#### 4.5.3 Results from using average temperature over a daily time scale

The original TINDEX and FTINDEX models were changed to allow average daily temperature to be used instead of the index derived by Ferguson (1984) and the models were re-run over both 1986 and 1987 data sets, using both linear and non-linear routing. The results are shown in Table 4.10, along with those from the combined parameter sets (as in 4.4.5 and 4.5.2). The SE and  $R^2$  values from the same model combinations using the Ferguson index are also shown for comparison.

From the optimised parameter values shown in Table 4.10 it can be seen that both E and A are now optimising to values that are not at the limit of the available range. Whilst this was the case for A, when using the six-hourly time step models, the values were only just within the limits; here they appear to be optimising to larger values. Whether or not this is a desirable feature can be questioned; whilst the snow covered area is now having an effect on the other parameters and the model performance it is also less easy to generalise. This problem is exacerbated by the fact that the values of A are not consistent between years: when using TINDEX the 1986 optimised areas are larger than those of 1987, yet when using FTINDEX with linear routing the 1987 area is larger than that for 1986! Encouragingly though, the relationship

YEAR	MODEL	ROUTING	PARAMETERS	E	R	A	M	W	SE	R <sup>2</sup>	FA	SE	R <sup>2</sup>
1986	TINDEX	Linear	Optimised	0.010	0.24	8.5	2.00	380	0.2016	0.700	4.08	0.2245	0.628
		Non-linear		0.009	0.72	7.2	3.30	380	0.1931	0.726	2.01	0.2116	0.672
	FTINDEX	Linear		0.010	0.56	7.0	3.20	310	0.2194	0.645	1.56	0.2318	0.610
		Non-linear		0.010	0.50	7.0	3.90	330	0.1963	0.715	0.96	0.2140	0.668
1987	TINDEX	Linear		0.006	0.52	7.0	2.00	150	0.1182	0.620	1.63	0.1197	0.582
		Non-linear		0.006	0.83	7.0	2.40	160	0.1313	0.550	0.99	0.1302	0.514
	FTINDEX	Linear		0.009	0.74	7.3	1.20	190	0.1298	0.469	4.64	0.1302	0.462
		Non-linear		0.006	0.68	7.0	1.40	170	0.1288	0.499	3.56	0.1302	0.452
1986	TINDEX	Linear	Combined	0.008	0.38	8.5	2.00	380	0.2052	0.689	3.93	0.2169	0.653
		Non-linear		0.008	0.78	7.2	2.85	380	0.1959	0.720	2.39	0.2169	0.653
	FTINDEX	Linear		0.010	0.65	7.0	2.20	310	0.2387	0.587	2.90	0.2458	0.556
		Non-linear		0.008	0.59	7.0	2.65	330	0.2153	0.661	2.19	0.2313	0.606
1987	TINDEX	Linear		0.008	0.38	7.0	2.0	150	0.1242	0.590	2.02	0.1281	0.485
		Non-linear		0.008	0.78	7.0	2.85	160	0.1367	0.487	0.35	0.1412	0.588
	FTINDEX	Linear		0.010	0.65	7.3	2.2	190	0.1552	0.252	2.84	0.1451	0.350
		Non-linear		0.008	0.59	7.0	2.65	170	0.1441	0.332	1.30	0.1441	0.314

Table 4.10

Results from running TINDEX and FTINDEX on the Mharcaidh data using average daily temperature to determine the degree-days.

The final two columns show the corresponding results when using Ferguson's index.

E = Environmental lapse rate ( $^{\circ}\text{C m}^{-1}$ ), R = Routing coefficient, A = Initial snow covered area ( $\text{km}^2$ ,

M = Melt coefficient ( $\text{mm}^{\circ}\text{C day}^{-1}$ ), W = Initial snowpack water equivalent (mm).

between the 1986 and 1987 E values is constant, the 1986 value always being larger, though the magnitude of the difference is not constant.

If the performance of the models using average daily temperature as the index to melt is compared to those using Ferguson's index it can be seen that, for these two data sets, the average daily temperature method is superior. Seven of the eight different model combinations have a lower SE and all eight have a higher  $R^2$  value. (The mean  $R^2$  increases from 0.574 to 0.616 (3 sf)). Six of the eight model combinations using the combined data sets also perform better, the two that do not are due to a large difference in the optimised melt coefficient (3.9 and 1.4, 3.2 and 1.2) affecting the 1987 model runs.

#### 4.5.4 Comparison of results so far

As the number of different models and model combinations was getting larger and the comparison of results becoming more complex it was decided to try and see if one particular method stood out as the best performer. If so, further development would be concentrated on this model/method.

The first comparison made was between the model run using the following time intervals and degree-day calculations:

- (1) Daily time interval, degree-day on Ferguson's index.

- (2) Daily time interval, degree-day on true mean temperature.
- (3) Six-hourly time interval, degree-day as true mean temperature.

The results from using both optimised and combined parameter sets on these three different models are shown in Table 4.11.

Criteria	Year and Rank	Model type		
		(1)	(2)	(3)
Standard Error	1986	0.2205	0.2026	0.2377
	Rank	2	1	3
	1987	0.1280	0.1270	0.1363
	Rank	2	1	3
R <sup>2</sup>	1986	0.645	0.697	0.653
	Rank	3	1	2
	1987	0.503	0.535	0.545
	Rank	3	2	1

Table 4.11 Summarised SE and R<sup>2</sup> values for all model runs using both combined and optimised parameter sets. For definitions of model types refer to main text above.

From these results it can be clearly seen that model type (2) (i.e. daily time interval and mean of 24 hourly temperature observations) performs better than either (1) or (3). When looking at the SE values, which the model optimises, it ranks as the best performer for both the 1986 and 1987 datasets. If the R<sup>2</sup> values are considered it also ranks first on the 1986 data (the snowier year and thus the

better test for the model) but comes second to the six-hourly model type on the 1987 data. If the mean  $R^2$  for both years are compared (0.616 for 1986 compared to 0.599 for 1987) it can be seen that method (2) is also the best performer when considering the  $R^2$  values.

The second comparison to be made was between different methods used in model types (1) - (3) above. The four approaches compared were as follows:

- (a) Simple model with linear routing.
- (b) Simple model with non-linear routing.
- (c) Freezing level with linear routing.
- (d) Freezing level with non-linear routing.

Table 4.12 shown the results from using both optimised and combined parameter sets on all model runs (i.e. model type (1) - (3) using approaches (a) - (d).

Criteria	Year and Rank	Model type			
		(a)	(b)	(c)	(d)
Standard Error	1986	0.2236	0.2101	0.2348	0.2125
	Rank	3	1	4	2
	1987	0.1239	0.1318	0.1338	0.1322
	Rank	1	2	4	3
$R^2$	1986	0.653	0.695	0.621	0.689
	Rank	3	1	4	2
	1987	0.588	0.551	0.472	0.497
	Rank	1	2	4	3

Table 4.12

Summary SE and  $R^2$  results for all parameter sets using modelling approaches (a) - (d) as defined in the main text.

The first point that can be made from these results is that approach (c) is clearly the worse, being ranked fourth for all SE and  $R^2$  values.

The relative performance of the remaining three approaches is not so clear, however. If the mean ranks are calculated the values are as follows:

Approach (a) = 2.0

Approach (b) = 1.5

Approach (c) = 2.5

From these values it can be said that when all model types are considered Approach (b) (no freezing level but with addition of non-linear routing) produces the best results. Approach (a) is second (no freezing level and linear routing). This confirms the results in 4.4.2 which showed that the addition of the freezing level weakened the model's performance. It also suggests that the addition of non-linear routing helps the models, though it must be noted that this improvement may be largely attributed to the influence of the six-hourly time series models (4.5.2) which show a marked improvement when using non-linear routing.

Whilst the results shown in Table 4.12 and discussed above were useful in summarising the results of all model runs so far they did not assist in determining a single best method

and approach that future development would be concentrated on. To do this Table 4.13 was constructed which shows the summary results from applying the four different approaches to model type (2) only, i.e. running over a daily time interval and calculating the number of degree-days from the true daily mean temperature.

Criteria	Year and Rank	Model type			
		(a)	(b)	(c)	(d)
Standard Error	1986	0.2034	0.1945	0.2291	0.2058
	Rank	2	1	4	3
	1987	0.1212	0.1340	0.1425	0.1364
	Rank	1	2	4	3
R <sup>2</sup>	1986	0.695	0.723	0.616	0.688
	Rank	2	1	4	3
	1987	0.601	0.518	0.360	0.416
	Rank	1	2	4	3

Table 4.13 Summary SE and R<sup>2</sup> results from all parameter sets using model approaches (a)-(d) on model type (1) only. Definitions as in main text.

These results very strongly indicate that the model performs better without the addition of the freezing level, approaches (c) and (d) being ranked 4 and 3 respectively for all cases. The addition of the freezing level has such a detrimental effect on method (2) in particular that six of the eight SE and R<sup>2</sup> values for approaches (c) and (d) are worse in Table 4.13 than 4.12.

Having discounted approaches (c) and (d) it was less easy to differentiate between (a) and (b), i.e. linear and non-

linear routing. They both have a mean rank of 1.5, coming first and second an equal number of times. If the mean SE and  $R^2$  are calculated they suggest that linear routing is the best performer, the mean SE being 0.1623 compared to 0.1643 and the mean  $R^2$  being 0.648 compared to 0.621. However, this difference is due to the 1987 values; those for the 1986 model runs indicate that the addition of non-linear routing might improve the models. As this was the snowier year (3.1) it could be argued that the results were more important than those of 1987.

Due to the difficulties in deciding a clear optimum model approach it was decided to continue the model development using model type (2) and approaches (a) and (b), i.e. TINDEK using average daily temperatures with both linear and non-linear routing. By doing this the number of different model combinations was reduced from 12 to two, greatly speeding up the computing and simplifying the analysis of any subsequent model changes.

#### 4.6 Final stages of TINDEK development

##### 4.6.1 Correction of over-prediction in the early stages of the model runs

Having decided to concentrate the model development on TINDEK using average daily temperatures with linear and non-linear routing functions the problem of over-prediction in the early stages of the model runs had to be dealt with.

This pattern was also found with some of the models used in the WMO project (WMO, 1986, Nemec, 1986), resulting in the WMO recommending that runoff be reduced during the period the snowpack was ripening, i.e. becoming isothermal and saturated. Whilst this recommendation was to reduce runoff over the first few days the Mharcaidh models over-predict for up to ten days. As it is unlikely that it takes the snowpack this long to become isothermal and saturated with melt water the over-prediction must be due to another factor.

Anderson (1968, 1973, 1976) reported a seasonal variation in the melt factor when applying the NWSRFS to data at the Central Sierra Snow Laboratory, California. For the contiguous US the seasonal variation could be represented by a sine function:

$$Mf = (MFMAX+MFMIN)/2 + \sin(n*2 /366) * (MFMAX-MFMIN)/2 \quad (4.28)$$

where

MFMAX = Maximum melt factor (on 21 June)

MFMIN = Minimum melt factor (on 21 December)

n = Day number beginning with 21 March

This sine function had to be adjusted when using the model on Alaskan data though the seasonal variation is still present (Figure 4.12). Anderson attributes this seasonal variation mostly to changes in radiation inputs throughout the year. Early in the melt season the albedo of the snow

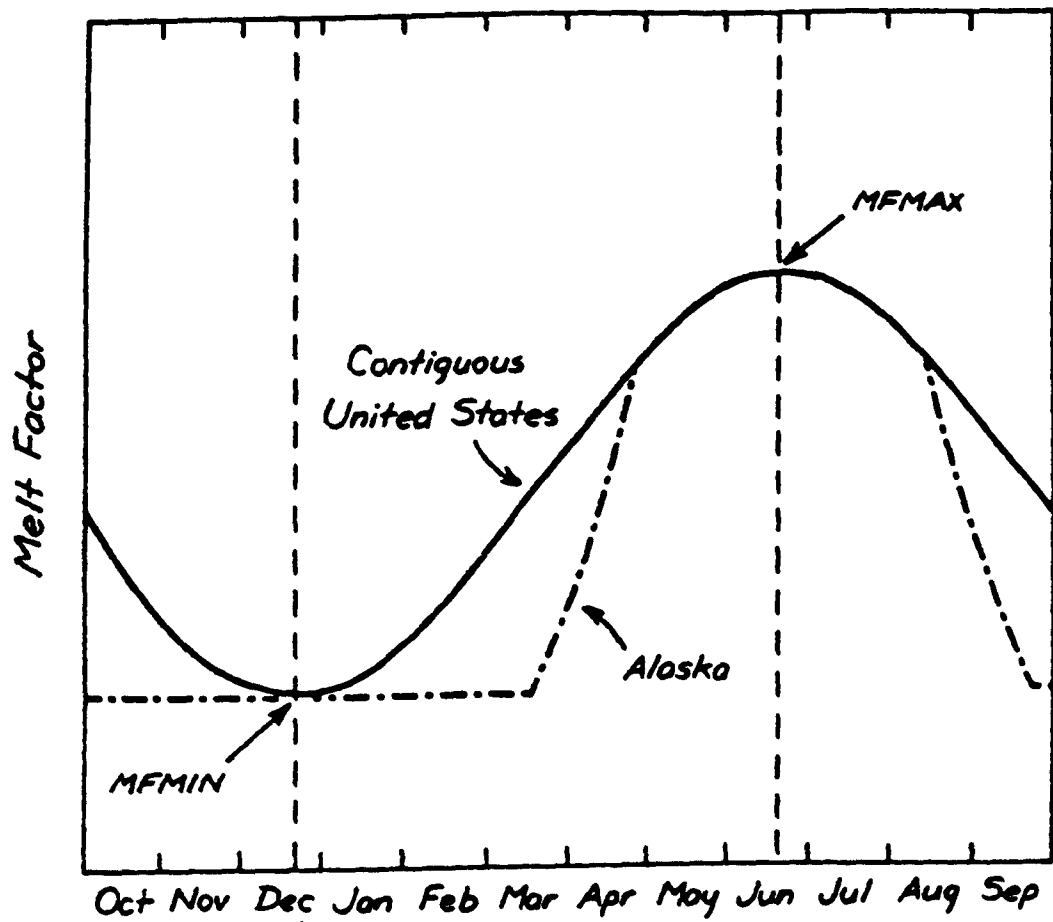


**Figure 4.12** The variation in melt factor determined by Anderson (1978) for North America. No scale for the y-axis is given by Anderson.

is high (typically 0.9) reflecting much of the incident (incoming) shortwave radiation. As the melt season progresses the albedo decreases (to approximately 0.5) as the snow characteristics alter, and the incident radiation inputs increase as a result of longer day length and decreasing zenith angle of the sun. This results in an increase in melt and Anderson corrects for this by increasing the melt factor. Rango and Martinec (1982) and Martinec (1980b) also vary the melt factor and attribute the changes to changing snow density in the early stages of the melt season.

Whilst the melt season for the Mharcaidh is usually only two-three months long it is possible that there is a need for the melt-factor to increase. As the time series plots indicate a consistent over-prediction only during the early stages this is most likely due to the changing albedo of the snowpack - radiation inputs will change more gradually as illustrated in Figures 3.8 and 3.9. Also, as mentioned in 1.3.2, the significance of radiation inputs to the energy balance is likely to be relatively low in Scotland due to the high incidence of cloudy weather.

It was thus decided to reduce the melt factor over the first ten days of the model run. This was initially done in two stages:

Days 1 - 7       $AM = M * X$       and

$$\text{Days } 8 - 10 \quad \text{AM} = M * Y \quad (4.29)$$

where

AM = Actual melt coefficient used for the melt calculation and

X and Y are constants such that  $0 < X < Y < 1$ .

Four different combinations of X, Y and routing function were tried. The values and results are shown in Table 4.14. These clearly indicate a dramatic improvement in the model performance, the mean  $R^2$  of the optimised model runs increasing from 0.644 to 0.750 and, more usefully, the mean  $R^2$  of the combined parameter set model runs increasing from 0.613 to 0.724. The increase in performance is most noticeable for the 1987 model runs (for example, the mean  $R^2$  of the 1987 combined parameter model runs increases from 0.513 to 0.687, an increase of 34%) which had previously shown the greatest over-prediction of runoff during the early stages of the model run (Figures 4.7 and 4.10).

In addition to performing well statistically it can be seen from Table 4.14 that the range of optimised parameters is smaller (for example,  $M = 2.1$  to  $3.2$ , Non-Linear Routing  $R = 0.65$  to  $0.82$ ). Whilst this explains the good performance of the model runs using the combined data sets it also increases the possibility of declaring the parameters as constants.

As this latest addition to the model was so successful it

Parameter Set	Year	Routing	E	R	A	M	W	X	Y	SE	FA	R <sup>2</sup>	SE	R <sup>2</sup>
Optimised	1986	Linear	0.010	0.840	9.0	2.30	340	0.6	0.80	0.1767	3.20	0.770	0.1931	0.726
		Non-lin	0.010	0.770	8.2	2.90	340	0.5	0.75	0.1547	2.28	0.774	0.1931	0.726
		Non-lin	0.010	0.820	9.1	2.40	320	0.4	0.70	0.1725	2.79	0.781	0.1931	0.726
		Linear	0.010	0.190	9.1	2.10	320	0.4	0.70	0.1742	3.40	0.776	0.2016	0.700
	1987	Non-lin	0.006	0.750	7.0	2.90	160	0.6	0.80	0.1136	0.00	0.674	0.1313	0.550
		Non-lin	0.006	0.720	7.1	3.00	160	0.5	0.75	0.1105	0.00	0.692	0.1313	0.550
		Non-lin	0.006	0.650	7.4	3.20	160	0.4	0.70	0.1080	0.00	0.693	0.1313	0.550
		Linear	0.006	0.560	8.0	2.40	140	0.4	0.70	0.0152	0.00	0.760	0.1182	0.620
Combined	1986	Non-lin	0.008	0.795	9.0	2.60	340	0.6	0.80	0.1817	2.39	0.762	0.1959	0.720
		Non-lin	0.008	0.745	8.2	2.95	340	0.5	0.75	0.1779	1.87	0.767	0.1959	0.720
		Non-lin	0.008	0.735	9.1	2.80	320	0.4	0.70	0.1818	1.71	0.761	0.1959	0.720
		Linear	0.008	0.375	9.1	2.25	320	0.4	0.70	0.1826	2.87	0.757	0.2052	0.689
		1987	Non-lin	0.008	0.795	9.0	2.60	340	0.6	0.80	0.1227	1.25	0.643	0.1367
Non-lin			0.008	0.745	7.1	2.95	160	0.5	0.75	0.1169	0.47	0.664	0.1367	0.487
Non-lin			0.008	0.735	7.4	2.80	160	0.4	0.70	0.1163	0.81	0.667	0.1367	0.487
		Linear	0.008	0.375	8.0	2.25	140	0.4	0.70	0.1038	1.17	0.772	0.1242	0.590

**Table 4.14** Results from running TINDEX with the melt factor increasing in two stages. The final two columns show corresponding results for TINDEX (both using average daily temperature). E = Environmental lapse rate ( $^{\circ}\text{C m}^{-1}$ ), R = Routing coefficient, A = Initial snow covered area ( $\text{km}^2$ ), M = Melt coefficient ( $\text{mm}^{\circ}\text{C day}^{-1}$ ), W = Initial snowpack water equivalent (mm).

was decided to develop it further. In reality the melt rate will increase gradually as the snowpack becomes saturated progressively up the catchment and the snow surface characteristics alter. It was thus decided to alter the model so that the melt factor increased gradually rather than in two discrete stages. After experimenting with different possible methods it was decided to use a negative exponential function in the form:

$$AM = M - (M - 1) * \exp (ALB * N) \quad (4.30)$$

where

AM = Melt factor on day n

M = Melt factor

ALB= Constant to be optimised

N = Day number

This function produced a series of asymptotic curves according to the value of ALB that approach the final melt factor. The effect of different values of k on the growth rate is shown in Figure 4.13 (k = ALB in Figure).

The model was then run using both linear and non-linear routing on combined and optimised data sets. The model was also run with the melt factor increase being calculated by substituting the cumulative number of degree-days for day number, along the lines of Rango and Martinec's (1982) later work discussed in Chapter 1. It was felt that this would allow for discrete observed events rather than

assuming a gradual change or, as before, selecting two arbitrary dates for the change to occur. The results from these model runs are shown in Table 4.15 and Figure 4.14 shows time series plots for the model runs using AM determined from day number.

#### 4.6.2 Results

If the results in Tables 4.14 and 4.15 are compared it can be seen that whilst the gradually increasing melt factor does not perform as well as the two-stage increase it is still superior to the constant melt factor for all model runs, the mean  $R^2$  being 0.722 compared to 0.677 for the optimised parameter sets and 0.697 compared to 0.630 for all model runs.

The visual improvement can be clearly seen in Figure 4.14. Whereas previous TINDEX model runs failed to match the flow during days 1-14 of the 1986 model run the addition of the gradually increasing melt factor resulted in the first peak on day 5 being well simulated, followed by a period of low and high flow that matches the observed data. The improvement is less noticeable on the non-linear plot, the statistical superiority of this approach being attributed to its ability to match flow on the recession limbs of the hydrographs much better.

The visual improvement resulting from the addition of the

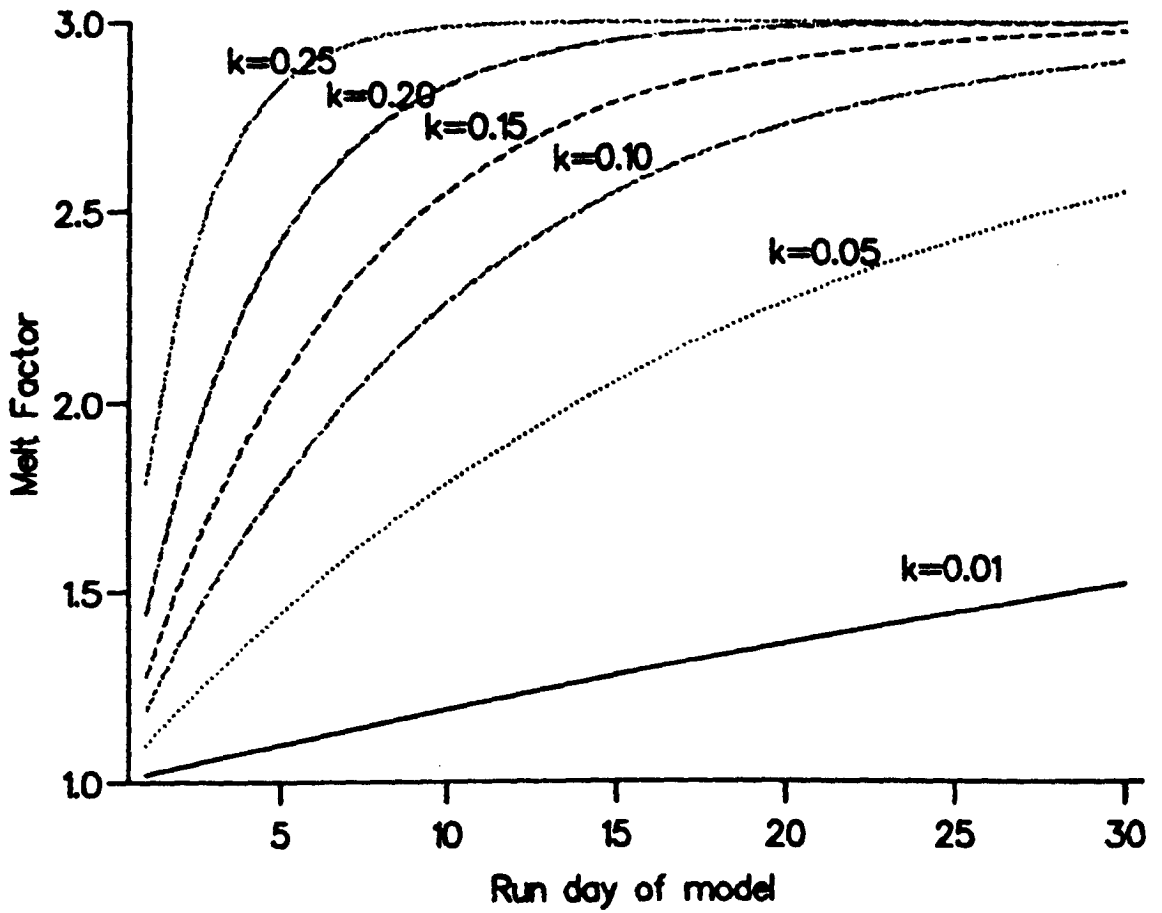


**Figure 4.13** The effect of the parameter  $k$  on the rate of growth of the gradually increasing melt factor. The maximum value for the melt factor in all cases is three.

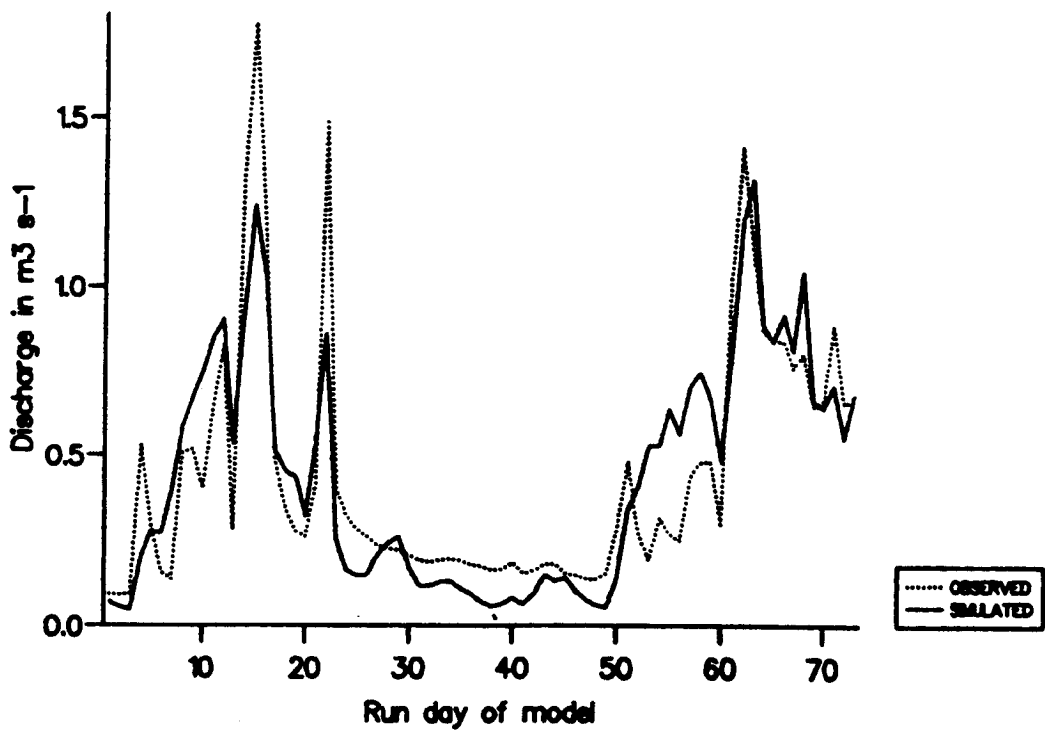
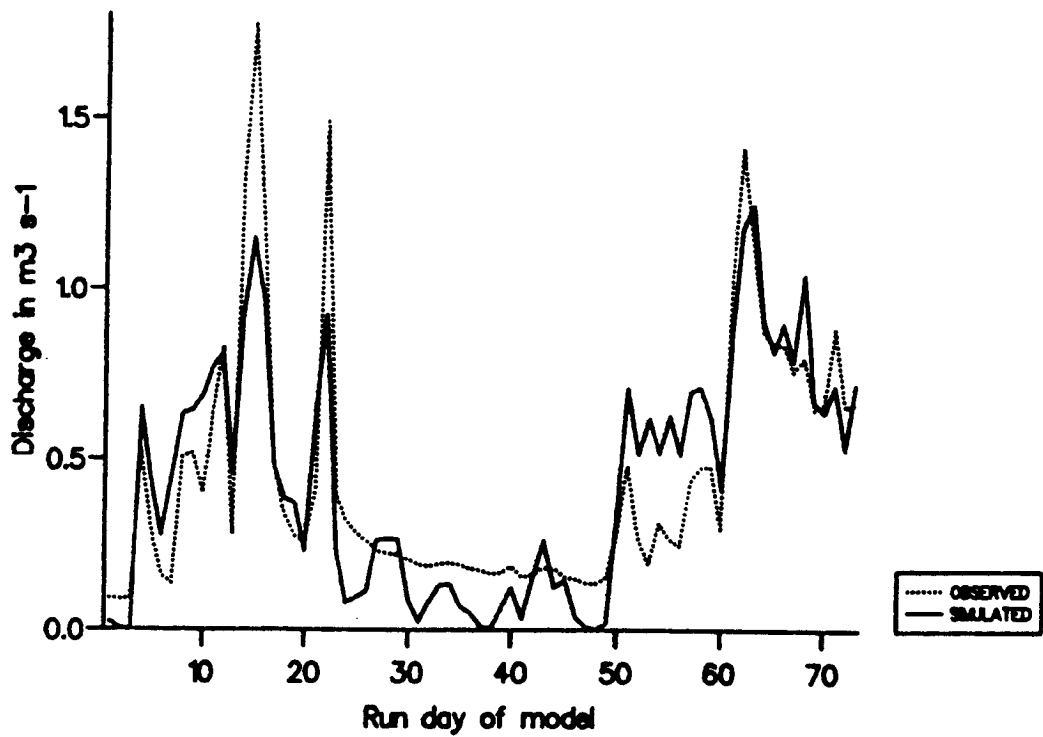


**Figure 4.14a** Time series plots from running TINDEK with a gradually increasing melt factor on the 1986 Mharcaidh data. The upper plot used linear routing and the lower used non-linear routing.

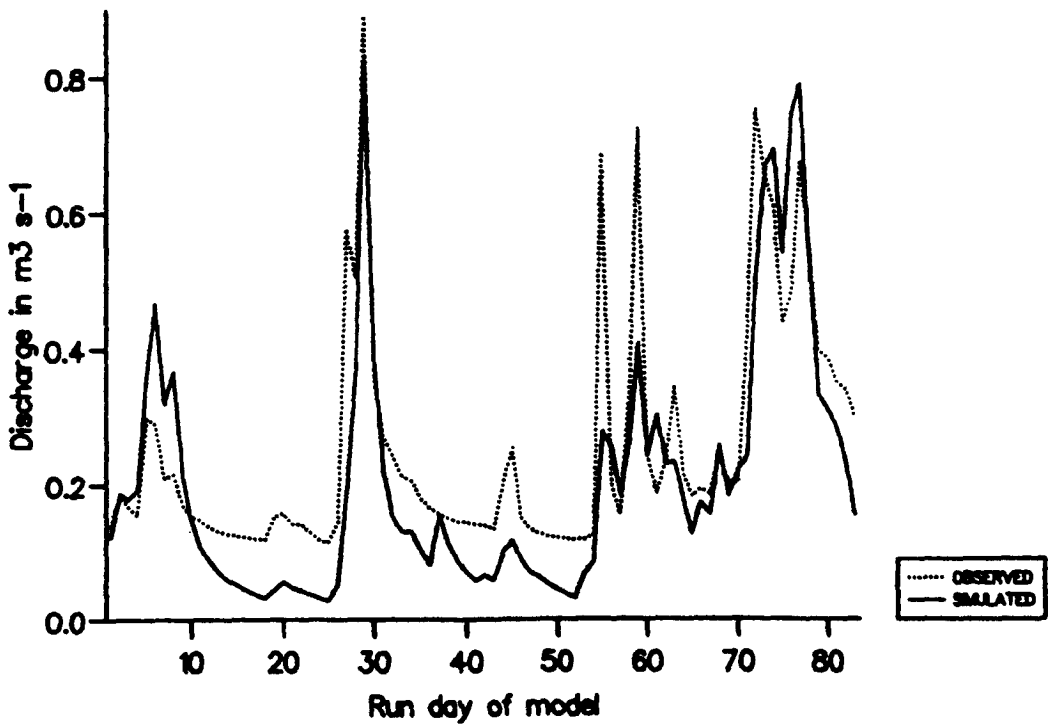
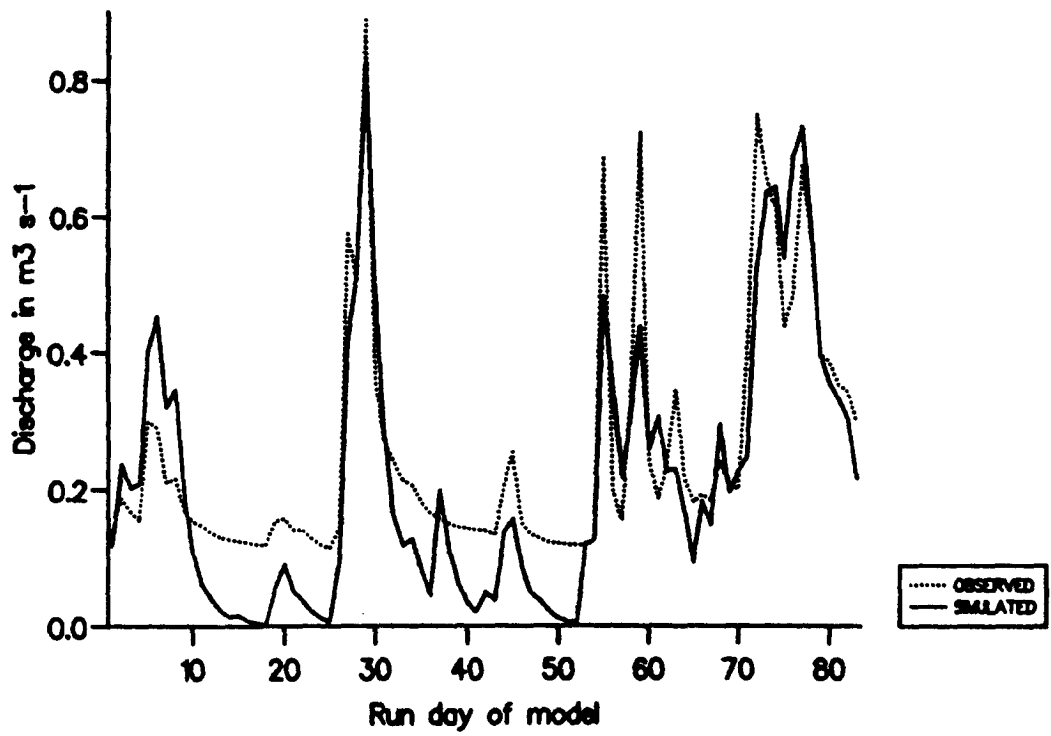


**Figure 4.14b** Time series plots from running TINDEK with a gradually increasing melt factor on the 1987 Mharcaidh data. The upper plot used linear routing and the lower used non-linear routing.

Parameter Set	Melt Factor	Year	Routing	E	R	A	M	W	K	SE	FA	R <sup>2</sup>	SE	R <sup>2</sup>
Optimised	Day	1986	Linear	0.010	0.260	7.9	2.80	330	0.14	0.1910	2.35	0.731	0.2016	0.700
			Non-lin	0.010	0.760	8.2	3.00	340	0.14	0.1856	2.15	0.746	0.1931	0.726
		1987	Linear	0.006	0.560	7.7	2.60	140	0.05	0.996	0.00	0.736	0.1182	0.620
			Non-lin	0.006	0.690	7.0	3.30	160	0.08	0.1127	0.00	0.673	0.1313	0.550
	Cumulative Degree-day	1986	Non-lin	0.010	0.750	8.3	3.10	330	0.05	0.1801	1.9	0.761	0.1931	0.726
			Non-lin	0.006	0.750	7.0	3.00	160	0.07	0.1199	0.00	0.629	0.1313	0.550
Combined	Day	1986	Linear	0.008	0.410	7.9	2.70	330	0.10	0.2014	2.27	0.701	0.2050	0.689
			Non-lin	0.008	0.725	8.2	3.15	340	0.11	0.1897	1.62	0.736	0.1959	0.720
		1987	Linear	0.008	0.410	7.7	2.7	140	0.10	0.1142	0.00	0.627	0.1242	0.590
			Non-lin	0.008	0.725	7.0	3.15	160	0.11	0.1187	0.00	0.645	0.1167	0.487
	Cumulative Degree-day	1986	Non-lin	0.008	0.775	8.3	3.05	330	0.06	0.1834	1.56	0.752	0.1959	0.720
			Non-lin	0.008	0.755	7.0	3.05	160	0.06	0.1272	0.48	0.587	0.1367	0.487

**Table 4.15** Results from using a gradually increasing melt factor (K) when applying TINDEX to the Mharcaidh datasets. The corresponding TINDEX results without the gradually increasing melt factor are shown in the final two columns. E = Environmental lapse rate ( $^{\circ}\text{C m}^{-1}$ ), R = Routing coefficient, A = Initial snow covered area ( $\text{km}^2$ ), M = Melt coefficient ( $\text{mm}^{\circ}\text{C day}^{-1}$ ), W = Initial snowpack water equivalent (mm).

gradually increasing melt factor is more noticeable for the 1987 plots. Earlier model runs over-predicted the first peak flows on days 5 and 6 by more than  $0.3\text{m}^3 \text{ s}^{-1}$ ; this has been reduced by more than a half in the plots shown in Figure 4.14. These also show the reason for the decrease in performance when using non-linear routing; on days 55 and 59 the model is less able to simulate the two short duration peak flow events. The superior performance of non-linear routing during receding flows can also be seen, accounting for the good  $R^2$  values. One final point to be made is that the model simulates the peak snowmelt flows well on days 29-30, 72 and 77 despite this being a less snowy year.

If the results from calculating the gradually increasing melt factor on cumulative degree-days and actual day-number shown in Table 4.15 are compared it can be seen that whilst there is a slight increase in statistical performance for the 1986 model runs, the decrease for the 1987 runs is much higher, resulting in the mean optimised  $R^2$  decreasing from 0.710 to 0.695 and the mean combined  $R^2$  decreasing from 0.691 to 0.670. It is not known why this is so; one would expect the cumulative degree-days method to perform better. The only possible explanation for this discrepancy is that, similar to the addition of the freezing level, making one particular point of the model more sophisticated than the rest knocks the model out of balance and weakens the overall performance.

The optimised values of the melt and recession coefficients are very close in Table 4.15, causing the combined parameter set model runs to perform well. This is a most useful characteristic and suggests that the model has potential for use in a general form, only needing to optimise the snowpack characteristics which will be unique to each catchment for each year.

Finally, Figure 4.15 shows the simulated and observed snowpack depletion curves for the 1986 non-linear and 1987 linear model runs using both optimised and combined parameter sets. It can be seen that the 1986 model run simulates the general depletion pattern well, starting with a period of depletion, then a stable, constant SCA, followed by a rapid depletion at the end of the season. The gradient (rate of depletion) of the final period is especially well matched though the model does over-predict the SCA during the stable period by more than 1.5 Km<sup>2</sup>.

The 1987 depletion curve provides a less good visual fit than the 1987 model run, though the final period of rapid depletion is very well matched. Whilst much of the poor visual fit can be attributed to the rises in observed SCA (3.1.1) due to fresh snowfall which was not catered for in the model, the model shows the same trends for the 1987 plots as it does for 1986; namely it under-predicts SCA at the start of the melt season, over-predicts it during the middle, stable period but ends by matching the final

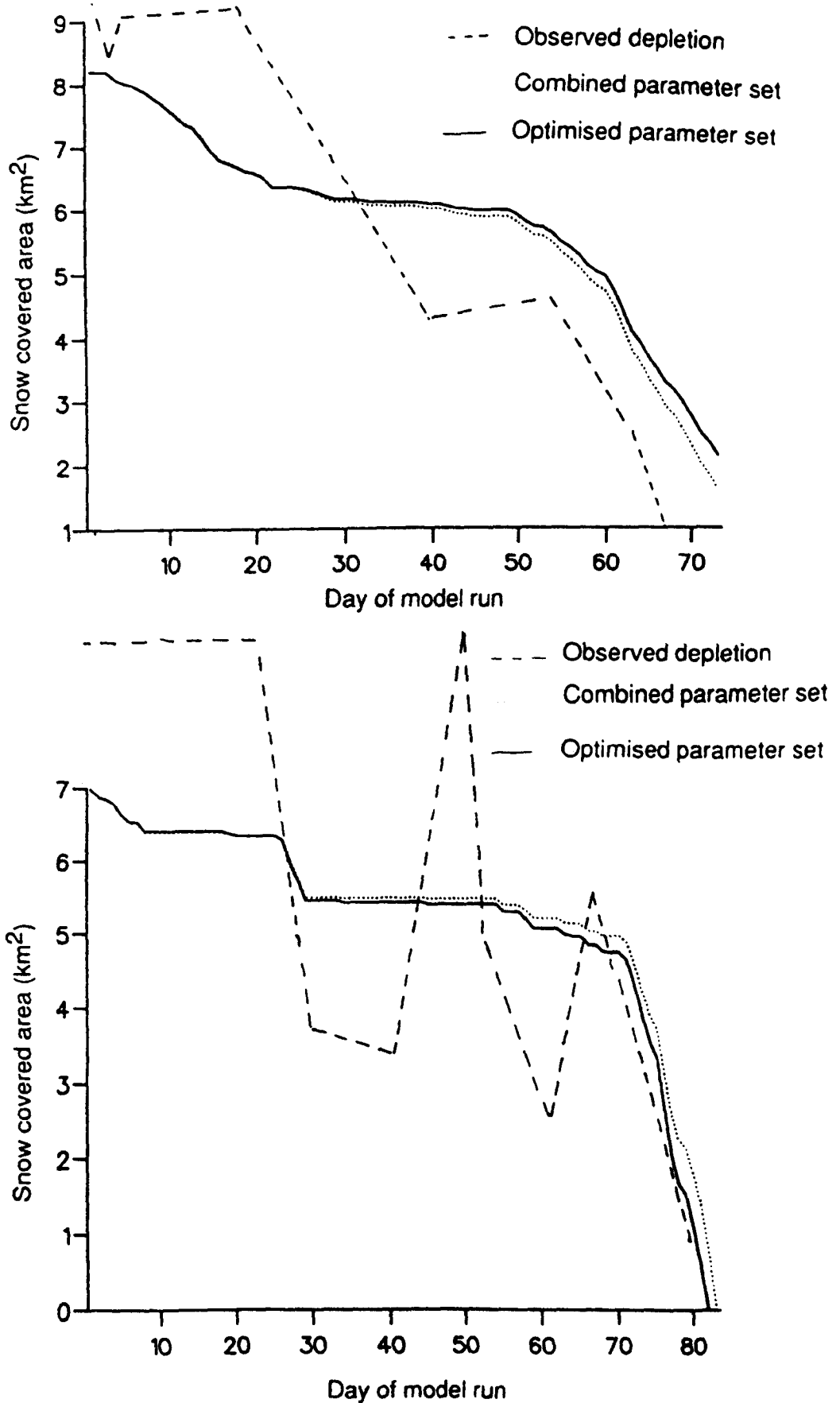


**Figure 4.15** Modelled and observed snow cover depletion curves for the 1986 and 1987 TINDEK model runs using the gradually increasing melt factor and non-linear routing. It is interesting to note that there is very little difference between the model runs using optimised and combined parameter sets.

depletion well. This suggested that the model was oversimplifying the snowpack representation and that this needed attention, possibly by dividing the catchment into a number of elevation zones along the lines of that used by Martinec (1975, 1980a) and modelling the snowpack within each of these zones.

One final point that can be made about the depletion curves shown in Figure 4.15 is that for both years there is little difference between the plots for the model runs using the optimised and combined parameter sets. This is again an encouraging sign suggesting that setting the lapse rate, recession and melt coefficients as constants does not severely limit the performance of the model, even for two years where the snowpack characteristics are so different.

#### 4.7 Conclusion

This chapter has described the development of the temperature-index model described by Ferguson (1984). It has shown that by making minor changes to the model its ability to simulate the observed runoff from a snow-covered catchment has been increased; the mean  $R^2$  for the first runs of TINDEX was 0.605, the final mean of  $R^2$  of the two optimised model runs using linear routing, a gradually increasing melt factor determined on day number and degree-days calculated on the true mean daily temperature was 0.734.

Whilst these developments have aided the models ability to simulate the observed flow the same can not be said of all the changes made to the model. The addition of a freezing level, reducing the time interval to six hours and determining the melt factor from the cumulated degree-days have hindered the performance. It is not clear if the addition of non-linear routing helps or hinders; because of this both methods will be used when applying the model to other datasets later in the project.

By using a depletion submodel within TINDEXT it was able to endogenously model the depletion of the snowpack as the melt season progressed, thus avoiding the need to update the snowpack characteristics as the melt season progresses. Although the modelled SCA depletion curve did not match the observed, the general patterns were similar for both years, as were the discrepancies. This suggests that it may be possible to more accurately model the SCA depletion by altering the snowpack structure within the catchment.

Although the overall performance of TINDEXT has been increased it is still unable to accurately simulate the observed peak flows, especially those occurring during rain-on-snow events.

Finally, the most encouraging point about the last TINDEXT model run is that the model is able to perform well when the lapse rate, recession and melt coefficients are set as

constants at the start of the model run, the model only optimising the snowpack characteristics. The mean  $R^2$  for the non-linear models run using the combined parameter set is 0.691, only 2.7% below the corresponding optimised value. This is accounted for by the optimised values of R and M being close and suggests the model has potential for use in real-time and on other datasets.

## CHAPTER 5 OTHER MODEL TYPES

### 5.1 Introduction

Chapter 4 described the development and results of TINDEX and FTINDEX, the two models based solely on the temperature index approach and treating the catchment as a homogenous unit. At this stage in the project it was felt that the development of these models had progressed such that there was little potential for further improvement. It was thus decided to try two different approaches, both using temperature as the index to melt but with significant differences to TINDEX and FTINDEX. The first alternative is the parametric energy balance approach which uses temperature and other readily available meteorological data as an approximation of the full energy balance and use this to calculate melt. The second alternative retains temperature as the sole index to melt but divides the catchment spatially into a number of elevation zones as pioneered by Martinec (1975).

### 5.2 Parametric energy balance approach

#### 5.2.1 Introduction

In 1.3 the three main methods used to model snowmelt were described, namely the full energy balance at a point, the

parametric energy balance and temperature index methods. As the final TINDEX model appeared to perform badly during rain/snow events, under-simulating the peak flows for both 1986 and 1987, it was decided to use the parametric energy balance method proposed by Anderson (1968, 1973, 1976) based on the model used by Anderson and Crawford (1964). The approach separates rain-on-snow from pure snowmelt events to calculate the melt, attempting to take account of the varying **sensible heat** contribution to melt by using windspeed data. During non-rain events Anderson used an empirically based melt factor routine which is essentially the same as the temperature index method. However, during rain-on-snow events Anderson showed that by making assumptions it is possible to adopt the energy-balance equation such that only universally available data are needed to calculate the energy balance.

The assumptions made were as follows:

- (1) During rain-on-snow events incoming solar radiation is negligible as overcast conditions are likely to prevail.
- (2) Incoming longwave radiation is essentially equal to blackbody radiation at the air temperature found at the base of the cloud cover. This in turn should be close to the prevailing air temperature.
- (3) The relative humidity is high (90%).

Using these assumptions it is possible to calculate the saturation vapour pressure from the observed air temperature. This is then used, along with air temperature, observed precipitation and a wind function (derived from observed wind speed) to calculate the theoretical melt during a rain-on-snow event.

It was hoped that this method would improve the performance of TINDEX given that the melt is calculated according to the energy balance during rain-on-snow events when the model performed less well. The high correlation coefficients between air temperature, windspeed, precipitation and observed flow found in 3.3 supported this hope.

#### 5.2.2 Model structure

TINDEX was adapted to allow for calculating melt during rain-on-snow events and re-named ANDERS. One extra value had to be optimised, WFUN, which was the average wind function during rain-on-snow periods ( $\text{mm mb}^{-1}$ ). Anderson only used windspeed data during rain-on-snow events though other authors (Braun and Lang, 1986) use it for all melt events.

When up to 1mm of rainfall was recorded at the AWS, melt was calculated using the same method as TINDEX. On occasions when the recorded rainfall was greater than or

equal to 1mm the parametric energy balance method was used to compute snowmelt in the following way:

- (1) Saturation Vapour Pressure (ESAT) was calculated using:

$$ESAT = 2.749 * 10^8 * \exp (-4278.6/ATEM + 242.8) \quad (5.1)$$

- (2) The atmospheric pressure (PA) was calculated from the height of the AWS using the 'standard-atmosphere' altitude-pressure relationship, approximated by:

$$PA = 1012.4 - (11.34 * EL) + (0.00745 * EL^{2.4}) \quad (5.2)$$

where

EL = Elevation for which PA was to be determined (hundreds of metres), calculated as the mean altitude of the snowpack.

- (3) WINDM, the total wind movement over the day (km) was calculated from the observed mean daily windspeed, and this was then used to calculate the average wind function during rain-on-snow events (UADJ) from:

$$UADJ = WINDM * WFUN \text{ (mm mb}^{-1} \text{ day}^{-1}\text{)} \quad (5.3)$$

- (4) The depth of melt during the rain on snow event was then calculated using:

$$\begin{aligned}
\text{WETM} = & 3.67 * 10^{-9} * (\text{ATEM}(\text{I}) - 273)^4 - 81.6 \\
& + 0.0125 * \text{PPT}(\text{I}) * \text{ATEM}(\text{I}) + 8.5 * \text{UADJ} * ((0.9 * \\
\text{ESAT} - 6.11) + & 0.00057 * \text{PA} * \text{ATEM}(\text{I})) \quad (5.4)
\end{aligned}$$

where

WETM = Depth of melt (mm) (After Anderson, 1976)

The precipitation itself was then added to the meltwater and routed through the store using the same methods as TINDEXT.

### 5.2.3 Results and further modification

ANDERS was applied to both the 1986 and 1987 Mharcaidh data sets using both linear and non-linear routing. The results are shown in Table 5.1, along with the results from using combined values of E, R, M and WFUN and optimised values of A, W and K using linear routing. TINDEXT R<sup>2</sup> values are shown for comparison.

From these results it can be clearly seen that the parametric energy balance approach performs less well than the temperature index method, the R<sup>2</sup> values being less for every model run and the mean R<sup>2</sup> for the whole dataset decreasing from 0.702 to 0.600. ANDERS was not run with the combined dataset using non-linear routing as the optimised model runs were so bad, the SE and R<sup>2</sup> values being worse than those of the combined parameter model runs using linear routing. Had these extra model runs been carried out, the mean R<sup>2</sup> for ANDERS would have decreased even

Year	Routing	E	R	A	M	W	K	WFUN	SE	FA	R <sup>2</sup>	TINDEX
1986	Linear	0.006	0.49	8.9	3.2	240	0.08	0.0035	0.2034	0.000	0.699	731
1987	Linear	0.006	0.68	4.2	5.0	180	0.42	0.0035	0.1253	0.000	0.547	736
1986	Non-lin	0.006	0.88	7.6	2.9	230	0.09	0.0020	0.2153	0.573	0.658	746
1987	Non-lin	0.006	1.10	7.3	1.8	90	0.08	0.0005	0.1274	0.792	0.479	673
1986	Linear	0.006	0.58	7.6	4.1	290	0.11	0.0035	0.2101	0.000	0.675	707
1987	Linear	0.006	0.58	4.4	4.1	170	0.42	0.0035	0.1272	0.000	0.545	627

Table 5.1 Results from applying the parametric energy balance model, ANDERS to the Mharcaidh 1986 and 1987 datasets. E = Environmental lapse rate ( $^{\circ}\text{C m}^{-1}$ ), R = Routing coefficient, A = Initial snow covered area ( $\text{km}^2$ ), M = Melt coefficient ( $\text{mm}^{\circ}\text{C day}^{-1}$ ), W = Initial snowpack water equivalent (mm).

further, whilst that for TINDEX would have only decreased by 0.001.

It was clear that the changes to the model were decreasing its ability to simulate melt during rain-on-snow events, the peaks being less well matched than when using TINDEX. This decrease was likely to be due to one or more of several reasons:

- (1) Anderson's assumptions were fundamentally incorrect.
- (2) The assumptions made by Anderson were not valid for use in Scottish conditions.
- (3) The method was being incorrectly used in the model.
- (4) There were errors in the precipitation data, causing the model to operate incorrectly on rainy days.

As (1) was highly unlikely it was disregarded, along with (4) as the data showed high rainfall occurring on days with high flow. This left (2) and (3). One of Anderson's assumptions was that the relative humidity was high (90%), indicating warm, humid and overcast conditions. The critical rainfall threshold value used for ANDERS was 1mm; above this value the parametric energy balance method was used. Closer reference to Anderson's work revealed that he used a critical value of 2.5mm, over a six-hour time period. Thus, it was thought that the poor performance of ANDERS was due to the critical rainfall value being too low. It is possible that, by setting the threshold too

low, too many days were assumed to be 'warm and wet' when the 'rainfall' may have just been due to the showers associated with the passing of a cold front or the melting of snow that had blown into the gauge.

As a result of this, ANDERS was re-run with the threshold rainfall value being re-set at 5mm and 10mm. By doing this the parametric energy balance would only be applied to days of high rainfall when the peak flows occurred, hopefully increasing the model performance. The results from these model runs are shown in Table 5.2, and Figures 5.1 and 5.2 show time series plots of some of the model runs. When using 5mm as the threshold linear routing gave the best results but, when using 10mm, non-linear model runs performed better. This is explained by the fact that a higher threshold makes the model more similar to TINDEK, which tended to perform better using non-linear routing, whilst a low threshold will make it more like the early version of ANDERS which performed better using linear routing.

From these results and those shown in Table 5.1 a number of points can be made:

- (1) The mean  $R^2$  has increased from 0.617 (all linear runs using 1mm as threshold) to 0.650 (5mm threshold) and 0.655 (10mm threshold). Thus, by only applying the parametric energy balance to high rainfall events the

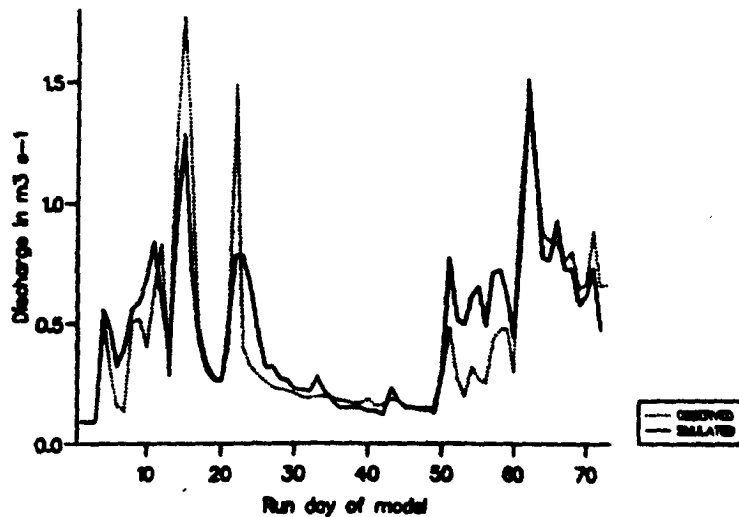
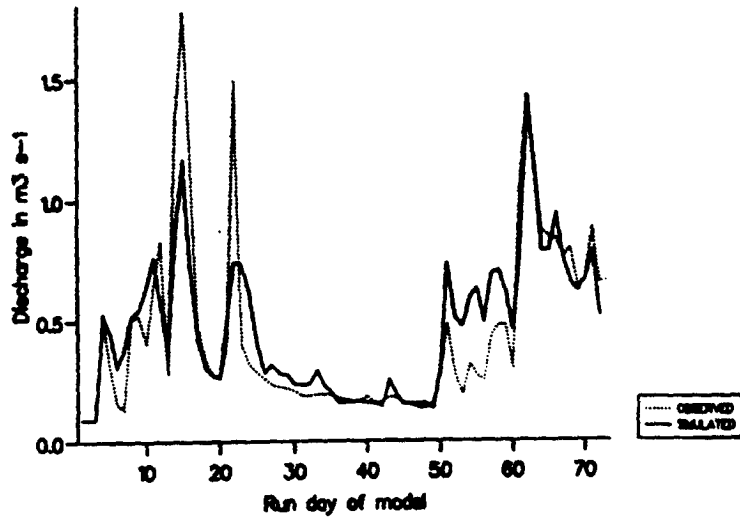
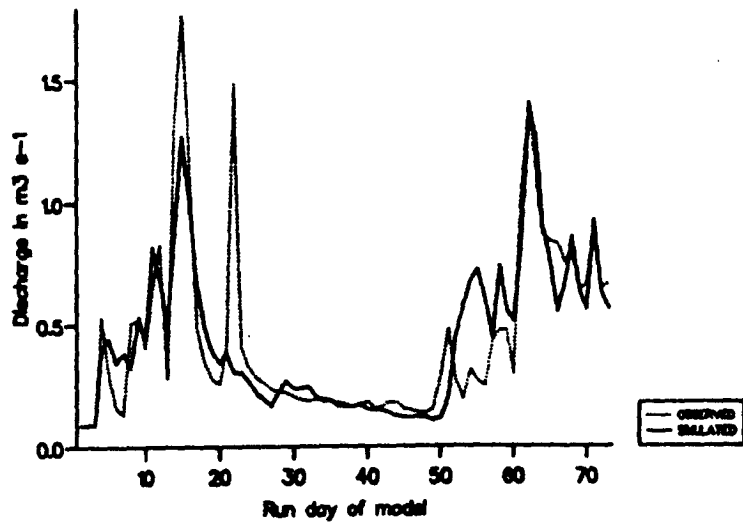


**Figure 5.1** Time series plots from running ANDERS on the Mharcaidh 1986 data. The upper plot shows the model using a rainfall threshold of 1mm and non-linear routing; the middle plot used a 10mm threshold and non-linear routing; the lower plot also used a 10mm threshold and non-linear routing but used the combined parameter set.

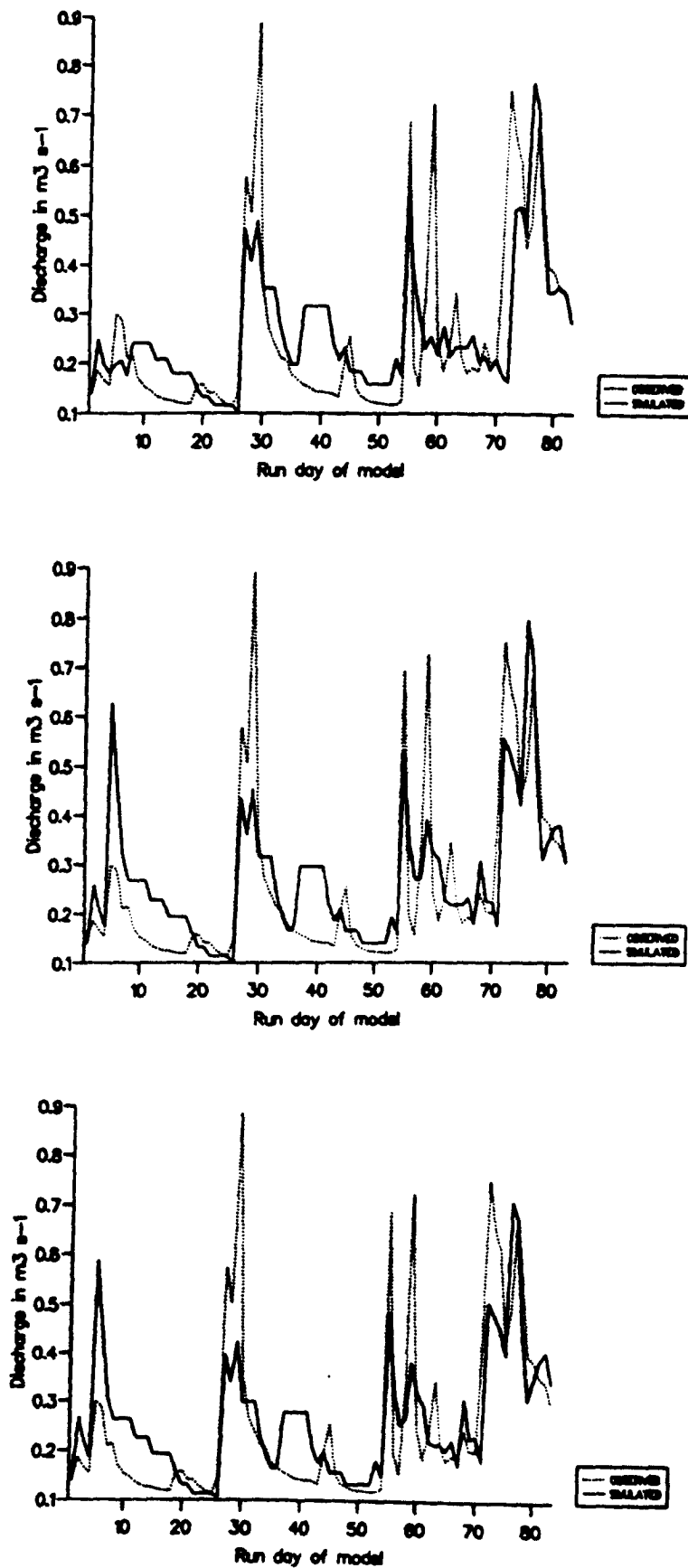


**Figure 5.2** Time series plots from running ANDERS on the Mharcaidh 1987 data. The upper plot shows the model using a rainfall threshold of 1mm and non-linear routing; the middle plot used a 10mm threshold and non-linear routing; the lower plot also used a 10mm threshold and non-linear routing but used the combined parameter set.

Data Set	Year	Routing	Threshold	E	R	A	M	W	K	WFUM	SE	FA	R <sup>2</sup>	INDEX Best Values
Optimised	1986	Linear	5	0.010	0.012	8.8	2.5	290	0.08	0.0001	0.2084	3.01	0.688	0.1910 0.731
Optimised	1987	Linear	5	0.006	0.590	4.9	4.1	160	0.30	0.0001	0.1137	0.00	0.657	0.996 0.736
Optimised	1986	Linear	5	0.008	0.300	7.4	3.3	310	0.10	0.0001	0.2142	1.68	0.652	0.2014 0.701
Optimised	1987	Linear	5	0.008	0.300	5.4	3.3	140	0.35	0.0001	0.1273	0.27	0.602	0.1142 0.627
Optimised	1986	Non-lin	10	0.010	1.250	8.8	2.3	280	0.08	0.0001	0.1917	3.11	0.737	0.1856 0.746
Optimised	1987	Non-lin	10	0.006	1.250	8.0	1.7	100	0.02	0.0001	0.1152	1.69	0.575	0.1127 0.673
Combined	1986	Non-lin	10	0.008	1.250	8.8	2.0	300	0.08	0.0001	0.1938	3.71	0.729	0.1897 0.736
Combined	1987	Non-lin	10	0.008	1.250	7.8	2.0	100	0.03	0.0001	0.0056	1.11	0.579	0.1187 0.645

Table 5.2 Results from applying ANDERS to the Mharcaidh 1986 and 1987 datasets using rainfall thresholds of 5 and 10mm. Results are only shown for the best routing method for each year. E = Environmental lapse rate ( $^{\circ}\text{C m}^{-1}$ ), R = Routing coefficient, A = Initial snow covered area ( $\text{km}^2$ ), M = Melt coefficient ( $\text{mm}^{\circ}\text{C day}^{-1}$ ), W = Initial snowpack water equivalent (mm).

- statistical performance of ANDERS has been increased.
- (2) Whilst the mean  $R^2$  has increased at the 5mm threshold, this is only due to a large increase in the 1987 values; the 1986  $R^2$  values have actually decreased.
  - (3) At the 10mm threshold the 1986  $R^2$  values show a marked increase, accounting for this being the best overall combination when using ANDERS. However, the 1987 optimised value is only slightly higher than that using the 1mm threshold (0.575 vs 0.547) and is less than that of the 5mm threshold model runs.
  - (4) The optimised R, M and WFUN parameter values for the 10mm threshold model runs are very close together, resulting in there being little loss in performance of ANDERS when using combined parameter values. Whilst this results in one of the SE values (1987) actually being lower for ANDERS than TINDEX the  $R^2$  values are still better for both TINDEX model runs.
  - (5) Whilst the SE value for the 1987 10mm threshold model run was lower when using the combined parameter set the  $R^2$  value actually increased. This highlights the problem of optimising the models on a single statistic and will be discussed further in Chapter 7.
  - (6) Despite the overall increase in performance of ANDERS when using a higher rainfall threshold value it still does not perform as well as TINDEX. At the 5mm level the mean  $R^2$  using ANDERS is 0.650 compared to the 0.699 of TINDEX and at the 10mm level the value is 0.655 compared to 0.700.

(7) Figure 5.1 shows that the visual performance of ANDERS is much less than that of TINDEK. Whilst it simulates well the final peak event of the season for both years the early peaks (more significant since they have a larger snowmelt contribution,) are poorly reproduced. Also, when run on the 1987 datasets the model produces a number of events where the flow is near constant at intermediate levels for a number of days. This is not so with the observed data and is another weakness of the model.

#### 5.2.4 Conclusions

It has been shown that by isolating the high magnitude rainfall events the performance of the ANDERS model is improved, especially for the 1986 dataset. Despite this improvement the model does not perform as well as TINDEK, both statistically and visually, despite the optimised parameters for the 10mm threshold being very close. Given that ANDERS is dependent on one extra meteorological variable than TINDEK and the problems likely to occur with applying this variable over a wide area it was felt that the parametric energy balance approach had little potential as a universally applicable model able to run in real time on readily available data. As other authors (Braun and Lang, 1976) have found that Anderson's method can increase the ability of a model to simulate snowmelt runoff by up to 5% more than the temperature index method the method must

not, however, be discounted. Further work is needed on this approach but as there was insufficient time to try all options in this project it was decided to try the second alternative outlined in 5.1.

### 5.3 Layered temperature index

#### 5.3.1 Introduction

In Chapter 3 seasonal patterns in the depleting snowpack characteristics with respect to elevation zones in the catchment were identified. As these patterns could be expressed in a general form that applied to all three years' snow survey data it was decided to incorporate them into one of the models. Some workers (for example, Speers et al, 1979 and Bergstrom, 1979) have used up to 20 different elevation bands. As it was possible to generalise the snowpack characteristics using only three zones in the Mharcaidh (3.1) it was decided to adopt the approach of Martinec (1975) who divided the catchment into three elevation zones and applied the model to each zone in turn, combining the resultant melt to calculate the catchment runoff.

#### 5.3.2 Model structure

The general structure of the model (called MART) was similar to that of TINDEX, i.e. it had a central core which acted as a link between the data input and output and the

subroutines that performed the calculation. Parameters were, where possible, kept the same as TINDEX, and the optimisation process worked in the same way. Data were input from external files and the model output was again sent direct to a file for further analysis.

### 5.3.3 Initial parameter/data input and modelling of the snowpack

The following data were read from an external file, ZONES.DAT: HMAX, HMIN, HMET, AB, AZ(n), where

AZ(n) = Area of zone n

The user then input a number of values of R, AA, M, W and ALB, where

ALB = Gradually increasing melt factor coefficient and other parameters are as described in Chapter 4.

The boundary heights of the three zones were declared:

HZ01 = HMIN

HZ12 = 600    Boundary between zones 1 and 2

HZ23 = 800    Boundary between zones 2 and 3

HZ34 = HMAX

and from these the mid heights (shown in Figure 5.3) of each zone were determined:

$$HZ(1) = (HZ01 + HZ12)/2 \quad (5.5)$$

$$HZ(2) = (HZ12 + HZ23)/2 \quad (5.6)$$

$$HZ(3) = (HZ23 + HZ34)/2 \quad (5.7)$$

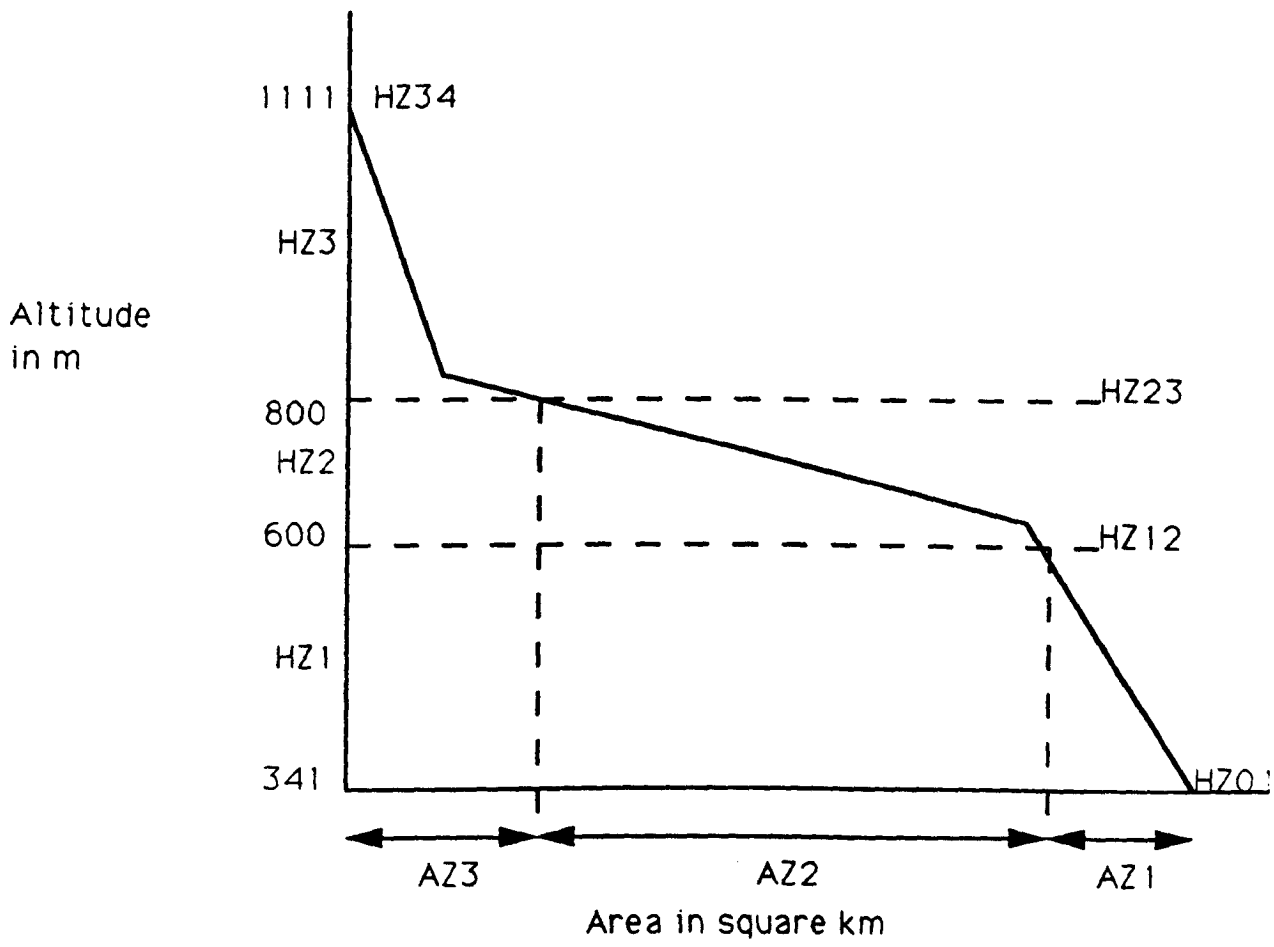


**Figure 5.3** Diagram to show the elevation zones used by MART for the Allt a Mharcaidh catchment.

The initial SCA for the three zones (SCA(n)) were then determined using AA (the initial snowpack area) and AZ(1), AZ(2) and AZ(3) from:

If  $AA > (AZ(2) + AZ(3))$  then

$$SCA(1) = AB - AA$$

$$SCA(2) = AZ(2)$$

$$SCA(3) = AZ(3)$$

Else if  $AA > AZ(3)$  then

$$SCA(1) = 0$$

$$SCA(2) = AA - AZ(3)$$

$$SCA(3) = AZ(3)$$

Else, if  $AA > 0$

$$SCA(1) = 0$$

$$SCA(2) = 0$$

$$SCA(3) = AA$$

Else all three SCA = 0

(5.8)

From this it can be seen that the model assumes a direct relationship between initial SCA and altitude, i.e. the snowpack will all lie upslope of a certain point. Whilst this assumption is clearly not valid later in the melt season when snow melts off exposed ridges and slopes at altitude whilst still lying in sheltered hollows lower down the catchment, it is a valid assumption at the start of the melt season when the snowpack has not started to melt, and is thus only used to determine the initial SCA for each zone.

The non-uniform depletion of the snowpack is due to a non-uniform areal distribution of snow, i.e. snowpack depth is not the same over the whole catchment, nor is it simply deeper at higher altitudes.

Field observations (shown in the snow survey results in Appendix B) show that deep and shallow snow cover can and does exist within the same elevation zone. As the layered model approach was being used in an effort to produce a closer representation of the snowpack characteristics observed in Chapter 3 the model allowed for this uneven snowdepth throughout the catchment by modelling the water equivalent for each zone.

From Figure 3.5 (a)-(c) it can be seen that whilst the snow depth is not uniform over the catchment it is possible to generalise the mean SWE distribution from zone to zone:

- (1) When all three zones contain snow, the mean SWE held in zones 2 and 3 is similar; this is also approximately twice the mean SWE of zone 1.
- (2) When only zones 2 and 3 contain snow then zone 3 initially contains more than zone 2, though this may change as the melt season progresses.

By incorporating these two observations as assumptions in the model it was possible to model the SWE in each zone using a constant  $S$  to distribute the SWE between the three

zones. The distribution in the three zones was determined by  $S_{MAX}(n)$  and  $S_{MIN}(n)$ , where

$S_{MAX}(n)$  = Maximum SWE in zone (n)

$S_{MIN}(n)$  = Minimum SWE in zone (n)

The snow was then distributed between the three zones in the following way (all values of  $S_{MIN}(n)$  and  $S_{MAX}(n) = 0$  unless stated otherwise):

Scenario 1      Snow in all three zones

$$S = (AA * WE) / (SCA(1) + 2 * SCA(2) + 2 * SCA(3)) \quad (5.9)$$

where

$$WE = W * (AB/AA) \quad (5.10)$$

$$S_{MAX} (1) = 2 * S$$

$$S_{MIN} (2) = S$$

$$S_{MAX} (3) = 3 * S$$

$$S_{MIN} (3) = S$$

$$S_{MAX} (3) = 3 * S \quad (5.11)$$

Scenario 2      Snow in zones 2 and 3

$$S = (AA * WE) / (SCA (2) + 2 * SCA (3)) \quad (5.12)$$

$$S_{MAX} (2) = 2 * S$$

$$S_{MIN} (3) = S$$

$$S_{MAX} (3) = 3 * S \quad (5.13)$$

### Scenario 3      Snow in zone 3

$$S_{MAX}(3) = 2 * WE \quad (5.14)$$

These three scenarios produced the three snowpack distributions represented in Figure 5.4.

Having determined the distribution of snow between the three zones the slope constants of the snowpack distribution for each zone (needed for depleting the snowpack) were calculated from:

$$KK(n) = (S_{MAX}(n) - S_{MIN}(n)) / SCA(n) \quad (5.15)$$

where

$$KK(n) = \text{slope constant for zone } (n)$$

The model then read in the meteorological data from an external file and proceeded to the meteorological submodel.

#### 5.3.4 Meteorological submodel

As TINDEX appeared to be very insensitive to changes in E and MART involved considerably more calculations than TINDEX it was decided to set E as a constant, thus reducing the number of parameters to be optimised. From the results shown in Chapter 4 it can be seen that E optimised to both ends of the physically reasonable range. Whilst this may have been due to the snow conditions for the two years (4.3.1), it might also have been a function of the model

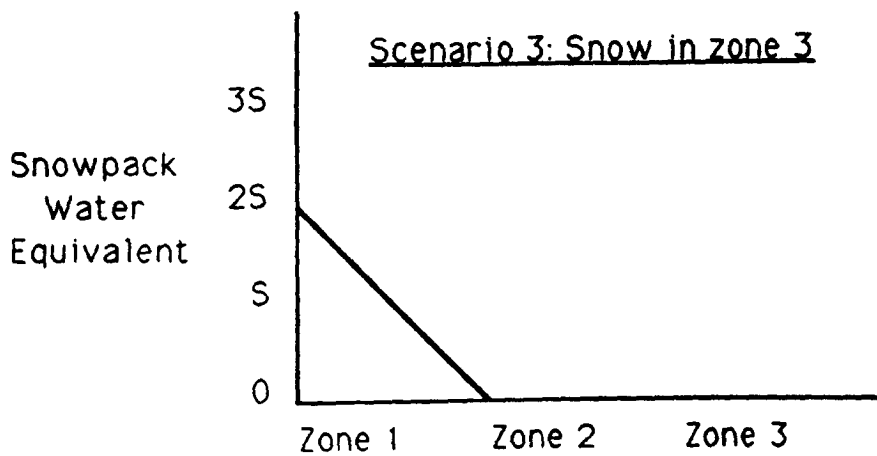
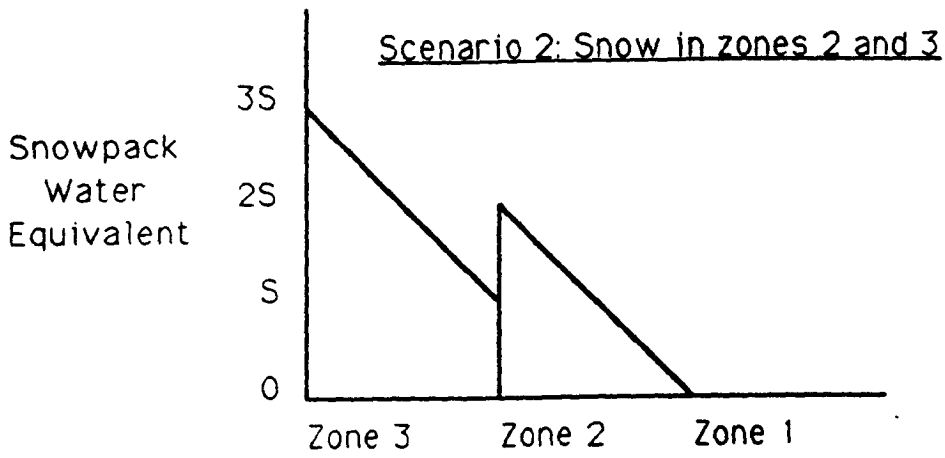
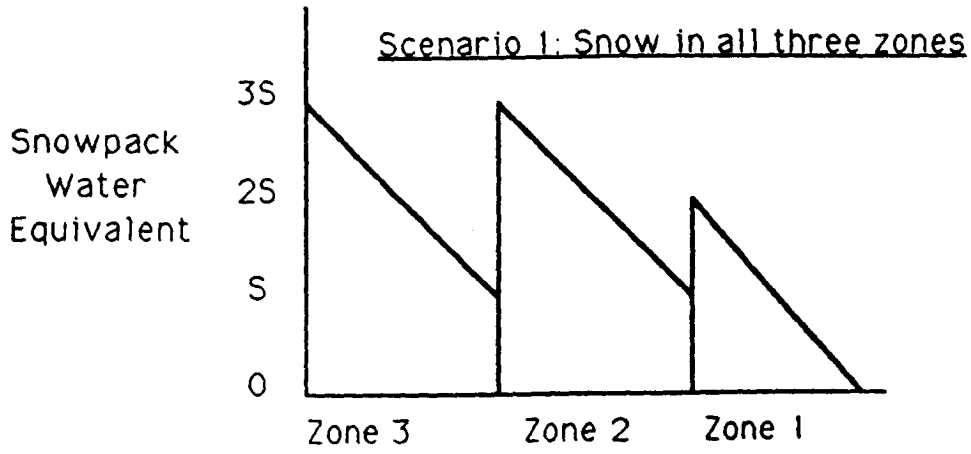


**Figure 5.4** Diagrammatic representation of the three different snow distribution scenarios catered for in MAT.

maximum temperatures (8.26°C), and both values produce lapse rates less than 0.01 optimised for the 1986 Mharcaidh model runs. M Birch (unpublished) carried out similar analysis using data collected at Glenmore Lodge (340m amsl) and in the Ciste Mhearad catchment to the east of Cairngorm and found similar results, attributing them to temperature inversions during periods of high pressure.

As temperature inversions do occur, resulting in warmer temperatures at altitude than in the valleys, and melt is associated with maximum rather than minimum temperatures, there is a case for using the mean difference in maximum daily temperatures to determine the true environmental lapse rate. This is confirmed by carrying out correlation and regression analysis on the data set used to construct Table 5.3, the strongest relationship being between the maximum temperature at each site ( $R^2 = \underline{65.8\%}$ ) and the lowest being for the minimum temperature ( $R^2 = \underline{3.7\%}$ ).

From Table 5.3 it can be seen that using the difference in maximum daily temperatures results in a lapse rate of  $0.0084^\circ\text{Cm}^{-1}$ ; this is close to the value obtained from the mean of the 1986 and 1987 TINDEK model runs and that found by Harding (1978) and optimised by Ferguson (1984) in his original model. It was thus decided to set E as a constant, the value being  $0.008^\circ\text{Cm}^{-1}$ .

The freezing level (FL) was determined in the same way as

FTINDEX (Eqn 4.19) using TMAX and, if this was above the mid-height for a zone, melt was applied to the whole SCA within the zone as done by Martinec (1975). In this way melt was maximised in an effort to simulate the peak flow events. The model then carried out the remainder of the meteorological and melt submodels one zone at a time.

The temperature difference (DT) between the zone mid-height and that of the AWS was determined using:

$$DT(n) = (H2(n) - HMET) * E \quad (5.16)$$

This was then used to determine if any precipitation recorded at the AWS fell as snow or rain in the snow (a critical temperature threshold of 0°C was used):

If  $(DT(n) + ATEM(1)) < 0$  then

$$SNEW(n) = PPT(i)$$

Else

$$WP(n) = AZ(n) * PPT(i) \quad (5.17)$$

where

SNEW(n) = depth of fresh snow (water equivalent) in

zone n

i = day number

### 5.3.5 Snowmelt submodel

The number of degree-days for the zone (DA) were determined using ATEM (i) and DT (n) as before. The volume of melt in

FTINDEX (Eqn 4.19) using TMAX and, if this was above the mid-height for a zone, melt was applied to the whole SCA within the zone as done by Martinec (1975). In this way melt was maximised in an effort to simulate the peak flow events. The model then carried out the remainder of the meteorological and melt submodels one zone at a time.

The temperature difference (DT) between the zone mid-height and that of the AWS was determined using:

$$DT(n) = (HZ(n) - HMET) * E \quad (5.16)$$

This was then used to determine if any precipitation recorded at the AWS fell as snow or rain in the snow (a critical temperature threshold of 0°C was used):

If  $(DT(n) + ATEM(1)) < 0$  then

$$SNEW(n) = PPT(i)$$

Else

$$VP(n) = AZ(n) * PPT(i) \quad (5.17)$$

where

SNEW(n) = depth of fresh snow (water equivalent) in  
zone n

i = day number

### 5.3.5 Snowmelt submodel

The number of degree-days for the zone (DA) were determined using ATEM (i) and DT (n) as before. The volume of melt in

the zone was then calculated from:

$$V(n) = A(n) * M * DA \quad (5.18)$$

where

A(n) = Snow covered area in zone n. On day 1 this equals SCA(n) but is altered by the depletion submodel.

### 5.3.6 Transformation submodel

The total volume of rainfall (VPT) and meltwater (VT) from the three zones were determined from:

$$VPT = VP(1) + VP(2) + VP(3) \quad (5.19)$$

$$VT = V(1) + V(2) + V(3) \quad (5.20)$$

These were then added together to give TW(i), the total amount of water produced on day 1. This was then added to STORE, the amount of water held in the store used for routing the rain and meltwater, the volume of the previous day's discharge being removed at the same time:

$$STORE = STORE + TW(i) - (86.4 * Q) \quad (5.21)$$

[Initial values of store were determined at the start of the model.] When linear routing was used:

$$STORE = Q/R; \quad (5.22)$$

the non-linear store was calculated from:

$$\text{STORE} = Q^{1/2}/R \quad (5.23)$$

The discharge was then calculated from the store:

$$Q = R * \text{STORE} \quad (5.24)$$

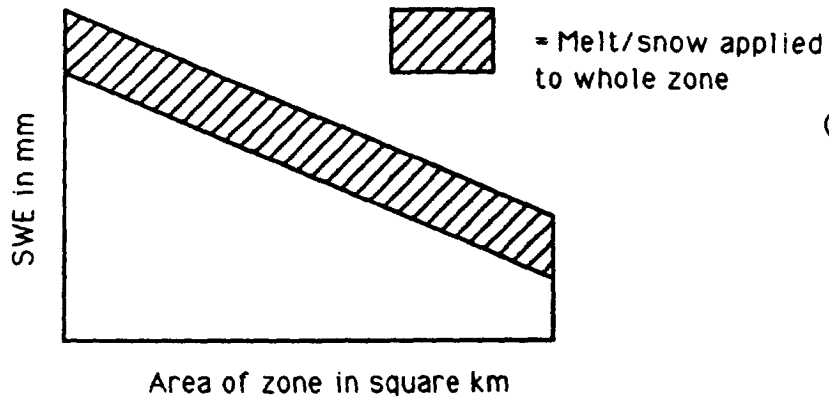
being used for linear routing and:

$$Q = (R * \text{STORE})^2 \quad (5.25)$$

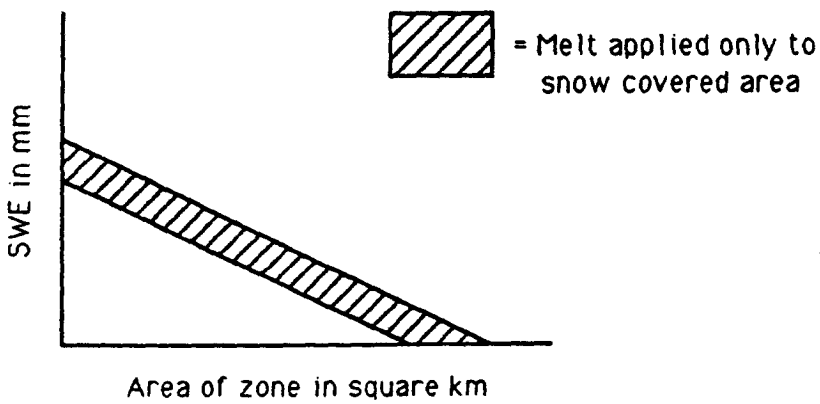
for non-linear routing.

### 5.3.7 Depletion submodel

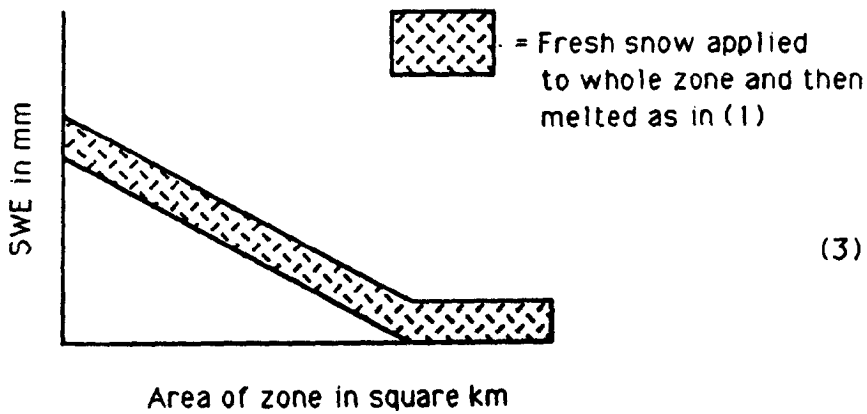
The depletion submodel was considerably more complex than that used in the TINDEXTYPE models as, in addition to being applied to the three zones, it also allowed for fresh snowfall in the zones. Along with the meteorological submodel it was based on the assumption that the air temperature at the mid-height of the zone governed the processes occurring over the whole zone. This was clearly a simplification that could, should it be so desired, be corrected by increasing the number of zones, thus decreasing the elevation range of each zone. The elevation range of the zones was, however, much smaller than that used by Rango and Martinec (1982) who set the elevation range for each zone at more than 400m. The depletion model applied the daily melt and snowfall, if any, to each of the zones in turn, the mode of application being dependent upon the SCA in each zone. Figure 5.5 shows the different scenarios described below.



- (1) Deep snow over whole zone, melt and fresh snow applied to whole zone



- (2) Less than complete snow cover, melt occurring in zone



- (3) Less than complete snow cover, snowfall applied to whole zone

**Figure 5.5** Diagram to show how melt or fresh snow was applied to the snowpack within each elevation zone.

Case 1      Complete snow cover over zone

Given 100% snow cover in the zone, melt or snow was applied at a uniform thickness over the whole zone in the following way:

If  $SNEW(n) > 0$

$$SMIN(n) = SMIN(n) + SNEW(n)$$

$$SMAX(n) = SMAX(n) + SNEW(n) \quad (5.26)$$

if  $V(n) > 0$

$$SMELT(n) = V(n)/A(n) \quad (5.27)$$

where

$$SMELT(n) = \text{Depth of melt in zone } n$$

When  $SMELT(n) < SMIN(n)$ , i.e. when there was sufficient depth of snow cover over the whole zone to allow the melt to be universally applied:

$$SMIN(n) = SMIN(n) - SMELT(n)$$

$$SMAX(n) = SMAX(n) - SMELT(n) \quad (5.28)$$

When  $SMELT(n) > SMIN(n)$ , i.e. when there was insufficient depth of snow to apply melt at a universal depth over the whole zone, equation 4.9 leads to:

$$A(n) = (A(n)^2 - 2 * V(n)/KK(n) + 2 * A(n) * SMIN(n)/KK(n))^{0.5}$$

$$SMIN(n) = 0$$

$$SMAX(n) = KK(n) * A(n) \quad (5.29)$$

This final stage resulted in the SCA dropping below AZ, i.e. there was no longer 100% snow cover over the zone.

Case 2      Incomplete snow cover over zone

During melt events the melt was applied at a uniform rate over the snow cover in a similar way to that in TINDEK (Eqn 4.9), the snowpack being depleted using:

$$A(n) = (A(n)^2 - 2 * V(n)/KK(n))^{1/2} \quad (5.30)$$

The major addition to the depletion submodel at this stage was in the application of the precipitation data. If Equation 5.26 determined that snow was falling in the zone, this was applied at a uniform depth over the whole zone using:

$$\begin{aligned} SMIN(n) &= SNEW(n) \\ SMAX(n) &= SMAX(n) + SNEW(n) \end{aligned} \quad (5.31)$$

Melt was then applied to this snowpack until depth SNEW(n) of snow had melted when the model continued to deplete the snowpack as above for incomplete cover, the SCA value prior to snowfall having been remembered. This was done in the following way:

$$SMELT(n) = V(n)/AZ(n) \quad (\text{determine depth of melt over whole zone}) \quad (5.32)$$

If  $SMELT(n) < SMIN(n)$  (determine if sufficient fresh

snow for melt) then

$SMIN(n) = SMIN(n) - SMELT(n)$  deplete fresh snow as

$SMAX(n) = SMAX(n) - SMELT(n)$  in Case 1, (Eqn 5.28)

However,

If  $SMELT(n) > SMIN(n)$  (i.e., if there was insufficient fresh snow to apply the calculated melt to)

$$A(n) = (A(n)^2 - 2 * V(n)/KK(n) + 2 * AZ(n) * SMIN(n)/KK(n))^{1/2}$$

$$SMAX(n) = 0$$

$$SMAX(n) = KK(n) * A(n) \quad (5.33)$$

If there was insufficient snow for Equation 5.33 to be satisfied  $A(n)$  was set to zero. Figure 5.5 shows the different depletion/snowfall scenarios that were represented and modelled for the three layers.

The total diminished snowpack area (AAA) was calculated after the snowfall/melt had been applied to each zone by adding together the individual SCAs for each zone.

The remainder of MART, including the optimisation method and handling of optimised parameter results, was essentially the same as TINDEX.

#### 5.3.8 Results from the layered model

MART was optimised on the 1986 and 1987 Mharcaidh datasets using both linear and non-linear routing, and also with

parameter sets containing combined values of R and M. When using the combined datasets, values of A, W and ALB were re-optimised as it was felt, since the aim of using the layered model approach was to accurately represent the snowpack characteristics, the model should be free to optimise the parameters relating directly to the snowpack. ALB was also re-optimised as this was dependent on the position within the whole melt season and was specific to each dataset.

The results from the optimised model runs using both parameter sets are shown in Table 5.4; Figures 5.6 and 5.7 show the time series plots for the 1986 and 1987 combined parameter sets using non-linear and linear routing. The corresponding  $R^2$  values for the TINDEK model run are also given in Table 5.4.

From these results it can be clearly seen that the MART model runs do not perform as well as TINDEK, the  $R^2$  value being less for every case. Despite this, reference to both Figures shows that MART does visually reflect the peak flows well for the non-linear plots. The poor statistical performance is caused by over-prediction during days 52-60 of the 1986 model runs and a general under-prediction (with the exception of the peak flow) over the 1987 model run.

Whilst the linear time series plots also match the peak flows well (especially the 1987 plot, where both the

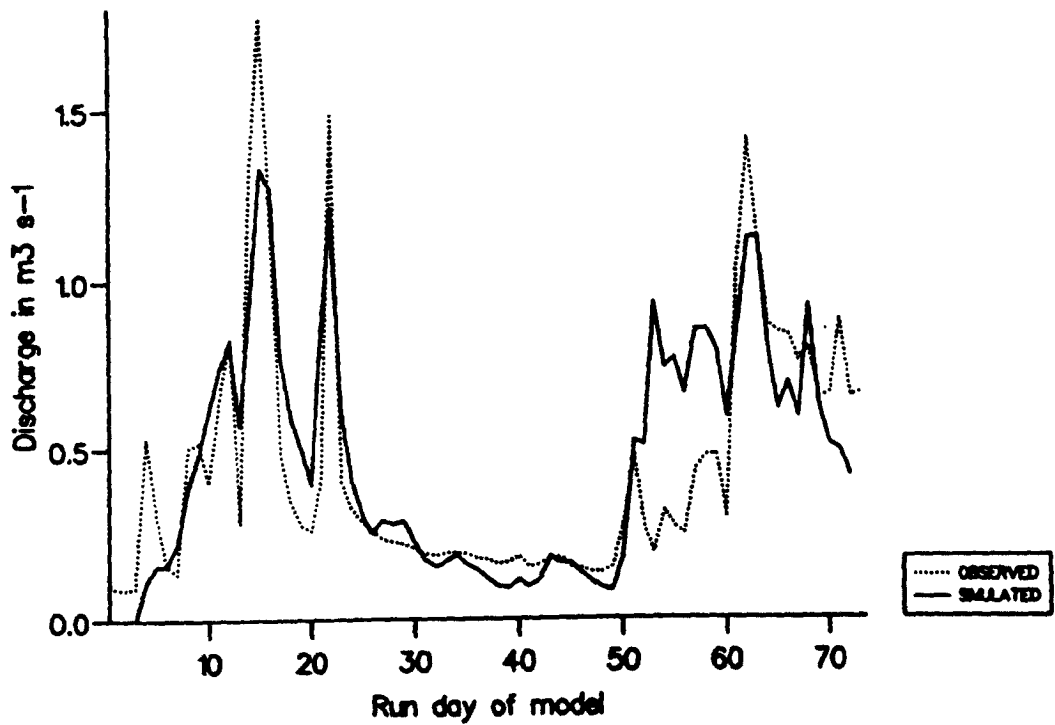
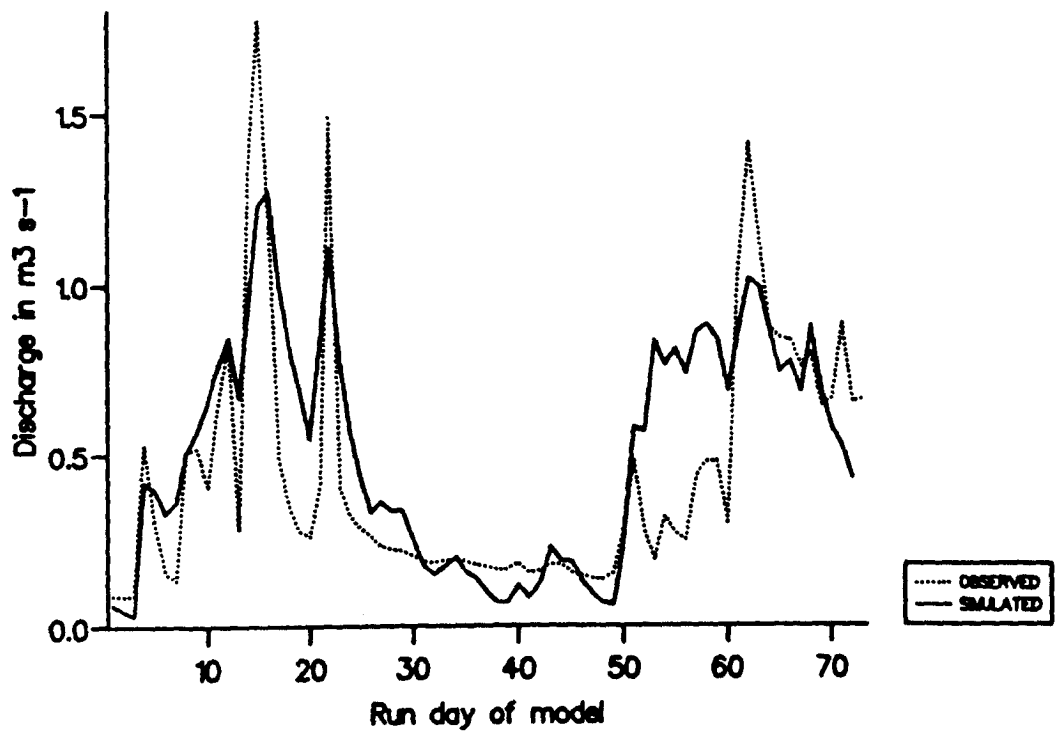


**Figure 5.6** Time series plots from running MART on the 1986 Mharcaidh data using combined parameter sets, The upper plot uses linear routing and the lower uses non-linear routing.

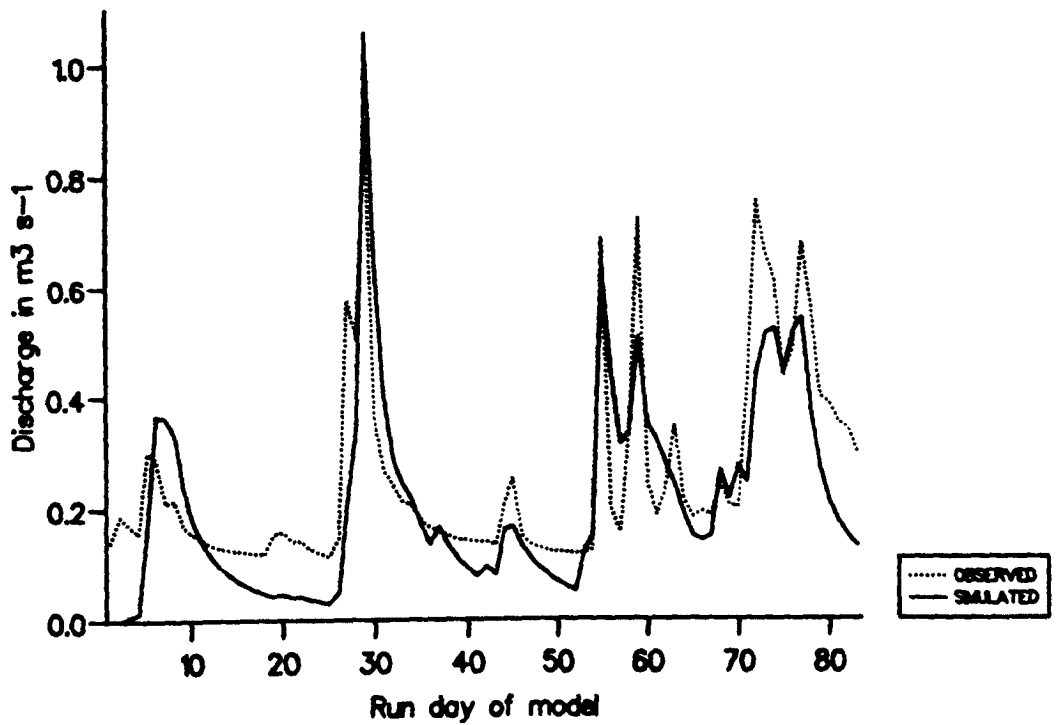
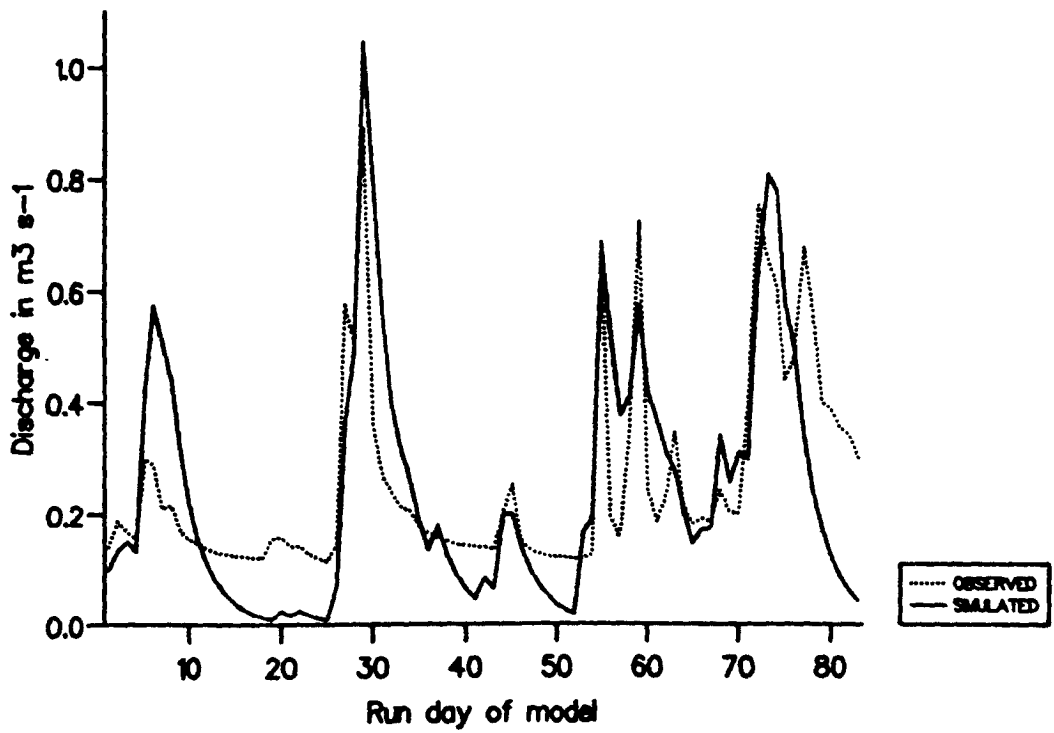


**Figure 5.7** Time series plots from running MART on the 1987 Mharcaidh data using combined parameter sets, The upper plot uses linear routing and the lower uses non-linear routing.

Year	Routing	Parameter	R	A	M	W	ALB	SE	FA	R <sup>2</sup>
1986	Non-lin	Optimised	0.0034	6.1	6.4	240	1.00	0.1182	0.156	0.724
1987	Non-lin	Optimised	0.0026	9.9	2.0	60	0.09	0.1133	0.000	0.595
1986	Linear	Optimised	0.0052	5.4	7.3	220	0.30	0.2046	0.000	0.670
1987	Linear	Optimised	0.0016	8.2	5.1	70	0.03	0.1136	0.000	0.589
1986	Non-lin	Combined	0.0030	7.5	4.2	250	1.00	0.2205	0.796	0.648
1987	Non-lin	Combined	0.0030	7.9	4.2	40	0.05	0.1180	0.120	0.611
1986	Linear	Combined	0.0034	6.2	6.2	240	0.40	0.2494	0.167	0.581
1987	Linear	Combined	0.0034	5.5	6.2	50	0.09	0.4770	0.000	0.303

**Table 5.4** Results from the first runs of MART using linear and non-linear routing as optimised and combined parameter sets.

E = Environmental lapse rate ( $^{\circ}\text{C m}^{-1}$ ), R = Routing coefficient, A = Initial snow covered area ( $\text{km}^2$ ),

M = Melt coefficient ( $\text{mm}^{\circ}\text{C day}^{-1}$ ), W = Initial snowpack water equivalent (mm).

highest flow and the later peaks are well matched) and show similar under and over-predictive patterns to the non-linear model runs, it is clear that the linear routing method is not able to deal with the variation in flow as well as the non-linear. Having a fixed routing coefficient results in the recession limbs of peak flow hydrographs not being steep enough, thus over-predicting during these periods, whilst at times of low flow the fixed routing coefficient results in the predicted flow being much lower than the observed. A further weakness of the 1987 linear model runs is a considerable over-prediction in the early stages of the model (days 4-12). Whilst this may be due to the combined parameter set using a higher melt factor than the optimised set (6.2 instead of 5.1mm°C day<sup>-1</sup>) the gradually increasing melt factor was also optimised to try and compensate for this. Clearly it was unable to do so; in order to reach the peak flows on day 30 the melt factor has to be high to compensate for the fixed routing coefficient.

The difference in performance of the two routing methods was studied further, Table 5.5 showing the R<sup>2</sup> values for subsets of model runs taken from Table 5.4. From this it can be seen that the non-linear routing method is statistically superior to the linear method. For example, the difference between the MART and TINDEX combined parameter set non-linear model runs is only 24.5% that of those using linear routing. The statistical superiority of

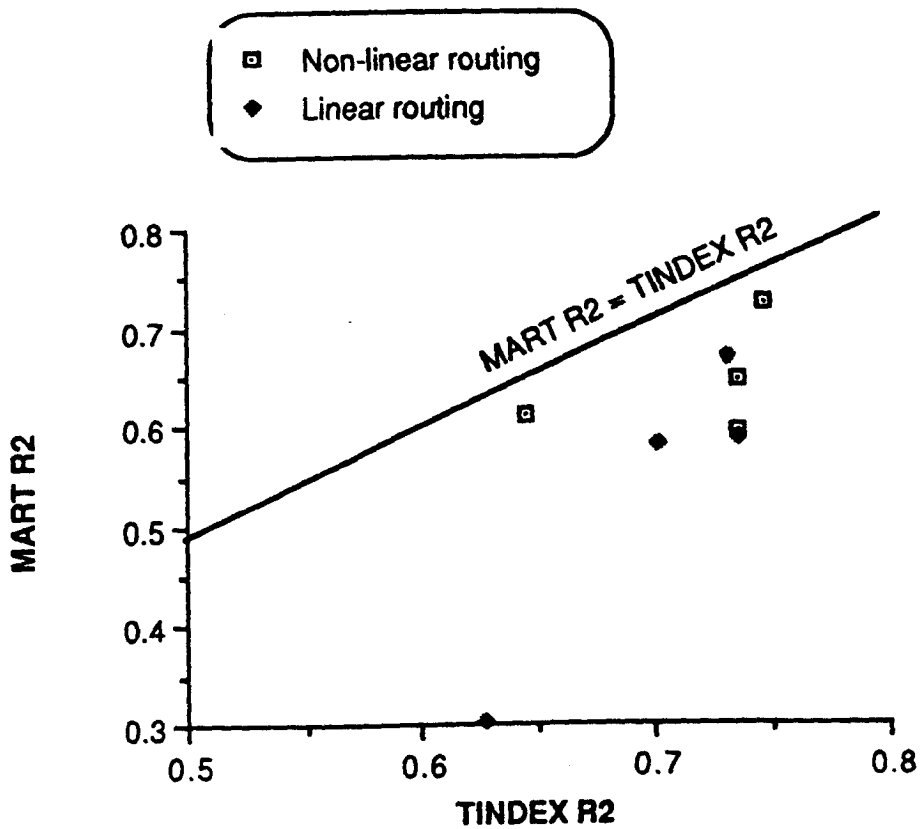


**Figure 5.8** A graph to show the statistical superiority of non-linear routing when using MART.

the non-linear model runs is graphically shown in Figure 5.8 which also highlights the poor performance of the 1987 combined parameter set model runs described above.

Subset of model runs	No. of model runs	Mean MART R <sup>2</sup>	Mean TINDEX R <sup>2</sup>	Difference
All runs	8	0.590	0.699	0.109
All optimised	4	0.645	0.722	0.077
All combined	4	0.534	0.677	0.143
All linear routing	4	0.534	0.699	0.165
Optimised linear	2	0.630	0.734	0.104
Combined linear	2	0.442	0.691	0.249
All non-linear	4	0.645	0.700	0.055
Optimised non-lin	2	0.660	0.710	0.050
Combined non-lin	2	0.630	0.691	0.061

Table 5.5 Comparison of TINDEX and MART R<sup>2</sup> values.

Given the visual and statistical superiority of non-linear routing against linear it was decided that any further work on MART would include only non-linear routing. It was realised that when developing TINDEX both routing methods were tried for all model changes. However, this was because there was no significant difference between the two methods and it was hoped that by retaining them both any differences would emerge. In the case of MART the differences were consistent and large from the beginning, thus justifying the decision to use only non-linear routing for all subsequent model runs.

## 5.4 Further developments to MART

### 5.4.1 Snowpack distribution

5.3.3 described the representation of the snowpack within the catchment in MART. As this was the major difference between the MART and TINDEX models it was decided to study the effect of different snowpack structures on the model performance. Eight different structures were chosen in addition to the original, the four that showed performance similar or superior to that of the original MART structure are shown in Figure 5.9.

Structure 1 (S1) had the mean SWE in each zone in the same ratios as the original structure, i.e 2:2:1. It differed in that SMIN (i.e. the minimum depth of snow in each zone) was set to 0. This catered both for the exposed ridges and spurs in the catchment that often had the snowfall blown off them by the wind before it had time to settle and other snow-free areas within each zone (eg stream channels, large boulders).

Structure 2 (S2) also had the mean SWE in each zone in the same ratio as the original structure. It formed an intermediate structure between S1 and the original in that zone 3 had SMIN set to 0 and SMAX at 4S whilst zone 2 had a less extreme distribution, SMIN being S and SMAX being 3S. This catered for both the exposed ridges that were more noticeable in zone 3 and the more uniform snowpack that was generally observed in zone 2, though it did not cater for very thin snowcover if the initial SCA covered all of zones 2 and 3.

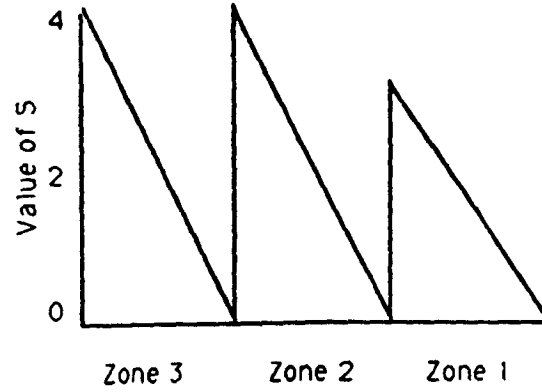
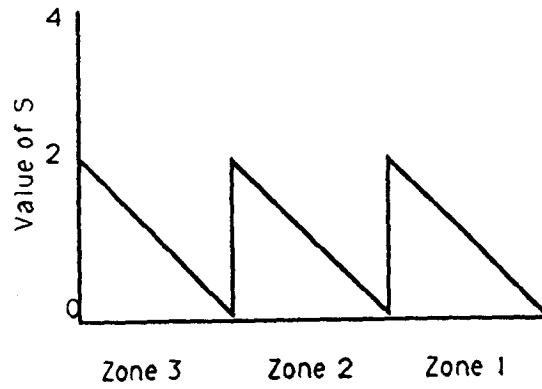
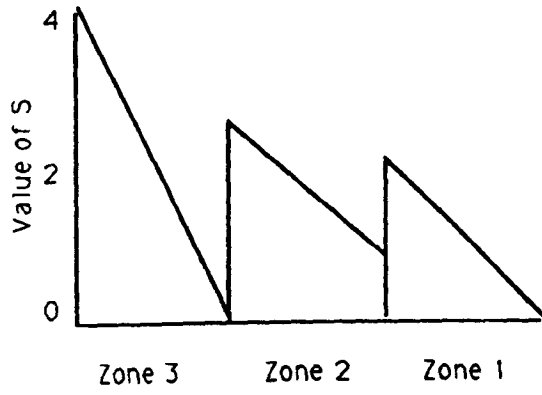
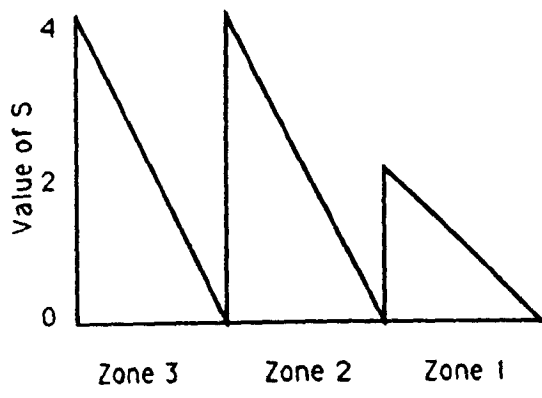


**Figure 5.9** The four snowpack distributions S1 (top) - S4 (bottom) that were used in MART.

Structure 3 (S3) had a uniform ratio of mean SWE between all zones, SMAX being set at 2S and SMIN being set to 0 for all three. Whilst catering for snow-free areas or thin cover in all zones and the near uniform distribution of snow over the three zones observed from the 1988 surveys (shown in the simplistic representation in Figure 3.6), it did not cater for the differences between zones that was observed in the 1986 surveys.

Structure 4 (S4) was similar to S1 in that the SMIN for each zone was set to 0. The ratio of mean SWE between zones was 4:4:3, i.e. the differences between the mean SWE in zones 2 and 3 and that in zone 1 were greater than S3 but less than all the other snowpack structures. This catered for snow-free areas or thin snowcover in all zones and also for a more uniform initial distribution of snow between the three zones.

It must be remembered that all the structures described above are for 100% initial snow covered areas. If the model optimised the SCA such that snow cover was incomplete over a zone then SMIN was accordingly set to 0 for that zone. In this way it was possible for the model to override the different structures in extreme cases.

MART was re-optimised on the 1986 and 1987 Mharcaidh datasets and then re-run using combined parameter sets re-optimising the snowpack parameters and ALB for each structure. The results from these four different structures, together with those of the original structure, are shown in Table 5.6. Figures 5.10-5.13 show

Structure	Year	Parameter	R	A	M	W	ALB	SE	FA	R <sup>2</sup>
0	1986	Optimised	0.0034	6.1	6.4	240	1.00	0.2182	0.156	0.724
	1987	Optimised	0.0026	9.9	2.0	60	0.09	0.1133	0.000	0.595
	1986	Combined	0.0030	7.5	4.2	250	1.00	0.2026	1.220	0.648
	1987	Combined	0.0030	7.9	4.2	40	0.05	0.1157	0.000	0.611
1	1986	Optimised	0.0034	4.6	9.9	210	10.00	0.1806	0.058	0.761
	1987	Optimised	0.0029	9.2	2.3	60	0.08	0.1114	0.078	0.625
	1986	Combined	0.0032	6.2	6.1	220	10.00	0.1931	0.743	0.728
	1987	Combined	0.0032	4.0	6.1	50	0.55	0.1140	0.000	0.634
2	1986	Optimised	0.0033	5.6	6.1	190	10.00	0.2116	0.642	0.675
	1987	Optimised	0.0021	9.8	3.4	70	0.07	0.1103	0.000	0.618
	1986	Combined	0.0027	6.8	4.8	230	10.00	0.2151	1.130	0.666
	1987	Combined	0.0027	9.9	4.8	60	0.01	0.1152	0.000	0.613
3	1986	Optimised	0.0034	4.6	9.9	210	10.00	0.1806	0.058	0.761
	1987	Optimised	0.0028	9.9	2.1	50	0.07	0.1099	0.547	0.630
	1986	Combined	0.0031	6.2	6.0	220	10.00	0.1939	0.778	0.726
	1987	Combined	0.0031	4.1	6.0	50	0.07	0.1224	0.000	0.567
4	1986	Optimised	0.0034	4.6	9.9	210	10.00	0.1806	0.058	0.761
	1987	Optimised	0.0027	9.7	2.4	60	0.07	0.1105	0.154	0.626
	1986	Combined	0.0031	6.2	6.2	220	10.00	0.1933	0.725	0.727
	1987	Combined	0.0031	4.0	6.2	50	0.60	0.1140	0.000	0.636

Table 5.6 Results from running MART with the five different snowpack structures. E = Environmental lapse rate ( $^{\circ}\text{C m}^{-1}$ ), R = Routing coefficient, A = Initial snow covered area ( $\text{km}^2$ ), M = Melt coefficient ( $\text{mm}^{\circ}\text{C day}^{-1}$ ), W = Initial snowpack water equivalent (mm).

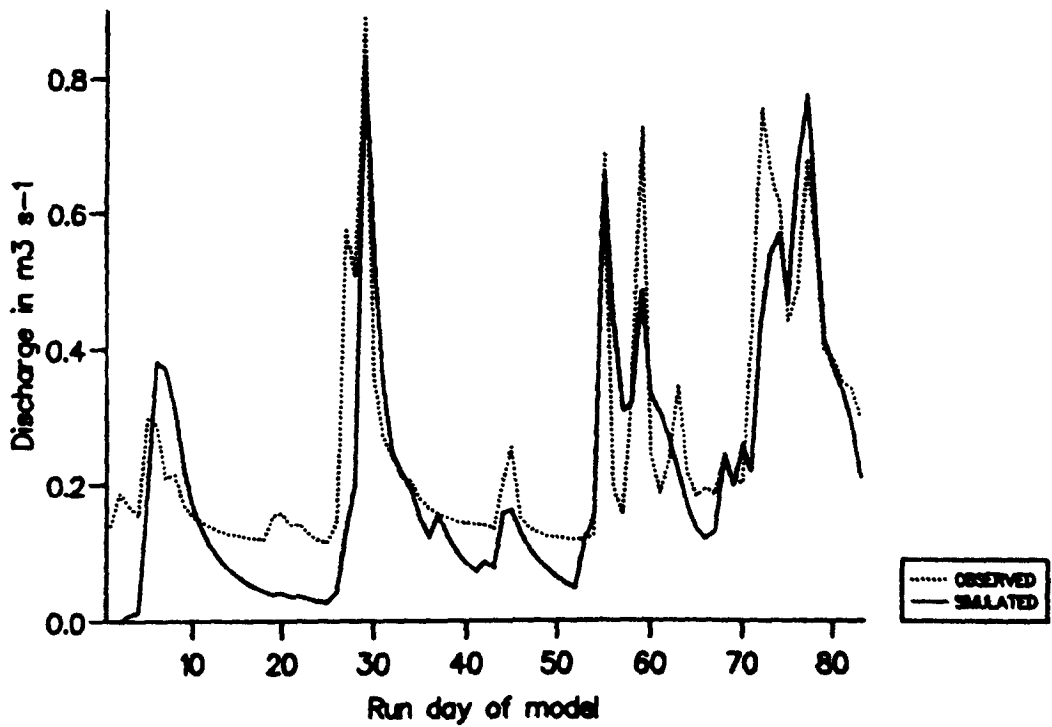
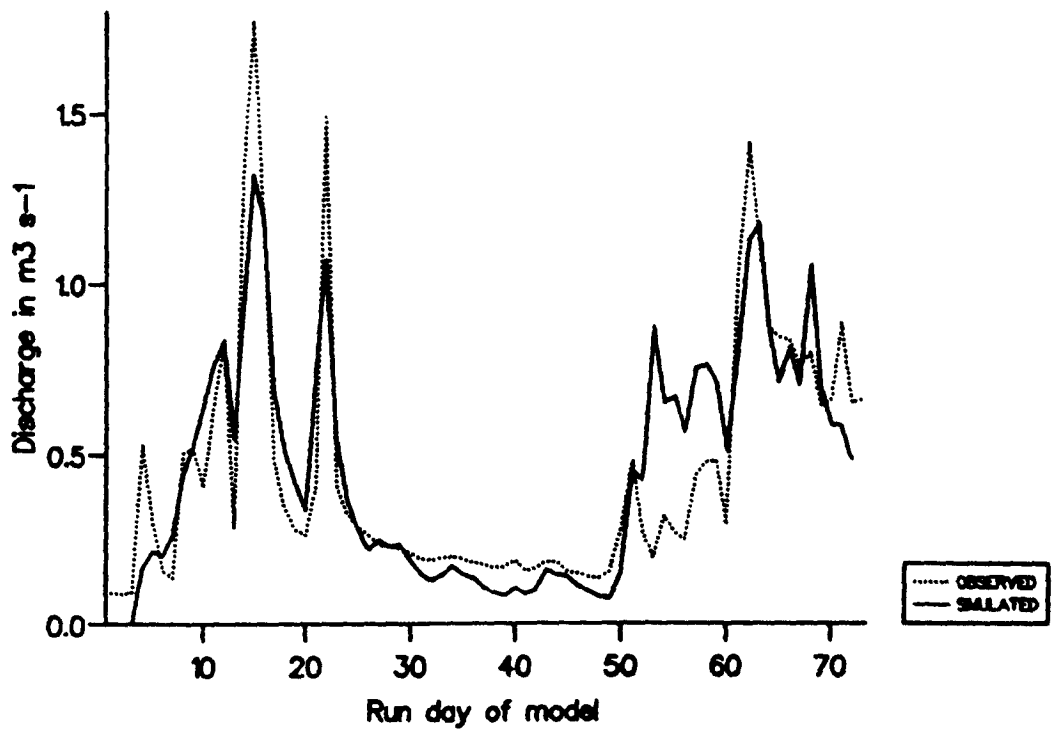


**Figure 5.10** Time series plots from running MART with a combined parameter set, non-linear routing and structure S1. 1986 = upper plot; 1987 = lower plot.

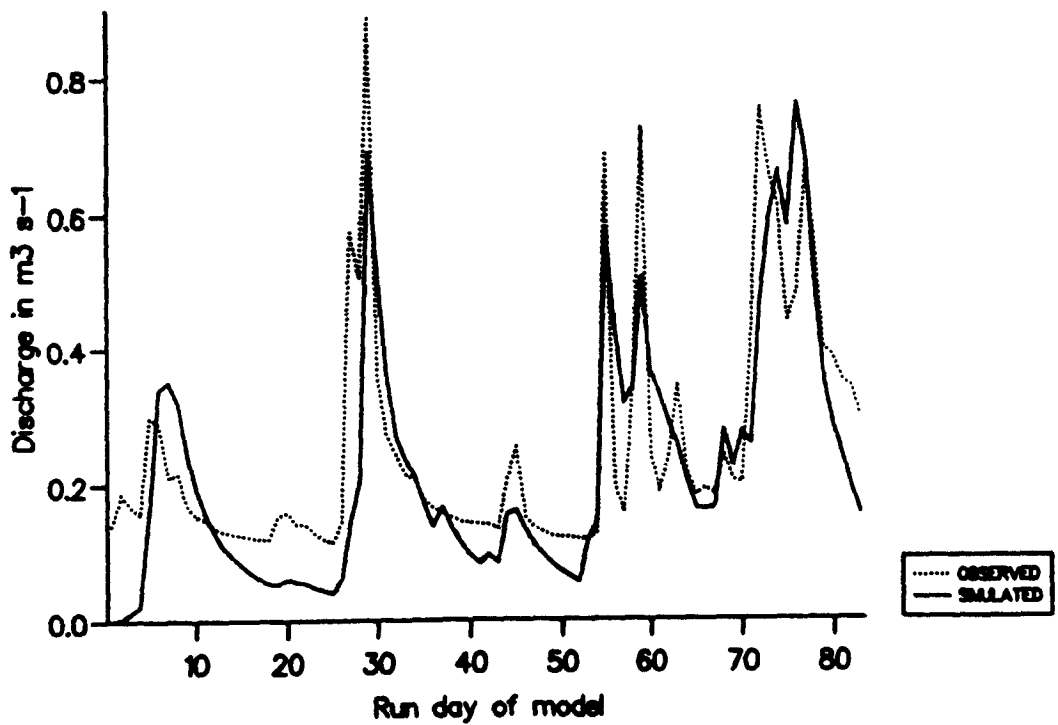
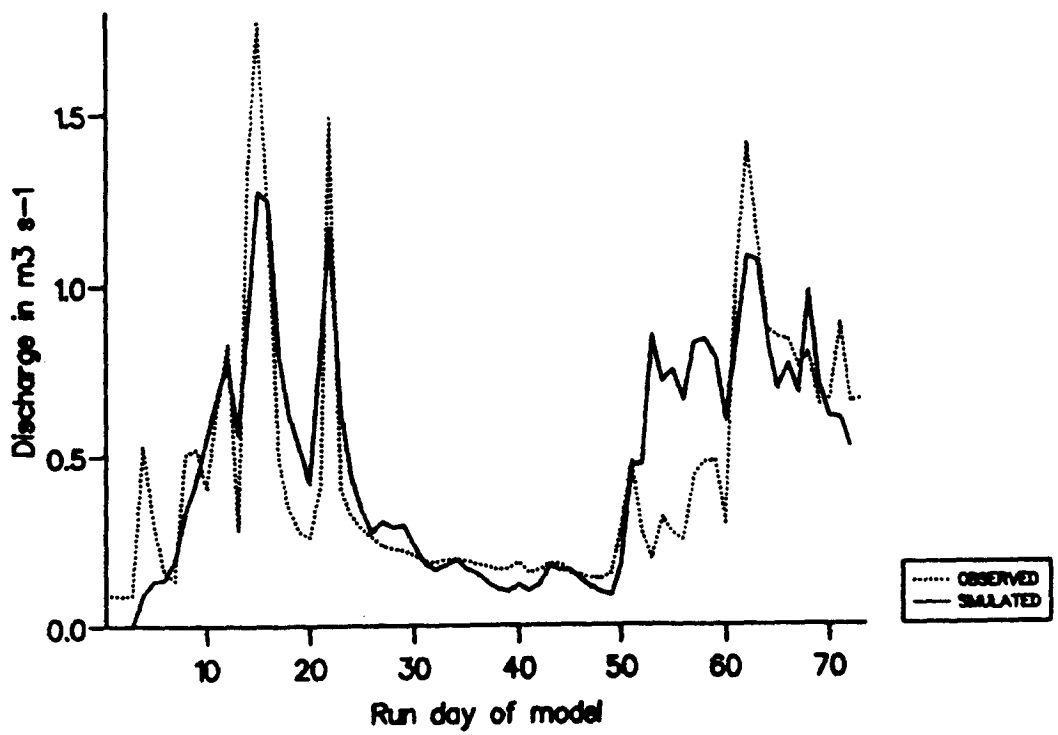


**Figure 5.11** Time series plots from running MART with a combined parameter set, non-linear routing and structure S2. 1986 = upper plot; 1987 = lower plot.

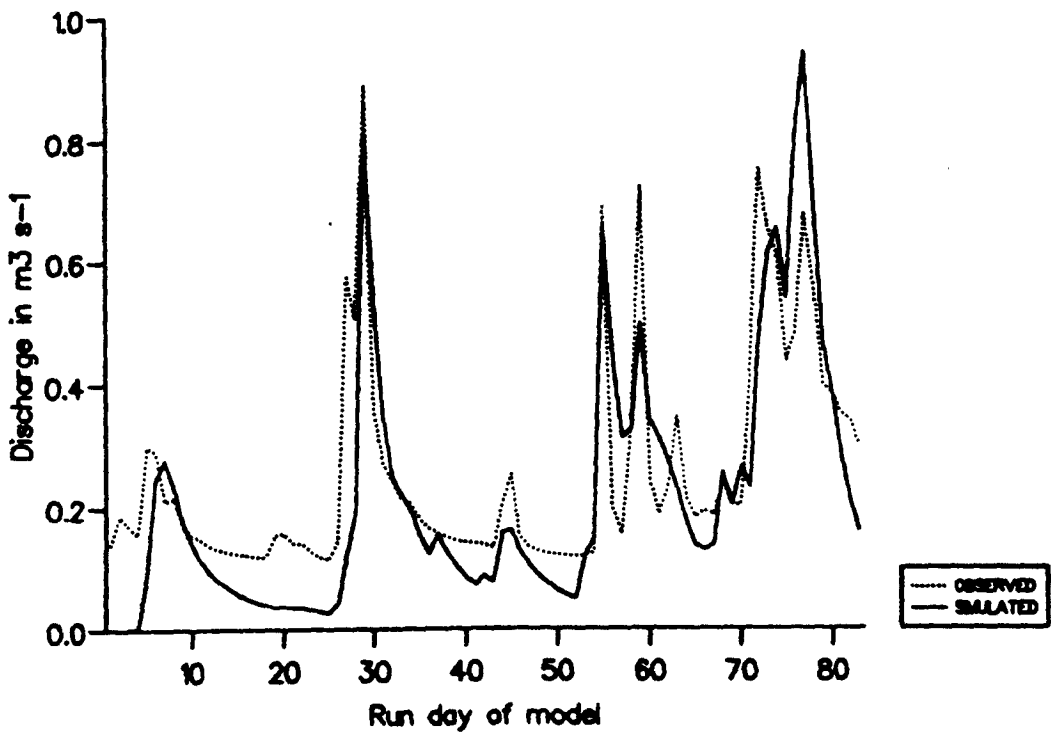
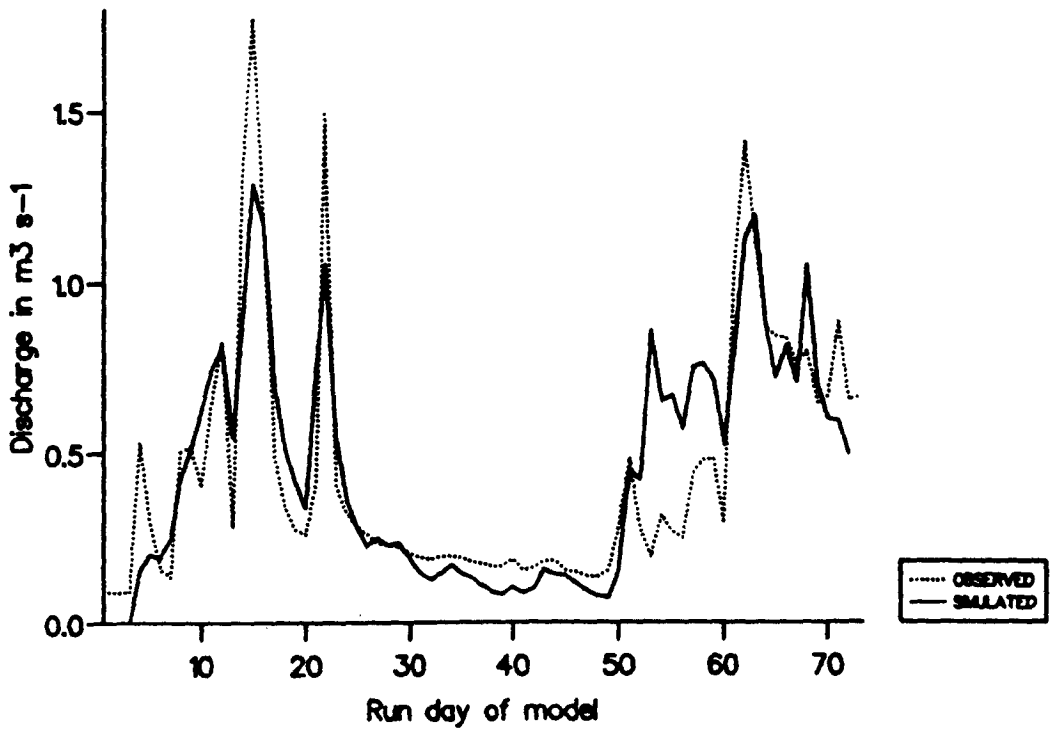
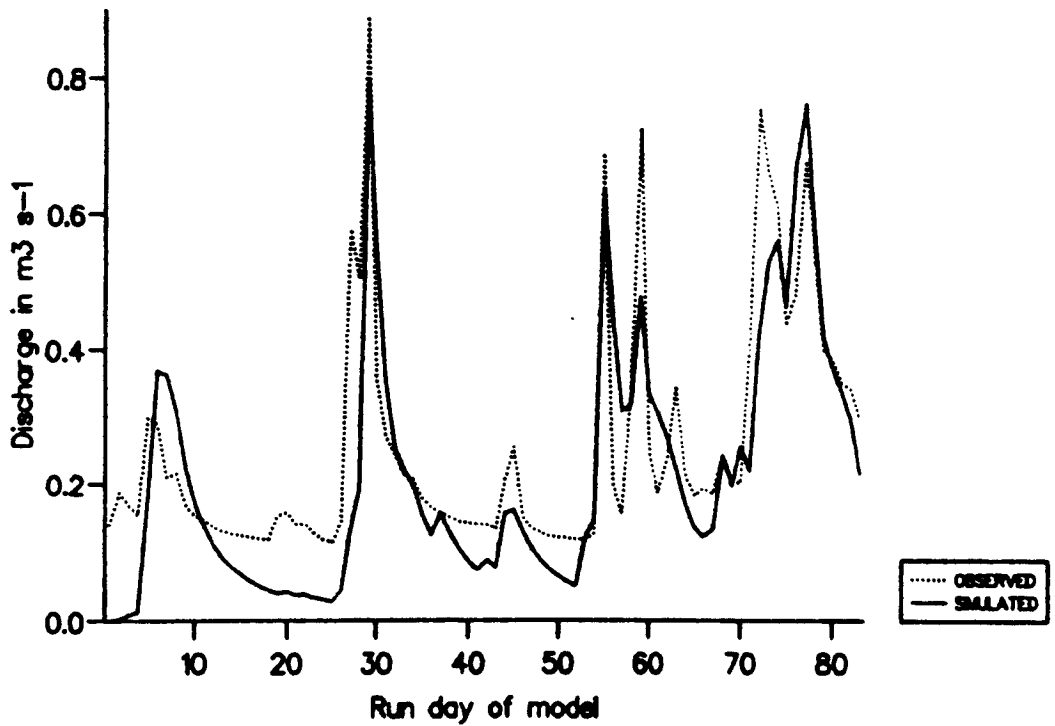
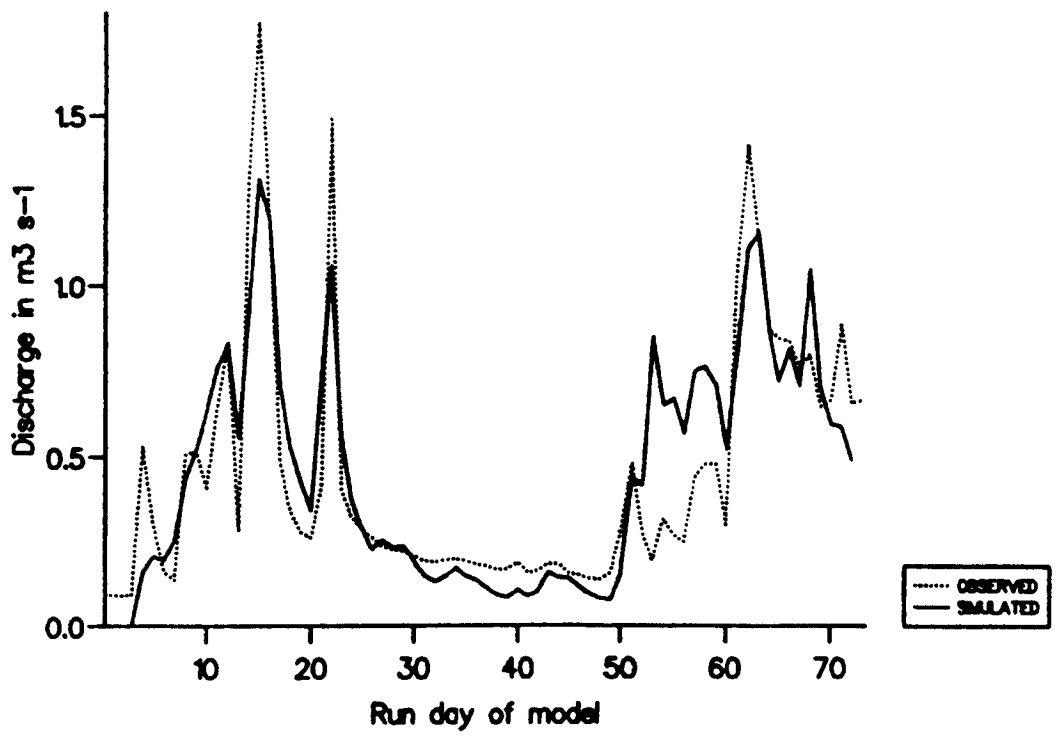


Figure 5.12 Time series plots from running MART with a combined parameter set, non-linear routing and structure S3. 1986 = upper plot; 1987 = lower plot.



**Figure 5.13** Time series plots from running MART with a combined parameter set, non-linear routing and structure S4. 1986 = upper plot; 1987 = lower plot.

the model runs for each of the different structures using the combined parameter sets.

To discuss these results it is clearer if a number of separate themes are isolated:

(a) Statistical performance

From the  $R^2$  values shown in Table 5.6 it can be seen that structures 1 and 4 (S1 and S4) outperform the other three, the mean  $R^2$  values for the model runs being 0.687 and 0.688 compared to 0.645, 0.643 and 0.671. The mean SE values also show this, the mean values for S1 and S4 being 0.1498 and 0.1496 compared to 0.1625, 0.1631 and 0.1517. S4 allows the model to perform better than S1, though the difference is very small. Of the remaining three structures S3 performs intermediately, whilst the original structure and S2 are both weak performers.

The mean  $R^2$  of the 'best' snowpack structure (S4) compares well with that of TINDEX (0.688 for S4 compared to 0.700), especially if it is remembered that the lapse rate was optimised for the TINDEX model runs whilst it was held constant for all MART runs. If the results of the combined parameter sets are compared (both had E set to  $0.008^\circ\text{C cm}^{-1}$ ) the  $R^2$  values are even closer, 0.682 for MART comparing to 0.691 for TINDEX.

It can be seen that the 1986 optimised model runs are the same for S1, S3 and S4. This is because the optimised SCA was such that zone 1 was snow-free, thus resulting in the snowpack distribution

being the same for both zones 2 and 3 for all structures. Any differences in the mean  $R^2$  for each structure are thus related to the structure's ability to model the 1987 snowpack and the influence this has on determining the combined values of the recession coefficient and melt factor.

(b) Visual performance

The visual differences between the five different snowpack structure combined parameter model runs shown in Figures 5.6, 5.7 and 5.10-13 are less easy to detect than the statistical. Taking the 1986 model runs first it can be seen that the model runs for S1, S3 and S4 are all the same for the reasons outlined above. Compared to the original structure they match the first peak equally well, are approximately  $0.1\text{m}^3\text{ s}^{-1}$  below the second peak but match the later peak on days 62-63 slightly better. Their major difference and benefit is that the over-prediction between days 50 and 60 is less than that of the original structure, thus decreasing the SE and increasing the  $R^2$  value. S2 is very similar to the original, the only major difference being that it under-predicts the three main peaks by approximately  $0.05\text{m}^3\text{s}^{-1}$  more whilst also over-predicting marginally less during days 50-60. It shows similar differences to S1, S3 and S4 as the original structure.

Taking the 1987 plots next, the S1 and S4 plots are again very similar. Compared to the original structure they under-predict the main peak by less than it over-predicts it, match the two peaks on days 55 and 59 as well as the original and are much better at matching the final two peaks, thus accounting for most of their

statistical improvement. S2 under-predicts the main peak by approximately  $0.15\text{m}^3\text{s}^{-1}$  more than S1 and S4 and is less able to match the peak on day 55. It is also better at matching the final two peaks than the original structure. It must be noted that in doing so it simulates these late peaks as higher magnitude events than the first and major peaks; neither S1, S4 or the original structure do this. Finally, S3 matches the first three peaks in a similar way to S1 and S4 and thus compares to the original structure similarly. Whilst it matches the first of the final two peaks well, it over-predicts the last one by more than  $0.25\text{m}^3 \text{ s}^{-1}$ , the simulated flow being even higher than the maximum observed flow on day 30. This is the major reason for poor performance of this structure.

Having compared the plots for the different structures S4 can be compared to the corresponding plots for the TINDEXT model runs. Figures 5.14 and 5.15 show the 1986 and 1987 combined parameter model runs for both TINDEXT and MART. On the 1986 dataset MART simulates the early flow better, being closer to the first two major peaks and over-predicting less over the first 14 days of the model run. The TINDEXT plot compensates for this later in the melt season by being closer to the observed intermediate flows over days 51-55 and matching the final peak on days 61-62 better than MART. It can thus be said that neither model outperforms the other on the 1986 dataset, both having good and bad periods. The same can not be said for the two 1987 model runs shown in Figure 5.15. TINDEXT over-predicts during the early stages of the model and whilst both models are very similar at simulating the main peak, TINDEXT is

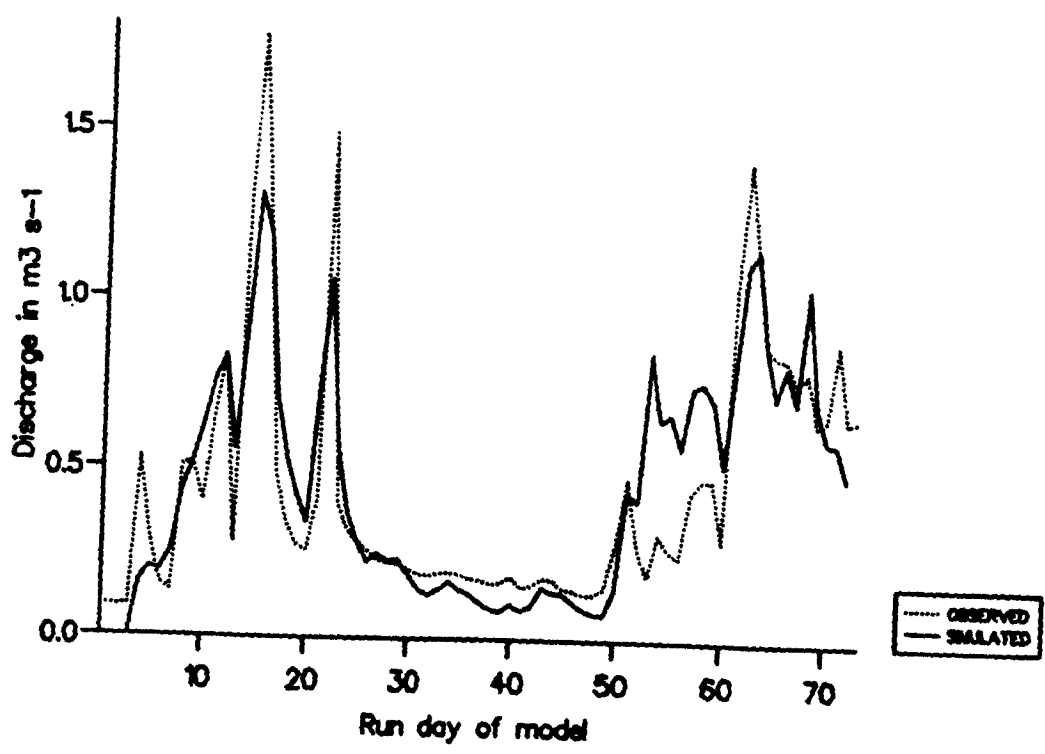
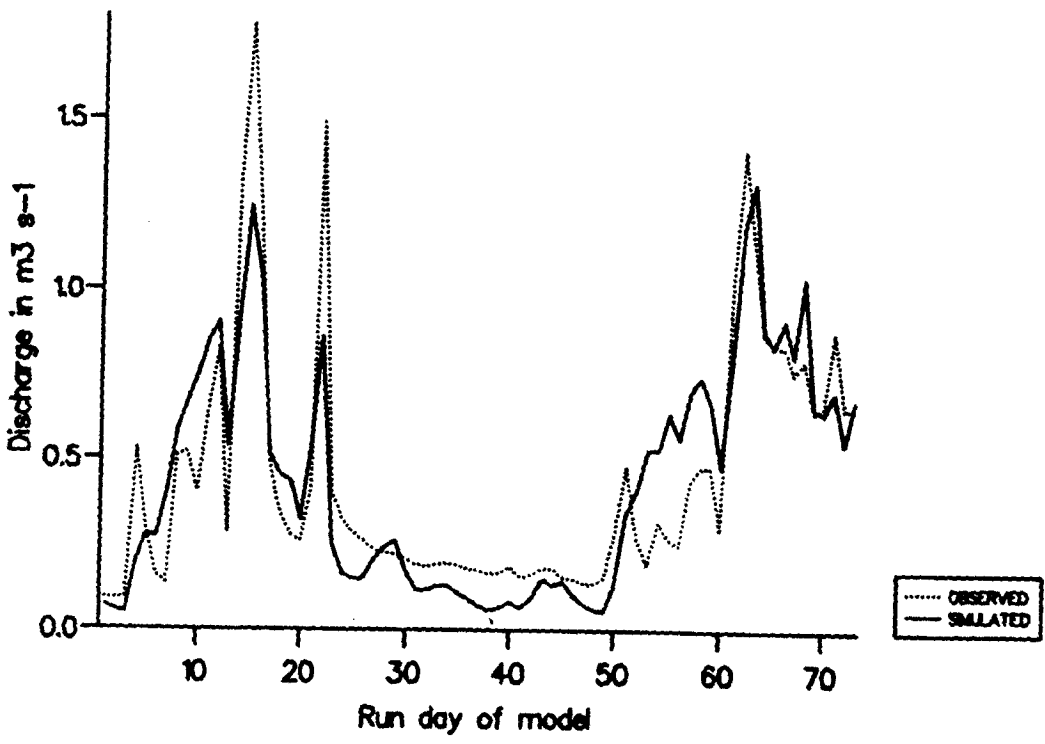


**Figure 5.14** Time series plots of TINDEX (upper) and MART (lower) running on the Mharcaidh 1986 data.

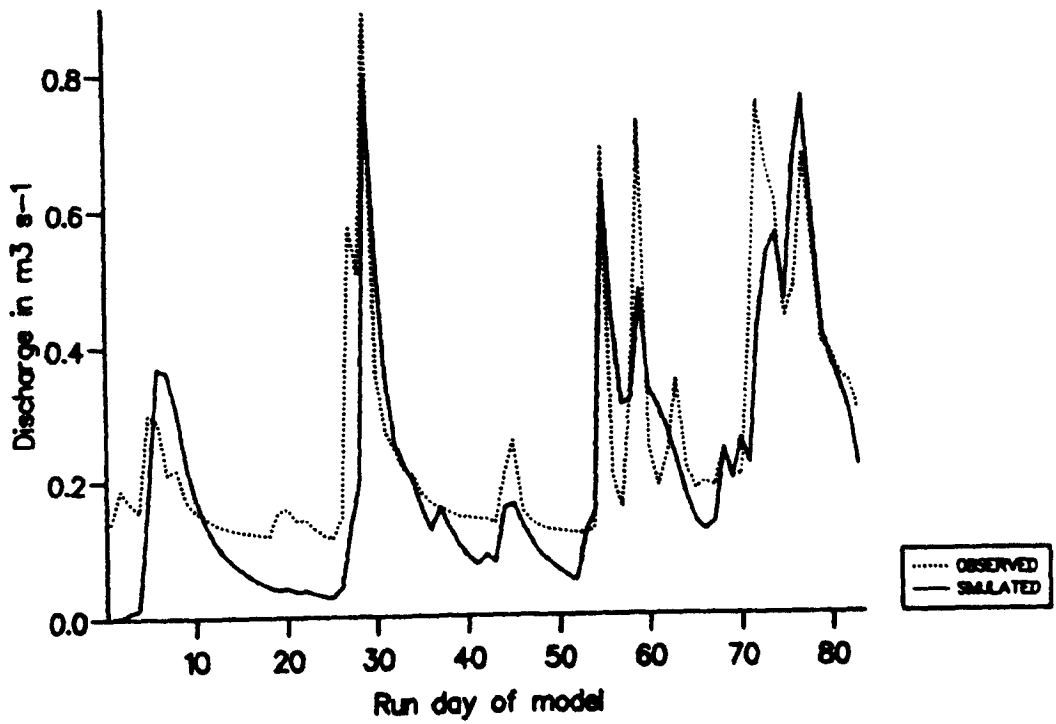
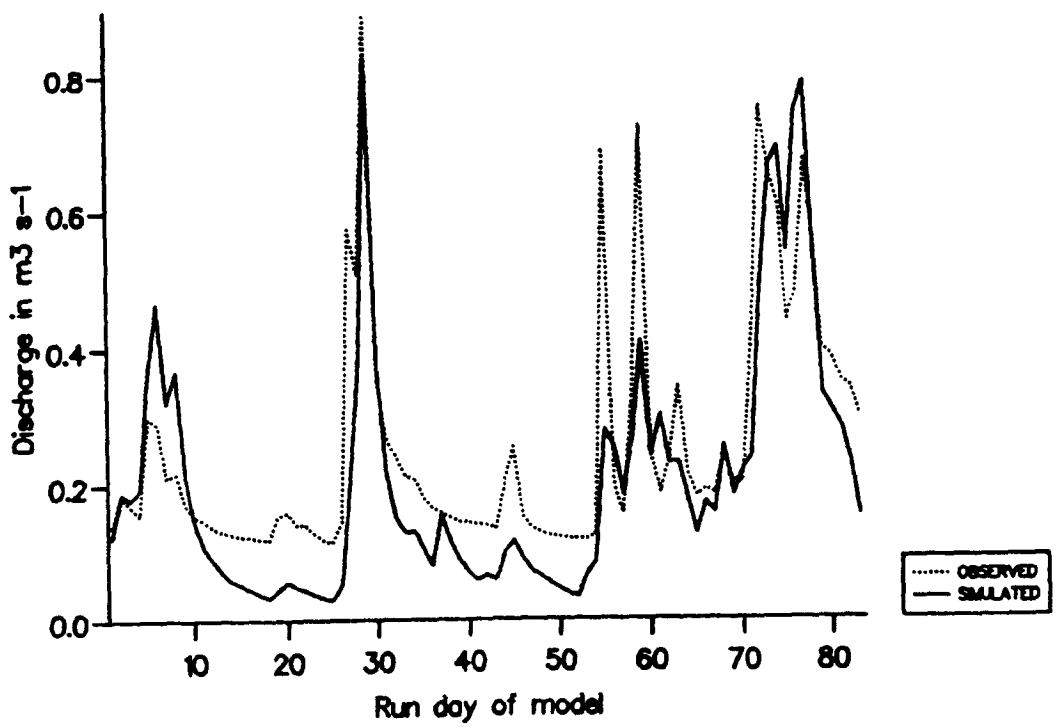


**Figure 5.15** Time series plots of TINDEX (upper) and MART (lower) running on the Mharcaidh 1987 data.

again much weaker at simulating the high flows observed on days 55 and 59. It does simulate the first of the final two peaks on day 74 better than MART but this is matched by MART simulating the final peak better. Thus, it can be said that visually MART performs better than TINDEK on the 1987 dataset.

(c) The parameter set values

From the data shown in Table 5.4<sup>6</sup> it can be seen that regardless of the snowpack structure used in the model all models optimise to give very similar recession coefficients for each year. The 1986 model runs optimise R to 0.0033 or 0.0034 in all cases whilst the 1987 values range from 0.0021 to 0.0029. Because of this the combined recession coefficients are also very similar, varying from 0.00270 to 0.00315, and being close to the optimised values for each year allow the model to perform well using the combined values. From these results two useful points can be made: firstly, the values all being so similar regardless of snowpack structure or year is encouraging if a universally applicable model is to be developed optimising as few parameters as possible; secondly, the optimised values differ consistently from year to year, i.e. the 1986 value is always higher than that for 1987. This would be expected, a higher recession coefficient being needed to allow the flow to increase from low to high flow conditions. Whilst non-linear routing allows for this later in the year a higher values is still needed for the first major melt event.

The melt coefficients vary widely for each model structure, the

greatest variation being present in the S1, S3 and S4 model runs where the 1986 values are all 9.9 and the 1987 values range from 2.1 to 2.4 mm°C day<sup>-1</sup>. The differences are less for S2 and the original structure, the 1986 values being 6.1 and 6.4, those for 1987 being 3.4 and 2. Despite these large differences the model is still able to perform well using a combined melt coefficient suggesting that it is not sensitive to this provided that it is free to optimise the snowpack characteristics.

Taking the snowpack parameters (A and W) together, Table 5.7 shows the initial snowpack volumes used by the five snowpack structures.

MODEL RUN	SNOWPACK STRUCTURE				
	0	S1	S2	S3	S4
1986 O	1.464	0.966	1.064	0.966	0.966
1987 O	0.594	0.552	0.686	0.496	0.580
1986 C	1.875	1.364	1.564	1.364	1.364
1987 C	0.316	0.200	0.595	0.205	0.200

Table 5.7 Snowpack volumes modelled by the optimised and combined MART model runs for the different snowpack structures. 0 = Original structure, O = Optimised and C = Combined parameter sets.

From these results the first point to be made is that the 1986 snowpack volume is always greater than that of 1987. Had it been otherwise the model would have had little potential for use in real-time forecasting, the snowpack parameters bearing no resemblance to the observed snowpack variation from year to year.

In addition to the relationship between the 1986 and 1987

snowpack volume being constant it can also be seen that the change in volume is constant between the optimised and combined parameter model runs for both years; the 1986 volume is always lower for the optimised parameter set whilst the 1987 volume increases. This constant change can be attributed to the respective changes in the melt factor; it decreases for all 1986 datasets and increases for all the 1987 model runs. It is best illustrated by referring to the 1987 model runs on S1, S3 and S4. The snowpack volumes show a decrease to approximately one third of the optimised values as a result of the associated near threefold increases in the melt factors.

If the initial volumes from the model runs are compared to those obtained from the snow surveys (approximately  $1.6 \times 10^6 \text{m}^3$  for 1986 and  $0.6 \times 10^6 \text{m}^3$  for 1987, shown in Figure 3.2) it can be seen that no structure is able to produce a volume close to the observed using both optimised and combined parameters. The original structure provides the closest values for the optimised datasets and S2 provides the closest for the combined. S1, S3 and S4 are all close on the 1987 optimised value and the 1986 combined but are very weak on the 1987 combined.

Whilst no particular snowpack structure is able to accurately replicate the data observed in the field, the values in Table 5.7 can shed some light on the differences observed between the time series plots described in (b)

above. The 1986 initial volume obtained from the original structure is more than  $0.5 \times 10^6 \text{m}^3$  larger than that of S1, S3 and S4 accounting for the greatest over-prediction late in the melt season between days 50 and 60. Similarly, the 1987 volume being smaller results in the simulated main peak for structures S1, S3 and S4 being less than that of the original.

Finally, whilst the optimised values of A and W shown in Table 5.6 do not directly reflect the observed snowpack at the start of the 1986 melt season (A is only  $4.6 - 6.1 \text{km}^2$  whereas the snow surveys show almost all of the catchment being covered) they do reflect the snowpack that was responsible for the major contribution to runoff for both melt seasons. 1986 was dominated by a deep snowpack that, once initial melt had taken place over the lower slopes, covered the upper two zones of the catchment. The 1987 snowpack was generally more variable, covering a large area with a thin initial snowcover which was able to melt at all elevations in the catchment, resulting in snow-free areas on both high and low ground.

(d) Snowpack depletion

Figures 5.16 and 5.17 show the depletion curves for the optimised and combined model on the 1986 and 1987 datasets respectively.

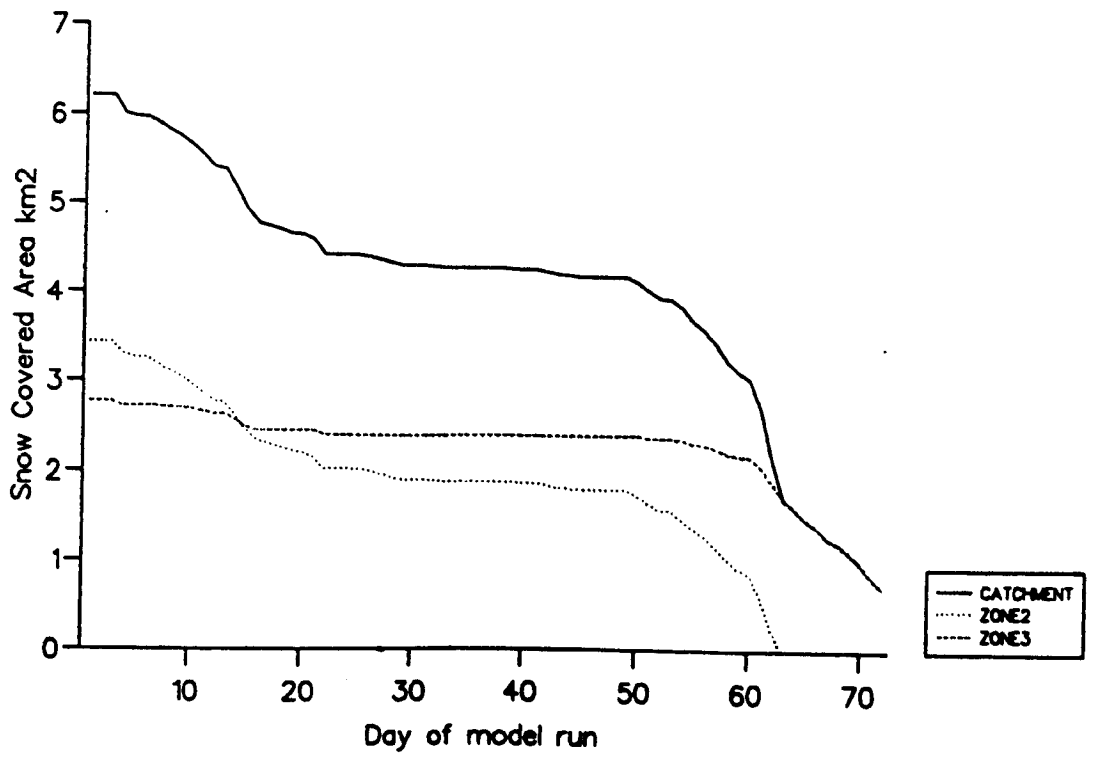
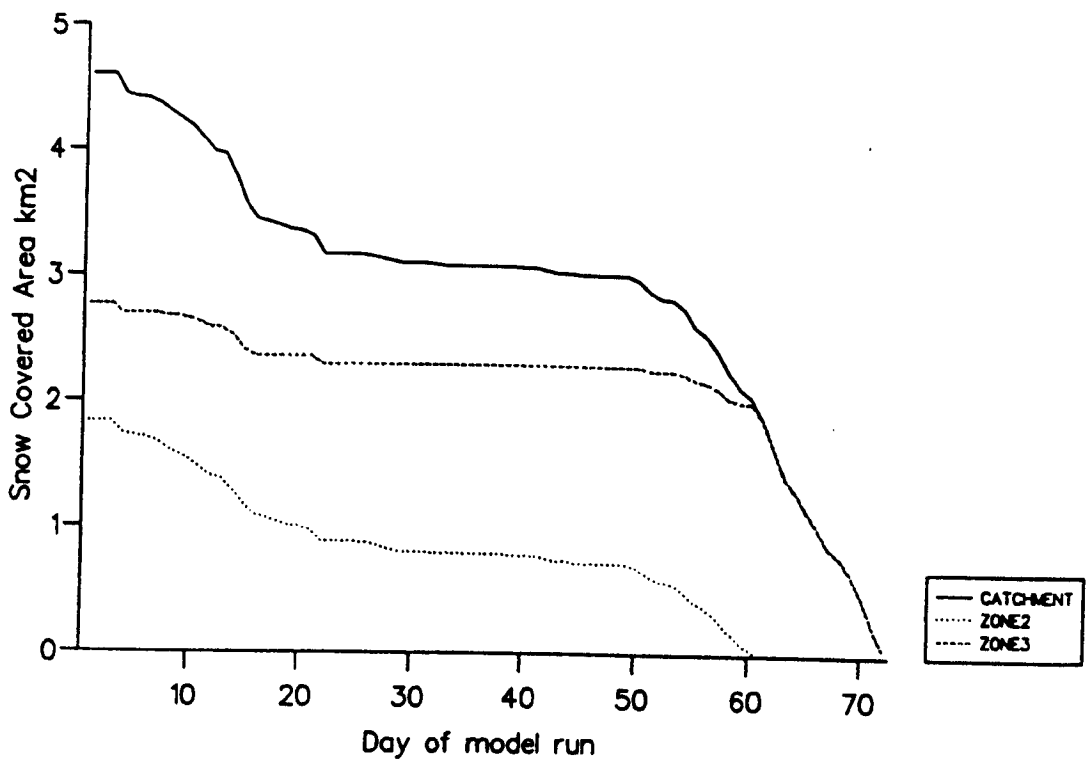


**Figure 5.16** Snow covered area depletion curves from the MART model run on the Mharcaidh 1986 data using optimised (upper) and combined (lower) parameters.

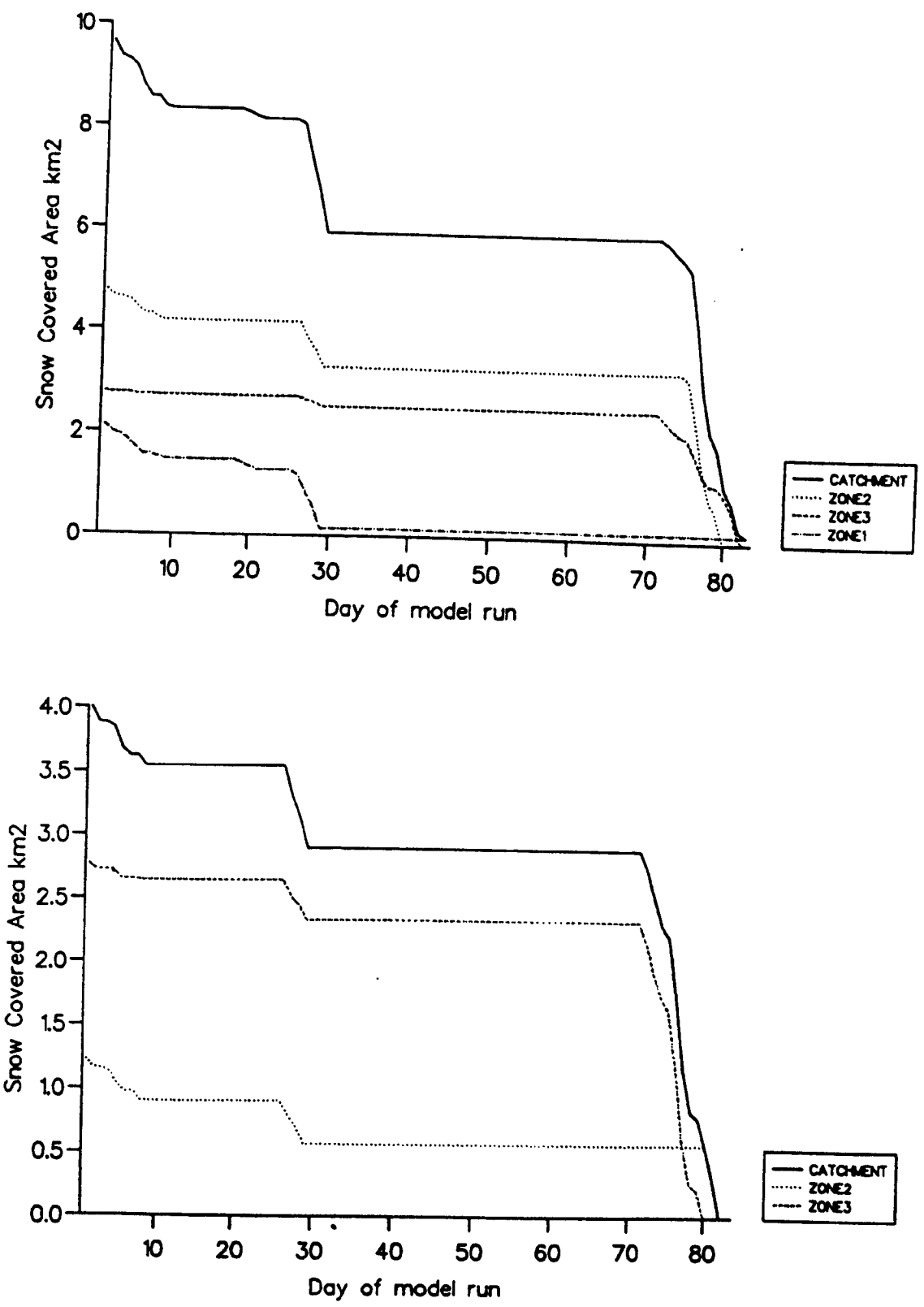


**Figure 5.17** Snow covered area depletion curves from the MART model run on the Mharcaidh 1987 data using optimised (upper) and combined (lower) parameters.

The 1986 plots show that despite the initial SCA being considerably higher in the combined parameter set (increasing from 4.6 to 6.2km<sup>2</sup>) and having a lower melt coefficient the model is able to produce a similar depletion curve for both zones 2 and 3.

SCA over zone 2 is rapidly depleted over days 1-20 of the model runs, coinciding with the major melt event of the year, and then stabilises between days 20 and 50 due to the period of cold and settled weather associated with the dominant high pressure system (3.3.1(a)). When the temperatures increase and melt re-starts after day 50 the snow cover rapidly depletes once more, reaching 0 on day 61 of the optimised model run and day 63 of the combined. It can be noted that despite the SCA on day 50 being so much higher on the combined model run than the optimised as a result of the higher initial SCA (values are 1.75 and 0.65km<sup>2</sup>) the model is still able to deplete this cover over a similar time-span. This helps explain the over-prediction in stream runoff over this period noted in Figure 5.14.

Zone 3 also shows a period of melt between days 1-20 of the model runs though, as it is closer to the freezing level, it is less rapid than zone 2. It is stable between days 20-50 and then starts to deplete once again, the rate of depletion increasing between days 50-60 as the temperatures increase. This is what would be expected in reality, and

represents an isothermal, saturated snowpack rapidly melting. By day 61 of the optimised model run and 63 of the combined, the snowcover in the zone is all that remains in the catchment, this being finally depleted on the final day of the optimised model run and down to 0.725km<sup>2</sup> on the combined.

Both sets of the 1987 depletion curves shown in Figure 5.15 also show similar patterns despite the initial values being so different. They start with a short reduction in SCA in all zones containing snow, after which they remain stable between days 8 and 25. There is then a period of rapid depletion between days 26 and 29 associated with the major melt and runoff event of the year, followed by another stable period between days 50 and 71. The snowcover then rapidly melts until the SCA is at or close to zero by day 83. It is interesting to note that no depletion is modelled and observed between days 55 and 65 yet the modelled and observed hydrographs show two major and one minor peak in this period; the same applies to days 22 to 24 of the 1986 model runs. Reference to Figure 3.9 shows that both periods contain high magnitude precipitation events at the AWS, thus accounting for the increase in runoff. (Whilst both the periods often have maximum temperatures above 0°C the mean daily temperature is always close to 0°C, thus accounting for the stable snowpack.)

The major difference between the two 1987 plots is that

because the initial SCA is higher for the optimised parameter set zone 2 has <sup>complete</sup> snow cover and zone 1 contains snow for the early part of the melt season, though this is completely depleted by the end of the first major melt event.

Comparing the 1986 and 1987 plots it can be seen that whilst both show similar patterns of alternating rapid depletion and stable snowpack the contribution of melt from individual zones is different. The 1986 snowpack, having a high SWE, depletes at a slower rate in zone 3 as the temperature differences have more significance. Thus, for the final 10-12 days of the model run it is the only zone containing snow in the catchment and contributing meltwater to the Mharcaidh burn. In contrast the 1987 snowpack is very shallow, resulting in the snowcover in zones 2 and 3 completely depleting within three days of each other.

## 5.5 Conclusion

It has been shown that whilst the initial model runs using a vertically layered snowpack structure did not perform statistically well, the model has been improved by altering the snowpack structure within each zone. This development to MART has resulted in the statistical performance being very close to that of TINDEX whilst the visual performance is as good if not better, especially for the 1987 model runs. The model is able to perform well using a combined

parameter set, optimising only the snowpack and gradually increasing melt factor parameters, suggesting that it may have potential for use in real-time.

One weakness of the model is that despite representing the general characteristics of the two snowpacks well, the initial snowpack for 1986 bears little resemblance to that observed in the snow surveys, the optimised snow covered area being much less than the observed. Even with this weakness the model is able to simulate the snowpack depletion curves for each zone, the contribution of melt from each zone being well represented for both years.

## CHAPTER 6 APPLYING THE MODEL TO OTHER CATCHMENTS

### 6.1 Introduction

It was stated in 1.4 that one of the aims of the project was to apply the various models to other catchments in the Cairngorms region for a number of different melt seasons. TINDEX and MART were thus run on the datasets shown in Table 6.1 for the Dee, Gairn and Feshie catchments. These datasets are shown in Appendix A. ANDERS was run on the 1986 data only for the Dee and Gairn. The TINDEX model run will be studied first, catchment by catchment, then the MART model runs and finally ANDERS.

### 6.2 TINDEX

#### 6.2.1 Running TINDEX on the Dee datasets

TINDEX was run on datasets covering the 1984, 1986 and 1987 melt seasons. The 1984 dataset used meteorological data collected at Braemar (325m amsl) close to the gauging station whilst the 1986 and 1987 data was that collected in the Mharcaidh. Thus, in addition to testing the ability of the model to simulate flow using data collected within the catchment, the 1986 and 1987 model runs would be testing the performance of the model using data collected some 21.5km from the gauging station (though only 6.5km from the north-west limit of the watershed).

Catchment	Year	Number of Days	Start Date	Finish Date	Mean Discharge
Dee	1984	60			17.44
	1986	73	1 March	12 May	18.99
	1987	83	1 February	24 April	11.34
Gairn	1979	52	11 April	1 June	8.83
	1980	53	25 March	16 May	4.52
	1981	35	7 March	10 April	5.13
	1984	60			5.92
	1986	73	1 February	24 April	4.36
Feshie	1979	52	11 April	1 June	10.26
	1980	53	25 March	16 May	5.52
	1981	35	7 March	10 April	5.87

**Table 6.1** Datasets used to apply TINDEK and MART to the Dee, Gairn and Feshie catchments. Mean discharge is in  $\text{m}^3\text{s}^{-1}$ . For details of the recording stations see main text.

The model was run using both linear and non-linear routing as neither had appeared significantly superior during the model development on the Mharcaidh datasets described in Chapter 4. As only daily minimum and maximum temperatures were available for 1984 the average daily temperature (ATEM) was calculated using:

$$\text{ATEM} = (\text{TMIN} + \text{TMAX}) / 2$$

In order to ensure consistency the 1986 and 1987 datasets were reproduced so that only minimum and maximum data were used. The model was run using both the new datasets and those using the daily mean of the hourly observations collected in the Mharcaidh. The results from all model runs are shown in Table 6.2, and Figure 6.1-6.3 shows six of the ten time series plots from the model runs.

Taking the 1984 runs first it can be seen from Figure 6.1 that whilst the model operates slightly better using non-linear routing, both routing methods produce a good visual fit. Discrepancies common to both routing methods are a failure to match the first peak on day 10, under-prediction on both the major melt events (days 13-14 and 19-20) and over-prediction on the final melt event (days 24-26). The discrepancies are much less for the non-linear routing model run which is also able to simulate the receding flow more closely. The  $R^2$  values are both very high (0.822 for the linear, 0.875 for the non-linear) supporting the strong

Year	Routing	A TEM	E	R	A	M	W	ALB	SE	R <sup>2</sup>	FA
1984	L	1	0.009	0.32	284	2.6	280	0.17	6.1	0.822	7
1986	L	1	0.006	0.24	285	3.1	420	0.11	11.0	0.575	114
1987	L	1	0.006	0.57	186	6.1	240	0.42	6.4	0.654	15
1986	L	2	0.006	0.29	284	3.3	420	0.09	10.0	0.649	111
1987	L	2	0.006	0.55	169	6.1	260	0.70	6.3	0.668	27
1984	NL	1	0.006	0.15	270	2.5	260	0.16	5.0	0.875	0
1986	NL	1	0.006	0.18	281	2.8	420	0.12	10.1	0.634	128
1987	NL	1	0.006	0.19	237	2.9	150	0.05	7.1	0.458	60
1986	NL	2	0.006	0.15	281	2.8	440	0.10	9.5	0.677	139
1987	NL	2	0.006	0.19	217	3.1	150	0.04	7.2	0.448	58

Table 6.2 Results from applying TINDEK to the Dee datasets.

L = Linear routing; NL = Non-linear routing; ATEM (1) = Mean of minimum and maximum;

ATEM (2) = Daily mean of 24-hourly temperature values.

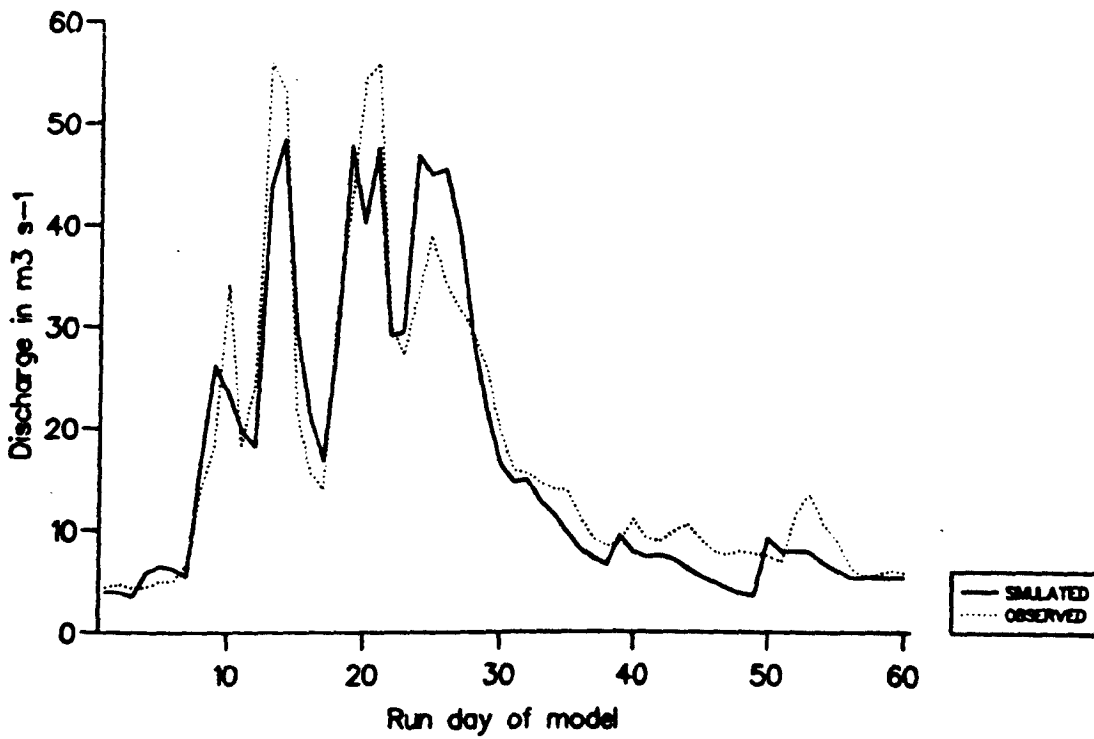
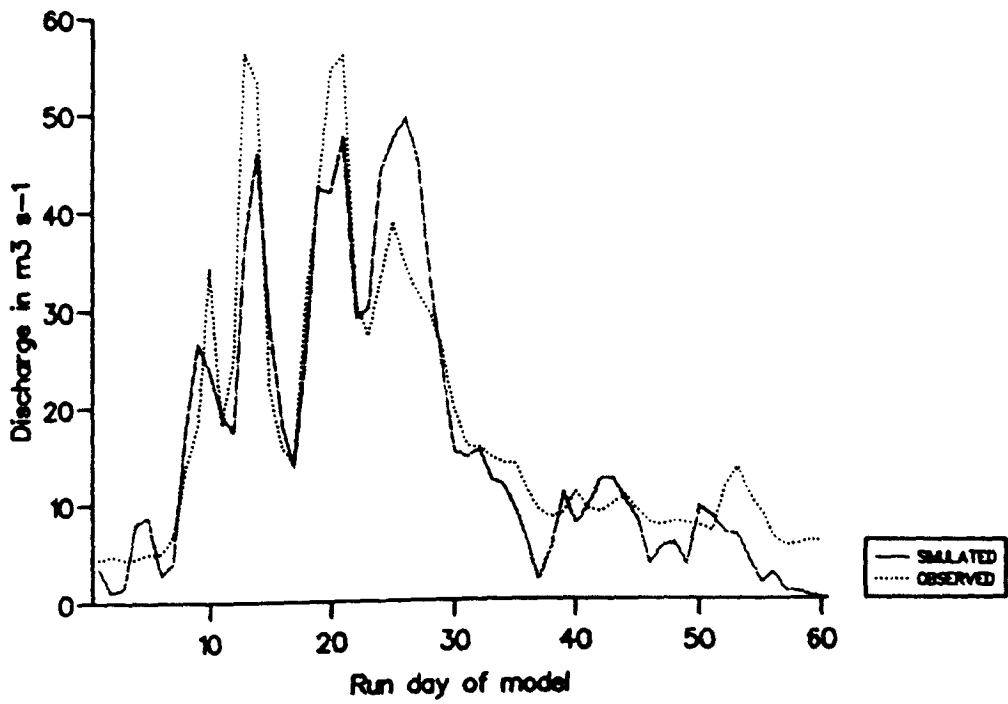


Figure 6.1 Time series plots from TINDEK running on the DEE 1984 data with linear (upper) and non-linear (lower) routing.

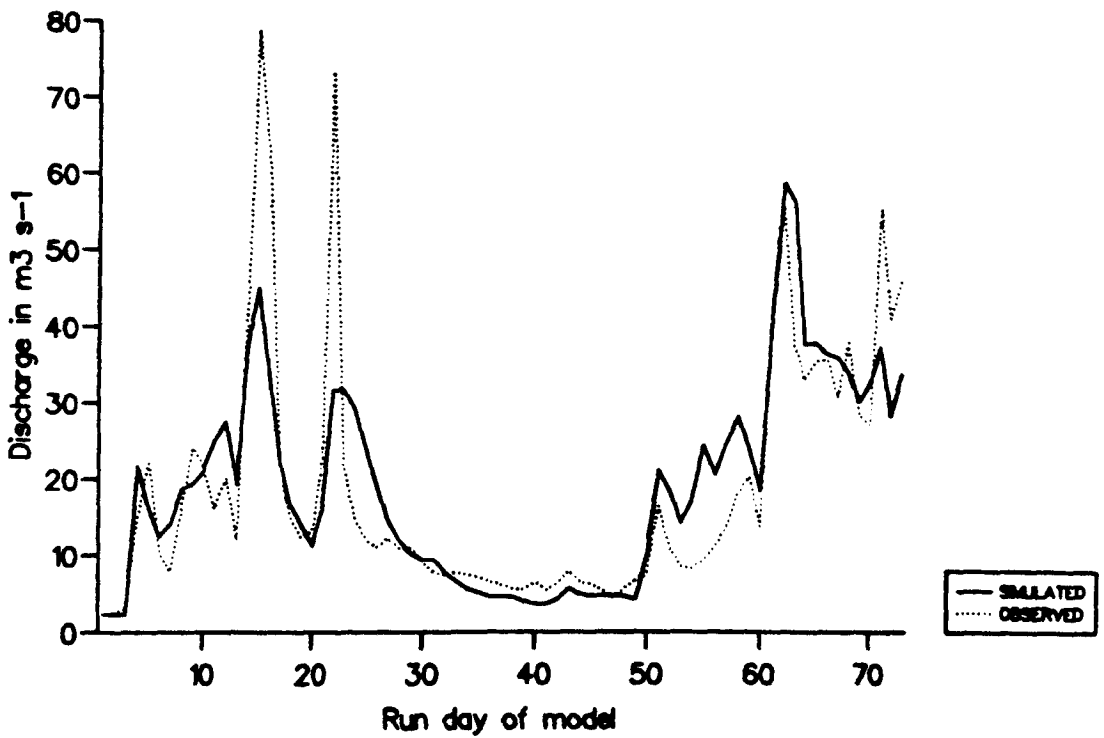
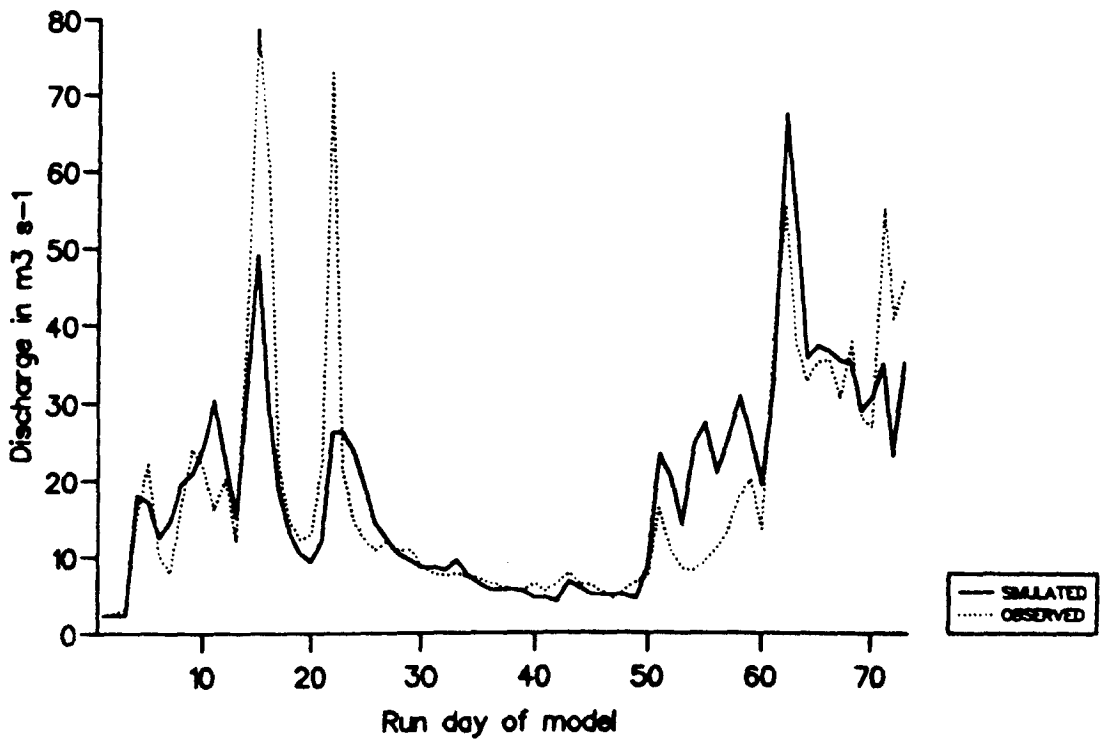


Figure 6.2 Time series plots from running TINDEK on the DEE 1986 data with non-linear (upper) and linear (lower) routing.

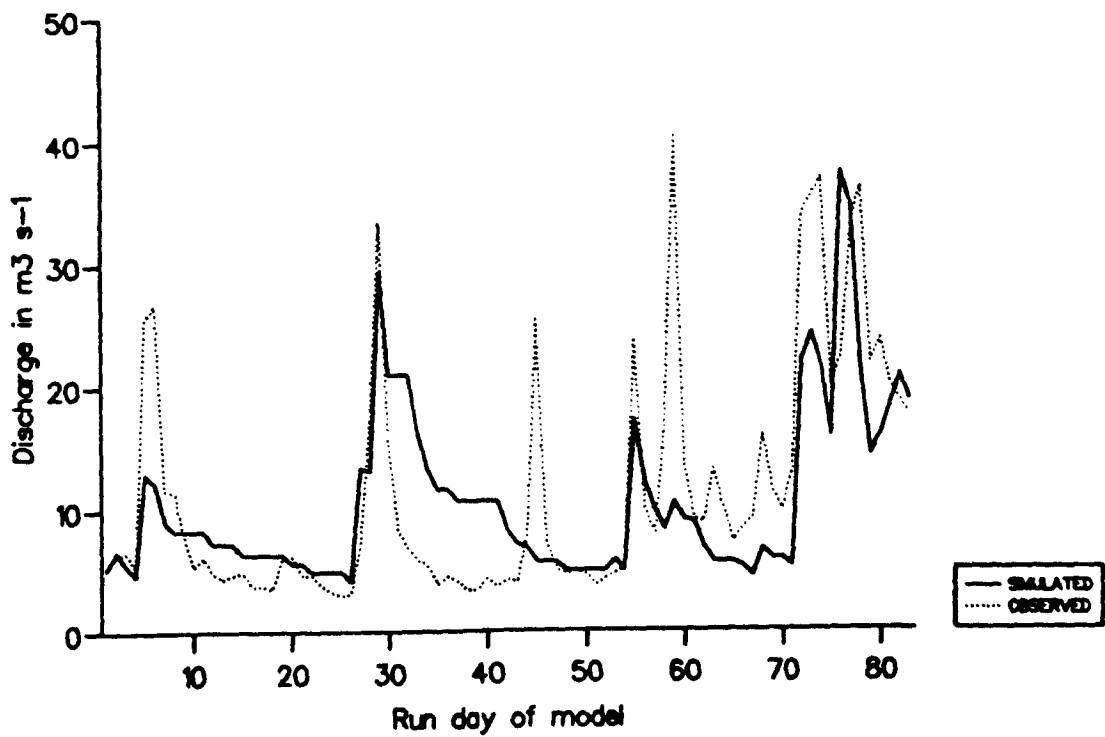
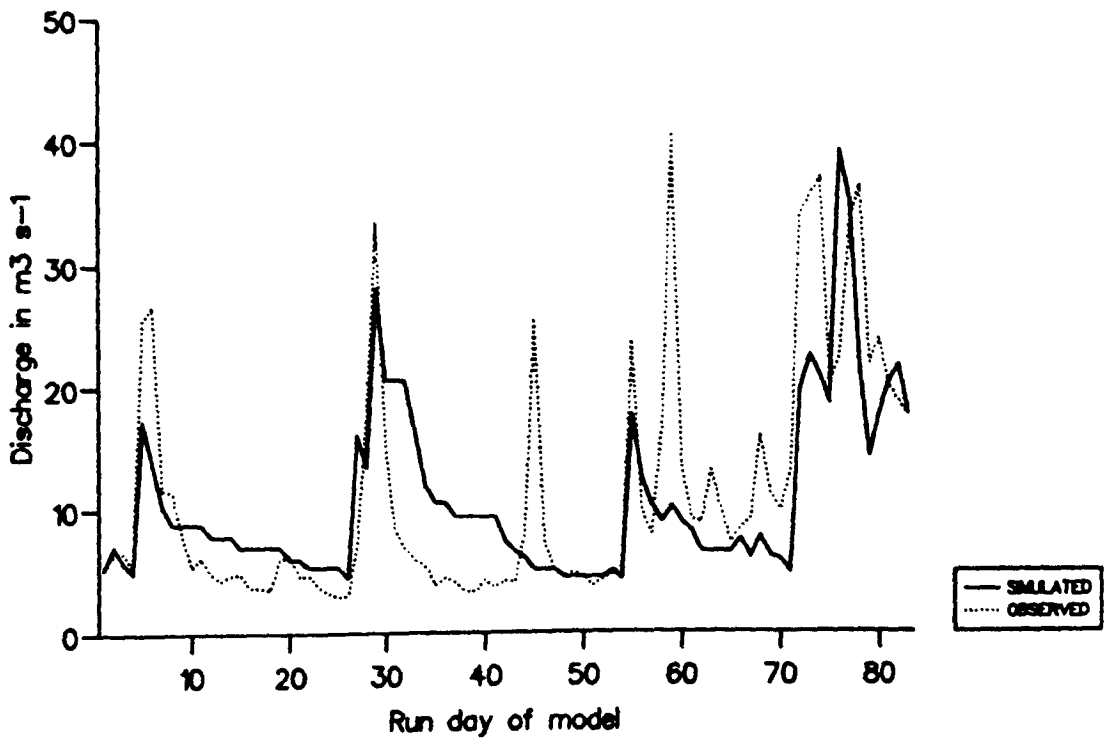


Figure 6.3 Time series plots from running TINDEK on the DEE 1987 data with non-linear (upper) and linear (lower) routing.

visual fit and confirming that in this case TINDEX is able to simulate the observed flow from a large, snow-covered catchment.

The 1986 plots shown in Figure 6.2 show a strong resemblance to those of the Mharcaidh, with high flows occurring on days 15-17 and 21-23, a period of low flow and then a final period of melt with high flows occurring on days 62 and 71. Like the TINDEX runs on the Mharcaidh dataset, the model is not able to match the early peak flows in magnitude, though the timing and general patterns are very similar. The non-linear run can again be seen to be better at matching the low flows, accounting for the higher  $R^2$  values recorded in Table 6.2. As TINDEX was unable to match the two early peak flows for the Mharcaidh using meteorological data collected within the catchment it was not expected that it would be able to match them for the Dee. Given this limitation, be it in the model or quality of the data, it can be said that for the rest of the 1986 melt season TINDEX is able to simulate the observed flow in the Dee using data collected in another catchment, the mean  $R^2$  for all model runs being 0.634.

Although the 1987 observed flows shown in Figure 6.3 are, on the whole, similar to those of the Mharcaidh there is a high flow event (day 45) that does not appear as significant on the Mharcaidh data. The flow on day 59 is also much higher in relation to the rest of the flow record

than it was for the Mharcaidh, and the highest flows are in general observed in the later part of the melt season.

Of the high flow events shown for the Dee in Figure 6.2 those over days 1-10, 26-33 and 71-83 are the main snowmelt events. TINDEX matches these events well, especially when using linear routing, the main weakness being a tendency to under-predict the first of the final two high flow events on days 72-74. This tendency was also present in the Mharcaidh model run and may be due to either a weakness in the depletion submodel (though this is unlikely as the later peak is well matched) or in the meteorological data.

The short duration, high peak flows observed on days 45, 55 and 59 are mainly derived from precipitation events and it can be seen that TINDEX is not able to simulate these events. Whilst this weakness can be partly attributed to the problems associated with quantifying precipitation inputs and applying these over a large area (especially the event on day 45), it is mainly due to TINDEX not being able to accurately model rainfall events, either when they are rain-on-snow or falling on snow-free areas.

If the two 1987 plots shown in Figure 6.3 are compared the reason for the statistical superiority of the model runs using linear routing (mean  $R^2$  of 0.656 compared to 0.454 for the non-linear routing) can be attributed to the poor performance of the non-linear model run over the receding

flows following the melt event on days 26-33.

One minor point of interest is that the non-linear model run simulates a minor peak on the rising limb of the hydrograph during this melt event that is not present in the observed flow record; the Mharcaidh observed data showed this peak but TINDEX was unable to simulate it! This suggests that the meteorological data is sufficient to model this particular event though TINDEX itself may not do so.

If the SE and  $R^2$  values shown in Table 6.2 are compared for the two different methods used to calculate the degree-days it can be seen that the availability of hourly temperature to determine the true mean daily temperature improves the performance of the model in most cases. The mean SE for all model runs drops from 8.65 to 8.25 and the mean  $R^2$  increases from 0.580 to 0.611. If the results for the 1987 model run using non-linear routing are discounted (it was an especially weak performer using both temperature indices) the difference becomes even larger, the SE dropping from 9.17 to 8.6 and the  $R^2$  increasing from 0.621 to 0.665. Whilst this improvement was not obvious in the respective time series plots it must be concluded that the performance of TINDEX is improved by the availability of hourly data to determine the true mean daily temperature.

When the results from the two different routing methods are

compared they show that for snowy years (1984 and 1986) non-linear routing performs better, the mean  $R^2$  being 0.755 compared to 0.699 for the linear routing model runs. As these years represent the years for which the model is most likely to be used it could thus be said that non-linear routing improves the ability of TINDEX to model snowmelt events. However, the 1987 dataset also contains snowmelt events, even if they are of smaller magnitude than the 1984 and 1986 events (peak snowmelt derived runoff rates being  $38\text{m}^3\text{ s}^{-1}$ ,  $57\text{m}^3\text{ s}^{-1}$  and  $79\text{m}^3\text{ s}^{-1}$  respectively) and the addition of non-linear routing decreases the mean  $R^2$  from 0.661 to 0.453. These results show that when TINDEX is applied to the Dee datasets the routing methods have similar effects to when running the model on the Mharcaidh data, non-linear performing better for snowy years whilst linear is better when the total snow volume is low and precipitation inputs are high. It is not therefore possible to decide which method should be used in a general model.

Finally, if the optimised parameter sets shown in Table 6.2 are considered it can be seen that the lapse rate, recession and melt coefficients all show a small range in values, especially for the non-linear routing parameter sets. With the exception of the 1987 linear routing parameter sets the melt coefficients all fall within the range  $2.5\text{--}3.3\text{mm}^\circ\text{C day}^{-1}$ , very similar to the range of melt coefficients for the corresponding Mharcaidh runs ( $2.6\text{--}3.3\text{mm}^\circ\text{C day}^{-1}$ ). The lapse rates mostly optimise to the lower

limit ( $0.006^{\circ}\text{C m}^{-1}$ ) and the routing coefficients for the non-linear model runs all fall within the 0.15–0.19 range. The 1987 linear routing parameter sets are anomalous in that both the recession and melt coefficients are more than twice the mean values of the 1984 and 1986 parameter sets (R value of 0.7 compared to 0.28, M value of  $6.1\text{mm}^{\circ}\text{C}^{-1}\text{ day}^{-1}$  compared to 2.85). Whilst this demonstrates the flexibility of TINDEX using linear routing, allowing it to simulate observed flow records, it also makes the linear routing method less applicable as a general model as the parameters are less easy to set as constants.

It can thus be concluded that from the TINDEX model runs on the Dee datasets the non-linear routing method offers the greatest potential for use in a general model. Whilst the  $R^2$  values using this method are low for 1987 (0.448 and 0.458) they are high for the snowy winters of 1984 and 1986 (0.875, 0.634 and 0.677) and the range of optimised parameters are low.

### 6.2.2 Running TINDEX on the Gairn datasets

TINDEX was run on datasets covering the 1979, 1980, 1981, 1984, 1986 and 1987 melt seasons. All flow data was collected at the North East River Purification Board gauging station on the Gairn above its confluence with the Dee at Ballater. The meteorological data for the 1984, 1986 and 1987 datasets were the same as those used for the

Dee model runs; the 1979, 1980 and 1981 were collected at Lagganlia Outdoor Education Centre (265m amsl) at the western edge of the Cairngorms. As the Gairn catchment was further east than the Dee and then even further away from the meteorological sites and has a lower mean elevation (Figure 1.8) it was expected that the results from the TINDEX runs would not be as good as those for the Dee.

The model was run using both linear and non-linear routing, and for 1986 and 1987 the two methods outlined in 6.2.1 for determining the degree-days were used. The results are shown in Table 6.3 and Figures 6.4-6.7 show nine of the 16 time series plots.

The plots shown in Figure 6.4 for the 1979-81 model runs all show TINDEX generally reflecting the observed flow. Surprisingly, the 1979 model run has the lowest  $R^2$  (0.599 linear, 0.511 non-linear) although it appears to simulate the observed flow well and represents a snowy winter. This can be attributed to the magnitude of flow during the 1979 melt season, the peak flow ( $25\text{m}^3 \text{s}^{-1}$ ) being three times that of 1980 and  $7\text{m}^3 \text{s}^{-1}$  greater than that of 1981 and matched all the major peaks well.

1979 was the year that Ferguson's (1984) model was initially tested on and simulated the observed flow for the Feshie catchment ( $R^2$  of 0.88) yet the model is not able to do this for the Gairn 1979 data, its main weakness being

Year	Routing	ATEM	E	R	A	M	W	ALB	SE	R <sup>2</sup>	FA
1979	L	1	0.006	0.53	150	1.7	190	3.00	3.00	0.599	0.0
1980	L	1	0.006	0.85	150	0.5	110	0.01	0.89	0.825	17.0
1981	L	1	0.006	0.65	61	4.4	140	0.01	2.25	0.699	11.0
1984	L	1	0.006	0.44	145	2.6	160	0.20	2.55	0.786	0.0
1986	L	1	0.006	0.45	134	2.0	250	0.05	2.69	0.620	2.3
1987	L	1	0.006	0.70	77	4.5	230	0.03	1.57	0.685	0.0
1986	L	2	0.006	0.44	135	2.0	250	0.01	2.53	0.663	5.7
1987	L	2	0.006	0.69	74	4.7	230	0.03	1.54	0.708	0.0
1979	NL	1	0.006	0.15	150	1.5	180	4.00	3.30	0.511	0.0
1980	NL	1	0.006	0.10	150	0.7	90	0.01	0.93	0.808	0.0
1981	NL	1	0.006	0.16	65	2.8	100	0.01	2.20	0.710	9.9
1984	NL	1	0.009	0.24	134	2.7	140	0.19	1.69	0.900	0.0
1986	NL	1	0.006	0.21	138	1.8	230	0.04	2.75	0.639	0.0
1987	NL	1	0.006	0.30	130	1.0	160	0.01	2.03	0.460	59.0
1986	NL	2	0.006	0.19	144	1.6	220	0.01	2.73	0.630	12.1
1987	NL	2	0.006	0.35	134	0.8	160	1.00	1.96	0.502	73.9

Table 6.3 Results from applying TINEX to the Gairn catchment.

L = Linear routing; NL = Non-linear routing; ATEM (1) = Mean of daily minimum and maximum;  
ATEM (2) = Daily mean of 24 hourly temperature values; E = Environmental lapse rate ( $^{\circ}\text{Cm}^{-1}$ )  
R = Recession coefficient; A = Initial SCA ( $\text{km}^2$ ); M = Melt coefficient ( $\text{mm}^{\circ}\text{C day}^{-1}$ );  
W = Initial SWE (mm); ALB = Gradually increasing melt factor coefficient.

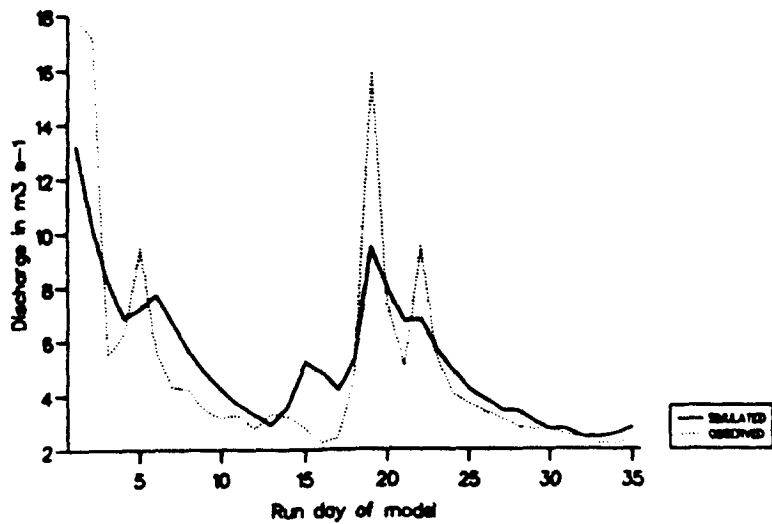
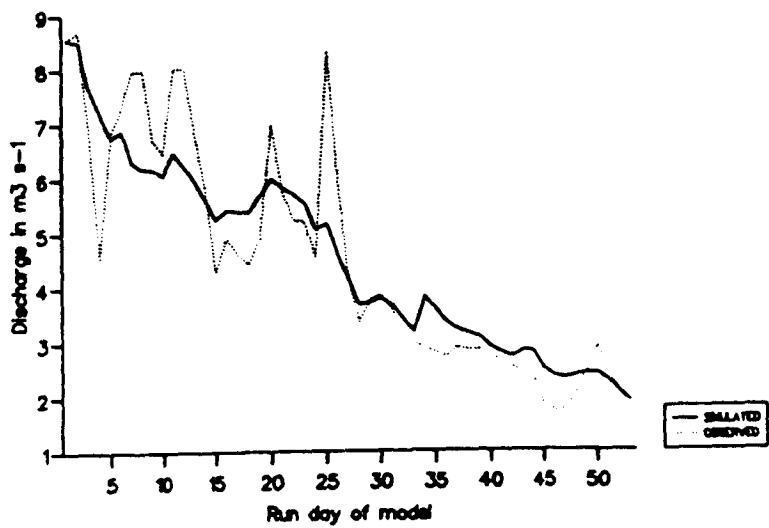
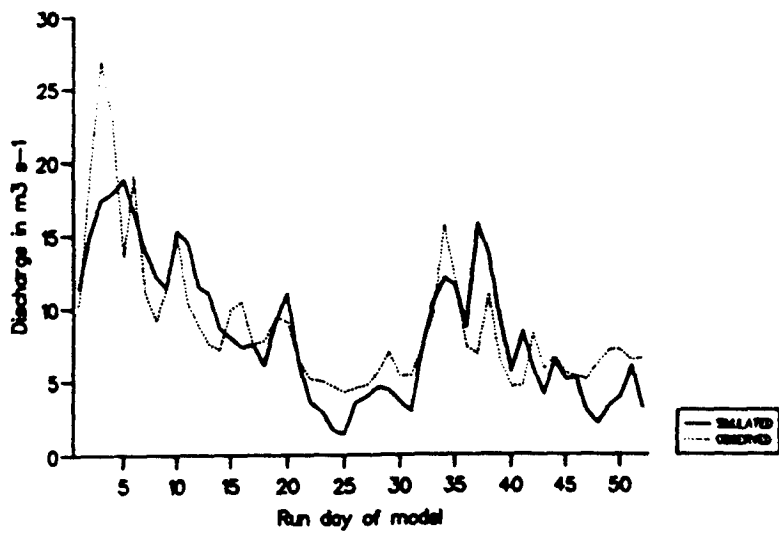


Figure 6.4 Time series plots from running TINDEK on the Gairn data; upper plot is for 1979 with linear routing, middle plot is for 1980 with linear routing and the lower plot is for 1982 with non-linear routing.

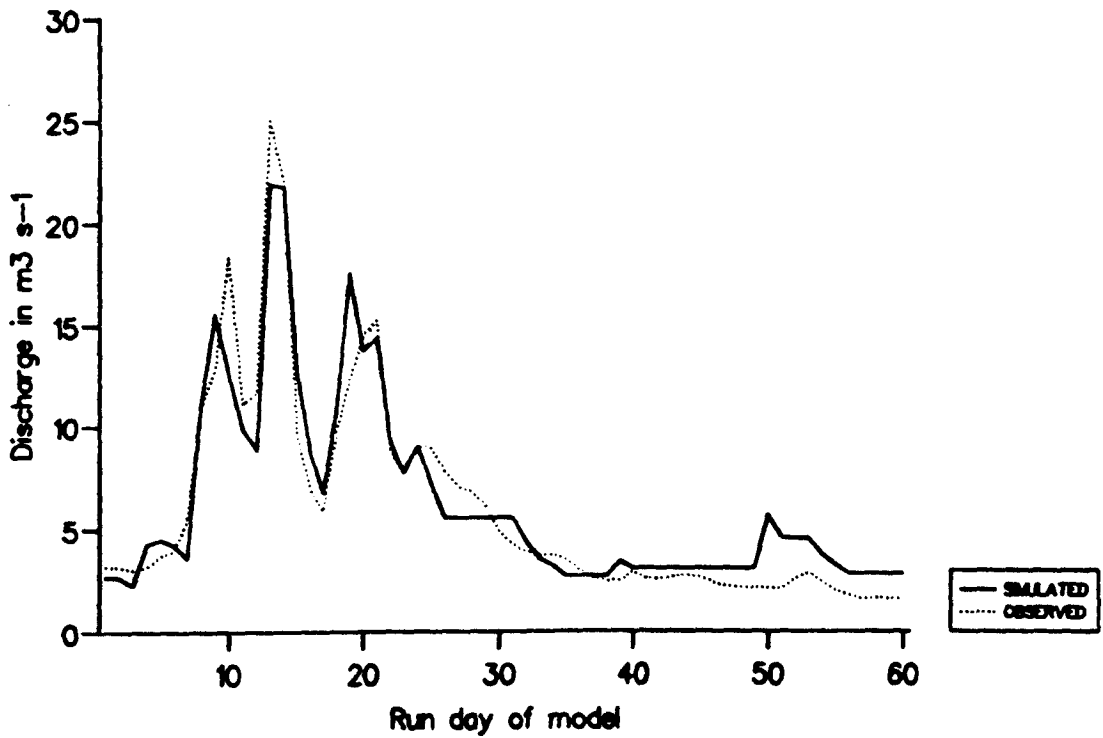
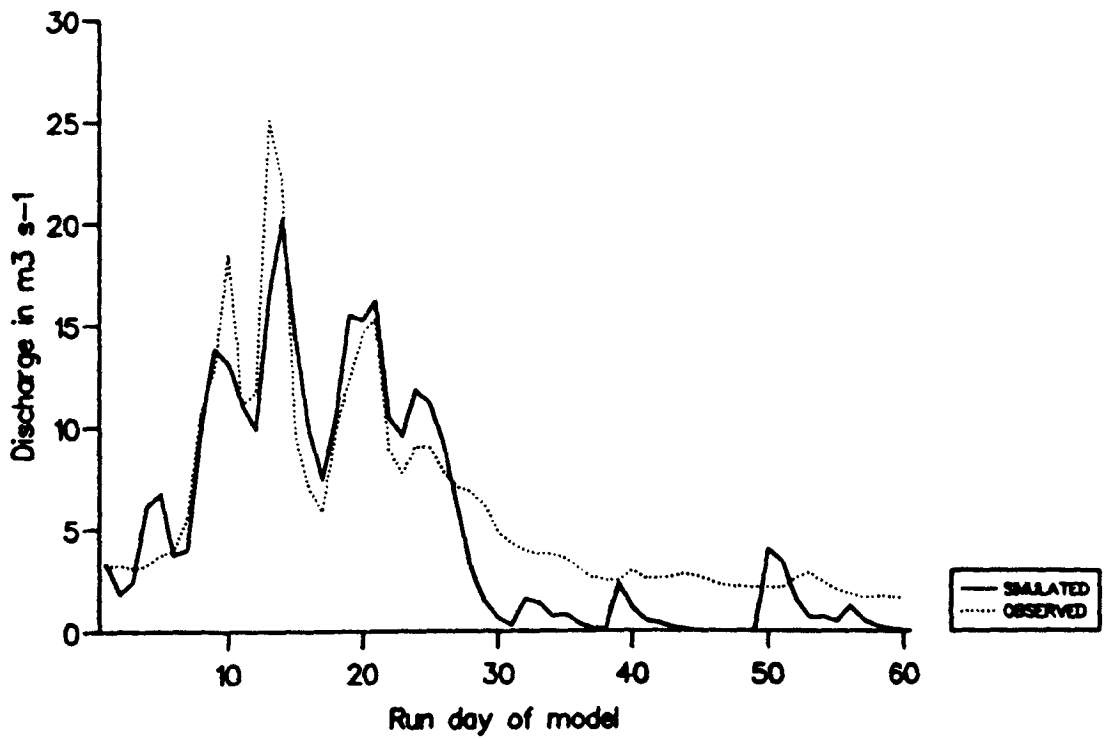


Figure 6.5 Time series plots from running TINDEK on the Gairn 1984 data with non-linear (upper) and linear (lower) routing.

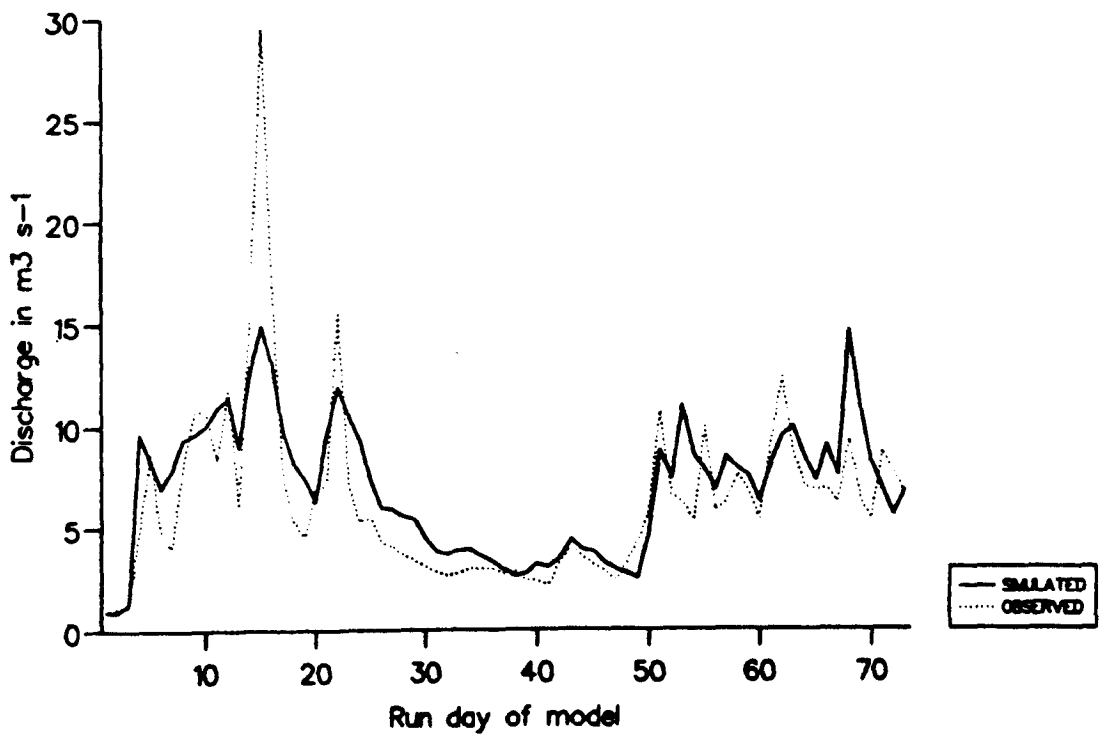
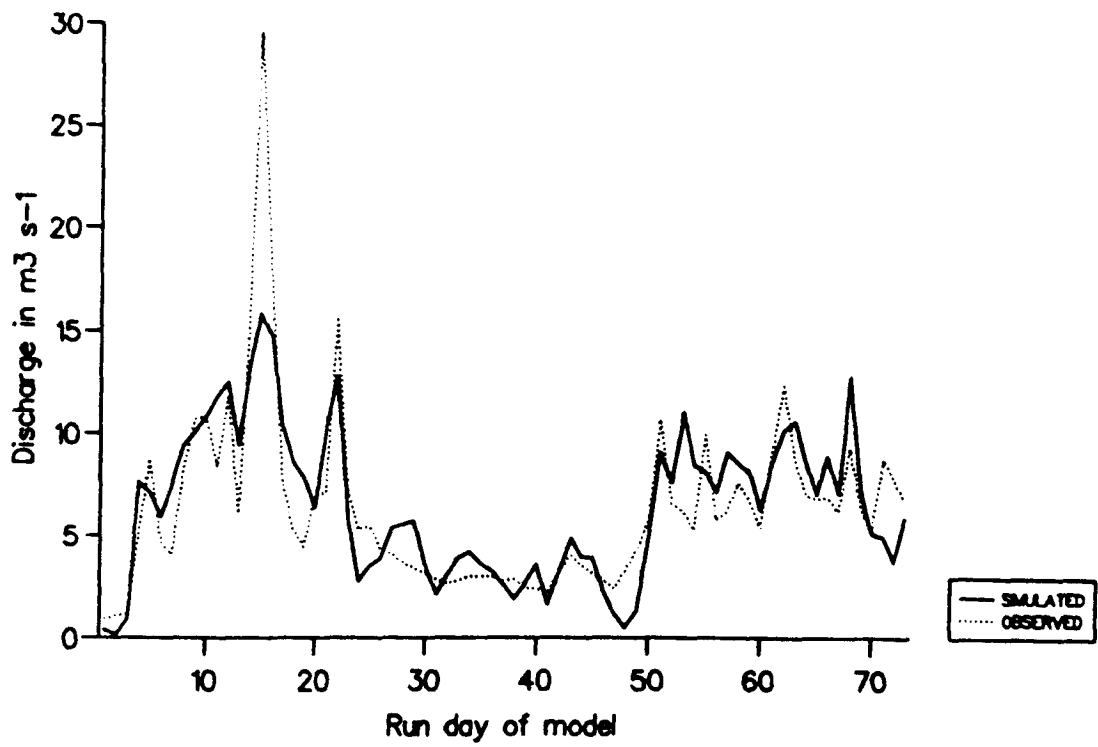


Figure 6.6 Time series plots from running TINDEK on the Gairn 1986 data with linear (upper) and non-linear (lower) routing.

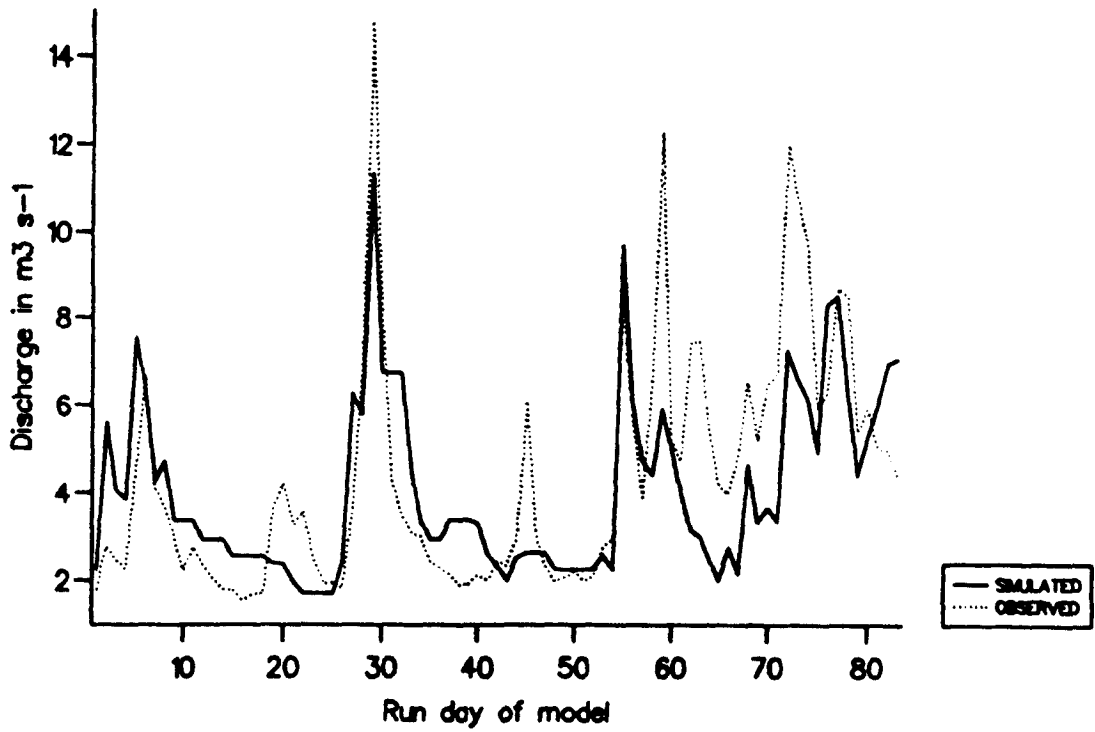
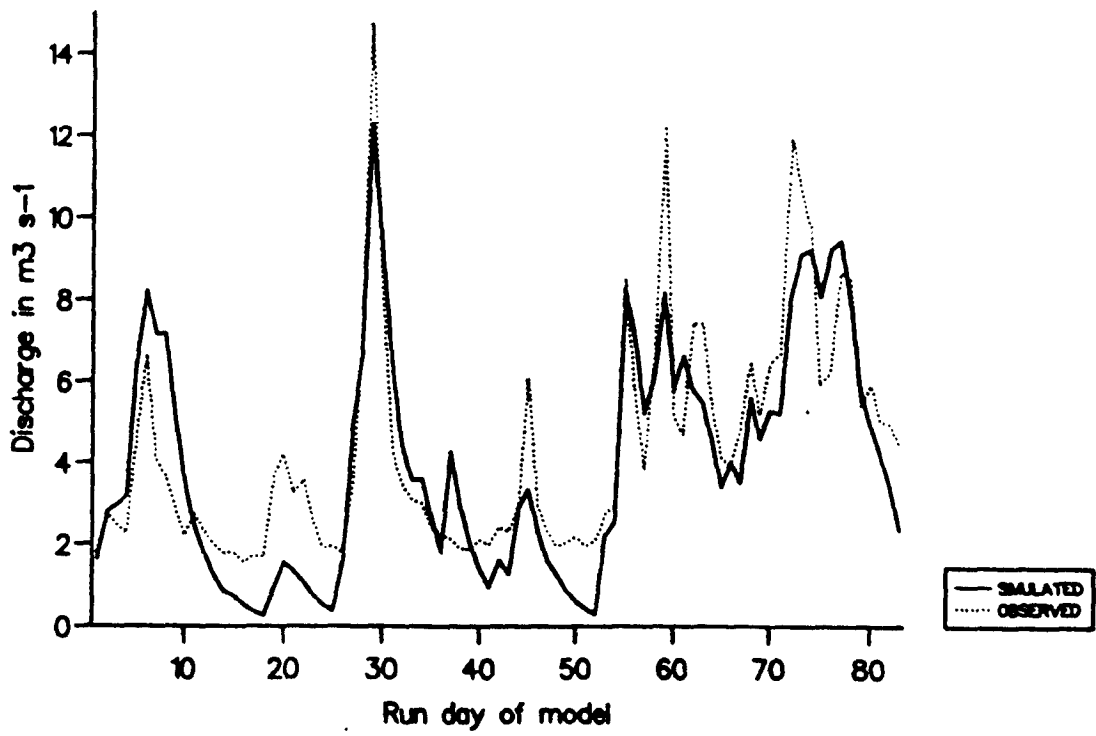


Figure 6.7 Time series plots from running TINDEK on the Gairn 1987 data with linear (upper) and non-linear (lower) routing.

the under-prediction of the first and largest peak by approximately one-third and over-prediction of days 36-38.

The 1980 flow is well simulated (linear  $R^2$  of 0.825, non-linear  $R^2$  of 0.808), the peak flows early in the melt season being closely matched though the sharp observed peak on day 25 is not replicated at all. This appears to be a rain-on-snow event, rising and falling very steeply, though this can not be verified from the meteorological data as this was collected some 48km to the west of the gauging station. There is also a peak on day 34 of the simulated flow that is not present on the observed. This corresponds to a low magnitude rainfall event at Lagganlia that may not have occurred over much of the Gairn catchment.

The 1981 flow record is also well simulated so far as the general pattern is concerned, but again TINDEK fails to simulate the major peak on day 19. In hindsight this may well be attributed to the flow at the start of the melt season; had the 'melt season' (which was selected mainly due to the data available) used for the model run started earlier or later by only a few days then the model may have performed better.

The 1984 model runs shown in Figure 6.5 show that TINDEK is able to simulate the observed flow well following a snowy winter with meteorological data collected close to the catchment. The non-linear plot in particular performs well

( $R^2 = 0.900$  compared to  $0.786$  for the linear plot), coming within 10% of the maximum peak flow and simulating the preceding and following peaks well. The superiority of the non-linear plot is not only due to the matching of the peak flows but also the very close fit with the observed low flows during the later part of the melt season. The higher  $R^2$  for the Gairn non-linear plot than that of the same Dee model run is due to a closer matching of the flow on days 17-22; on the Dee model run TINDEX over-predicted the flow whilst it is closely matched for the Gairn data.

From Figures 6.6 and 6.7 it can be seen that when TINDEX is applied to the Gairn using meteorological data collected in the Mharcaidh it behaves in a similar way to when it is applied to the Dee and Mharcaidh datasets. The 1986 peak flow is poorly matched, though the later rain-on-snow peak is well simulated as it is proportionally lower for the Gairn. Low flows during the middle of the 1986 melt season and the intermediate flows during the final melt are well matched, especially when non-linear routing is used. (It is interesting to note that these final flows are relatively lower in the Gairn than the Dee and Mharcaidh as a result of its generally lower topography shown in Figure 1.9).

The majority of the peak flows during the 1987 melt season shown in Figure 6.7 are well matched, especially when using linear routing, though the rain-on-snow events of days 45

and 60 are again poorly simulated on the non-linear model run thus accounting for the drop in mean  $R^2$  from 0.697 to 0.481. Reference to the optimised snowpack parameters in Table 6.3 show that this is not due to the initial snowpack volume optimised by the model as it is actually lower for the linear model run ( $77\text{km}^2 \times 230\text{mm} = 17.71 \times 10^6 \text{ m}^3$  for the non-linear run). The shortfall at the end of the melt season is due to the non-linear model predicted flows being much higher than those of the linear model run, especially during days 1-5, 10-22, 32-34 and 46-52.

The SE and  $R^2$  values in Table 6.3 again show that the availability of hourly data to calculate the mean daily temperature allows TINDEX to perform better than when using only minimum and maximum data, the mean SE falling from 2.26 to 2.19 and the mean  $R^2$  rising from 0.601 to 0.623 for the 1986 and 1987 model runs.

It is again not clear whether linear or non-linear routing allows the model to perform better. If the six model runs that calculated the degree-days on the minimum and maximum temperatures are compared, three (1979, 1980 and 1987) perform better with linear routing whilst three (1981, 1984 and 1986) perform better using the non-linear method. The mean  $R^2$  for all six model runs is 0.702 for those using linear routing and 0.671 for those using non-linear. If it is also considered that when hourly data are used to determine the mean temperature, the mean  $R^2$  decreases from

0.686 to 0.566 for the 1986 and 1987 model runs, then linear routing may be considered the best method.

However, this does not take account of the importance of individual years or the likely data available in real time. It is not yet possible to predict hourly temperatures for the following 48 hours yet this can be accurately done for minimum and maximum values (S J Harrison, pers comm) suggesting that the minimum and maximum method only should be considered. Also, as 1986 and 1984 were two of the snowiest three winters (the third being 1979) the results from their model runs should perhaps have more importance. This would suggest that non-linear routing may provide the best routing method though, as before with the Mharcaidh and Dee model run, the distinction is not at all clear.

The parameter sets shown in Table 6.3 show similar characteristics to those of the Dee model run shown in Table 6.2. The recession and melt coefficients show a smaller range of optimised values for the non-linear model runs than the linear, the melt coefficients again being in the physically reasonable range and similar to those found for the Mharcaidh and Dee model runs. The snowpack parameters are similar for both routing methods, the only major differences being for 1987 which is represented as a small and deep snowpack for the model runs using linear routing and a larger but thinner snowpack for the non-linear model run. As no field data are available for the

Gairn it is not possible to say which of these is the most realistic, though the snow-surveys in the Mharcaidh do suggest that the large but shallow representation of the non-linear routing model run may be closer to reality.

One final point to be made regarding the values of ALB, the gradually increasing melt factor coefficient. Whilst the values are generally consistent when the two different routing methods are compared, the only major difference being for the 1987 non-linear model run, there are anomalies in the variation of ALB from year to year. The values of ALB are physically reasonable for the 1979, 1984, 1986 and 1987 model runs, being high for 1979 when the model starts with high flows and low for 1984, 1986 and 1987 when there are periods of low flow prior to the onset of melt. However, the optimised values of ALB are low for the 1980 and 1981 model runs (0.01 for both routing methods) when the highest flows are observed on day 1. This might be because the model is still having to route the high volume of water already present in the store, be it linear or non-linear, through the transformation submodel when there is little actual melt taking place (this accounting for the very steep initial recession limits visible at the start of both the observed time series plots). Whilst this can explain the reason for the model optimising such a low value of  $k$  it also suggests that  $k$  may have little relationship with reality and is merely a 'fudge factor' that the model needs to be able to

optimise; this possibility is also supported by earlier findings in 4.6.2 that there is a decrease in performance of TINDEX if  $k$  is optimised on cumulative degree-days rather than day number.

### 6.2.3 Running TINDEX on the Feshie datasets

TINDEX was also run on datasets covering the 1979, 1980 and 1981 melt season for the Feshie catchment. Flow data was collected at Glenfeshie Lodge (360m amsl) by R I Ferguson and the meteorological data was the same as that used for the Gairn model runs, Lagganlia being just over 10km from the gauging point.

As the Feshie has a higher mean elevation than the Gairn (resulting in snowmelt having a larger influence on the river regime) and is closer to the meteorological station it was initially expected that the model would perform better than it did on the Gairn datasets.

Table 6.4 shows the results from applying TINDEX to the three years' data and Figures 6.8 - 6.10 show the time series plots for the model runs.

Figure 6.8 shows that irrespective of the routing method used TINDEX is able to operate well on the 1979 data matching all of the observed peaks well. This was to be expected as this was the original melt season that Ferguson

Year	Routing	E	R	A	M	W	ALB	SE	R <sup>2</sup>	FA
1979	L	0.006	0.32	100	3.1	440	0.27	2.39	0.833	22
1980	L	0.006	0.66	76	2.6	320	0.44	1.36	0.683	8
1981	L	0.006	0.23	104	5.6	110	0.01	2.67	0.683	0
1979	NL	0.007	0.21	106	2.6	370	0.14	2.90	0.754	27
1980	NL	0.006	0.21	84	2.0	260	0.17	1.31	0.709	10
1981	NL	0.006	0.43	105	6.6	100	0.01	2.23	0.765	0

Table 6.4 Results from applying TINDEK to the Feshie datasets.

L = Linear routing; NL = Non-linear routing; E = Environmental lapse rate ( $^{\circ}\text{Cm}^{-1}$ )  
R = Recession coefficient; A = Initial SCA ( $\text{km}^2$ ); M = Melt coefficient ( $\text{mm}^{\circ}\text{C day}^{-1}$ );  
W = Initial SWE (mm); ALB = Gradually increasing melt factor coefficient.

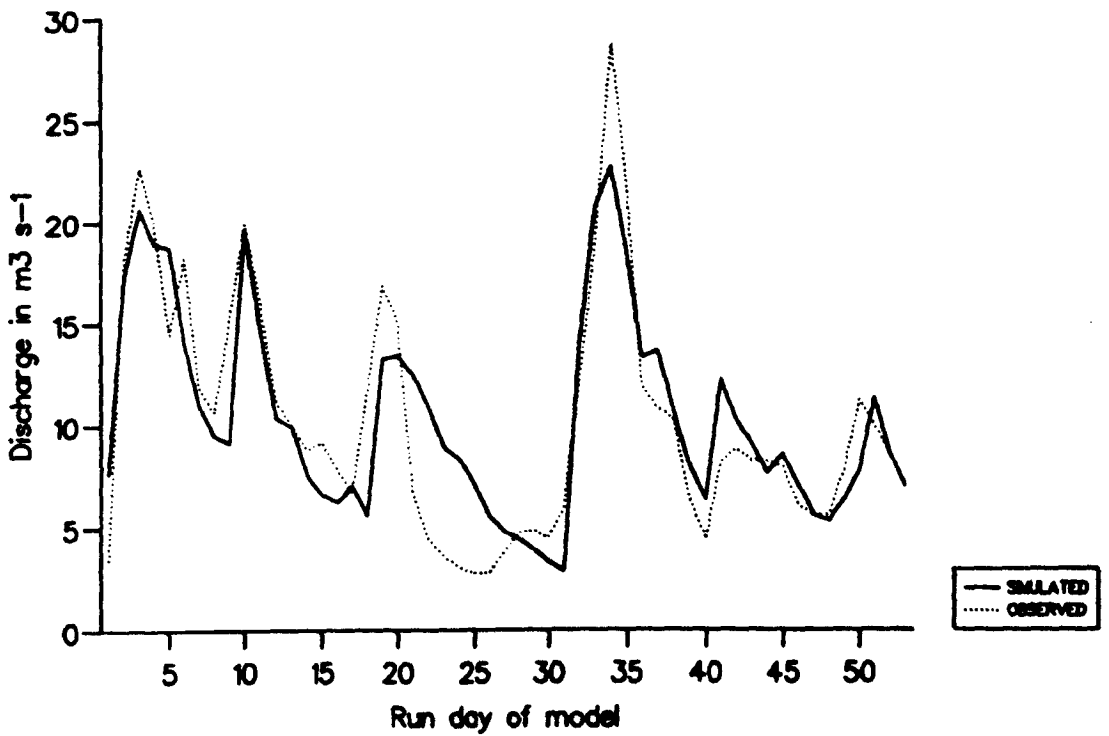
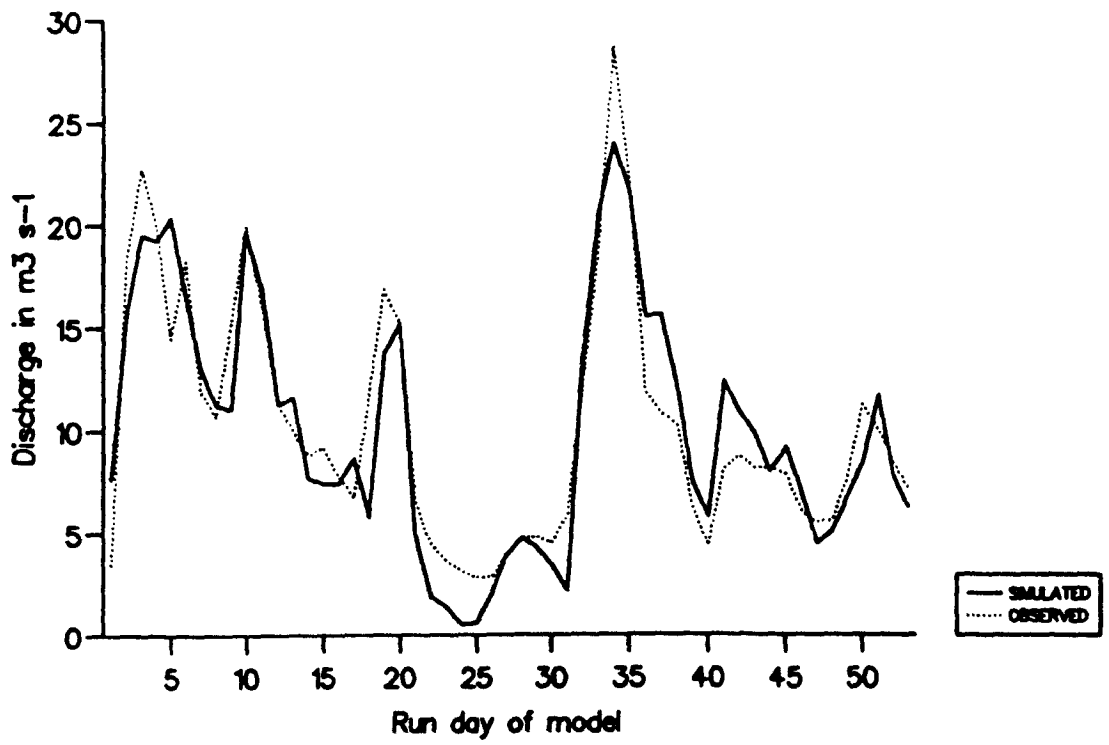


Figure 6.8 Time series plots from running TINDEK on the Feshie 1979 data with linear (upper) and non-linear (lower) routing.

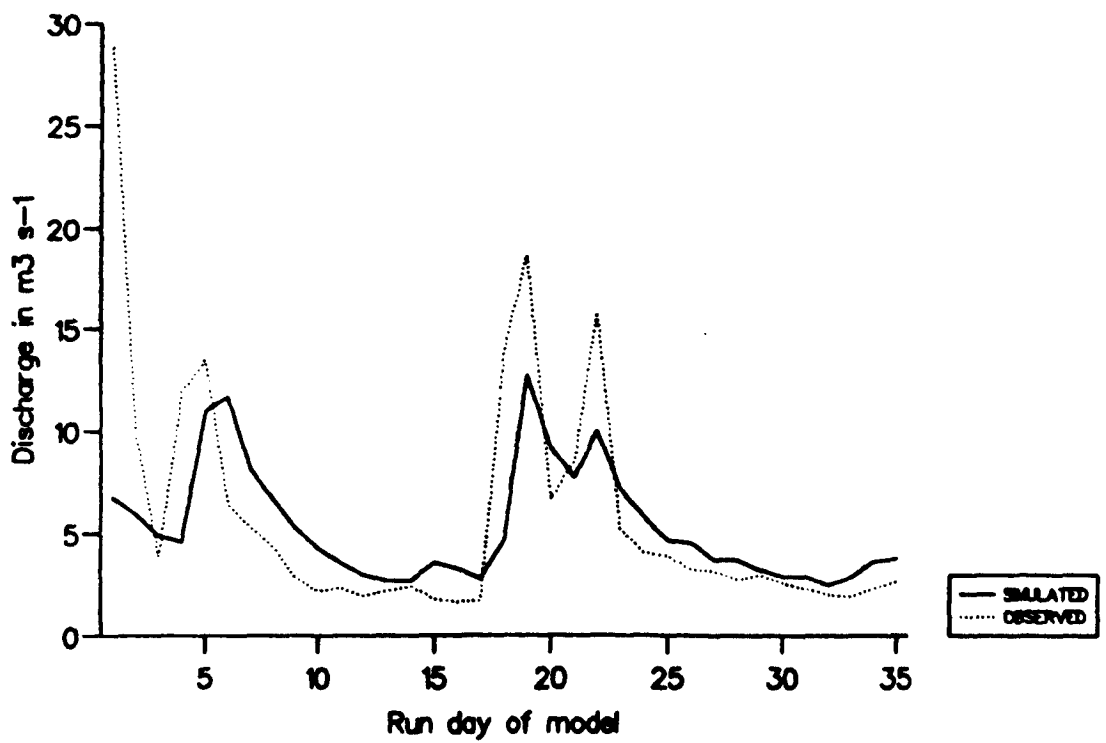
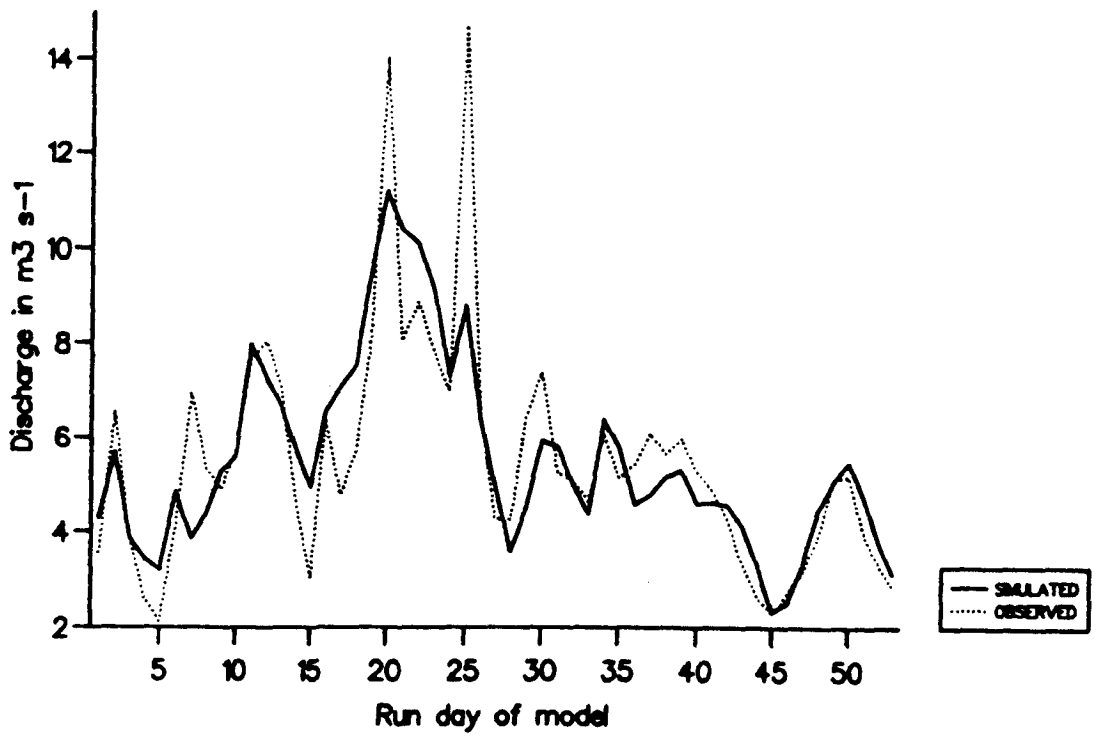


Figure 6.9 Time series plots from running TINDEK on the Feshie 1980 data with linear routing (lower) and on the 1981 complete data set with non-linear routing.

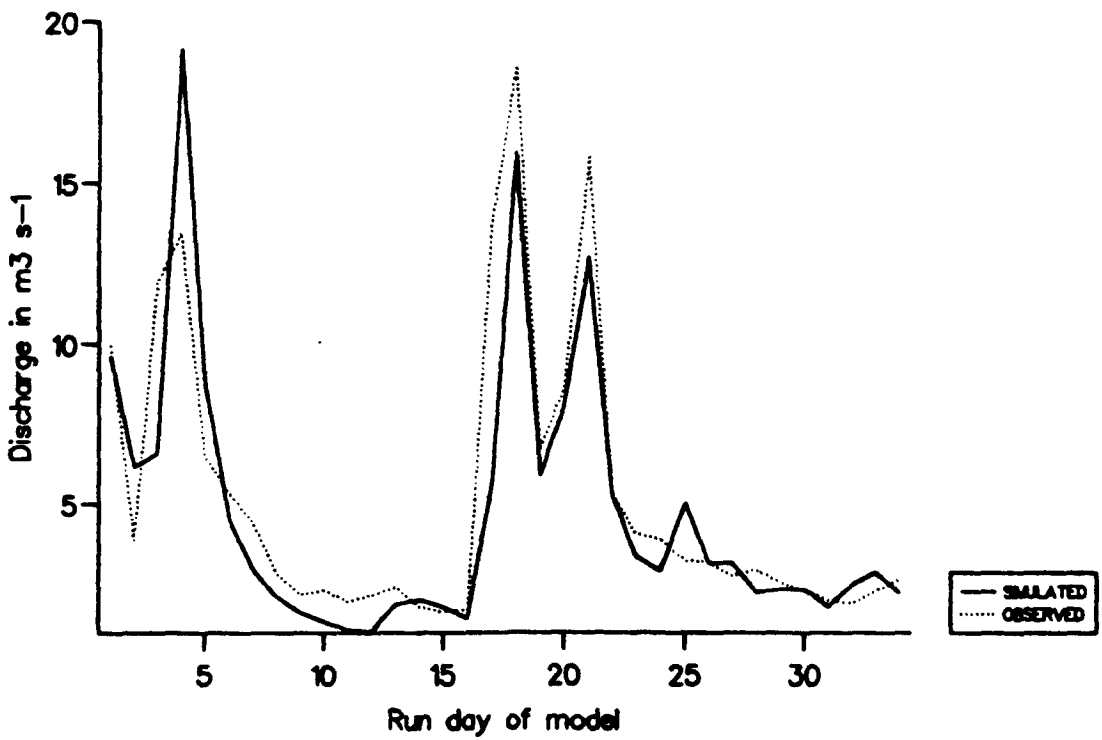
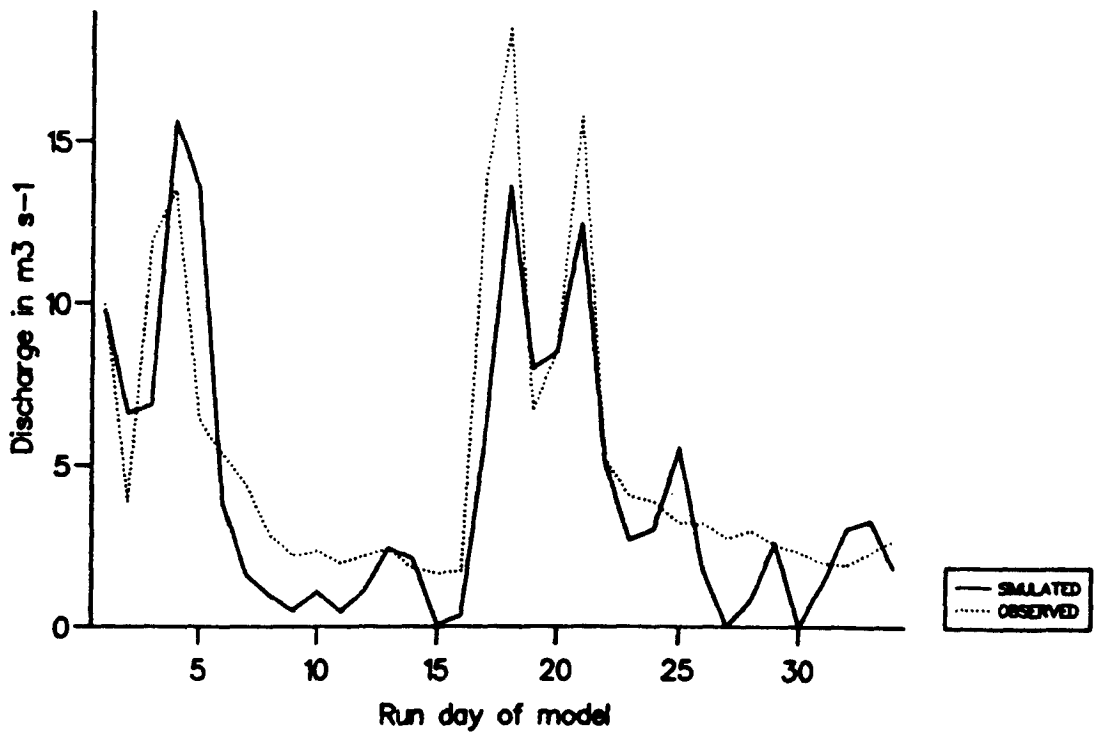


Figure 6.10 Time series plots from running TINDEK on the Feshie 1981 data with the first day's values missing using linear (upper) and non-linear (lower) routing.

(1984) ran his model on, producing a  $R^2$  value of 0.88. The major difference between the two plots is between days 20 - 28 when the non-linear model run over-predicts the flow, accounting for the higher SE and lower  $R^2$  values.

The 1980 model runs shown in Figure 6.9 also matches the observed flow record well, the main exceptions being on days 20 and 24.

The 1981 plot shown in Figure 6.9 is very similar to that of the Gairn in Figure 6.4 and shows the model poorly matching three minor snowmelt peaks, the dataset starting with a rapidly receding observed flow following a previous high melt event. It was thus decided to re-run TINDEK on the 1989 dataset with the first day's data removed. This reduced  $Q_0$  from almost  $20\text{m}^3 \text{ s}^{-1}$  to  $10\text{m}^3 \text{ s}^{-1}$ . The time series plots shown in Figure 6.10 show that by removing these data the model is able to perform much better, especially when non-linear routing is used. Whilst the first peak on day 4 is over-predicted the later peaks on days 18 and 21 are well matched, along with the intermediate low events. The linear routing method is less able to match these two later peaks and the low flows though it does come close to the first peak on day 4.

The first comment to be made about the results shown in Table 6.4 is that for the 1979 model run TINDEK is less able to simulate the observed Feshie flow than the original

model described by Ferguson (1984), the  $R^2$  value being 0.833 compared to 0.880. However, the 1980  $R^2$  value has slightly increased on the linear routing model run compared to that of Ferguson, increasing from 0.680 to 0.683. This is improved even further when non-linear routing is used, the  $R^2$  value being 0.709. There is also an improvement in the  $R^2$  value for the 1981 model run when non-linear routing is used, the  $R^2$  rising from 0.683 to 0.765. If the mean  $R^2$  of all model runs is calculated for each routing method it suggests that the addition of non-linear routing is slightly beneficial, the value increasing from 0.734 to 0.743. However, as the 1979  $R^2$  value decreases, and this should perhaps be considered the most important year as it was the snowiest, then it can also be argued that the addition of non-linear routing is detrimental to TINDEK. It can thus be said that the Feshie results are the opposite of those for the Dee and Mharcaidh model runs which showed non-linear routing being the best method for snowy years whilst linear is the best for years with a low initial snowpack and volume.

The results are, however, consistent with those from the Gairn 1979, 1980 and 1981 model runs; the addition of non-linear routing decreases the  $R^2$  for the 1979 model run, increases it for the 1981 and has little effect on the 1980 data. This is reassuring, as is the fact that the mean  $R^2$  of the Feshie 1979 and 1980 model run is higher than that for the corresponding Gairn model run (0.746 compared to

0.686). The 1981 results are not comparable as the Gairn model run included the extra day's data.

The range of recession coefficients for each routing method in Table 6.4 are comparatively similar, the maximum value being approximately twice that of the minimum. There is, however, no consistency in the year to year variation; the maximum linear routing coefficient being in the 1980 parameter set and the maximum non-linear value being for 1981. There is more consistency in the snowpack parameters and gradually increasing melt factor coefficients. The 1979 model runs optimise a large and deep snowpack, the 1980 pack is also deep but smaller in areal extent, and 1981 has a large but shallow snowpack. The non-linear model runs all optimise a snowpack that has a smaller volume than when optimised by the linear routing method.

Catchment	Routing	1979	1980	1981
Feshie	Linear	44.00	24.32	11.44
Feshie	Non-linear	39.22	21.84	10.50
Gairn	Linear	28.50	16.50	8.54
% of Feshie value		64.8%	67.8%	74.6%
Gairn	Non-linear	27.00	13.50	6.50
% of Feshie value		68.8%	61.8%	61.9%

Table 6.5 The optimised snowpack volumes for both the Feshie and Gairn model runs ( $*10^6\text{m}^3$ )

These data show that the Gairn model runs also optimise a lower initial snowpack volume when non-linear routing is

used. In addition to this common characteristic between catchments it can also be seen that the Gairn always has a lower optimised snowpack than the Feshie and that the relative reduction is similar for all years and routing methods. The mean Gairn snowpack volume is 66.6% that of the Feshie, all values falling within 8% of this. This is a most useful property of the TINDEX model runs and it was decided to investigate this further. Table 6.6 shows the optimised initial snowpack volumes for the Dee and Gairn model runs using both routing methods. It can be seen that with one exception (Gairn, 1987) the non-linear model runs again optimised a snowpack volume lower than that of the linear routing model run. It can also be seen that for the two snowy winters (1984 and 1986) the Gairn snowpacks are all a similar fraction of the corresponding Dee snowpack volume, the mean being 27.65% and all four values being within 1.55% of this. The 1987 Gairn snowpacks are a larger fraction which can be accounted for by remembering that snowfall was lower that year and is thus likely to have been more variable.

These results indicate that whilst the relative initial SCA and SWE values may vary from catchment to catchment TINDEX optimises consistent relative initial snowpack volumes. It may thus be possible to apply the results from snow surveys in one catchment to others nearby, thus reducing the time spent on collecting field data.

Catchment	Routing	1984	1986	1987
Dee	Linear	79.52	119.70	44.64
	Non-linear	70.20	118.02	35.55
Gairn	Linear	23.20	33.50	17.71
	% of Dee	29.2%	27.8%	39.7%
% of Dee	Non-linear	18.76	31.74	20.80
	% of Dee	26.7%	26.9%	58.5%

Table 6.6 Optimised initial snowpack volumes for the Dee and Gairn 1984, 1986 and 1987 TINDEK model runs. Values are  $\times 10^6 \text{ m}^3$ .

#### 6.2.4 Summary of TINDEK results

It has been shown that TINDEK is able to simulate the observed snowmelt runoff from three catchments over several melt seasons using data collected at a number of meteorological stations. The model performs particularly well when the initial snowpack volume is high, the meteorological data are collected within or close to the catchment and the melt season does not contain many precipitation events.

More specifically several points can be made about the performance of TINDEK from the results shown in 6.2.1 - 6.2.3:

- (1) For the snowy winters of 1981, 1984 and 1986 the addition of non-linear routing allows TINDEK to perform better than when linear routing is used. The

exception to this is the model runs for the 1979 melt season when linear routing is the better performer.

- (2) Generally, the use of non-linear routing results in a smaller range of the optimised recession and melt coefficients. This is useful if a general model is to be used, allowing these parameters to be set as constants.)
- (3) TINDEX simulates the timing of the peak snowmelt flows well, suggesting that the conceptual basis of the model is sound, though it does tend to slightly under-predict the main peak flows. This is especially so for all the 1986 melt season model runs.
- (4) Whilst the snowmelt peak flows are well matched the same cannot be said for the rain or rain-on-snow peak flows which are usually under-predicted and sometimes not simulated at all.
- (5) TINDEX is able to operate well using meteorological data collected at a site within or very close to the catchment. As the distance from meteorological station to catchment increases the performance of TINDEX decreases, presumably due to the errors associated with applying the precipitation data.
- (6) Whilst TINDEX is able to perform well calculating the degree-days from the minimum and maximum daily temperatures, its performance is increased when 24-hourly data are available to calculate the true mean daily temperature.
- (7) TINDEX does not perform well when  $Q_0$  is high. It is

unable to match the early high flows and, in trying to do so, performs poorly over the rest of the melt season. This problem might be overcome by starting the melt season earlier with a lower  $Q_0$  but due to missing data it was not possible to test this.

- (8) Whilst the optimised snowpack parameters show variation from catchment to catchment there is consistency in the relative snowpack volume, whichever routing method is used. This suggests that the depletion submodel and snowpack representation are both conceptually sound though minor changes may be necessary.

These points suggest that TINDEX has potential for use in real time and will be able to produce acceptable results in a general form, only needing to optimise the snowpack and gradually increasing melt factor parameters. At present it can only be said that non-linear routing will tend to perform better for snowy winters though linear routing shows superior performance under other conditions.

### 6.3 MART

MART was also optimised on data covering several melt seasons for the Dee, Gairn and Feshie catchments. Following the results of Chapter 5, snowpack structure 4 and non-linear routing were used for all model runs. The environmental lapse rate was also set to  $0.008^{\circ}\text{Cm}^{-1}$  for all

model runs.

### 6.3.1 Running MART on the Dee datasets

Table 6.7 contains the optimised parameter sets and results from running MART on the 1984, 1986 and 1987 Dee datasets. Figure 6.11 shows time series plots of the model runs. Following the results in 6.2 MART was run on the 1986 and 1987 data using both methods of determining the degree-days (i.e. mean hourly temperatures and mean of the minimum and maximum values).

From Figure 6.11 it can be seen that MART is able to simulate the 1984 snowmelt events well, the two main peaks being very closely matched (better than those of TINDEXT in Figure 6.1). It over-predicts the peak flow following the main snowmelt events, as does TINDEXT, but more importantly also under-predicts the first peak on day 10 and the low flows from day 26 onwards more than TINDEXT, this accounting for the lower  $R^2$  value than the TINDEXT non-linear routing model run (0.836 compared to 0.875). It does, however, perform better than the TINDEXT linear routing model run and it must be remembered that MART does not optimise the lapse rate value.

The 1986 plot shown in Figure 6.11 appears similar to that of TINDEXT in Figure 6.2, the main peaks being under-predicted but the low flows matched well. Close study

Year	ATEM	R	A	M	W	ALB	SE	R <sup>2</sup>	FA	Tindex NL R <sup>2</sup>	Tindex L R <sup>2</sup>
1984	1	0.00072	289	4.1	240	10.00	6.5	0.836	4	0.875	0.822
1986	1	0.00063	275	4.5	390	0.20	10.3	0.621	51	0.634	0.575
1987	1	0.00064	289	4.4	130	0.02	5.0	0.749	28	0.458	0.654
1986	2	0.00068	253	4.5	410	0.25	9.3	0.690	70	0.677	0.649
1987	2	0.00063	243	3.6	130	10.00	5.2	0.742	49	0.448	0.668

**Table 6.7 Results from applying MART to the Dee datasets. All model runs used non-linear routing and**

**had the Environmental lapse rate set to 0.008°C m<sup>-1</sup>. ATEM(1) = Mean of minimum and maximum;**

**ATEM(2) = Daily mean of 24 hourly temperature values; R = Recession coefficient;**

**A = Initial SCA (km<sup>2</sup>); M = Melt coefficient (mm°C day<sup>-1</sup>); W = Initial SWE (mm);**

**ALB = Gradually increasing melt factor coefficient.**

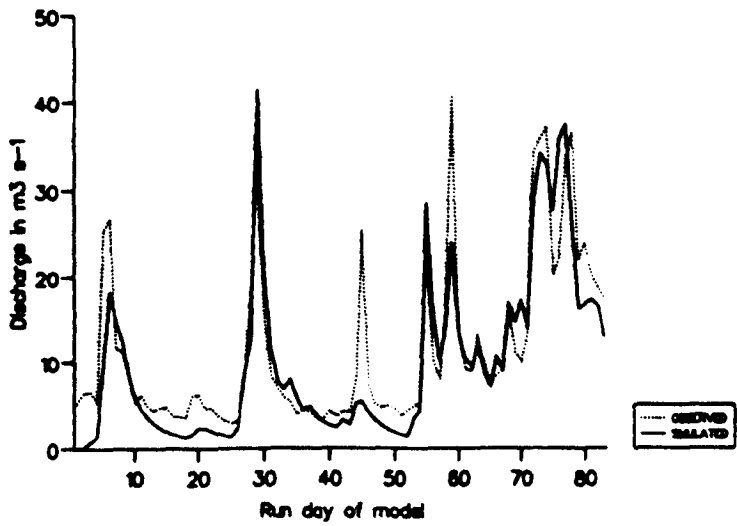
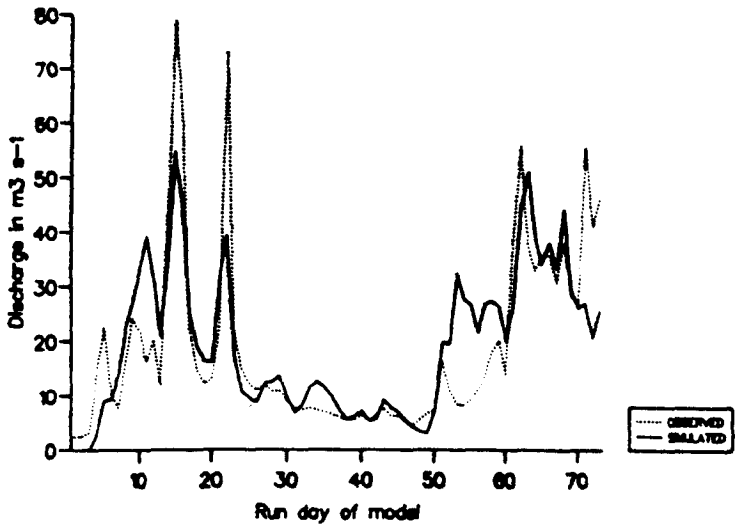
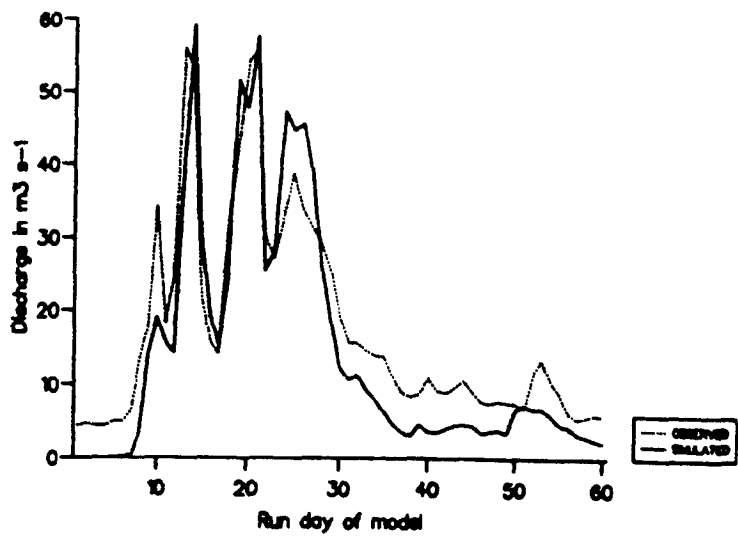


Figure 6.11 Time series plots from running MART on the Dee 1984 (upper), 1986 (middle) and 1987 (lower) data, all with non-linear routing.

reveals that MART matches the two peaks on days 17 and 22 better than TINDEX (it is more than  $5\text{m}^3 \text{ s}^{-1}$  closer) and also matches the first of the final melt event peaks better. Its lower  $R^2$  value (0.621 compared to 0.634) is explained by over-predicting more than TINDEX on days 9-13 and being less stable during the low flow period running between days 25 and 50. The increase in flow variability during this period can be attributed to the layered structure allowing small melt events to occur when the mean temperature is close to  $0^\circ\text{C}$  in the lower elevation zones.

The 1987 plot in Figure 6.11 shows the greatest improvement over the TINDEX plots. With the exception of the peak on day 45 that, it is thought is a rain-on-snow event, all other peaks are better matched than by TINDEX, the greatest improvement being for days 55 and 59 and the final melt between days 73 and 79. In addition to matching the peak flows well MART is also able to return to low flow condition in a much shorter space of time, this being the major factor that causes the dramatic increase in  $R^2$  from 0.456 to 0.749.

The data shown in Table 6.7 suggests that, like TINDEX, MART has potential for use in real time as a general model; the range of recession coefficients is small (0.00063 to 0.00072), as is that of the melt coefficients (4.1 to 4.5 for the minimum and maximum model runs, 3.6 to 4.5 for all model runs). The SE and  $R^2$  results show an increase in

performance for the 1986 model run when 24-hourly temperatures are present and a slight decrease for the 1987 data; overall there is an increase in the  $R^2$  value from 0.685 to 0.716.

Comparing the MART results to those of TINDEX it can be seen that all MART model runs are better than the TINDEX model runs using linear routing. The distinction is less clear for the TINDEX model runs using non-linear routing. Whilst the mean MART  $R^2$  is higher (0.735 compared to 0.656) this is only due to the 1987 value. It could be argued that the increase is not due to MART but arises from TINDEX performing badly in this case. If the mean of the TINDEX 1984 and 1986 non-linear and 1987 linear routing model run is calculated it is much closer to that of the MART model run (0.721 compared to 0.735).

Concluding, the MART model runs using the Dee datasets all perform well visually, the peak flows being closer matched than when using TINDEX. The optimised recession and melt coefficient ranges are small suggesting that it has potential for use in real time as a universal model. Like TINDEX the model is able to perform better if hourly data are used to calculate the degree-days, though the improvement is not consistent for all years. Finally, MART is much better than TINDEX at simulating the observed flow, this improvement being the most noticeable benefit of the layered model.

### 6.3.2 Running MART on the Gairn datasets

The results from running MART on the 1979, 1980, 1981, 1984, 1986 and 1987 datasets are shown in Table 6.8 and Figures 6.12 and 6.13. As with the Dee the 1986 and 1987 model runs were optimised for both methods of calculating the degree-days.

The time series plots for 1979, 1980 and 1981 all show that whilst MART is better than TINDEX at simulating the early high flows (though it does struggle on days 1-4 of the 1980 model run) there is little or no simulation of the melt events later in the season. Whilst TINDEX was also generally poor at simulating these events (days 3-35 for 1979, days 20-25 for 1980 and days 18-23 for 1981) it did at least simulate a rise in mean daily runoff. MART fails even to do this for the 1979 and 1980 model runs, though a minor increase is present for the 1981 model run. Although it has been argued earlier in the project that the representation of the major peaks is most important, the model is also expected to simulate the minor melt events to some degree and MART fails to do this.

Reference to this initial snowpack parameters in Table 6.8 shows that for all three years MART optimises a large but shallow snowpack in order to match the high initial flows. This reveals a possible flaw in the representation of the snowpack in MART. Structure 4, the structure chosen to use

Year	ATEM	R	A	M	W	ALB	SE	R <sup>2</sup>	FA	Tindex NL R <sup>2</sup>	Tindex L R <sup>2</sup>
1979	1	0.00030	150	10.0	140	10.000	4.46	0.368	0.0	0.511	0.599
1980	1	0.00026	150	10.0	120	10.000	1.72	0.488	0.0	0.808	0.825
1981	1	0.00085	150	10.0	50	10.000	2.56	0.685	0.0	0.710	0.699
1984	1	0.00110	107	5.9	140	10.000	2.40	0.845	0.0	0.900	0.786
1986	1	0.00100	69	7.8	180	0.150	2.37	0.709	2.0	0.639	0.620
1987	1	0.00510	150	7.5	80	0.010	1.57	0.671	0.0	0.460	0.685
1986	2	0.00082	53	10.0	180	10.000	2.43	0.692	1.7	0.630	0.663
1987	2	0.00062	109	9.9	70	0.015	1.64	0.681	6.5	0.502	0.708

Table 6.8 Results from applying MART to the Gairn datasets.

All model runs used non-linear routing and had the Environmental lapse rate set to 0.008°C m<sup>-1</sup>.

ATEM(1) = Mean of minimum and maximum; ATEM(2) = Daily mean of 24 hourly temperature values;

R = Recession coefficient; A = Initial SCA (km<sup>2</sup>); M = Melt coefficient (mm°C day<sup>-1</sup>); W = Initial

SWE (mm); ALB = Gradually increasing melt factor coefficient.

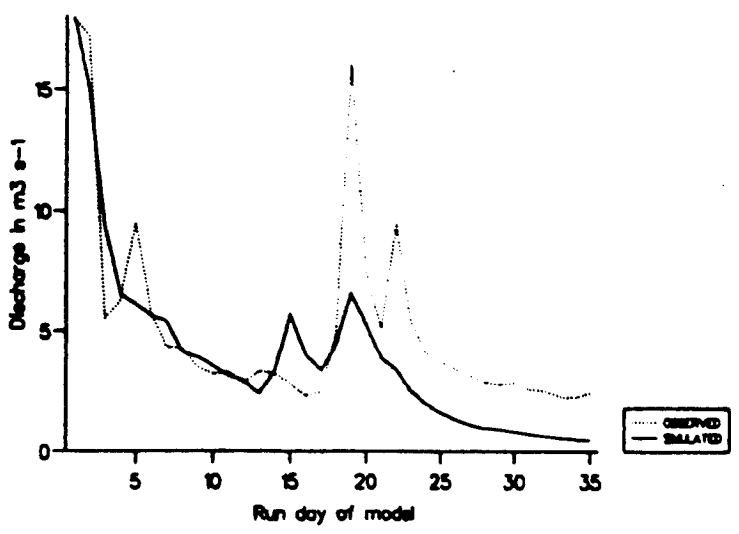
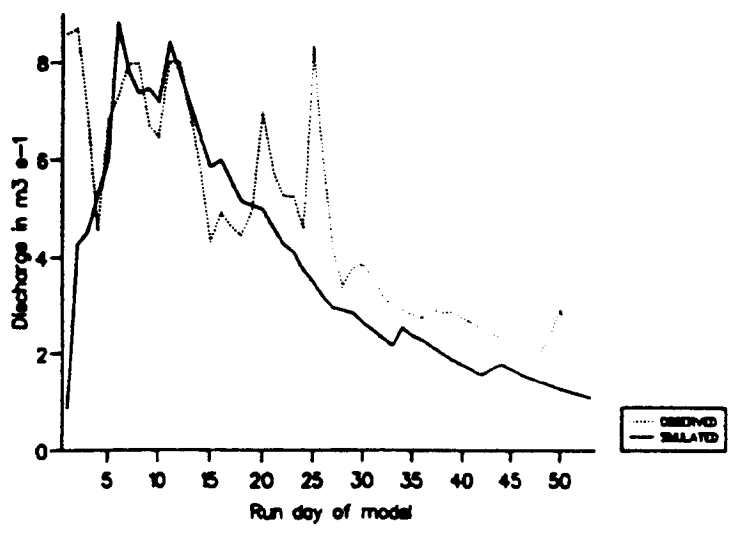
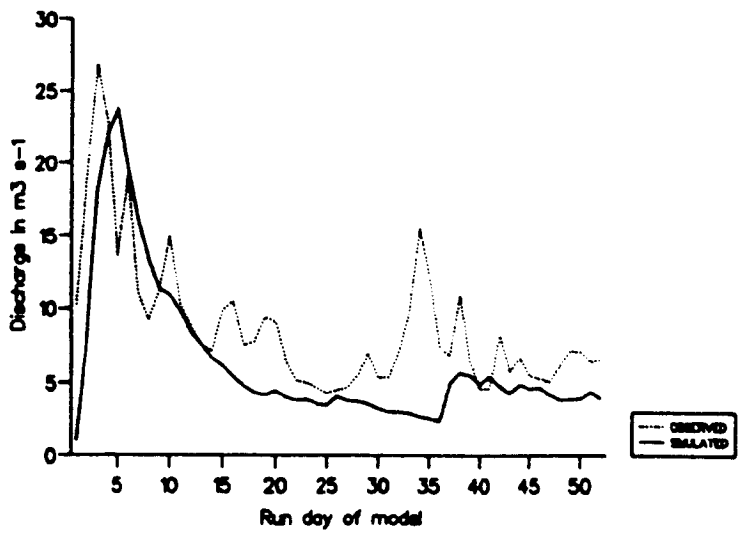


Figure 6.12 Time series plots from running MART on the Gairn 1979 (upper), 1980 (middle) and 1981 (lower) data, all with non-linear routing.

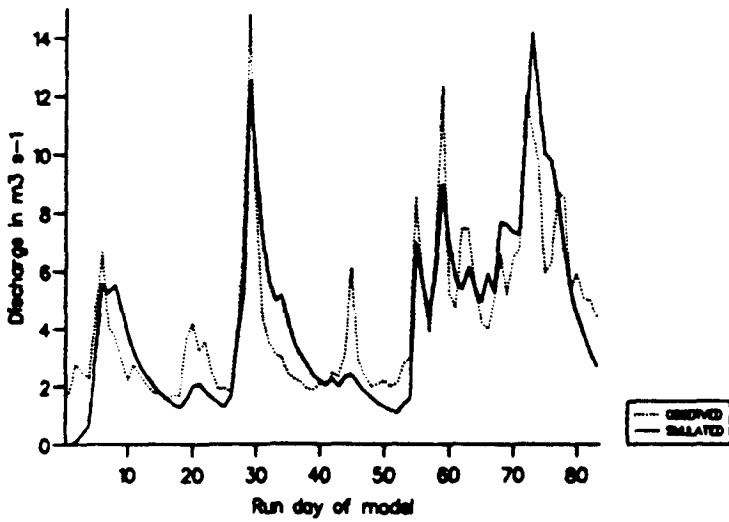
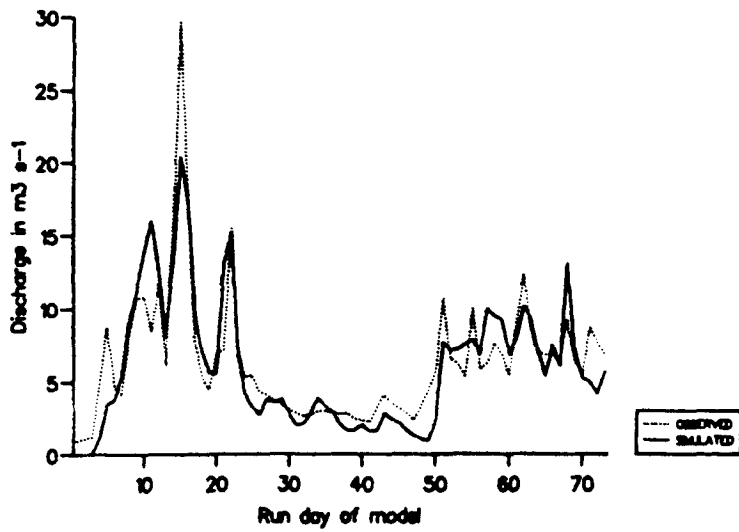
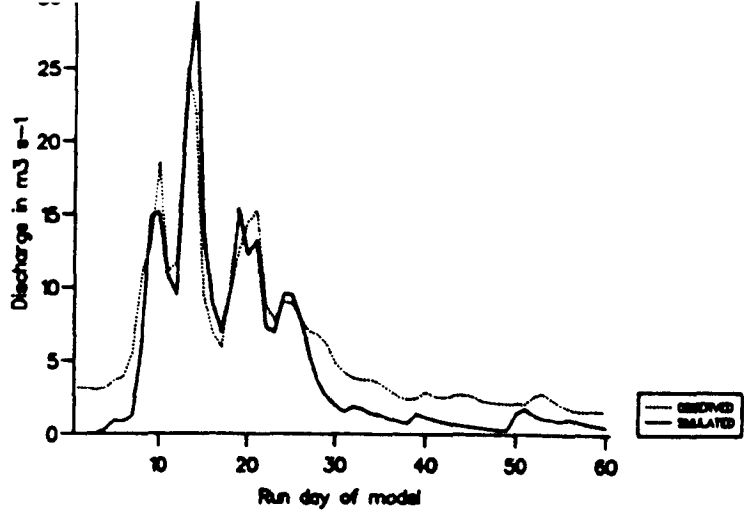


Figure 6.13 Time series plots from running MART on the Gairn 1984 (upper), 1986 (middle) and 1987 (lower) data, all with non-linear routing.

when applying MART to other datasets, assumed a low initial variation in snowpack volume between the three zones (zone 1 = 3 units, zone 2 = 4 units, zone 3 = 4 units). Given the flow patterns present in the 1979-1981 datasets it is likely that towards the end of the melt season the snowpack is small in areal extent, thus limiting the ability of MART to simulate later melt events.

Had the initial snowpack volume ratio been different, possibly 1:2:2 or 1:2:3 instead of 3:4:4, then MART may have been able to match the initial runoff and still have a reasonable snow covered area later in the melt season to allow it to simulate later melt events. This difference in the ratio of snow held in each zone is likely to be a function of the different hypsometric curves of each catchment and can only be confirmed by carrying out snow surveys similar to those in the Mharcaidh but for other catchments. The results from these surveys would then allow the snowpack structure to be modelled more accurately for each catchment.

The 1984, 1986 and 1987 plots shown in Figure 6.13 are similar to those of the Dee and show similar visual improvements over the corresponding TINDEK plots in Figures 6.5 - 6.7. The peak flows are all well matched, especially those of 1984 and 1987, and like the Dee MART model run the main peak of 1986 is better simulated by more than  $5\text{m}^3 \text{s}^{-1}$ , though it still significantly underestimates the observed

value. The 1984 plot shows a tendency to simulate the low flows lower than the observed, and all three plots show that MART has difficulty in making the observed flow over the first 4-6 days, this also being a characteristic of the 1979 and 1980 model runs.

From the results shown in Table 6.8 it can be seen that the ranges of recession and melt coefficients are larger than those observed for both the Dee model run (even if it is taken into account that there are more model runs and the ranges are thus likely to be larger) and the corresponding TINDEK parameter sets shown in Table 6.3. Whilst these large variations may be attributed to the model trying to compensate for weakness in the snowpack representation they do show that, in its present form, MART is not likely to be successfully applied to the Gairn catchment in real time as a universal model.

Comparing the  $R^2$  values of the MART and TINDEK model runs shown in Table 6.8 it can be seen that when the results are taken as a whole MART is less able to simulate the observed Gairn runoff than TINDEK. However, it can also be seen that for the 1986 and 1987 model run MART performs better than the corresponding TINDEK run, suggesting that, in addition to the snowpack structure varying from catchment to catchment, it may be necessary to alter it from year to year as a result of field observations. This is supported by the fact that the 1984 and 1981 model runs which, by

optimising the initial SCA less than the catchment areas are able to perform similarly to TINDEX.

Finally, if the results for the two different methods used to calculate the degree-days are compared it can be seen that there is little difference in the  $R^2$  values, the 1986 value decreasing whilst the 1987 value increases. Whilst this suggests that the model may be able to operate well on limited data for these two years it might also be that limitations in the model do not allow it to be improved by more detailed input data.

### 6.3.3 Running MART on the Feshie datasets

The results from running MART on the Feshie 1979, 1980 and 1981 datasets are shown in Table 6.9 and Figures 6.14 and 6.15 show the corresponding time series plots.

The 1979 plot in Figure 6.14 shows a very good similarity between the simulated and observed flows, the only major difference being over-prediction by MART on days 6 and 37. The 1980 plot, also shown in Figure 6.14, shows that once again MART is poor at simulating the flow during the first few days of the model run. With this exception MART is as good as TINDEX at simulating the observed flow, especially on day 20, though like TINDEX, MART is unable to match the peak on day 25.

Year	R	A (km <sup>2</sup> )	M (mm°Cday <sup>-1</sup> )	W (mm)	K	SE	R <sup>2</sup>	FA (km <sup>2</sup> )	TIND NLR <sup>2</sup>	TIND LR <sup>2</sup>
1979	0.0010	106	4.9	390	10.00	3.88	0.567	19.9	0.754	0.833
1980	0.00072	106	3.7	230	10.00	1.87	0.439	11.8	0.709	0.686
1981	0.0014	106	6.0	110	0.08	3.67	0.624	18.7	0.765	0.683

Table 6.2 Results from applying MART to the Feshie 1979, 1980 and 1981 datasets. The final two columns give the corresponding TINDEX results using both types of routing.

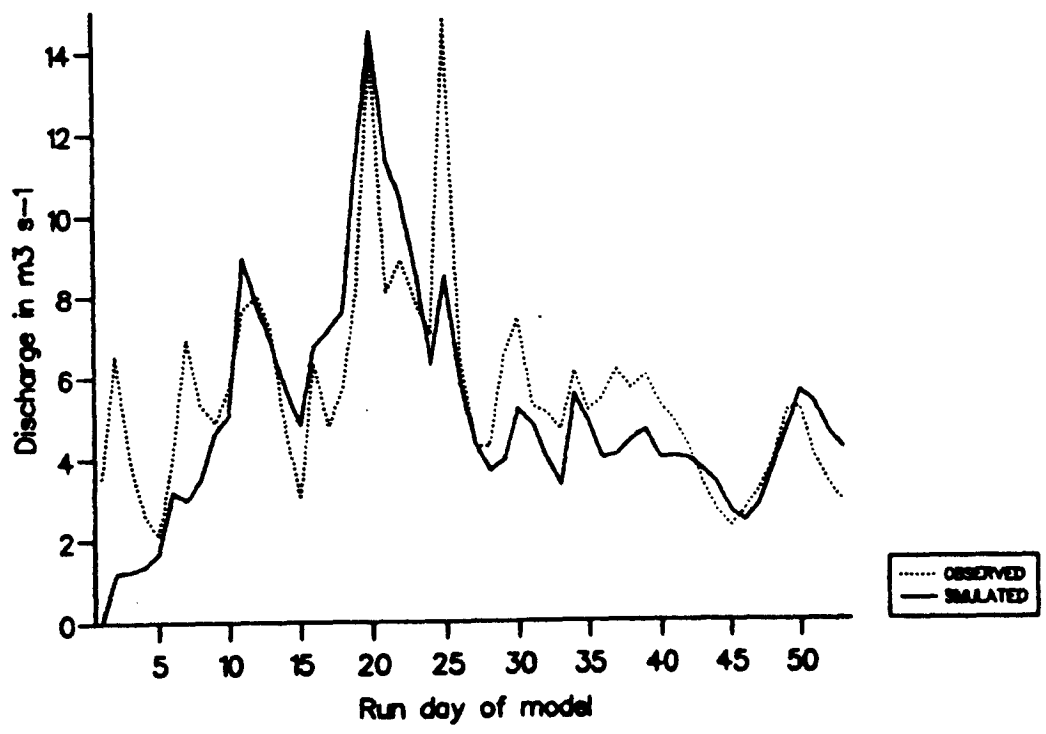
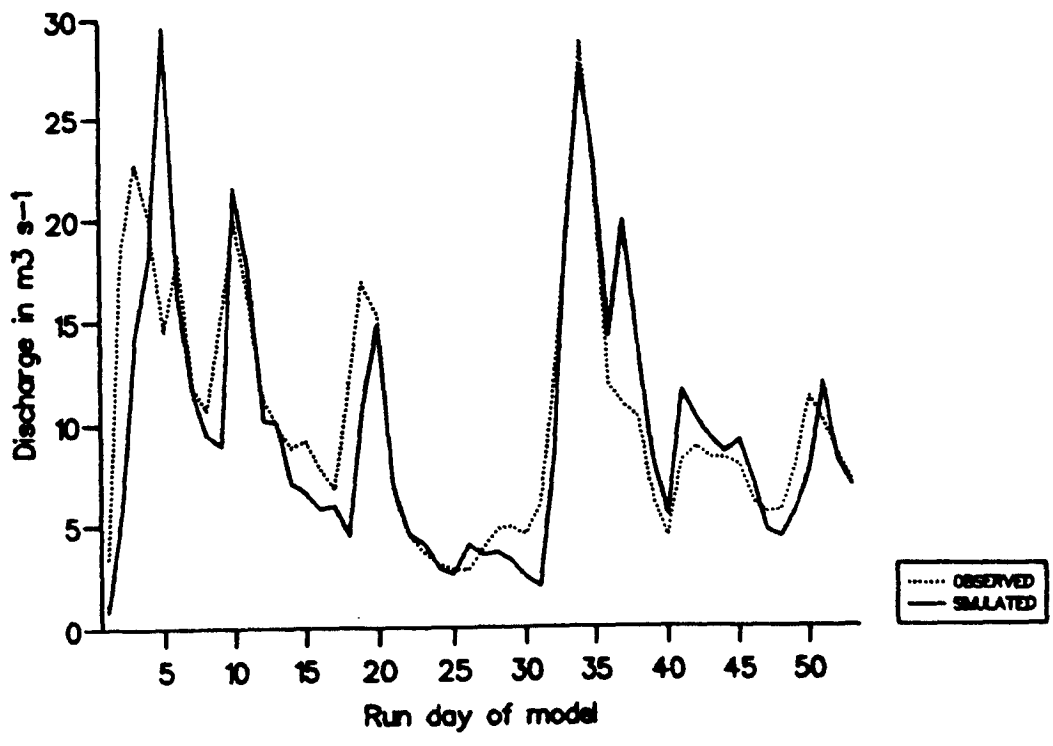


Figure 6.14 Time series plots from running MART on the Feshie 1979 (upper) and 1980 (lower) data, both with non-linear routing.

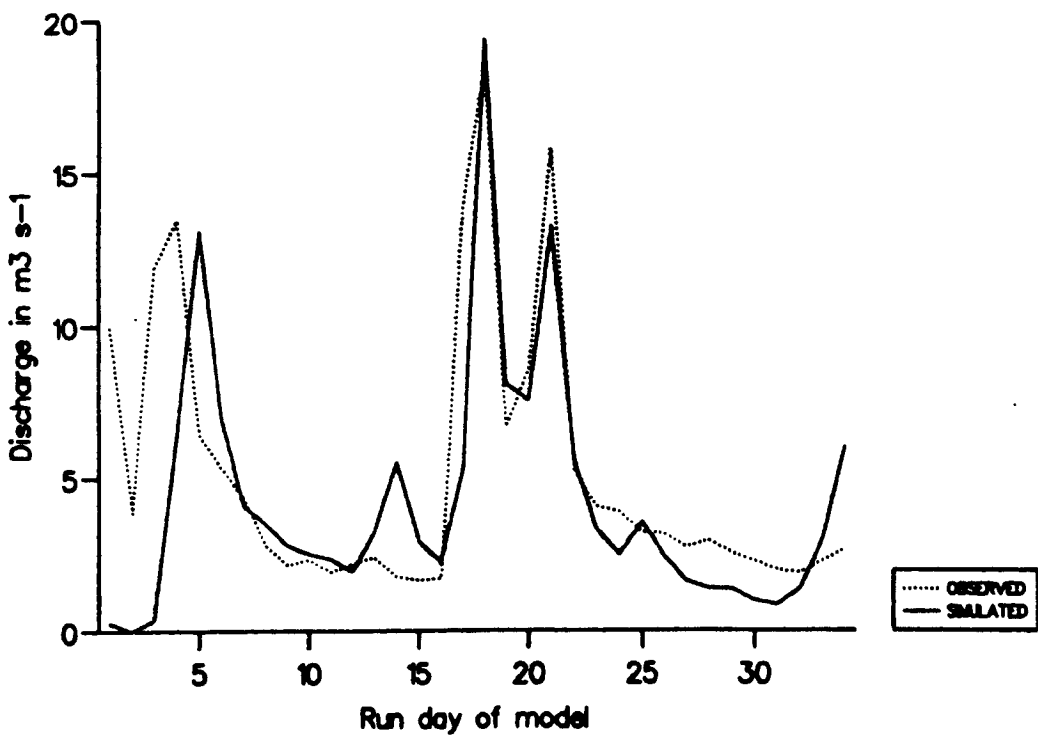
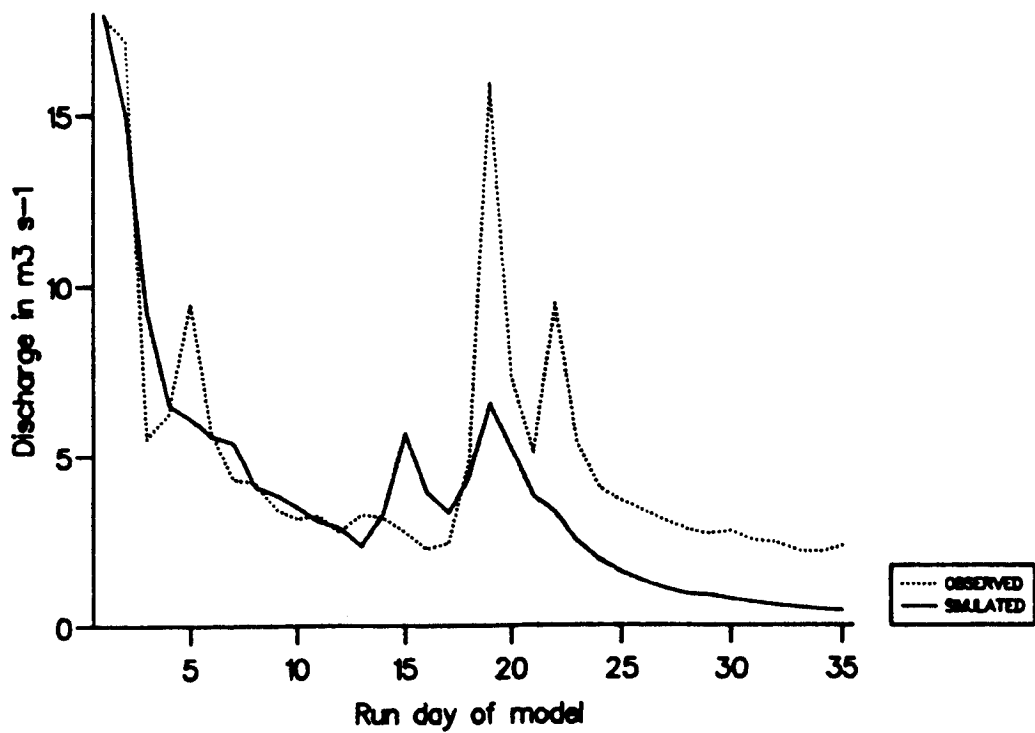


Figure 6.15 Time series plots from running MART on the Feshie 1981 complete dataset (upper) and with the first day's data removed (lower), both with non-linear routing.

From Figure 6.15 it can be seen that when the whole 1981 dataset is used, MART is able to simulate the later melt events much better than TINDEX, though it does struggle once again during the first few days of the model run. Removing the first day's data actually results in MART simulating the observed peak flow on day 22 less well than when the whole dataset was used, though the peak on day 18 is matched better. The most dramatic improvement is in the ability to simulate the peak flows between days 2 and 6. Whilst MART predicts this peak one day later than observed the magnitude is almost exactly the same. As MART has difficulty in attaining high flows during the early stages of the model run this lag in the peak flow is likely to be a result of this not due to a conceptual weakness in the model. This is supported by the fact that for the model run using the extra day's data the timing of the peak is better though the magnitude is less due to problems with the snowpack representation for the Feshie.

From the results shown in Table 6.9 it appears that the snowpack representation derived from the Mharcaidh snow surveys is not the best possible structure for the Feshie, despite the catchment's geographical proximity, as the initial SCA is representative of a snow cover over the whole catchment. This is for reasons similar to the Gairn catchment, even though the hypsometric curve of the Feshie is closer to that of the Mharcaidh, and once again suggests that snow surveys may need to be carried out in the Feshie

to allow successful application of MART. Another alternative, which may be quicker and more cost effective, is to try different snowpack representation in the model using the same methods described in Chapter 5 for the Mharcaidh. Due to time limitations this was not possible for this project but is clearly an area where further investigation may prove beneficial.

The melt and recession coefficients both show a considerable range in values given that only three model runs were carried out. Given the likelihood that the snowpack structure hinders MART these may be due to the model compensating elsewhere. It can also be seen that the MART  $R^2$  values are all less than those of the corresponding TINDEX model runs, again suggesting that further work is needed before MART can be applied to the Feshie in real time as a universal model.

#### 6.3.4 Summary of MART results

It has been shown that, given certain conditions, MART is able to simulate snowmelt events as well as if not better than TINDEX. These conditions are as follows:

- (1) The catchment must have a similar hypsometric curve to the Mharcaidh.
- (2) Meteorological data must have been collected within or close to the catchment.

(3)  $Q_0$  must be low.

(4) A run-in period of at least five days' low flow is needed to permit the transformation submodel to stabilise.

Given these conditions MART is able to simulate the observed peaks better than TINDEX, though low flows in the later part of the melt season do tend to be under-predicted.

Whilst condition (1) above is the most crucial, if any of the four are not met the performance of MART is severely limited. Condition (2) can be met by all catchments used in this project; it was not done so when testing the models partly because the datasets used were readily available but also to test the applicability of the models using data collected at a remote site. Conditions (3) and (4) are likely to be met if the model is used in real time for predictive purposes as the observed flow would be readily available; they were not met in some of the model runs due to data limitations and again to provide a stronger test for the models.

Having shown that it should normally be possible to meet conditions (2), (3) and (4) leaves only condition (1) to be considered. This condition came about as a result of developing MART on the Mharcaidh snow survey data. Had the surveys been carried out in another catchment then the pre-

requisite would be that the model could only be accurately used on catchments with similar hypsometric curves to that catchment, i.e. the performance of MART is specific to different snowpack structures which in turn depend on different hypsometric curves. It could also be argued, with a lesser degree of certainty, that the performance of MART is also related to the snowpack characteristics of individual years as MART performs better on the 1986 and 1987 datasets which were used to develop the snowpack structure. As other authors (Davison, 1987; Green, 1973, 1975; Manley, 1969, 1971; Spink, 1980) have noted the variability of the snowcover from year to year in the Scottish Highlands, the snow survey results in Chapter 3 confirming this, one can say that in order to apply MART successfully to a catchment it would help if snow survey data were available to allow accurate modelling of the snowpack. Whilst this is not a particularly large task for a catchment the size of the Mharcaidh it is for those the size of the Dee and Gairn and reduces the potential of MART as a universal model. As mentioned earlier, an alternative solution is to develop different snowpack structures using computer simulations as in this project. However, even this will require field data both to develop the model further and to allow the appropriate structure to be chosen at the start of the melt season.

#### 6.4 ANDERS

Although ANDERS had performed weakly on the Mharcaidh it was decided to run the model on the Dee and Gairn 1986 data. It was not run on the 1987 data (the only other year that contained windspeed data needed for the model) as it had performed so badly on the Mharcaidh.

Figure 6.16 shows the linear model runs for the Dee and Gairn which have  $R^2$  values of 0.675 and 0.689. Linear routing performed better than non-linear which had corresponding  $R^2$  values on 0.666 and 0.617. These plots and  $R^2$  values compare favourably with those of the TINDEX and MART model runs described in 6.2 and 6.3. The model is especially good at matching the pattern of the flow variation although, like the Mharcaidh model runs, it is unable to match the magnitude of the peak flows.

As ANDERS performs reasonably well on larger catchments it is worth considering how it might be further developed so that it can be used in real time to predict snowmelt runoff. This is not possible at present due to the dependence of the model on windspeed data from a meteorological site. As windspeed is so variable in both space and time, especially in an area such as the Highlands which have such wide ranging topography and relief, it is not possible to predict it in advance (Barry, 1981). Davison (1987) also found this and used the geostrophic

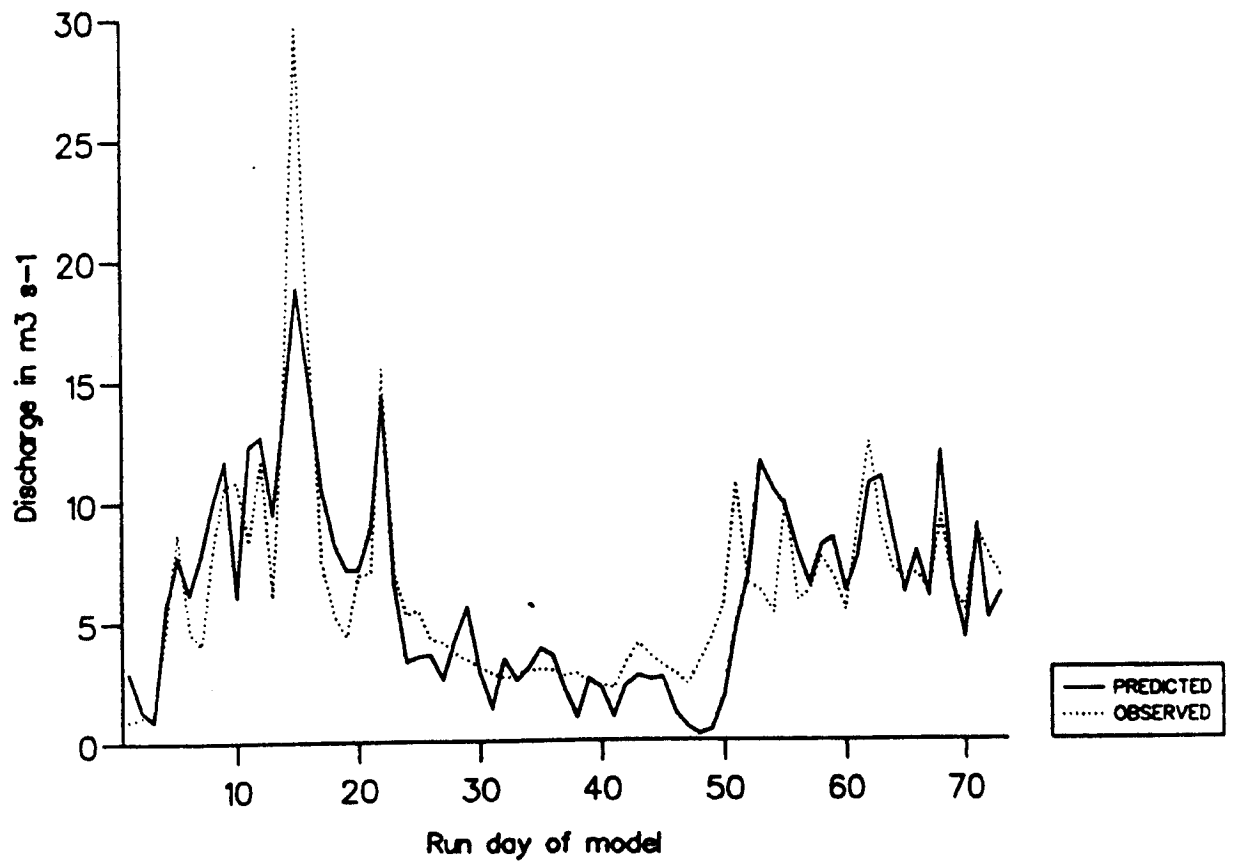
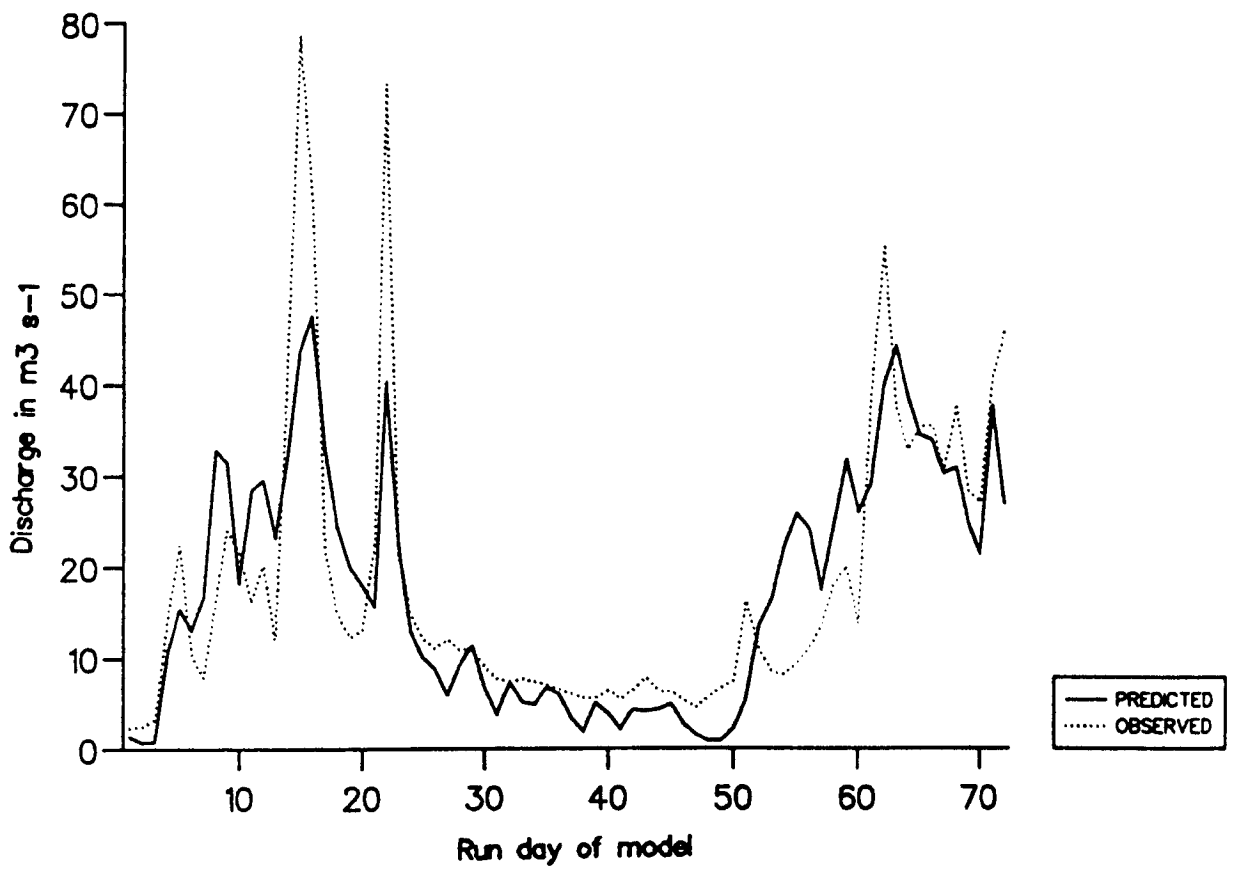


**Figure 6.16** Time series plots from running ANDERS on the Dee (upper) and Gairn (lower) datasets. Both model runs used linear routing and a rainfall threshold of 10mm.

wind to model snowdrift in the Cairngorms. Given that the geostrophic wind may be more representative of the atmospheric conditions than a low level wind that is affected by local influences it can be argued that it should be used instead of the low-level windspeed as an index to the energy balance conditions. As it is also possible to predict the geostrophic wind (Barry and Chorley, 1976) this would allow ANDERS to be used in real time to predict snowmelt runoff.

From Figures 3.8 and 3.9 it can be seen that the windspeed and runoff for the 1986 data in particular show a similar pattern in variation. This is confirmed by the correlation coefficient of 0.493 shown in Table 3.5. Given this relationship (less for 1987 with a correlation coefficient of 0.185) it can be seen that future developments of ANDERS might also include using the windspeed for every day, as done by Braun and Lang (1986), rather than just for rain-on-snow events.

## 6.5 Conclusion

This chapter has described the application of the models developed in Chapters 4 and 5 to the Dee, Gairn and Feshie catchments.

From the TINDEX results it can be seen that the model is generally able to perform well, especially for snowy

winters, and the lapse rate, recession and melt coefficients all fall within a narrow range for each catchment. This leads to the conclusion that TINDEX has potential for use in real time.

The MART results show that, for catchments with a similar hypsometric curve to the Mharcaidh, the model is able to perform well. However, for the Gairn and Feshie, whose hypsometric curves differ from that of the Mharcaidh, the results are not as good. The results indicate that the snowpack structure within the model may need to be specific to different hypsometric curves, similar to the depletion curves of Rango and Martinec (1982), and may even need to be specified for different snowpacks within the same catchment.

The ANDERS results are similar to those of the Mharcaidh model runs in Chapter 5, the model simulating the flow variation well but failing to match the magnitude of the peak flows.

Given that TINDEX and MART demonstrate potential for use in real time the next logical step is to evaluate this potential. This is done in the following chapter.

## CHAPTER 7 TOWARDS A UNIVERSALLY APPLICABLE MODEL

### 7.1 Comparison of different models

Chapters 4-6 have described the results from developing and applying three different snowmelt runoff models to four Highland catchments over several melt seasons. Having tested the models on meteorological datasets that vary in size, detail and proximity to the catchments it is possible to discuss the results with a view to the ultimate aims of the project outlined in Chapter 1, namely, the development of a universal snowmelt runoff model that can be applied to different catchments in real time.

TINDEX, the model based on the temperature index method of calculating snowmelt was developed using data collected in the Allt a Mharcaidh catchment. Whilst a number of changes hindered the model's performance, namely the addition of the freezing level concept, shortening the time interval and determining the melt factor from the cumulated degree-days, the model was successfully improved by making several changes. These were calculating the degree-days on the mean daily temperature, the use of a gradually increasing melt factor and, in some cases, the addition of a non-linear routing transformation for the modelled meltwater.

These changes allowed TINDEX to satisfactorily simulate the observed Mharcaidh runoff during the 1986 and 1987 melt seasons, accounting for more than 70% of the observed flow variation using fully optimised parameter sets. More encouragingly more than 69% of the variation was accounted for by using averaged lapse rate, recession and melt coefficients, suggesting that the model has potential for use on other datasets and possibly in real time. However, whilst the timing of the flow variation was well matched for both years, the model was unable to simulate the magnitude of the main melt peaks for the 1986 data and some of the rain-on-snow events of 1987, though these were of a lower magnitude.

When applied to other Highland catchments (the Dee, Gairn and Feshie) TINDEX is also able to simulate the observed flow patterns, showing similar general results to those of the Mharcaidh datasets. The meteorological data for these model runs were always collected either outside the catchment or close to the gauging station, resulting in the data having to be lapsed up considerable altitudes. This was in contrast to the Mharcaidh where the data were collected close to the mean hypsometric elevation, thus minimising the effect the lapse rate had on the model, and shows once again that TINDEX has potential for use as a general model. This is supported by noting that whilst TINDEX gave better results when using the mean of the hourly temperature values to calculate the degree-days it

showed only a small drop in performance using daily minimum and maximum temperatures which can be predicted with reasonable accuracy two to three days in advance (S J Harrison, pers comm).

Whilst TINDEX generally performed well when applied to these larger catchments it still performed poorly during rain-on-snow events, especially when the data were collected at remote sites. This consistent characteristic in TINDEX suggests that it is an area that needs further study.

MART also had the melt routine based on the temperature index melt calculation but differed from TINDEX in that the catchment was divided into three distinct elevation zones. The snowpack was modelled within each zone, the daily melt being calculated for each zone and the snowpack in turn depleted according to the value of melt. By using data collected from snow surveys in the Allt a Mharcaidh different snowpack structures were represented and the 'best' structure used to apply MART to other catchments.

By trying the different snowpack structures on the Mharcaidh data the performance was increased until it was statistically similar to that of TINDEX when applied to the 1986 and 1987 Mharcaidh melt seasons. Visually, MART performed similarly to TINDEX on the 1986 data but was able to match the 1987 peak flow events better than TINDEX as a

result of the snowpack being largely determined by the 1987 data. This gave hope that MART also had potential for use in real time, though the representation of the snowpack within the model was clearly a major factor in determining the success of its application. One factor that was clear from the MART model runs on the Mharcaidh data was that non-linear routing gave much better results than linear and was thus used for applying MART to other catchments.

The results from applying MART to the other catchments were both encouraging and discouraging. When the meteorological data were collected close to the catchment,  $Q_0$  was low, there was a 'run-in period' of low flow and, most importantly, the catchment had a similar hypsometric curve to that of the Mharcaidh, MART was able to perform as well if not better than TINDEX. Statistical results were similar but MART was able to match the peak flows during the high snow winters of 1984 and 1986 better than TINDEX.

MART was, however, less able to simulate the observed flow during winters with intermediate or low initial snowpack volumes, when  $Q_0$  was high or when the hypsometric curve of the catchment was different to that of the Mharcaidh. Whilst the  $Q_0$  factor can easily be overcome when applying MART in real time by starting the model run during the low flow period preceding the spring melt, the remaining two points lead to the conclusion that annual snow-survey data is needed to determine the snowpack structure for

catchments with different hypsometric curves.

These surveys need not be as numerous as those carried out in the Mharcaidh. By carrying out a single, detailed survey covering either the whole catchment or representative areas within the catchment prior to the start of the melt season it should be possible to obtain enough information to select/develop the appropriate structure. If this were carried out for a number of years it may then be possible to either produce a general structure for each catchment or to establish inter-catchment relationships that subsequently reduce the number of surveys that need to be carried out.

It can thus be seen that whilst the results of applying MART to some of the datasets show that it does have potential for use as a universal model that is capable of matching the observed peak flows well it is not yet suitable to apply to all datasets. The fact that given certain conditions it is able to both statistically and visually perform better than TINDEK for snowy years means that it should not be discounted merely because it performs badly on some datasets.

Finally, the model based on the parametric energy balance method, ANDERS, also showed that it is able to simulate the timing of meltwater runoff peaks but is very poor at matching the magnitude. By making simple changes to

ANDERS, it was possible to significantly increase its performance, though it was still not as good as either TINDEK or MART, particularly on the 1987 data.

The results in Chapter 6 showed that whilst the statistical performance of ANDERS was weak when applied to the Dee and Gairn 1986 datasets it did match the pattern of the observed flow well, suggesting that the approach has potential for use in a universal model even though ANDERS itself is clearly not suitable in its present form.

The limitations of ANDERS in the form used for this project are highlighted by the fact that it was only possible to apply it to two of the six melt seasons due to lack of windspeed data. Because of this and the problems associated with applying point source wind data to an area as topographically variable as the Highlands it was suggested that it may be beneficial to try alternative indices of windspeed with a view to improving the specific performance of the model and also to making it suitable for use in predicting snowmelt runoff as a general model.

## 7.2 The application of models in 'real time'

### 7.2.1 Introduction

Given the results of the different model runs described above it was decided to try and simulate the use of TINDEK

and MART in real time. The importance of this was stated by Rango (1988) and, because of this, was one of the project aims outlined in Chapter 1. It was initially intended to try this on a dataset covering the 1988 melt season in the Allt a Mharcaidh. However, as the model(s) are unlikely to be usefully applied to such a small catchment that is so well instrumented, and given that the data had not yet been transferred from Wallingford to Stirling and converted into a form suitable for use in the model, it was decided to re-use a dataset that both models performed well on. By doing this any decrease in performance would be easily detectable and the models could be more easily compared.

It was decided to run the models on the 1984 melt season dataset for the Dee catchment. When used to simulate the observed flow both models gave good results using non-linear routing (TINDEX  $R^2 = 0.875$ , MART  $R^2 = 0.836$ ) and this was the routing method chosen for the model run. As the dataset met the criteria outlined in Chapter 6 for the successful application of both models it was felt that any problems likely to arise due to the use of the models in predicting runoff would be clearly visible and not complicated by other factors.

It was realised that by using 'observed' rather than true predicted meteorological data the simulations caused the models to perform better than they might in real time but

the aim of the exercise was only to see if the models had potential for use in this way. Had true predicted data been available they would have been used but the fact that they were not used does not make the results any less significant so long as the limitations are remembered.

In Chapters 4 and 5 it was shown that both TINDEK and MART were able to perform well optimising only the snowpack (i.e. initial SCA and SWE) and albedo parameters; environmental lapse rate (E), recession and melt ( $\text{mm}^\circ\text{C day}^{-1}$ ) coefficients were all fixed at the mean of the values optimised over the two Mharcaidh melt seasons. It was shown, using the results of these model runs that the models were able to perform well though the parameters may have shown consistent variations from year to year (for example, the lapse rate was optimised to a higher value for the snowy winters when it would be expected that the air would cool at a greater rate due to travelling over a larger snowpack). Had linear routing been used it would have been necessary to optimise this parameter for each year's data as the magnitude of flow variation is clearly related to the nature of the snowpack. The method outlined by Wheeler et al (1986) would be appropriate if this routing method had been used, optimising the coefficient on a tailored calibration period which, in this case, would have been one of the recession limbs on the observed hydrograph. By using a non-linear routing submodel the recession coefficient had less need to be optimised as it

automatically adjusted to the magnitude of flow variation.

Whilst there was some variation in these three parameters for all the Dee model runs it was very small (6.2.1, 6.3.1) and less than the variation between catchments. As one would expect both the recession and, to a lesser extent, the melt coefficient to be specific to each catchment it was decided to take the mean values of the parameters from the model runs that used non-linear routing and calculate melt from the mean of the observed daily minimum and maximum temperatures. These parameters were then set as constants in both TINDEX and MART, the values being shown in Table 7.1.

Parameter	TINDEX	MART
Environmental lapse rate ( $^{\circ}\text{C m}^{-1}$ )	0.006	0.008
Recession coefficient	0.17	0.00066
Melt coefficient ( $\text{mm}^{\circ}\text{C day}^{-1}$ )	2.7	4.3

Table 7.1 Values of the environmental lapse rate, recession and melt coefficients set as constants for the TINDEX and MART simulated real time model runs.

Before applying TINDEX and MART in simulated real time the literature was searched to seek guidance on a suitable method. Fountain and Tangborn (1985) summarised the methods used by several authors in applying predictive models to snow-covered and glacierised areas. Whilst the

models varied in sophistication, time-step and results they were all applied to large snow-covered areas that bear little resemblance to the conditions found in the Scottish Highlands. Jones et al (1984) applied the SRM developed by Martinec and Rango (1983, 1986) to the Cache la Poudre catchment in Colorado for the 1983 melt season to forecast flood potentials. By predicting over periods of one to three days using forecast air-temperature and precipitation data; and obtaining snow-cover elevation from aircraft flights over the catchment the authors were able to forecast runoff values within 20% of the observed data. By using the depletion submodel both MART and TINDEK were able to endogenously simulate the snow-cover elevation, thus reducing the required forecast data to just temperature and precipitation. Whilst Jones et al predicted up to three days in advance it was felt that, though this may be feasible for temperature data, it was not so for precipitation in the Highlands. It was thus decided, for the purposes of the project, to 'predict' mean daily runoff two days in advance and update parameters every two days. In reality the parameters could be updated daily but, given the amount of computing required, it was decided to initially run using the two-day updating time-span.

Having decided on the values to be optimised and updated as the number of days increased, the parameters and their respective values to be set as constants for each model and the time-interval over which the flow could be predicted it

was then possible to run the models under simulated real time conditions as follows:

- (1) The model was optimised over the first five days' data.
- (2) Using the values optimised in step (1) the model was then run using the next five days' temperature and precipitation data to predict the runoff. (This was the only five-day time-step used, the reasons for this will be explained later).
- (3) The three parameters were then re-optimised on the 10 days' observed flow data.
- (4) The optimised parameters from (3) were then used, along with the meteorological data, to predict the next two days' runoff.
- (5) Steps (3) and (4) were repeated at two-day intervals until the three parameters remained constant. These were then used to predict the flow for the remainder of the melt season.

Initially two five-day time-steps were used at the start of the model runs as it was felt that the models would initially be insensitive to the snowpack parameters due to the catchment having a large and deep snowpack that would not be significantly altered during the low flow "run-in" period of the model run. Whilst this was the case for the MART model run it was not so for TINDEK which subsequently had the parameters updated after eight days. This

demonstrates that in using the model it is safe to update at the two-day time-step interval; if no changes are needed then all that is lost is some computing time whilst, if they are needed, the performance of the model can be increased for little additional cost.

Using this method the runoff was predicted for the Dee catchment during the 1984 melt season using both TINDEX and MART. The updated parameter sets for both model runs are shown in Tables 7.2 and 7.3 and Figures 7.1 and 7.2 show the observed, simulated and predicted flows for the two model methods (the predicted plots were constructed by appending together all the two-day predicted runoff values).

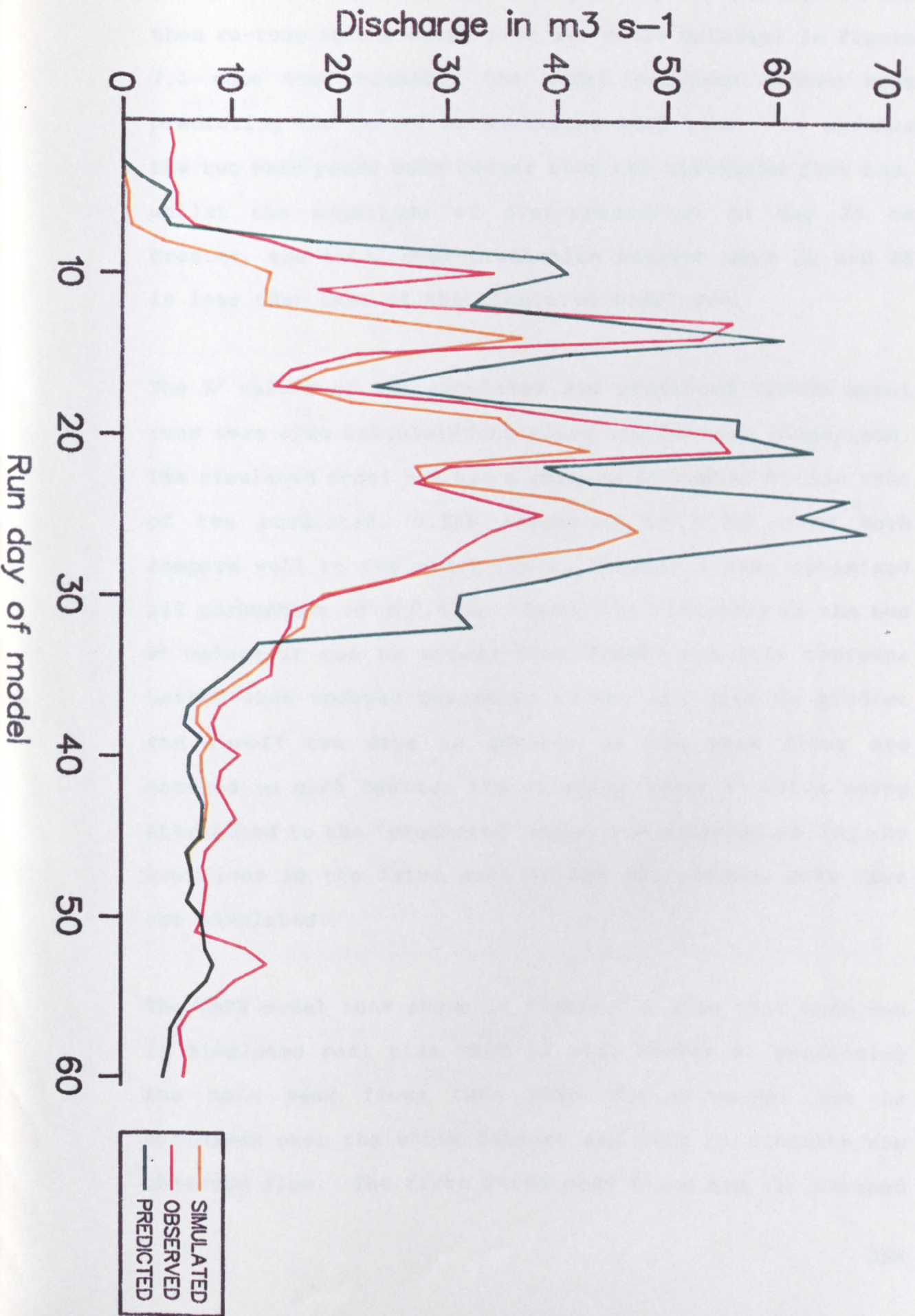
From Figure 7.1 it can be seen that TINDEX has great potential for use in real time forecasting. Whilst the first peak on day 10 is under-predicted ( $23\text{m}^3 \text{s}^{-1}$  compared to the observed value of  $34\text{m}^3 \text{s}^{-1}$ ) the two major high flow events are predicted exceptionally well, the magnitude of both ( $55\text{m}^3 \text{s}^{-1}$ ) being matched to within  $1\text{m}^3 \text{s}^{-1}$ , i.e. less than 2% difference. Although the fourth peak on day 25 is over-predicted by some  $15\text{m}^3 \text{s}^{-1}$  it is only for one day and is less than the over-prediction noted for either of the TINDEX model runs on the same data but optimising all parameters in Chapter 6.

Comparison of the predicted and simulated plots (i.e. that

Number of Days	Initial SCA (km <sup>2</sup> )	Initial SWE (mm)	Albedo Factor	SE
5	210	500	0.45	
8	267	500	0.07	4.55
10	270	500	0.08	4.49
12	270	500	0.09	4.24
14	271	500	0.09	4.64
16	270	360	0.10	4.56
18	271	270	0.10	5.93
20	271	250	0.10	5.74
22	269	280	0.10	7.12
24	267	220	0.10	6.12
26	271	210	0.10	6.11
28	273	220	0.10	6.29
30	271	230	0.10	6.22
32	264	240	0.15	6.20
34	260	250	0.15	6.20
36	260	250	0.15	6.12
38	256	260	0.15	6.04
40	256	260	0.15	6.04
42	256	260	0.15	6.04
44	251	270	0.20	5.75
46	251	270	0.20	5.68
48	250	280	0.20	5.62
ALL (60)	250	280	0.20	5.17

Table 7.1 Parameter sets obtained from applying TINDEK in simulated real-time on the Dee 1984 dataset.

Figure 7.1 (overleaf) Time series plots from running TINDEX on the Dee 1984 dataset under different conditions. The simulated plot had the environmental lapse rate, recession and melt coefficients set as constants and optimised the snowpack and gradually increasing melt factor parameters from the whole dataset; the predicted plot optimised the same parameters at two day increments, the plot being derived by appending the two day flow predictions as explained in the text. Both model runs used non-linear routing.



using all the observed data to optimise the parameters and then re-running the model over the whole dataset) in Figure 7.1 show that visually the model performs better when predicting the runoff in simulated real time. It matches the two main peaks much better than the simulated flow and, whilst the magnitude of over-prediction on day 25 is greater, the total over-prediction between days 22 and 28 is less than that of the simulated model run.

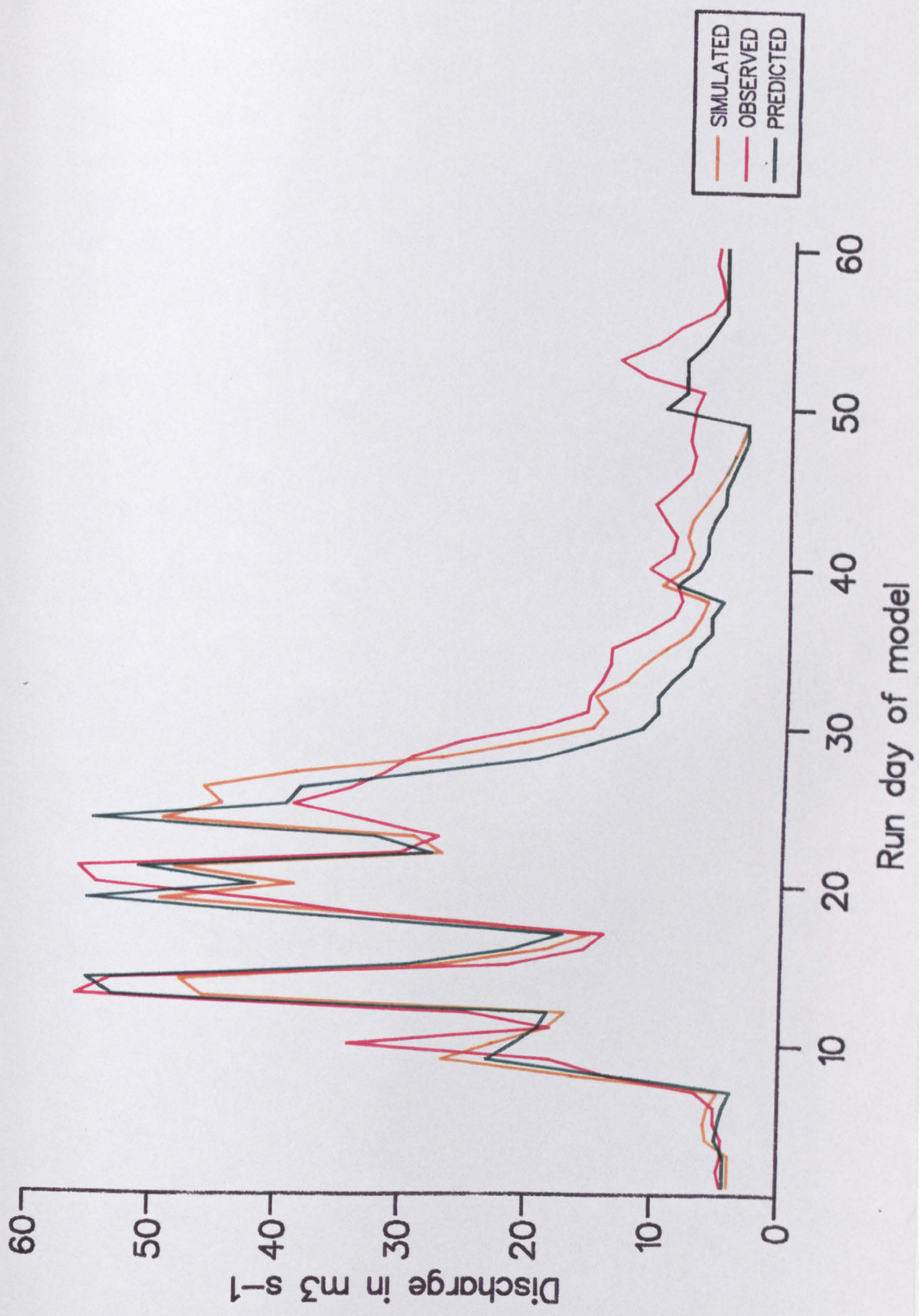
The  $R^2$  values of the simulated and predicted TINDEX model runs were also calculated to allow statistical comparison. The simulated model run had a marginally higher  $R^2$  than that of the predicted, 0.868 comparing to 0.841, and both compare well to the model run in Chapter 6 that optimised all parameters ( $R^2 = 0.875$ ). Given the closeness of the two  $R^2$  values it can be argued that TINDEX actually performs better when updated parameter values are used to predict the runoff two days in advance as the peak flows are matched so much better; the slightly lower  $R^2$  value being attributed to the 'predicted' model run underestimating the low flows in the later part of the melt season more than the simulated.

The MART model runs shown in Figure 7.2 show that when run in simulated real time MART is also better at predicting the main peak flows than when the parameter set is optimised over the whole dataset and used to simulate the observed flow. The first three peak flows are all matched

Number of Days	Initial SCA (km <sup>2</sup> )	Initial SWE (mm)	Albedo Factor	SE
5	289	500	10.00	8.54
10	289	500	10.00	5.54
12	223	20	10.00	5.35
14	266	10	0.15	8.49
16	212	30	10.00	6.80
18	208	30	10.00	7.26
20	197	40	10.00	7.11
22	192	40	10.00	10.17
24	167	90	10.00	12.00
26	151	80	10.00	12.09
28	151	80	10.00	12.40
30	151	80	10.00	12.33
32	150	470	10.00	9.68
34	150	470	10.00	9.45
36	150	480	10.00	9.21
38	150	490	10.00	8.82
40	150	490	10.00	8.82
42	150	500	10.00	8.45
44	150	500	10.00	8.45
46	150	510	10.00	7.48
ALL (60)	150	510	10.00	7.48

Table 7.2 Parameter sets obtained from running MART in simulated real-time on the Dee 1984 dataset.

Figure 7.2 (overleaf) Time series plots from running MART on the Dee 1984 dataset under different conditions. The simulated plot had the environmental lapse rate, recession and melt coefficients set as constants and optimised the snowpack and gradually increasing melt factor parameters from the whole dataset; the predicted plot optimised the same parameters at two day increments, the plot being derived by appending the two day flow predictions as explained in the text. Both model runs used non-linear routing.



much better than the simulated model run and the low flows over the later part of the melt season are also well simulated. Reference to Figure 6.11 shows that MART was equally good at replicating the two main peaks as the predicted model plot in Figure 7.2, though the first peak and later low flows are not as well matched.

Despite these beneficial points the MART predicted plot shown in Figure 7.2 does show one period of consistent over-prediction (days 22-32) that is much worse than the simulated model run. Whilst the simulated model run does over-predict the flow during part of this period it is much less than that of the predicted plot. This period of over-prediction results in the MART predicted model run having a low  $R^2$  value of 0.482 compared to the 0.759 of the simulated model run and leads to the conclusion that MART needs further work before it can be used in real time to predict snowmelt runoff.

The parameter sets shown in Tables 7.2 and 7.3 also raise some interesting points:

- (1) The SE values during the period of over-prediction during the MART model run increase suddenly and drop once this period comes to an end. It may be that by observing the SE values as the model is applied it is possible to determine a degree of confidence in the predicted flow. Whilst this is an area that would

clearly need extra work it may enable MART to be successfully used.

- (2) Whilst the parameters are, on the whole, slow to change, there are periods when the rate of change increases (for example, days 14-20 of the TINDEK SWE values, days 22-24 of the MART SCA values and days 30-32 of the MART SWE values). It may be possible that by reducing the time interval to one day for the updating of parameters (though not adjusting the models predicting two days in advance) the errors described above can be reduced by using intermediate values during periods of rapid change.
- (3) Both models take similar lengths of time to reach the optimum set of parameters (48 days for TINDEK, 46 for MART) which was more than 75% of the modelled melt season.
- (4) Although both models showed periods during which the optimised parameters were stable (for example, days 38-42 of TINDEK, days 26-32 of MART) but then the parameters started changing. This shows that it is not possible to stop updating the parameters as soon as the same values are obtained on consecutive days. Instead, the updating process needs to be carried out until the end of the melt season.

From the results described above it can be seen that whilst MART does have potential for use in real time it still needs further work to be accurately applied, even though it does appear to match the important peak flows well. TINDEK not only has potential for predictive use but appears to need little extra work, though it must be remembered that it is poor at simulating rain-on-snow events. Given the high statistical and visual performance of TINDEK operating in simulated real time it was decided to carry out sensitivity analysis on the model to see how robust it is. The TINDEK simulated model run on the Dee 1984 dataset was used as an example to carry out sensitivity analysis.

### 7.3 Sensitivity analysis

Whilst the <sup>simulated</sup> plot in Figure 7.1 did not visually perform as well as the model run using updated parameters it must be remembered that the model was optimised on a statistical index and in order to be consistent it was necessary to study the effect of parameter variability on this index. Since the aim of the exercise was to evaluate the universal version of the model that treated the environmental lapse rate, recession and melt coefficients as constants only the snowpack and albedo parameters were varied. Before the model is actually used in real time it is advised that sensitivity analysis is carried out on the three constants.

TINDEX was re-run using 10 different values of initial SCA, SWE and ALB, the values and corresponding SE values being written to an external file. From these data it was then possible to construct Figure 7.3 which shows the variation of SE with each of the three parameters. For each plot the remaining two parameters were set to the optimum values obtained from the simulation run using all days' data; this ensured that any variation in SE could be attributed specifically to each parameter. The plots also show two horizontal lines that correspond to an increase in 5 and 10% of the SE value.

Taking the three plots separately it can be seen that the model is relatively insensitive to changes in initial SCA. The parameter can vary by  $20\text{km}^2$  below and  $15\text{km}^2$  above the optimised value (total range = 12% of catchment area) and still only affect the model by 5%. However, as one moves further away from the optimum value the rate of increase in SE increases, reflecting a more significant effect on the model performance. Reference to Table 7.2 shows that after only eight days of data TINDEX is able to optimise the initial SCA to within the 10% boundary, though it does take longer (32 days) to reach the 5% range of values. Those results show that the increments used for optimising the initial SCA in the model may have been smaller than was needed to produce acceptable results; a  $1\text{km}^2$  final increment was used whereas a  $5\text{km}^2$  increment would appear to have been sufficient.

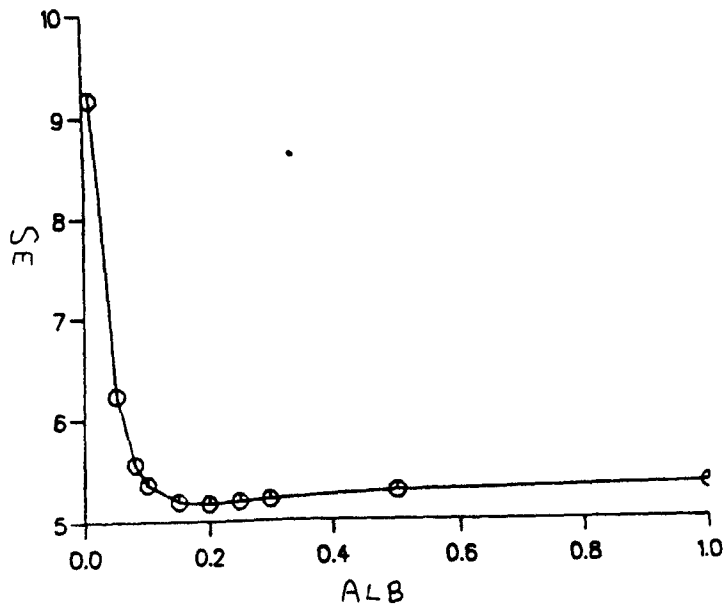
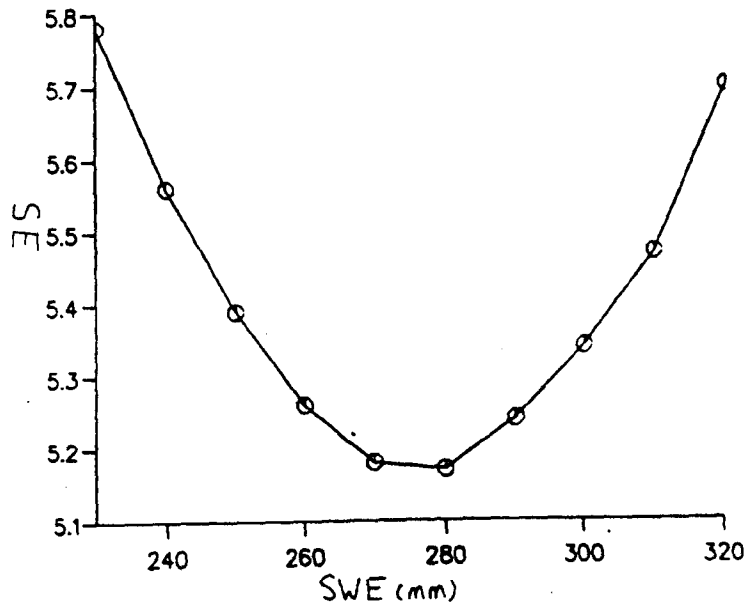
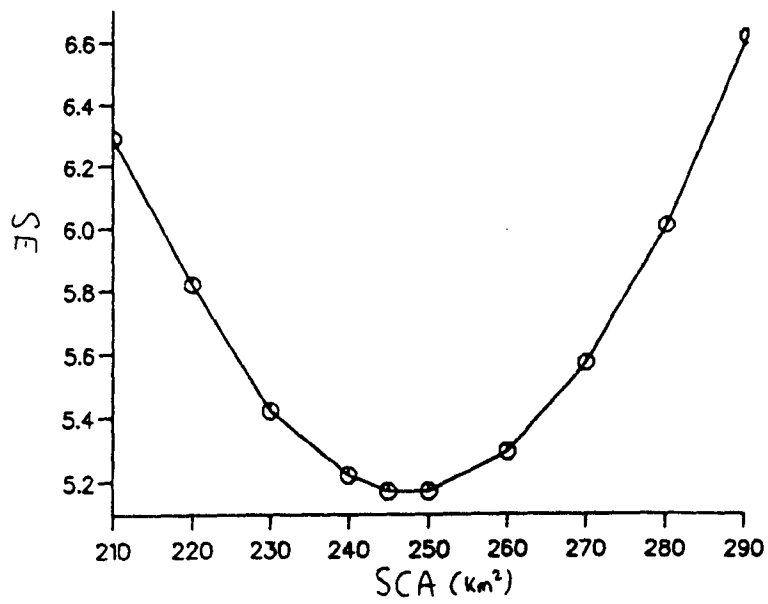


**Figure 7.3** Plots of the response surface of the TINEX simulated model run varying one of the three optimised parameters at a time and holding the other two at the optimised value.

The SWE plot is similar to that of the initial SCA in that it is parabolic in nature reflecting the increasing rate of decrease in model performance the further the parameter value is from the optimum. The curve appears to be symmetric, unlike that of the SCA which is affected by the upper SCA value at the catchment area, and shows that SWE can vary by 30 mm either side of the optimum and still allow the model to perform within 5% of the statistical optimum. Beyond this threshold the model performance decreases sharply, a further 10 mm variation resulting in the 10% threshold being reached. These results show that the increment used to optimise SWE during the model run (10 mm) was suitable given the insensitivity of the model to SWE. Had the increment been reduced to 5 mm a lower SE value would have been obtained but, given the nature of the response surface in Figure 7.3(b), this improvement would have been less than 0.5% of the optimum SE value (the Optimum SWE appears to be 275 mm), suggesting that it would not be worth the extra computing.

The plot of the effect different ALB values have on the SE values of TINDEX runs is very different to that of the SCA and SWE. This is due to the negative exponential function used to calculate the gradually increasing melt factor outlined in 4.6.1 and illustrated in Figure 4.12. From Figure 4.12 it could be seen that a given change in ALB (then called  $k$  in the early TINDEX models) when ALB itself was small resulted in a large change in the rate at which

the melt factor increased. As values of ALB increased above 0.1 there was little relative increase in the rate of melt factor change for the same given change. Because of this the increments used for optimising ALB depended on the range of values that ALB appeared to be optimising on. For example, when ALB appeared to fall between 0.01 and 0.09 the increments were 0.01; when ALB appeared to be between 0.1 and 1 the increments were 0.05. In this way it was intended to optimise ALB as efficiently as possible.

The plot shown in Figure 7.3 is based on this range in increments and shows that the concept of varying the increments is sound and appears to reflect the variation in SE, the density of points being highest where the response surface shows the greatest rate of change. The model is clearly sensitive to a decrease in ALB below the optimised value when this value is below or close to 0.1. (This value causes the actual melt factor to be within 25% of the final melt factor after only 10 days.) It can also be seen from Table 7.2 that TINDEX was quickly able to optimise ALB within the 10% threshold (after 8 days) and needs only 12 days' data to optimise ALB within the 5% threshold. Thus, whilst it has been shown that TINDEX is sensitive to changes in ALB when the optimised value is below or close to 0.1 the model is able to compensate for this by optimising the parameter to a reasonable value using little data.

In addition to evaluating the sensitivity of TINDEX to changes in individual parameters it was decided that it would also be useful to study the combined effect of varying two of the three parameters. This was done by taking two-dimensional 'slices' through the three-dimensional response surface of TINDEX, the 'slices' being taken through the optimum value of the parameter set being studied. These three slices are shown in Figure 7.4. On all plots the lowest contour value of 5.4 corresponds to 5% threshold in model performance, a contour of 5.7 corresponding to the 10% threshold.

From the lower two of the three plots it can be seen that the relationship of both SCA and SWE with ALB on TINDEX is a straightforward combination of the plots shown in Figure 7.3. For example, if the SCA/ALB plot (the middle of the three) is considered it can be seen that at the optimum ALB value of 0.2 the range of SCA values within the 5% contour is the same as that in Figure 7.3(b). Similarly, at the optimum SCA value of 250km<sup>2</sup> the range of ALB values is also the same as in Figure 7.3(c). As either value moves from the optimum the range of the other parameter values within the 5% threshold decreases accordingly. Due to the sensitivity of the model to ALB the contours indicate a steeper response surface as ALB decreases, the effect of SCA on the model performance being almost completely cancelled by this.

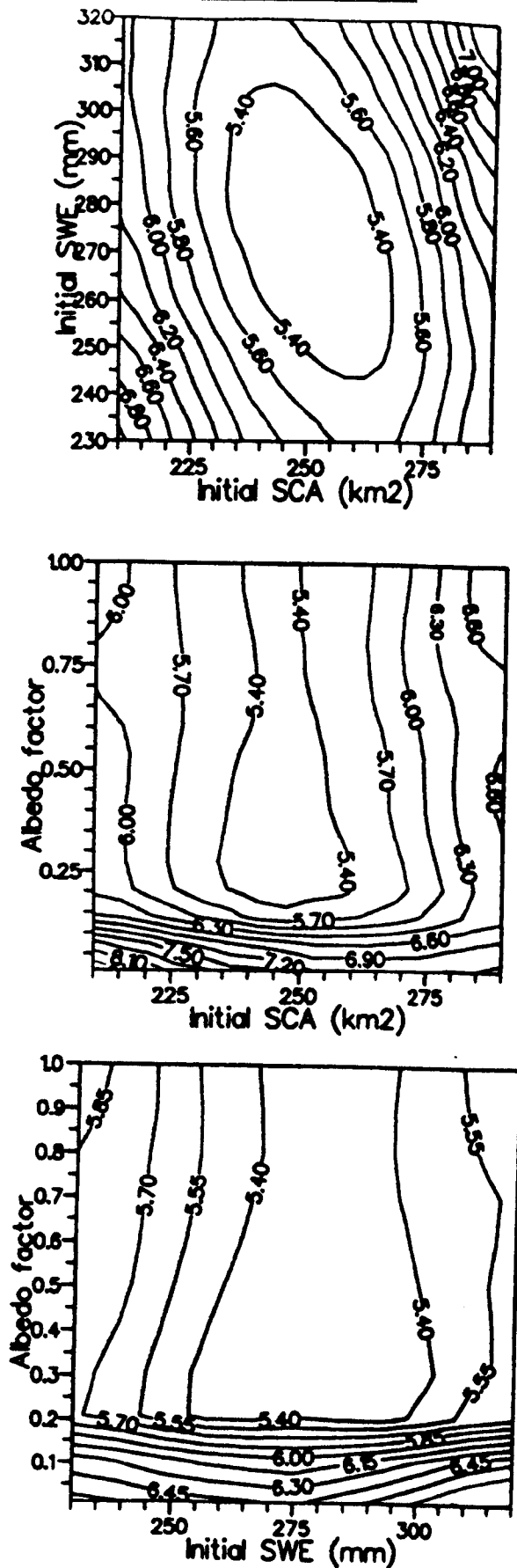


Figure 7.4 Two-dimensional slices through the three-dimensional response surface of the TINDEK simulated model run, the slice being taken through the optimised value of the third parameter.

The SWE/ALB plot in Figure 7.4(c) shows similar characteristics, the effect of SWE on model performance also being cancelled out at low values of ALB due to the sensitivity of TINDEXT to this parameter.

The SCA/SWE plot in Figure 7.4(a) is more interesting in that given the plots in Figure 7.3(a) and (b) one would have expected a series of concentric contour lines oriented parallel to either the x or y axis of the plot. Instead it can be seen that whilst there is indeed a set of concentric contour lines these are oriented along a diagonal axis that tends towards the 'top left to bottom right' diagonal of the plot. This skewed orientation of the response surface suggests that there is, as one would hope, a relationship between the two variables that influence the performance of TINDEXT. The orientation of the contours shows that a decrease in SCA will, when accompanied by an increase in SWE, not have as much effect on the performance of TINDEXT as it would if the SWE were lower. The opposite also applies, namely an increase in SCA has less effect on the model when SWE is decreased. Ferguson (1984) also noted a limited trade-off of SCA and SWE when applying TINDEXT to the Feshie catchment. These observations are encouraging and show that whilst TINDEXT is a conceptual, parametric model, the treatment of the snowpack is such that changes in one snowpack parameter cause a physically reasonable change in the other.

Concluding, the sensitivity analysis shows that TINDEX is tolerant of a wide range of initial snowpack characteristics and that it is able to approximate these values after only a few days observed flow to within the 5% thresholds. The interaction of the SCA and SWE has been observed by producing a two-dimensional plot of the response surface and this interaction is physically reasonable. TINDEX is more sensitive to the gradually increasing melt factor ALB, particularly when it is optimised to below or close to 0.1. Despite the high degree of sensitivity to this parameter the model is able to approximate the optimum value after a very short time-span to within the 5% threshold.

#### 7.4 Conclusions and guidelines for use in real time

This chapter has shown that both TINDEX and MART are able to closely simulate the observed flow of the Dee catchment during the 1984 melt season with the environmental lapse rate recession and melt coefficients set as constants. By running the models in simulated real time, predicting flow two days in advance, it has also been shown that both models are able to match the observed high flows with a high degree of accuracy. Visually it can be seen that by running the models in real time, updating the snowpack and gradually increasing melt factor parameters every two days, the models are able to perform better than when the whole dataset is available to optimise the parameters on, even

though the statistical performance is lower. This suggests that both models have potential for predictive use. Of the two models TINDEX is the better performer, both statistically and visually, due to MART over-predicting for a period of more than 10 days during the last melt event. Because of this it was concluded that whilst MART has potential for predictive use it needs further work before it can be used with any confidence.

As TINDEX was the better performer sensitivity analysis was carried out on the optimised parameters. This analysis showed that TINDEX is able to tolerate a reasonable range in the parameters without the statistical performance of the model run being affected too much. By using suitable increments in the optimisation process TINDEX is able to approximate all three parameters to reasonable values in a relatively short time-span. This is most important for the gradually increasing melt factor ALB which the model is particularly sensitive to and is able to approximate after less than 10 days' data for the Dee 1984 dataset.

When this ability to approximate the parameters on limited observed data is combined with the fact that by using an endogenous snowpack depletion submodel within TINDEX the snowpack parameters are automatically updated during the model runs it can be seen that the need for field data is minimised. Whilst snowpack data are useful for calibrating and developing the model and providing initial estimates of

the parameters, it is obviously preferable if the need for snow surveys is minimised, especially in the larger catchments where they would present logistic difficulties.

If TINDEX is to be used in real time for predictive purposes it is clearly useful if a set of guidelines can be given for use when applying the model. From the results of this thesis the guidelines for TINDEX in its present form would be as follows:

- (1) A number of previous years' data should be used to evaluate the performance of TINDEX when all data is known. In addition to providing an idea of the likely suitability of the model to the particular catchment this would also provide the mean for calibrating the environmental lapse rate, recession and melt coefficients.
- (2) When TINDEX is used to predict runoff from a catchment the model run should be started during the low flow period prior to the main melt seasons. This provides a 'running-in' period for the model.
- (3) Initially snowpack parameters will need to be input into the model until a change occurs in the observed flow. These parameters should preferably be from snow surveys but, as experience is gained after a number of years using the model, it may be possible to use

estimates for these values.

- (4) Whilst the results from 7.2 suggest that a two-day time-step is sufficient to obtain good results from TINDEX it is most likely that shortening this interval and updating the three parameters daily will increase the performance of the model, particularly during periods of rapid change in either the parameter set or observed flow data.
- (5) Whilst the parameters are updated at a daily time interval it should still be possible to predict the flow two days in advance given suitable meteorological data. Whilst the predicted flow for the following day is likely to be more accurate, the two day forecast will still provide a useful indication of the runoff. The meteorological data should be collected from a site as close to the catchment as possible for updating the parameters though the site will be less critical for the predicted temperature and precipitation data.
- (6) By recording the SE values for the cumulating model runs it may be possible to attach confidence levels to the predicted flow. Quite how this can be done is not yet clear but it is a point that would benefit from further study.

- (7) The parameter set should be re-optimised at the given time-step (daily or two-daily) for the whole of the melt season. It is possible that the parameter will stabilise for periods within the melt season but then change again and it is only by continuing with the updating process that any errors due to this are avoided.

Given these guidelines the results from this chapter show that TINDEX, a conceptual model based on the temperature index method of calculating snowmelt and endogenously depleting the snowpack in a similar way to that used by Ferguson (1984), has potential for use in predicting snowmelt runoff events.

## CHAPTER 8 CONCLUSION AND FURTHER WORK

### 8.1 Summary of Results

The project has managed to complete the five aims outlined in Chapter 1 with some success. Detailed snow surveys were carried out in the Allt a Mharcaidh, a small experimental Highland catchment used in the SWAP project. From these surveys it was possible to determine general patterns in the snowpack characteristics over several melt seasons. These patterns were related to the observed hydrological and meteorological data collected over the same period.

By studying the meteorological and hydrological data it was possible to identify a number of modelling approaches that had potential for use in Highland catchments. Regression analysis showed that whilst the meteorological data could account for almost 70% of the variation in flow for single years it was not able to do so when applied to more than one year's data. By establishing a regression equation on the data from two melt seasons it was shown that this method could not be used in a general form to predict snowmelt runoff.

The temperature index model described by Ferguson (1984) was adapted and applied to the Allt a Mharcaidh for the

1986 and 1987 melt seasons. It was found that the performance of the model could be improved by a number of changes:

- (1) Calculating melt from true mean daily temperature.
- (2) Incorporating a gradually increasing melt factor to allow for snowpack ripening and changes in albedo.
- (3) Non-linear routing for snowy years.

The development of the model also showed that other changes made to the model that were close to reality hindered its performance. It is thought that this was due to changes in one particular submodel knocking the rest of the model out of balance, suggesting that the degree of complexity should be similar for all stages of the model.

The endogenous depletion submodel was able to replicate the observed pattern and rate of snowpack depletion, though the modelled SCA was different to that observed from the snow surveys.

Two other model types were also adapted and applied to the Mharcaidh datasets. These were:

- (1) The parametric energy balance outlined by Anderson (1973) that attempted to represent the energy balance at the snow/air interface during rain-on-snow events using temperature, precipitation and windspeed data.

(2) The vertically layered temperature index model used by Martinec (1975) that divided the catchment into a number of elevation zones and modelling separate snowpacks within each zone.

The parametric energy balance model was very good at replicating the observed pattern of runoff though it was not as good as the temperature index model at matching the magnitude of peak flows. By adjusting the rainfall threshold value to differentiate between rain-on-snow and pure melt events it was possible to increase the performance of the model.

The vertically layered model did not appear to be as good as the temperature index model when first applied. By trying a number of different snowpack structures for each zone it was possible to improve the performance of the model until it was similar to that of the temperature index model.

All three models were then applied to three other Highland catchments ranging in size from 106 to 289km<sup>2</sup>. The parametric energy balance method replicated the pattern of runoff well but was unable to match the magnitude of peak flows. It was thus concluded that the model had no potential for predictive use without further development.

The vertically layered temperature index model performed

well on certain datasets, namely those that were from a snowy winter and for catchments that had a similar hypsometric curve to the Allt a Mharcaidh. It was concluded that whilst the model had potential for use in its current form to certain catchments, it might perform better if the snowpack structure was determined for each catchment from field data and, possibly, for each year.

The temperature index approach was the best of the three at simulating the observed flow pattern in these large catchments suggesting that it had potential for use in real time.

Given these results the vertically layered and temperature index models were applied to the Dee catchment for the 1984 melt season in simulated real time. By setting three parameters as constants it was demonstrated that both models were able to predict the observed flow well, even matching the peak flows better than when simulating the observed flow from the complete dataset. The temperature index model was the better of the two as it matched later melt runoff better, though both models over-predicted during these events. Sensitivity analyses were carried out on the temperature index model and showed that it was tolerant to fluctuations in the two snowpack parameters. It was, however, sensitive to the gradually increasing melt factor coefficient but was able to closely approximate the optimum value using only a few days' data.

From these results it is concluded that the conceptual temperature index model is suitable for use as a means of predicting snowmelt runoff from Highland catchments. If the guidelines given in Chapter 7 are followed the model should be able to closely match the important peak flows, though low flow events may be poorly predicted.

## 8.2 Further work

Whilst the project appears to have achieved the aims outlined in Chapter 1 it has also identified a number of areas where future work could be carried out. These are as follows:

- (1) To try and develop a more accurate means of predicting rain-on-snow events as all models are weak at this.
- (2) To further develop the parametric energy balance model along the lines outlined in Chapter 6, i.e. to try using geostrophic winds, possibly for all days of the model run, as these can be predicted.
- (3) To try different snowpack structures in the vertically layered model for different catchments and to see if relationships between catchments exist that can be used to reduce the need for the snow survey data that the model seems to require.

- (4) To compare the depth of melt from all methods to that calculated by the energy balance in a model such as IHDM. This would then facilitate the accurate development of the snowmelt submodels.

Given these recommendations it should be possible to further develop the models so that all snowmelt runoff events can be accurately predicted.

## BIBLIOGRAPHY

Anderson, E A, 1968.

Development and testing of snowpack energy balance equations. Water Resources Research, 4(1): 19-37.

Anderson, E A, 1973.

National Weather Service River Forecast System - Snow Accumulation and Ablation Model. NOAA Technical Memorandum, NWS 17.

Anderson, E A, 1976.

A point energy and mass balance model of a snow cover. NOAA Technical Report, NWS 19.

Anderson, E A, 1978.

National Weather Service River Forecast System - Snow Accumulation and Ablation Model: User's Manual and Guidance for Use. NOAA Technical Memorandum.

Anderson, E A and Crawford, N H, 1964.

The synthesis of continuous snowmelt runoff hydrographs on a digital computer. Department of Civil Engineering Technical Report No 36, Stanford University, Stanford, California.

Archer, A C, 1970.

Studies of snow characteristics in the north-eastern Ben Ohau mountains, New Zealand. Journal of Hydrology (NZ), 9(1): 4-21.

Archer, D R, 1981.

Severe snowmelt runoff in north-east England and its implications. Proceedings of the Institution of Civil Engineers, Part 2, 71: 1049-1060.

Archer, D R, 1983.

Computer modelling of snowmelt flood runoff in north-east England. Paper 8613, Proceedings of the Institution of Civil Engineers, 75: 155-173.

- Archer, D R, 1986.  
Snowmelt and river flooding. Unpublished paper presented to the Royal Society of Edinburgh.
- Bagchi, A K, 1983.  
Areal value of degree-day factor. Hydrological Sciences Journal, 24: 499-511.
- Bailey, R A and Waters, J S, 1986.  
Rain - the raw material: ways to measure, model and manage it.
- Barry, R G, 1981  
Mountain weather and climate, Methuen - London.
- Barry, R G and Chorley, R J, 1976.  
Atmosphere, weather and climate. Methuen, London.
- Beaumont, R T, 1965.  
Mount Hood pressure pillow snow gauge. Journal of Applied Meteorology, 4: 626-631.
- Bergstrom, S, 1976.  
Development and application of a conceptual runoff model for Scandinavian catchments. Department of Water Resources Engineering, Lund Institute of Technology, University of Lund, Bulletin Series, A(52).
- Bergstrom, S, 1978.  
Spring flood forecasting by conceptual models in Sweden. In Colbeck, S C and Ray, M (editors), Modelling of Snow Cover Runoff: 397-406.
- Bernier, P Y, 1965.  
Extrapolating snow measurements on the Marmot Creek experimental basin. Nordic Hydrology, 17: 83-92.
- Bevan, K J and O'Connell, P E, 1982.  
On the role of physically-based distributed modelling in hydrology. Institute of Hydrology Report, 81.
- Braun, L N and Lang, H, 1986.  
Simulation of snowmelt runoff in lowland and lower Alpine regions of Switzerland. IAHS, 155: 125.

- Brundson, G P and Sargent, R J, 1982.  
The Haddington flood warning system. IASH, 134: 257-272.
- Charbonneau, R, Lardeau, J P and Obled, C, 1981.  
Problems of modelling a high mountainous drainage basin with predominant snow yields. Hydrological Sciences Bulletin, 26(4): 345-361.
- Chinn, T J H, 1969.  
Snow survey techniques in the Waitaki catchment, South Canterbury. Journal of Hydrology (NZ), 8(2): 68-76.
- Colbeck, S C, 1972.  
A theory of water percolation in snow. Journal of Glaciology, 2(63): 369-385.
- Colbeck, S C, 1974.  
Water flow through snow overlying an impermeable boundary. Water Resources Research, 10(1): 119-123.
- Colbeck, S C, 1975.  
A theory for water flow through a layered snowpack. Water Resources Research, 11(2): 261-266.
- Davison, R W, 1987.  
The supply of snow in the Eastern Highlands of Scotland: 1954-5 to 1083-4. Weather, 42(2): 42-50.
- Deas, A, 1986.  
Modelling of snowmelt runoff from Scottish Highland catchments. Unpublished BSc dissertation, Department of Environmental Science, University of Stirling.
- Dickison, R B B and Daugharty, D A, 1978.  
A square grid system for modelling snow cover in small watersheds. In Colbeck, S A and Ray, M (editors), 1978. Modelling of snow cover runoff, CRREL, Hanover, NH: 71-76.
- Dunne, T, Price, A G and Colbeck, S C, 1976.  
The generation of runoff from subarctic snowpacks. Water Resources Research, 12(4).

- Elder, K, Kattelmann, R and Ferguson, R I, 1990.  
Refinements in dilution gauging for mountain streams.  
IAHS, 193: 247-254.
- Ferguson, R I, 1984.  
Magnitude and modelling of snowmelt runoff in the  
Cairngorm Mountains, Scotland. Hydrological Sciences  
Journal, 29: 49-62.
- Ferguson, R I, 1985.  
High densities, water equivalents and melt rates of  
snow in the Cairngorm Mountains, Scotland. Weather,  
40: 272-277.
- Ferguson, R I, 1986.  
Parametric modelling of daily and seasonal snowmelt  
using snowpack water equivalent as well as snow-  
covered area. IAHS, 155: 151-162.
- Ferguson, R I and Morris, E M, 1987.  
Snowmelt modelling in the Cairngorms, NE Scotland.  
Transactions of the Royal Society of Edinburgh, Earth  
Sciences, 78: 261-267.
- Fitzharris, B B, 1978.  
Problems in estimating snow accumulation with  
elevation on New Zealand mountains. Journal of  
Hydrology (NZ), 17(2): 78-90.
- Fitzharris, B B and Grimmond, S, 1982.  
Assessing snow storage and melt in a New Zealand  
mountain environment. IAHS, 138: 161-168.
- Fohn, P M B, 1980.  
Snow transport over mountain crests. Journal of  
Glaciology, 26: 469-480.
- Forth River Purification Board, 1977.  
Proposals for a flood warning scheme for Haddington on  
the river Tyne. Technical report no 6, FRPB  
Edinburgh.
- Fountain, A G and Tangborn, W, 1986.  
Overview of contemporary techniques. IAHS, 149: 27-  
41.

- Gillies, A J, 1964.  
Review of snow survey methods, and snow surveys in the Fraser catchment, Central Otago. *Journal of Hydrology (NZ)*, 3(1): 3-16.
- Goodison, B E, Ferguson, H L and McKay, G A, 1981.  
Measurement and data analysis. In Gray, D M and Male, D H, *Handbook of Snow*, Pergamon Press: 191-235.
- Green, F H W, 1973.  
Changing incidence of snow in the Scottish Highlands. *Weather*, 30(7): 226-235.
- Green, F H W, 1975.  
The transient snow-line in the Scottish Highlands. *Weather*, 28(11): 428-437.
- Harding, R J, 1978.  
The variation in the altitudinal gradient of temperature within the British Isles. *Geogr. Ann.* 60A:43-49.
- Harding, R J, 1986.  
Exchanges of energy and mass associated with a melting snowpack. *IAHS*, 155: 3-15.
- Harrison, W, 1986 (a).  
Seasonal accumulation and loss of snow from a Block Mountain catchment in Central Otago. *Journal of Hydrology (NZ)*, 25(1): 1-17.
- Harrison, W, 1986 (b).  
Effects of snow fences on the snowpack of a Block Mountain in Otago. *Journal of Hydrology (NZ)*, 25(1): 18-40.
- Institution of Civil Engineers, 1978.  
*Flood and reservoir safety: engineering guide.*
- Jackson, M C, 1977.  
A method of estimating the probability of occurrence of snow water equivalents in the United Kingdom. *Hydrological Sciences Bulletin*, 22(1): 127-142.

- Jenkins, A, 1989.  
Storm period hydrochemical response in an unforested Scottish catchment. *Hydrological Sciences Journal*, 34(4): 393-404.
- Johnson, P and Archer, D R, 1972.  
Current research on British snowmelt river flooding. *Hydrological Sciences Bulletin*, 17(4): 443-451.
- Jones, E B, Frich, D M, Barker, P R and Allum, J, 1984.  
Application of a snowmelt runoff model for flood prediction. Unpublished report, Resource Consultants Inc, Fort Collins, Colorado.
- Kopanev, I D, 1972.  
Estimate of the accuracy of determination of snow cover characteristics and recommendations on the rationalisation of the snow measurement network. *Soviet Hydrology: Selected papers*, 2: 122-128.
- Kuusisto, E, 1972.  
The energy balance of a melting snow cover in different environments. *IAHS*, 155: 37-45.
- Kuusisto, E, 1986.  
The energy balance of a melting snow cover in different environments. *IAHS*, 155: 37-45.
- Lichtenegger, J, Seidel, K, Keller, M and Haefner, H, 1981.  
Snow surface measurements from Landsat MSS data. *Nordic Hydrology*, 12: 272-288.
- Male, D H and Gray, D M, 1981.  
Snowcover ablation and runoff. In Gray, D M and Male, D H, 1981, *Handbook of Snow*, Pergamon Press: 360-436.
- Manley, G, 1969.  
Snowfall in Britain over the past 300 years. *Weather*, 28(7): 428-437.
- Martinec, J, 1960.  
The degree-day factor for snowmelt-runoff forecasting. *IAHS*, 51: 468-477.

- Martinec, J, 1965.  
A representative watershed for the research of snowmelt-runoff relations. IAHS, 66(2): 494-501.
- Martinec, J, 1975.  
Snowmelt runoff models for operational forecasts. Nordic Hydrology, 16(3): 129-136.
- Martinec, J, 1976.  
Snow and ice. In Rodda, J C (editor), Facets of Hydrology, John Wiley & Sons, Chapter 4: 85-118.
- Martinec, J, 1980 (a).  
Snowmelt-runoff forecasts based on automatic temperature measurements. IAHS, 129: 239-246.
- Martinec, J, 1980 (b).  
Limitations in hydrological interpretations of the snow coverage. Nordic Hydrology, 2: 209-220.
- Martinec, J and Rango, A, 1983.  
The snowmelt-runoff model (SRM) user's manual. NASA reference publication 1100: 118.
- Martinec, J and Rango, A, 1986.  
Parameter values for snowmelt runoff modelling. Journal of Hydrology, 84: 197-219.
- Mason, B J and Seip, H M, 1985.  
The current state of knowledge on the acidification of surface waters and guidelines for future reserch. Ambio, 14(1): 45-51.
- Meier, M F, 1975.  
Application of remote-sensing techniques to the study of seasonal snow cover. Journal of Glaciology, 15: 251-265.
- Moore, R D and Owens, I F, 1984 (a).  
Modelling alpine snow accumulation and ablation using daily climate observations. Journal of Hydrology (NZ), 23(2): 73-83.

- Moore, R D and Owens, I F, 1984 (b).  
A conceptual runoff model for a mountainous rain-on-snow environment, Craigieburn, New Zealand. *Journal of Hydrology (NZ)*, 23(2): 84-99.
- Morris, E M, 1980.  
Forecasting flood flows in grassy and forested basins using a deterministic distributed mathematical model. *IAHS*, 129: 247-255.
- Morris, E M, 1982.  
Sensitivity of the European Hydrological System snow models. *IAHS*, 138: 221-231.
- Morris, E M, 1983.  
Modelling the flow of mass and energy within a snowpack for hydrological forecasting. *Annals of Glaciology*, 4: 198-203.
- Morris, E M, 1986.  
Modelling preferential elution of pollutants during snowmelt. *International Conference on Water Quality Modelling in the Inland Natural Environment*, Paper N2: 503-516.
- Morris, E M, Blyth, K and Clarke, R T, 1980.  
Watershed and river channel characteristics and their use in a mathematical model to predict flood hydrographs. In Froud, G (editor), *Remote Sensing Application in Agriculture and Hydrology*.
- Morris, E M and Godfrey, J, 1978.  
The European Hydrological System snow routine. In Colbeck, S C and Ray, M (editors), 1978. *Modelling of snow cover runoff*, CRREL, Hanover, NH: 26-28.
- Morris, E M and Thomas, A G, 1985.  
Preferential discharge of pollutants during snowmelt in Scotland. *Journal of Glaciology*, 31: 190-193.
- Morris, E M and Thomas, A G, 1985(b).  
Transient acid surges in an upland stream. *Proceedings of the International Symposium on Acid Precipitation, Muskoka, 15-20 September 1985*. Water, Air and Soil Pollution.

- Nash, J E and Sutcliffe, J V, 1970.  
River flow forecasting through conceptual models, Part I - a discussion of principles. *Journal of Hydrology*, 10: 282-290.
- Nemec, J, 1986.  
Hydrological forecasting. D Reidel Publishing Company.
- Natural Environment Research Council, 1975.  
Conceptual catchment modelling of isolated storm events. Vol I, Section 7.3 of the Flood Studies Report, NERC.
- Nolan, A J and Lilly, A, 1985.  
The soils of the Allt a Mharcaidh catchment. A Macauley Land Use Research Institute survey for the SWAP project.
- Obled, C and Rosse, B, 1977.  
Mathematical models of a melting snowpack at an index plot. *Journal of Hydrology*, 32: 139-163.
- Olyphant, G A and Isard, S A, 1987.  
Some characteristics of turbulent transfer over alpine surfaces during the snowmelt-growing season: Niwot Ridge, Front Range, Colorado, USA. *Arctic and Alpine Research*, 19(3): 261-269.
- Price, A G and Dunne, T, 1976.  
Energy balance computations of snowmelt in a subarctic area. *Water Resources Research*, 12(4): 686-694.
- Prowse, T D and Owens, I F, 1982.  
Energy balance over melting snow, Craigieburn Range, New Zealand. *Journal of Hydrology (NZ)*, 21(2): 133-147.
- Rango, A, 1988.  
Progress in developing an operational snowmelt-runoff forecast model with remote sensing input. *Nordic Hydrology*, 19: 65-76.

- Rango, A and Itten, K I, 1976  
Satellite potentials in snowcover monitoring and runoff prediction. *Nordic Hydrology*, 7: 209-230.
- Rango, A and Martinec, J, 1979.  
Application of a snowmelt-runoff model using Landsat data. *Nordic Hydrology*, 10: 225-238.
- Rango, A and Martinec, J, 1981.  
Accuracy of snowmelt-runoff simulation. *Nordic Hydrology*, 12(4/5): 265-274.
- Rango, A and Martinec, J, 1982.  
Snow accumulation derived from modified depletion curves of snow coverage. *IAHS*, 138: 83-90.
- Rasmussen, W and Ffolliott, F, 1979.  
Prediction of water yield using satellite imagery and a snowmelt simulation model. In Deutsch, Wiesnet and Rango (editors), *Satellite Hydrology*, American water resources association.
- Reed, D W, 1984.  
A review of British flood forecasting practice. Institute of Hydrology Report No 90.
- Rogers, C C M and Anderson, M G, 1986.  
Spatial variability of hillslope hydrological parameters and the problems of optimal model design. Final Report, NERC research grant GR3/4840.
- Rogers, C C M, Beren, K J, Morris, E M and Anderson, M G, 1985.  
Sensitivity analysis, calibration and predictive uncertainty of the Institute of Hydrology distributed model. *Journal of Hydrology*, 81: 179-191.
- Shafer, B, Leaf, C and Marron, J, 1979.  
Landsat derived snow cover as an input variable for snowmelt runoff forecasting in south central Colorado. In Deutsch, Wiesnet and Rango (editors), *Satellite Hydrology*, American water resources association.

- Skartveit, A and Gjessing, Y T, 1979.  
Chemical budgets and chemical quality of snow and runoff during spring snowmelt. *Nordic Hydrology* 10(2): 141-154.
- Speers, D D, Keuhl, D and Schermerhorn, V, 1978.  
Development of the operational snow band SSARR model. In Colbeck, S C and Ray, M (editors), *Modelling of Snow Cover Runoff*: 369-379.
- Spink, L V, 1980.  
A summary of summer snow surveys in Scotland: 1965-1978. *Journal of Hydrology*, 5: 105-111.
- Strangeways, I C, 1972.  
Automatic weather stations for network operation. *Weather*, 27(10): 403-408.
- Strangeways, I C, 1985.  
A cold region automatic weather station. *Journal of Hydrology*, 79: 323-332.
- Strangeways, I C and Wyatt, R J, 1990.  
A cold regions automatic weather station. Unpubl.
- Totts, H L, 1937.  
Snow surveys and runoff forecasting from photographs. *Transactions American Geophysical Union*, 34(3): 370-388.
- Ward, R G W, 1984.  
Avalanche predictions in Scotland: II. Development of a predictive model. *Applied Geography*, 4: 109-133.
- Wheater, H S, Bishop, K H and Bech, M B, 1986.  
The identification of conceptual hydrological models for surface water acidification. *Hydrological Processes*, 1(1): 89-109.
- Wiesnet, D R, 1974.  
The role of satellites in snow and ice measurement. NOAA Technical Memorandum NESS58, National Oceanic and Atmospheric Administration, US Department of Commerce, Washington DC.

Work, R A, Stockwell, H J, Freeman, T G and  
Beaumont, R T, 1965.

Accuracy of field snow surveys, western United States,  
including Alaska. Technical Report 163, CRREL,  
Hanover, NH.

World Meteorological Organisation, 1976.

International working seminar on snow studies by  
satellites. Final Report, Geneva.

World Meteorological Organisation, 1986.

Intercomparison of models of snowpack runoff.  
Operational Hydrology Report 23, Geneva.

## APPENDIX A

Datasets used for the model development.

Those with nine columns contain data collected from the AWS in the Allt a Mharcaidh. Columns represent: Minimum temperature; maximum temperature; next minimum temperature; mean temperature; net radiation; total incoming radiation; total precipitation; average windspeed and mean discharge.

Those with five columns contain data collected from a standard meteorological station. The columns represent:

Minimum temperature; maximum temperature; next minimum temperature; total precipitation and mean discharge.

MINTEM	MAXTEM	NMINTM	AVGTEM	INRADN	SOLRAD	TOTPPN	AVGW	SP	AVGFLOW
-7.5	-5.5	-7.6	-6.6	-60.5	0.0	0.0	2.0	0.091	
-7.6	-5.0	-6.0	-6.3	24.6	179.8	0.0	1.5	0.091	
-6.0	-4.2	-6.5	-4.8	55.0	248.7	0.0	1.4	0.090	
-6.5	-4.3	-4.5	-6.0	-42.5	0.0	0.0	2.1	0.091	
-4.5	-2.8	-2.0	-3.8	-42.4	0.0	0.0	1.3	0.091	
-2.0	0.8	-0.6	-0.6	23.4	137.0	0.0	1.2	0.091	
-0.6	1.6	-2.8	0.6	61.4	221.2	0.0	3.2	0.088	
-2.8	-1.8	-2.1	-2.3	-54.7	0.0	0.0	4.4	0.088	
-2.1	-1.4	-1.7	-1.8	-50.4	0.0	0.0	7.9	0.088	
-1.7	-0.6	-1.0	-1.1	17.5	141.2	0.0	9.0	0.088	
-1.0	1.4	1.4	0.6	23.6	147.0	0.0	11.4	0.091	
1.4	2.0	1.9	1.7	-23.2	0.0	0.0	12.0	0.091	
1.9	3.9	4.7	3.1	-10.2	0.0	0.5	13.1	0.091	
4.7	6.3	6.3	5.7	41.7	60.3	0.0	8.6	0.099	
6.3	6.9	5.7	6.6	60.7	79.4	0.0	6.1	0.181	
5.7	6.6	1.7	6.4	-6.0	0.0	0.0	6.7	0.536	
1.7	5.4	1.0	3.5	-17.3	0.0	0.5	5.8	0.992	
1.0	1.6	1.5	1.2	6.2	83.2	0.5	7.5	0.632	
1.5	2.0	1.6	1.6	23.0	132.9	0.0	11.5	0.357	
1.6	2.1	1.0	1.9	-14.3	0.0	0.0	7.1	0.267	
1.0	2.1	0.2	1.5	-16.3	0.0	0.0	6.4	0.213	
0.2	0.8	1.0	0.6	1.6	89.6	0.0	6.4	0.185	
1.0	1.7	1.3	1.3	11.5	138.9	1.0	6.3	0.170	
1.3	1.6	1.8	1.5	-13.6	0.0	0.0	6.7	0.155	
1.8	2.4	2.4	2.1	-12.8	0.0	0.0	5.6	0.143	
2.4	3.7	3.3	3.1	31.4	142.1	0.0	6.1	0.136	
3.3	3.8	2.7	3.6	56.1	153.4	0.0	7.0	0.134	
2.7	3.3	3.5	3.0	-32.1	0.0	0.0	9.3	0.135	
3.5	4.0	3.3	3.8	-44.9	0.0	0.0	11.8	0.135	
3.3	3.8	3.1	3.5	63.8	105.5	0.0	13.2	0.149	
3.1	3.7	2.7	3.5	106.6	150.2	0.0	11.8	0.316	
2.7	3.6	2.4	3.1	-12.6	0.3	1.5	12.7	0.677	
2.4	2.7	2.8	2.6	-12.1	0.0	1.0	11.2	0.685	
2.8	3.6	3.8	3.1	91.8	134.8	0.0	9.9	0.506	
3.8	4.4	3.3	4.1	122.7	173.5	0.0	8.0	0.587	
3.3	3.7	2.8	3.5	-18.8	0.0	0.0	5.4	0.611	
2.8	3.3	2.8	3.0	-8.6	0.0	1.0	4.4	0.435	
2.8	4.1	4.1	3.2	56.4	80.1	0.5	3.7	0.402	
4.1	4.8	2.8	4.4	93.1	138.7	0.0	2.9	0.461	
2.8	3.8	2.3	3.3	-40.1	0.0	0.0	5.0	0.478	
2.3	2.5	2.4	2.5	-46.8	0.0	0.0	10.6	0.335	
2.4	3.8	4.4	3.0	90.3	125.3	0.0	12.7	0.270	
4.4	5.9	4.6	5.2	72.7	102.3	0.5	12.1	0.338	
4.6	6.7	4.4	5.7	-15.7	0.0	0.0	12.6	0.696	
4.4	5.7	4.9	5.2	-36.3	0.0	0.0	11.3	0.921	
4.9	5.8	4.0	5.2	172.3	226.4	0.0	10.0	1.014	
4.0	4.8	1.0	4.4	119.7	184.8	0.0	9.6	1.278	
1.0	3.8	0.1	2.4	-44.1	0.1	0.0	13.2	0.849	
0.1	3.3	0.8	1.2	-57.1	0.0	0.0	9.8	0.481	
0.8	3.0	1.3	2.0	124.9	181.6	0.0	6.4	0.343	
1.3	2.7	2.1	2.3	133.4	206.4	0.0	12.1	0.289	
2.1	2.5	2.5	2.3	-10.7	0.0	0.0	13.3	0.262	
2.5	4.1	5.6	3.0	-22.6	0.1	0.0	14.2	0.264	
5.6	6.5	6.2	6.3	47.6	75.0	0.0	11.9	0.371	
6.2	7.1	6.0	6.7	79.8	121.8	0.0	10.1	0.956	
6.0	6.6	6.1	6.3	-7.5	0.0	0.0	10.1	1.536	
6.1	6.7	6.1	6.4	-10.6	0.0	0.0	14.2	1.698	
6.1	6.5	6.4	6.3	31.5	53.2	0.0	13.8	1.714	
6.4	6.9	6.1	6.7	48.0	78.0	0.0	12.4	1.618	
6.1	6.4	4.7	6.2	-13.6	0.2	0.0	14.1	1.782	
4.7	6.1	4.7	5.5	-11.0	0.0	0.0	11.4	1.935	
4.7	5.0	4.2	4.8	60.0	87.3	1.0	10.7	2.040	
4.2	5.8	2.8	5.0	87.2	132.1	0.0	7.3	1.651	
2.8	3.8	0.5	3.4	-40.2	0.2	0.5	6.3	0.961	
0.5	3.1	-0.2	1.8	-25.6	0.0	0.5	5.1	0.725	

-0.5	0.7	-1.3	0.1	-5.5	0.0	0.0	2.2	0.202
-1.3	-0.5	-0.3	-0.8	-8.0	0.8	0.0	1.6	0.193
-0.3	1.3	1.9	0.6	51.8	213.3	3.0	2.0	0.186
1.9	3.8	0.0	2.8	141.9	349.9	0.0	2.5	0.193
0.0	0.7	0.1	0.4	-34.2	0.0	0.0	2.2	0.209
0.1	0.4	0.7	0.3	-10.0	2.5	0.0	1.9	0.198
0.7	3.6	1.0	2.0	154.8	277.5	0.5	2.5	0.187
1.0	3.1	-0.2	1.7	93.4	150.4	0.0	3.6	0.191
-0.2	0.6	-0.4	0.0	-15.7	0.0	0.0	2.5	0.197
-0.4	-0.2	-0.3	-0.2	-9.1	3.0	0.0	2.8	0.189
-0.3	1.8	1.5	0.7	117.3	220.3	1.0	4.1	0.181
1.5	2.5	0.1	2.1	109.5	179.3	0.0	4.2	0.181
0.1	0.7	-0.2	0.4	-12.7	0.0	0.0	2.8	0.182
-0.2	0.3	0.0	0.0	-7.7	5.3	0.0	3.8	0.176
0.0	1.9	1.1	1.2	130.5	263.8	0.0	3.6	0.173
1.1	2.5	-1.3	1.9	125.7	225.9	0.0	3.0	0.177
-1.3	0.6	-2.2	-0.4	-54.2	0.0	0.0	2.0	0.181
-2.2	-0.4	0.4	-1.3	-25.7	7.0	0.0	3.5	0.172
0.4	2.3	0.5	1.6	185.8	361.4	0.0	5.1	0.166
0.5	2.6	-1.1	1.9	147.1	282.0	0.0	6.2	0.167
-1.1	-0.2	-0.7	-0.8	-54.3	0.0	0.0	5.1	0.166
-0.7	-0.6	-0.1	-0.7	-46.8	11.1	0.0	6.7	0.161
-0.1	3.9	2.4	2.0	306.4	479.3	0.0	6.8	0.158
2.4	4.3	-0.2	3.8	208.0	334.8	0.0	5.5	0.163
-0.2	1.1	0.7	0.2	-42.2	0.0	0.0	5.7	0.175
0.7	1.5	2.1	0.9	-5.8	6.8	0.0	4.3	0.166
2.1	3.2	0.8	2.6	84.5	124.7	1.0	5.7	0.162
0.8	2.7	-0.5	1.8	138.1	194.1	0.5	8.0	0.188
-0.5	0.7	-1.2	0.0	-15.0	0.0	0.0	8.0	0.206
-1.2	-0.3	-1.0	-0.8	-11.8	4.4	0.0	7.2	0.184
-1.0	0.4	-0.1	-0.3	100.5	156.2	0.0	5.2	0.169
-0.1	0.9	-1.9	0.5	85.5	141.2	0.0	3.8	0.158
-1.9	-0.4	-1.3	-1.2	-31.8	0.0	0.0	1.3	0.154
-1.3	0.2	0.4	-0.3	-11.7	6.1	0.0	3.0	0.149
0.4	3.5	3.0	2.0	85.7	124.6	0.0	6.5	0.147
3.0	4.2	1.8	3.5	73.8	106.6	0.5	6.1	0.150
1.8	2.5	1.1	2.1	-6.3	0.0	0.0	3.5	0.167
1.1	1.4	1.6	1.3	-6.0	13.1	0.0	1.9	0.173
1.6	3.9	1.6	2.6	205.5	299.9	2.0	1.9	0.166
1.6	4.4	-0.2	3.0	84.7	125.7	0.5	2.1	0.182
-0.2	1.5	-0.8	0.6	-14.0	0.0	0.0	2.4	0.197
-0.8	-0.1	0.2	-0.5	-7.5	14.1	0.0	1.0	0.180
0.2	2.7	1.4	1.8	283.4	401.3	0.5	2.5	0.166
1.4	3.1	1.2	2.3	179.3	257.9	0.0	8.1	0.178
1.2	1.4	1.5	1.3	-21.6	0.0	0.0	10.7	0.200
1.5	2.1	2.1	1.8	-12.5	8.9	0.0	7.5	0.180
2.1	2.7	1.2	2.3	80.7	137.7	0.5	4.0	0.166
1.2	2.4	-0.1	1.7	88.9	129.6	0.0	5.1	0.156
-0.1	1.1	-0.9	0.6	-11.6	0.0	0.0	4.5	0.155
-0.9	-0.4	-0.2	-0.7	-7.5	18.0	0.0	6.2	0.149
-0.2	1.0	0.4	0.3	62.0	321.4	0.0	7.8	0.146
0.4	1.5	0.1	0.8	54.7	259.3	0.0	6.8	0.150
0.1	0.8	0.0	0.4	-7.4	0.1	0.0	7.0	0.150
0.0	0.5	-0.2	0.2	-6.1	5.8	0.0	9.0	0.148
-0.2	0.1	-0.2	0.0	13.2	132.7	0.0	9.2	0.144
-0.2	0.1	-0.8	-0.1	6.4	96.0	0.0	9.5	0.142
-0.8	-0.5	-1.4	-0.7	-9.4	0.0	0.0	7.8	0.139
-1.4	-0.8	-0.6	-1.1	-14.1	11.9	0.0	5.2	0.135
-0.6	1.5	1.1	0.6	76.4	398.7	0.0	6.0	0.134
1.1	1.9	-3.5	1.5	56.2	251.8	0.0	4.3	0.137
-3.5	0.4	-3.3	-2.1	-58.1	0.4	0.0	2.4	0.137
-3.3	-2.6	-2.0	-3.0	-39.0	24.6	0.0	3.1	0.133
-2.0	3.4	1.8	1.3	230.8	571.9	0.0	4.5	0.129
1.8	3.3	1.3	2.3	124.5	239.1	0.5	4.2	0.148
1.3	1.6	0.9	1.5	-15.6	0.5	0.0	2.7	0.173
0.9	1.8	2.2	1.5	-2.6	26.7	0.0	2.2	0.158

2.2	3.8	2.9	3.1	257.8	409.4	0.0	7.0	0.149
2.9	4.1	2.7	3.6	136.5	193.3	1.5	12.9	0.209
2.7	3.7	3.2	3.1	-14.1	0.0	1.0	16.3	0.314
3.2	4.7	4.0	3.7	-3.6	7.7	3.5	13.5	0.318
4.0	5.8	3.7	4.6	170.3	231.7	2.5	4.3	0.523
3.7	6.1	1.8	5.1	143.3	201.4	0.0	4.9	0.632
1.8	3.0	0.3	2.3	-42.9	0.7	0.0	3.7	0.537
0.3	1.1	2.2	0.7	-31.4	26.7	0.0	3.2	0.325
2.2	6.6	4.5	5.1	402.2	547.5	0.5	2.4	0.245
4.5	7.3	0.2	6.0	220.5	331.1	0.0	3.5	0.278
0.2	2.9	0.0	1.5	-35.7	0.2	0.0	1.7	0.336
0.0	1.0	1.0	0.6	-7.8	3.5	0.0	2.7	0.251
1.0	1.3	1.5	1.1	33.7	149.7	5.5	4.6	0.211
1.5	1.9	1.5	1.8	10.6	154.7	7.0	2.7	0.200
1.5	1.7	1.4	1.6	-7.6	0.0	0.0	1.0	0.192
1.4	1.8	2.2	1.6	-8.8	20.7	0.0	1.0	0.184
2.2	8.1	4.4	4.6	154.4	472.3	0.0	1.1	0.179
4.4	7.7	1.3	6.4	181.6	378.2	0.0	2.7	0.369
1.3	3.9	1.1	2.3	-46.4	0.3	0.0	1.5	0.423
1.1	2.7	4.4	1.6	-19.9	33.1	0.0	1.9	0.273
4.4	8.3	5.2	6.8	378.4	525.0	0.0	1.4	0.219
5.2	9.0	2.6	7.4	200.5	291.9	0.0	2.8	0.266
2.6	4.6	1.0	3.5	-35.7	1.2	0.0	1.8	0.330
1.0	2.0	2.6	1.4	0.8	16.3	0.0	1.4	0.258
2.6	6.6	4.4	5.2	206.5	291.4	0.5	2.0	0.216
4.4	6.8	1.9	5.7	103.8	154.2	0.0	3.9	0.241
1.9	3.1	2.5	2.3	-12.2	0.0	0.0	3.9	0.278
2.5	2.9	3.1	2.6	-3.5	13.7	2.0	6.9	0.249
3.1	4.9	5.7	4.0	174.4	236.2	2.0	7.1	0.271
5.7	6.5	4.7	6.1	222.6	306.3	0.0	6.6	0.460
4.7	5.4	4.1	5.0	-15.4	1.2	0.0	7.2	0.540
4.1	4.9	4.7	4.6	1.3	24.4	0.0	7.0	0.414
4.7	5.6	5.6	5.1	150.3	206.4	0.5	5.2	0.398
5.6	7.3	4.2	6.4	142.2	216.0	0.0	5.4	0.530
4.2	5.8	3.4	5.1	-39.1	2.5	0.0	8.5	0.566
3.4	3.8	3.9	3.6	-8.9	19.2	0.0	11.3	0.433
3.9	6.0	4.0	5.0	227.3	314.5	0.5	9.8	0.360
4.0	7.4	2.1	5.7	138.4	207.9	1.5	5.9	0.638
2.1	3.2	2.0	2.5	-51.3	1.4	0.0	6.2	0.564
2.0	2.5	3.0	2.1	-4.6	45.6	0.0	6.1	0.376
3.0	5.3	3.2	4.3	347.6	463.5	0.0	7.7	0.310
3.2	5.8	2.4	4.4	148.6	224.0	0.5	7.2	0.308
2.4	2.9	2.8	2.6	-45.4	1.7	0.0	7.0	0.303
2.8	3.1	5.1	3.0	-1.0	17.1	0.5	11.1	0.276
5.1	8.7	9.1	7.5	169.1	224.6	0.5	11.5	0.268
9.1	9.7	9.0	9.5	42.7	60.9	0.0	8.6	0.605
9.0	9.6	7.8	9.3	-7.7	0.0	0.0	8.5	1.192
7.8	9.0	8.4	8.6	-11.2	8.6	0.0	9.3	1.466
8.4	11.1	11.5	9.7	396.5	531.9	0.0	12.0	1.489
11.5	13.1	8.1	12.5	381.2	550.2	0.0	9.7	1.830
8.1	10.7	6.6	8.9	-35.8	23.6	0.0	7.1	1.608
6.6	7.6	7.8	7.1	-51.0	8.6	0.0	4.9	1.033
7.8	13.2	12.7	10.9	343.7	478.9	0.0	7.1	0.890
12.7	14.6	7.3	14.0	306.7	450.1	0.0	6.1	1.305
7.3	10.4	5.6	8.9	-12.0	3.9	0.5	3.6	1.307
5.6	6.8	5.6	6.1	-5.1	1.1	0.0	3.0	1.034
5.6	8.5	7.4	6.9	76.4	111.4	0.0	2.3	0.898
7.4	9.8	5.8	9.0	88.8	128.8	0.5	3.8	0.899
5.8	6.9	5.9	6.3	-12.2	3.7	0.5	4.8	0.912
5.9	6.8	7.1	6.3	-3.7	3.7	0.0	2.9	0.844
7.1	10.1	8.3	8.7	211.1	305.4	0.0	3.5	0.790
8.3	10.4	6.8	9.6	355.5	506.0	0.0	6.6	0.893
6.8	7.3	6.8	7.1	-22.4	14.8	0.0	5.5	0.932
6.8	7.4	6.9	7.1	-20.8	5.1	0.0	5.3	0.779
6.9	8.8	6.2	7.7	159.4	218.8	3.5	6.4	0.766
6.2	7.8	5.7	6.9	91.5	128.6	0.0	4.6	0.998

5.7	6.8	5.3	6.1	-12.3	0.1	1.0	3.3	0.832
5.3	6.7	5.8	5.9	-9.2	11.8	1.0	4.5	0.760
5.8	9.6	9.5	7.5	284.8	392.5	0.0	5.8	0.721
9.5	10.9	7.5	9.9	324.1	455.0	0.0	6.9	0.795
7.5	8.9	6.1	7.9	-14.9	25.9	0.0	5.1	0.847
6.1	7.8	4.7	6.8	-21.9	1.5	0.0	2.5	0.711
4.7	5.3	4.1	4.9	19.6	34.0	7.0	4.2	0.726
4.1	6.3	3.4	5.4	67.1	99.4	1.5	4.9	0.961
3.4	4.7	5.1	3.9	-9.7	7.5	2.5	10.9	0.790
5.1	5.7	5.9	5.5	-11.2	14.9	0.0	8.8	0.718
5.9	9.1	7.5	7.7	192.8	276.1	0.0	5.7	0.674
7.5	10.0	6.2	8.9	150.4	234.3	0.0	5.8	0.708
6.2	7.1	6.1	6.6	-22.1	6.9	0.0	5.2	0.676
6.1	7.0	7.3	6.4	-33.2	12.9	0.0	6.3	0.594
7.3	8.3	7.9	7.9	103.3	163.7	0.0	7.0	0.539
7.9	10.0	8.5	9.0	183.3	260.5	0.0	8.9	0.619
8.5	8.9	8.0	8.7	-23.7	5.3	0.5	6.6	0.715
8.0	8.6	8.5	8.2	-10.6	5.7	0.0	9.6	0.668
8.5	10.0	9.3	9.5	158.6	218.0	1.0	9.7	0.838
9.3	10.1	7.6	9.8	127.1	184.2	0.0	9.7	0.950
7.6	9.2	6.5	8.2	-7.1	13.1	0.5	9.1	0.930
6.5	7.6	6.3	7.2	-9.9	1.0	0.5	6.9	0.824
6.3	7.0	7.5	6.6	49.3	74.6	0.5	7.5	0.750
7.5	8.5	4.0	8.0	112.6	168.2	0.0	6.5	0.704
4.0	7.5	5.9	5.6	-24.9	12.4	0.0	3.0	0.665
5.9	6.9	7.4	6.4	-12.4	5.2	2.0	6.1	0.594
7.4	10.2	8.2	8.8	278.0	376.8	1.0	8.1	0.590
8.2	10.8	6.7	9.4	234.1	336.8	0.5	9.1	0.700
6.7	7.8	6.7	7.0	-24.2	9.8	0.5	8.1	0.729

-7.6	-4.2	-4.5	-5.9	-5.8	107.1	0.0	1.7	0.091
-4.5	1.6	-2.1	-1.5	-3.1	89.5	0.0	2.5	0.088
-2.1	2.0	1.9	-0.2	-8.1	72.0	0.0	10.1	0.091
1.9	6.9	1.0	5.4	21.6	34.9	0.5	8.6	0.532
1.0	5.4	0.2	2.1	-0.6	54.0	1.0	8.0	0.299
0.2	2.1	1.8	1.2	-4.2	57.1	1.0	6.4	0.157
1.8	3.8	2.7	2.9	10.6	73.9	0.0	7.0	0.135
2.7	4.0	2.4	3.5	28.2	64.0	1.5	12.4	0.507
2.4	4.4	2.8	3.3	45.9	77.1	1.0	8.6	0.519
2.8	4.8	2.3	3.5	25.2	54.7	1.5	4.0	0.402
2.3	6.7	1.0	4.1	25.1	56.9	0.5	12.0	0.640
1.0	5.8	0.1	4.3	52.9	102.8	0.0	11.0	0.830
0.1	3.3	2.5	2.0	47.6	97.0	0.0	10.4	0.281
2.5	7.1	6.1	5.6	24.3	49.2	0.0	11.6	1.323
6.1	6.9	2.8	6.4	13.9	32.9	0.0	13.6	1.776
2.8	6.1	-0.2	4.7	24.0	54.9	1.5	8.9	1.191
-0.2	4.0	-0.2	2.1	69.4	149.7	0.5	7.7	0.484
-0.2	3.8	-1.4	2.3	9.0	59.8	0.5	8.0	0.342
-1.4	5.4	-0.1	2.5	59.6	127.4	0.0	6.9	0.277
-0.1	4.1	-0.2	1.4	4.2	39.2	1.0	13.3	0.260
-0.2	4.5	0.6	2.8	15.2	64.8	9.5	7.4	0.410
0.6	7.9	-1.1	5.1	14.3	30.5	3.5	10.3	1.488
-1.1	0.5	-2.5	-0.4	-8.0	76.4	0.0	6.0	0.403
-2.5	0.8	0.4	-0.6	0.5	145.8	0.5	5.6	0.322
0.4	2.0	0.0	1.2	-9.2	73.3	0.5	6.4	0.286
0.0	2.8	1.0	1.4	5.9	132.8	0.0	7.4	0.261
1.0	3.7	0.7	2.1	2.1	92.3	1.5	8.8	0.234
0.7	3.7	0.7	2.2	4.0	146.0	0.0	8.6	0.226
0.7	3.6	-2.0	2.0	31.3	108.7	1.0	4.9	0.221
-2.0	2.4	-3.3	0.3	24.8	127.2	0.5	4.3	0.206
-3.3	2.8	-1.4	0.0	17.1	106.1	0.0	2.6	0.191
-1.4	5.6	-0.5	1.4	60.3	138.8	0.0	2.6	0.186
-0.5	5.2	-1.3	1.3	54.9	100.7	1.5	1.5	0.193
-1.3	3.8	-0.2	0.7	37.9	141.0	3.0	2.1	0.197
-0.2	3.6	-0.4	1.0	55.6	107.6	0.5	2.6	0.190
-0.4	2.5	-1.3	0.7	51.2	100.6	1.0	3.5	0.179
-1.3	2.5	-2.2	0.7	48.6	123.7	0.0	3.1	0.175
-2.2	2.6	-0.7	0.3	63.2	162.6	0.0	5.0	0.164
-0.7	4.3	-0.5	1.3	106.4	206.3	0.0	6.2	0.166
-0.5	3.2	-1.9	1.3	50.4	81.4	1.5	6.5	0.186
-1.9	0.9	-1.3	-0.4	35.6	75.5	0.0	4.4	0.154
-1.3	4.2	-0.2	1.8	35.4	59.3	0.5	4.8	0.162
-0.2	4.4	-0.8	1.9	67.6	109.7	2.5	2.1	0.181
-0.8	3.1	-0.1	1.2	108.4	168.3	0.5	5.5	0.181
-0.1	2.7	-0.9	1.6	36.4	69.1	0.5	5.3	0.154
-0.9	1.5	-0.8	0.2	25.4	149.7	0.0	7.0	0.148
-0.8	0.5	-3.5	-0.1	1.0	58.6	0.0	8.9	0.138
-3.5	1.9	-3.3	-0.3	15.1	165.7	0.0	4.5	0.135
-3.3	3.4	0.9	0.5	75.2	209.0	0.5	3.6	0.154
0.9	4.1	1.8	2.8	94.4	157.4	2.5	9.6	0.283
1.8	6.1	0.2	3.9	66.8	110.4	6.0	6.6	0.482
0.2	7.3	0.0	3.3	138.9	226.4	0.5	2.7	0.272
0.0	1.9	1.3	1.3	7.2	77.0	12.5	2.8	0.192
1.3	8.1	1.1	3.7	70.2	217.9	0.0	1.6	0.317
1.1	9.0	1.0	4.8	130.8	212.8	0.0	2.0	0.268
1.0	6.8	2.5	3.7	74.7	115.5	0.5	2.8	0.249
2.5	6.5	4.1	4.4	94.5	139.4	4.0	6.9	0.437
4.1	7.3	2.1	5.3	63.7	112.3	0.5	6.5	0.478
2.1	7.4	2.0	4.2	76.4	135.7	2.0	8.3	0.480
2.0	5.8	2.8	3.3	111.6	183.7	0.5	7.0	0.292
2.8	9.7	7.8	7.3	50.8	75.7	1.0	9.9	1.036
7.8	13.1	6.6	9.9	182.7	278.6	0.0	9.5	1.419
6.6	14.6	5.6	10.2	146.9	235.3	0.5	5.4	1.135
5.6	9.8	5.9	7.1	37.0	61.2	1.0	3.5	0.873
5.9	10.4	5.7	7.9	135.1	207.5	0.0	4.6	0.844
5.7	8.8	5.3	6.9	54.4	88.1	4.5	4.9	0.837

-1.2	0.9	-1.1	-0.5	42.5	42.2	2.0	2.4	0.185
-1.1	5.4	-0.8	2.1	78.3	100.9	5.0	4.5	0.243
-0.8	4.5	-1.0	1.0	125.9	151.4	0.5	4.1	0.204
-1.0	2.9	-1.8	0.6	60.2	113.6	5.0	4.6	0.201
-1.8	5.1	1.8	2.3	149.6	200.4	0.5	4.8	0.418
1.8	7.7	2.7	5.4	77.2	87.4	3.0	5.4	0.754
2.7	8.5	1.5	6.3	73.1	89.1	0.0	8.7	0.659
1.5	9.0	1.1	5.7	138.9	199.3	0.5	5.3	0.610
1.1	9.0	1.3	4.4	114.8	172.6	0.0	3.0	0.437
1.3	16.1	7.3	8.8	152.6	219.1	0.0	3.6	0.482
7.3	11.2	4.8	9.4	105.3	158.1	0.0	6.1	0.678
4.8	7.9	2.1	6.5	116.3	157.4	0.0	8.1	0.558
2.1	5.6	5.4	3.8	94.7	111.2	0.0	5.6	0.398
5.4	8.3	5.8	6.5	80.5	93.3	0.0	4.9	0.386
5.8	10.3	7.2	7.6	88.6	120.0	0.0	6.4	0.352
7.2	11.5	4.3	9.1	97.7	138.2	0.0	5.5	0.341
4.3	13.9	7.1	9.6	61.8	95.6	0.0	2.2	0.297

Dee 1984

-0.90	3.60	-6.30	0.10	4.4000
-6.30	6.80	-2.30	0.00	4.7000
-2.30	4.30	-0.20	0.00	4.4000
-0.20	5.60	-4.20	0.00	4.4000
-4.20	8.60	-2.70	0.00	5.0000
-2.70	4.10	-1.80	0.20	5.0000
-1.80	4.70	2.00	0.70	6.6000
2.00	6.30	2.70	0.20	13.6000
2.70	7.20	1.60	1.20	18.2000
1.60	6.40	1.70	1.80	34.3000
1.70	5.20	-0.90	0.10	18.2000
-0.90	7.70	3.60	0.50	24.9000
3.60	10.80	5.90	0.00	56.1000
5.90	10.10	0.20	0.90	53.2000
0.20	8.10	0.00	2.40	21.8000
0.00	6.60	-2.30	1.30	15.7000
-2.30	8.60	2.60	1.40	14.1000
2.60	9.60	5.20	0.10	31.4000
5.20	12.60	3.50	0.00	41.6000
3.50	12.70	7.40	0.00	54.5000
7.40	12.20	-2.20	0.00	55.9000
-2.20	13.10	-2.00	0.00	30.3000
-2.00	16.60	-0.70	0.00	27.2000
-0.70	22.70	0.80	0.00	32.9000
0.80	22.20	0.70	0.00	38.8000
0.70	24.50	0.80	0.00	34.2000
0.80	23.40	-0.40	0.00	31.5000
-0.40	19.10	1.20	0.00	29.4000
1.20	14.70	0.10	0.00	25.6000
0.10	12.20	-1.10	0.00	19.5000
-1.10	15.40	-1.80	0.00	15.8000
-1.80	15.70	-1.40	1.50	15.6000
-1.40	13.70	-1.20	0.70	14.6000
-1.20	15.10	-0.30	0.10	14.0000
-0.30	11.80	3.30	0.50	13.9000
3.30	6.70	0.10	0.00	11.2000
0.10	6.60	-1.00	0.00	9.1000
-1.00	12.70	2.70	0.00	8.4000
2.70	10.20	3.30	2.40	8.8000
3.30	8.30	4.20	0.10	11.0000
4.20	11.10	4.00	0.00	9.2000
4.00	14.50	1.80	0.00	8.9000
1.80	17.20	1.90	0.00	9.8000
1.90	16.10	2.40	0.00	10.6000
2.40	15.30	0.60	0.00	9.1000
0.60	11.30	4.40	0.00	7.8000
4.40	13.80	4.90	0.00	7.5000
4.90	14.20	0.40	0.00	7.9000
0.40	15.10	2.20	0.00	7.7000
2.20	10.90	4.30	4.10	7.5000
4.30	12.80	6.70	1.70	6.9000
6.70	16.30	7.00	0.00	11.5000
7.00	21.30	4.60	0.00	13.5000
4.60	16.60	4.10	0.40	10.6000
4.10	9.80	2.40	0.20	8.9000
2.40	8.40	1.50	1.00	6.3000
1.50	11.50	4.00	0.00	5.4000
4.00	15.50	0.30	0.00	5.6000
0.30	17.30	1.30	0.00	6.0000
1.30	15.70	8.40	0.00	5.8000

Dee 1986

-7.60	-4.20	-4.50	0.00	2.3300	5.30	10.90	3.40	1.00	30.7100
-4.50	1.60	-2.10	0.00	2.4700	3.40	7.80	5.10	10.50	37.9000
-2.10	2.00	1.90	0.00	3.2100	5.10	10.00	6.10	0.00	28.2800
1.90	6.90	1.00	0.50	14.7000	6.10	10.00	7.60	0.50	27.1300
1.00	5.40	0.20	1.00	22.4500	7.60	10.10	4.00	1.50	55.5600
0.20	2.10	1.80	1.00	10.2400	4.00	8.50	5.90	1.00	40.9300
1.80	3.80	2.70	0.00	7.8700	5.90	10.80	3.60	4.00	46.0700
2.70	4.00	2.40	1.50	16.2300					
2.40	4.40	2.80	1.00	24.1100					
2.80	4.80	2.30	1.50	21.7300					
2.30	6.70	1.00	0.50	16.1700					
1.00	5.80	0.10	0.00	20.2200					
0.10	3.30	2.50	0.00	12.0100					
2.50	7.10	6.10	0.00	42.4000					
6.10	6.90	2.80	0.00	78.8900					
2.80	6.10	-0.20	1.50	61.1000					
-0.20	4.00	-0.20	0.50	21.8700					
-0.20	3.80	-1.40	0.50	14.9000					
-1.40	5.40	-0.10	0.00	12.2800					
-0.10	4.10	-0.20	1.00	13.0000					
-0.20	4.50	0.60	9.50	22.5200					
0.60	7.90	-1.10	3.50	73.3500					
-1.10	0.50	-2.50	0.00	21.6100					
-2.50	0.80	0.40	0.50	14.9800					
0.40	2.00	0.00	0.50	12.1700					
0.00	2.80	1.00	0.00	10.9800					
1.00	3.70	0.70	1.50	12.1000					
0.70	3.70	0.70	0.00	10.7900					
0.70	3.60	-2.00	1.00	10.9100					
-2.00	2.40	-3.30	0.50	8.9600					
-3.30	2.80	-1.40	0.00	7.7400					
-1.40	5.60	-0.50	0.00	7.4500					
-0.50	5.20	-1.30	1.50	7.7500					
-1.30	3.80	-0.20	3.00	7.4100					
-0.20	3.60	-0.40	0.50	7.0600					
-0.40	2.50	-1.30	1.00	6.5200					
-1.30	2.50	-2.20	0.00	6.0700					
-2.20	2.60	-0.70	0.00	5.6000					
-0.70	4.30	-0.50	0.00	5.5600					
-0.50	3.20	-1.90	1.50	6.4400					
-1.90	0.90	-1.30	0.00	5.4300					
-1.30	4.20	-0.20	0.50	6.4600					
-0.20	4.40	-0.80	2.50	7.8400					
-0.80	3.10	-0.10	0.50	6.3600					
-0.10	2.70	-0.90	0.50	6.2300					
-0.90	1.50	-0.80	0.00	5.3300					
-0.80	0.50	-3.50	0.00	4.4900					
-3.50	1.90	-3.30	0.00	5.6600					
-3.30	3.40	0.90	0.50	6.7100					
0.90	4.10	1.80	2.50	7.4500					
1.80	6.10	0.20	6.00	16.3300					
0.20	7.30	0.00	0.50	10.8800					
0.00	1.90	1.30	12.50	8.5100					
1.30	8.10	1.10	0.00	8.2000					
1.10	9.00	1.00	0.00	9.2900					
1.00	6.80	2.50	0.50	11.0600					
2.50	6.50	4.10	4.00	13.4700					
4.10	7.30	2.10	0.50	17.9600					
2.10	7.40	2.00	2.00	20.1100					
2.00	5.80	2.80	0.50	13.6700					
2.80	9.70	7.80	1.00	39.2200					
7.80	13.10	6.60	0.00	55.7600					
6.60	14.60	5.60	0.50	37.6200					
5.60	9.80	5.90	1.00	32.9500					
5.90	10.40	5.70	0.00	35.4400					
5.70	8.80	5.30	4.50	35.6000					

## Gairn 1979

0.60	8.50	1.40	5.80	10.2600
1.40	12.40	4.30	0.30	18.8900
4.30	11.20	5.30	0.00	26.8500
5.30	9.80	2.50	0.00	22.7700
2.50	13.10	3.10	9.00	13.5800
3.10	9.90	3.40	0.10	19.1000
3.40	7.70	-1.60	0.00	11.1200
-1.60	12.30	0.00	0.00	9.1900
0.00	11.10	7.40	0.10	11.2800
7.40	12.20	3.30	0.00	15.0000
3.30	11.20	2.10	1.70	10.3700
2.10	8.10	3.30	0.20	8.8400
3.30	9.00	1.10	1.30	7.5400
1.10	7.30	2.10	0.80	7.0900
2.10	7.20	2.00	1.60	9.9000
2.00	7.80	3.00	0.20	10.4700
3.00	8.30	-1.60	0.00	7.5100
-1.60	9.40	4.90	0.30	7.7600
4.90	12.80	6.40	0.10	9.3800
6.40	9.60	-0.70	3.10	9.0500
-0.70	4.50	-2.50	0.30	6.4100
-2.50	4.50	-0.50	1.00	5.1400
-0.50	3.60	-2.60	2.60	5.0100
-2.60	4.80	-1.80	0.30	4.6100
-1.80	4.90	-2.00	1.50	4.2800
-2.00	7.00	-0.20	5.60	4.5100
-0.20	8.60	-0.20	0.60	4.6900
-0.20	8.50	-2.40	1.90	5.5400
-2.40	10.20	-1.00	1.10	7.0000
-1.00	8.20	-5.70	0.10	5.3200
-5.70	11.70	5.80	0.40	5.3800
5.80	14.10	6.90	0.50	7.2200
6.90	18.50	8.80	0.00	9.6000
8.80	19.70	11.90	0.00	15.6600
11.90	13.00	6.10	0.80	12.1700
6.10	12.50	1.70	0.00	7.3500
1.70	9.40	4.60	16.50	6.8600
4.60	7.70	2.30	6.80	10.9500
2.30	7.50	0.40	2.40	6.4900
0.40	11.00	4.20	0.00	4.5900
4.20	15.40	5.80	5.50	4.6500
5.80	12.70	4.60	0.10	8.3100
4.60	13.70	-1.00	0.00	5.7700
-1.00	11.00	5.60	5.70	6.7100
5.60	13.30	-1.90	1.20	5.5000
-1.90	13.60	-1.60	3.20	5.3100
-1.60	13.60	2.30	0.00	5.0900
2.30	12.60	2.90	0.40	6.1500
2.90	13.40	5.90	2.50	7.1300
5.90	13.90	8.30	2.40	7.0800
8.30	16.30	7.20	4.80	6.3800
7.20	13.50	2.70	0.00	6.5800

## Gairn 1980

2.40	8.00	3.00	0.50	8.5800
3.00	7.70	-0.40	4.80	8.7000
-0.40	5.20	1.00	0.40	6.9400
1.00	5.90	1.30	0.00	4.5300
1.30	5.40	1.60	1.10	6.8000
1.60	10.00	-3.50	1.00	7.2900
-3.50	9.70	2.20	0.60	7.9700
2.20	7.40	1.80	0.00	7.9800
1.80	9.00	-0.70	1.20	6.7000
-0.70	11.20	3.90	0.10	6.4500
3.90	12.90	-5.60	0.00	8.0200
-5.60	16.20	-5.30	0.00	8.0200
-5.30	15.50	0.90	0.10	6.8800
0.90	8.00	0.80	0.10	5.8000
0.80	7.40	3.60	0.20	4.3000
3.60	11.00	4.10	0.50	4.9100
4.10	9.40	2.10	0.00	4.6000
2.10	11.90	5.00	0.00	4.4300
5.00	14.80	4.30	0.00	4.9300
4.30	17.40	3.80	0.00	6.9800
3.80	11.90	0.50	0.00	5.7400
0.50	16.60	1.90	0.00	5.2400
1.90	11.60	0.70	1.30	5.2200
0.70	9.60	5.80	0.00	4.5600
5.80	15.20	2.40	0.00	8.3300
2.40	5.60	0.80	0.00	6.0400
0.80	7.80	-5.20	0.00	4.1800
-5.20	8.40	3.10	1.30	3.3700
3.10	10.20	6.00	1.20	3.7800
6.00	12.20	2.60	0.10	3.8500
2.60	11.20	-3.60	0.30	3.5700
-3.60	14.80	-3.50	0.00	3.1900
-3.50	14.30	5.10	0.00	2.9700
5.10	12.10	2.80	4.50	2.9000
2.80	11.30	-0.80	0.00	2.8100
-0.80	10.20	5.20	0.70	2.7300
5.20	10.40	3.00	0.00	2.9100
3.00	14.60	3.50	0.00	2.8500
3.50	14.30	-1.10	0.00	2.8600
-1.10	15.00	2.20	0.00	2.7400
2.20	15.10	2.10	0.00	2.6400
2.10	15.50	3.90	0.00	2.5300
3.90	7.10	2.70	2.10	2.4100
2.70	4.40	-1.50	1.90	2.3400
-1.50	10.50	2.40	0.00	1.8800
2.40	12.50	5.40	0.00	1.7100
5.40	15.30	6.50	0.00	1.7600
6.50	19.80	6.80	0.00	2.0200
6.80	21.60	9.60	0.00	2.4300
9.60	22.30	4.70	0.00	2.9100
4.70	20.80	-1.00	0.00	2.4000
-1.00	22.30	-1.30	0.00	2.0800
-1.30	24.40	-3.80	0.00	1.9000

## Gairn 1981

0.30	12.80	5.20	2.10	17.8800
5.20	8.60	2.10	0.60	17.1700
2.10	8.20	-0.40	0.80	5.5200
-0.40	11.40	4.70	0.70	6.2600
4.70	15.30	5.50	0.30	9.4900
5.50	11.80	-3.60	2.00	5.6600
-3.60	11.10	-0.30	2.90	4.3200
-0.30	6.10	-0.80	0.80	4.2500
-0.80	5.60	-2.10	1.90	3.4500
-2.10	3.60	-0.60	1.50	3.1700
-0.60	5.80	0.70	1.10	3.2700
0.70	3.30	-0.10	1.40	2.7700
-0.10	5.60	-0.60	0.30	3.2900
-0.60	6.40	-0.50	3.60	3.1900
-0.50	0.60	-4.30	6.30	2.7700
-4.30	2.80	-2.50	0.20	2.2600
-2.50	3.90	0.50	1.00	2.4200
0.50	8.90	2.50	4.00	4.8000
2.50	13.50	4.10	6.20	15.9600
4.10	8.40	2.40	1.60	7.3400
2.40	11.50	6.60	0.50	5.0800
6.60	11.70	-1.80	1.20	9.4500
-1.80	13.90	-4.80	0.00	5.4000
-4.80	14.20	-4.90	0.00	4.0800
-4.90	15.00	0.70	0.00	3.6900
0.70	13.90	-2.40	0.00	3.3800
-2.40	12.70	-7.60	0.00	3.1000
-7.60	13.80	-6.90	0.00	2.8500
-6.90	15.30	4.20	0.40	2.7200
4.20	8.40	-3.40	0.00	2.8100
-3.40	9.80	2.40	0.00	2.5200
2.40	8.70	3.70	0.00	2.4600
3.70	11.90	5.10	0.00	2.2100
5.10	14.20	5.80	0.00	2.2000
5.80	17.80	2.50	0.10	2.3700

## Gairn 1984

-0.90	3.60	-6.30	0.10	3.1700
-6.30	6.80	-2.30	0.00	3.1800
-2.30	4.30	-0.20	0.00	3.0200
-0.20	5.60	-4.20	0.00	3.1800
-4.20	8.60	-2.70	0.00	3.7000
-2.70	4.10	-1.80	0.20	3.9300
-1.80	4.70	2.00	0.70	5.5800
2.00	6.30	2.70	0.20	10.8200
2.70	7.20	1.60	1.20	12.7700
1.60	6.40	1.70	1.80	18.5100
1.70	5.20	-0.90	0.10	11.1100
-0.90	7.70	3.60	0.50	11.6500
3.60	10.80	5.90	0.00	25.0300
5.90	10.10	0.20	0.90	21.9900
0.20	8.10	0.00	2.40	9.4800
0.00	6.60	-2.30	1.30	6.9200
-2.30	8.60	2.60	1.40	5.8600
2.60	9.60	5.20	0.10	9.7500
5.20	12.60	3.50	0.00	12.3300
3.50	12.70	7.40	0.00	14.4800
7.40	12.20	-2.20	0.00	15.2800
-2.20	13.10	-2.00	0.00	8.8700
-2.00	16.60	-0.70	0.00	7.7000
-0.70	22.70	0.80	0.00	9.0200
0.80	22.20	0.70	0.00	8.9400
0.70	24.50	0.80	0.00	7.7700
0.80	23.40	-0.40	0.00	7.0500
-0.40	19.10	1.20	0.00	6.8100
1.20	14.70	0.10	0.00	6.1600
0.10	12.20	-1.10	0.00	4.8600
-1.10	15.40	-1.80	0.00	4.2300
-1.80	15.70	-1.40	1.50	3.8800
-1.40	13.70	-1.20	0.70	3.7400
-1.20	15.10	-0.30	0.10	3.7400
-0.30	11.80	3.30	0.50	3.4900
3.30	6.70	0.10	0.00	3.0100
0.10	6.60	-1.00	0.00	2.5800
-1.00	12.70	2.70	0.00	2.4200
2.70	10.20	3.30	2.40	2.4600
3.30	8.30	4.20	0.10	2.9200
4.20	11.10	4.00	0.00	2.5600
4.00	14.50	1.80	0.00	2.5200
1.80	17.20	1.90	0.00	2.6400
1.90	16.10	2.40	0.00	2.7400
2.40	15.30	0.60	0.00	2.6200
0.60	11.30	4.40	0.00	2.3500
4.40	13.80	4.90	0.00	2.1800
4.90	14.20	0.40	0.00	2.1400
0.40	15.10	2.20	0.00	2.1000
2.20	10.90	4.30	4.10	2.1100
4.30	12.80	6.70	1.70	2.0800
6.70	16.30	7.00	0.00	2.5700
7.00	21.30	4.60	0.00	2.8400
4.60	16.60	4.10	0.40	2.3900
4.10	9.80	2.40	0.20	2.0100
2.40	8.40	1.50	1.00	1.7900
1.50	11.50	4.00	0.00	1.5800
4.00	15.50	0.30	0.00	1.6300
0.30	17.30	1.30	0.00	1.6200
1.30	15.70	8.40	0.00	1.5600

-7.60	-4.20	-4.50	0.00	0.9100	5.30	10.90	3.40	1.00	6.2100
-4.50	1.60	-2.10	0.00	1.0800	3.40	7.80	5.10	10.50	9.2800
-2.10	2.00	1.90	0.00	1.1600	5.10	10.00	6.10	0.00	6.3300
1.90	6.90	1.00	0.50	4.8500	6.10	10.00	7.60	0.50	5.3700
1.00	5.40	0.20	1.00	8.7300	7.60	10.10	4.00	1.50	8.7600
0.20	2.10	1.80	1.00	4.6300	4.00	8.50	5.90	1.00	7.6900
1.80	3.80	2.70	0.00	4.0500	5.90	10.80	3.60	4.00	6.7200
2.70	4.00	2.40	1.50	8.1600					
2.40	4.40	2.80	1.00	10.6800					
2.80	4.80	2.30	1.50	10.8200					
2.30	6.70	1.00	0.50	8.3600					
1.00	5.80	0.10	0.00	11.7900					
0.10	3.30	2.50	0.00	6.0800					
2.50	7.10	6.10	0.00	15.6500					
6.10	6.90	2.80	0.00	29.6400					
2.80	6.10	-0.20	1.50	17.3600					
-0.20	4.00	-0.20	0.50	7.5100					
-0.20	3.80	-1.40	0.50	5.3100					
-1.40	5.40	-0.10	0.00	4.4400					
-0.10	4.10	-0.20	1.00	6.9700					
-0.20	4.50	0.60	9.50	7.0900					
0.60	7.90	-1.10	3.50	15.5300					
-1.10	0.50	-2.50	0.00	7.0900					
-2.50	0.80	0.40	0.50	5.2800					
0.40	2.00	0.00	0.50	5.4700					
0.00	2.80	1.00	0.00	4.2900					
1.00	3.70	0.70	1.50	4.1000					
0.70	3.70	0.70	0.00	3.6700					
0.70	3.60	-2.00	1.00	3.3800					
-2.00	2.40	-3.30	0.50	3.0800					
-3.30	2.80	-1.40	0.00	2.8200					
-1.40	5.60	-0.50	0.00	2.6300					
-0.50	5.20	-1.30	1.50	2.7300					
-1.30	3.80	-0.20	3.00	2.9600					
-0.20	3.60	-0.40	0.50	2.9800					
-0.40	2.50	-1.30	1.00	2.9500					
-1.30	2.50	-2.20	0.00	2.7300					
-2.20	2.60	-0.70	0.00	2.8200					
-0.70	4.30	-0.50	0.00	2.4200					
-0.50	3.20	-1.90	1.50	2.3600					
-1.90	0.90	-1.30	0.00	2.1600					
-1.30	4.20	-0.20	0.50	3.2100					
-0.20	4.40	-0.80	2.50	4.0300					
-0.80	3.10	-0.10	0.50	3.5200					
-0.10	2.70	-0.90	0.50	3.1200					
-0.90	1.50	-0.80	0.00	2.8100					
-0.80	0.50	-3.50	0.00	2.3400					
-3.50	1.90	-3.30	0.00	3.2500					
-3.30	3.40	0.90	0.50	4.2800					
0.90	4.10	1.80	2.50	5.6900					
1.80	6.10	0.20	6.00	10.6800					
0.20	7.30	0.00	0.50	6.5300					
0.00	1.90	1.30	12.50	6.2100					
1.30	8.10	1.10	0.00	5.2800					
1.10	9.00	1.00	0.00	9.9800					
1.00	6.80	2.50	0.50	5.8100					
2.50	6.50	4.10	4.00	6.2200					
4.10	7.30	2.10	0.50	7.5900					
2.10	7.40	2.00	2.00	6.7800					
2.00	5.80	2.80	0.50	5.3800					
2.80	9.70	7.80	1.00	9.0500					
7.80	13.10	6.60	0.00	12.3500					
6.60	14.60	5.60	0.50	8.7200					
5.60	9.80	5.90	1.00	7.0200					
5.90	10.40	5.70	0.00	6.8100					
5.70	8.80	5.30	4.50	6.8800					

-3.00	3.40	2.10	0.00	1.8100	-1.20	0.90	-1.10	2.00	4.9000
2.10	5.20	-0.70	0.00	2.7600	-1.10	5.40	-0.80	5.00	6.5300
-0.70	4.20	0.40	1.50	2.4800	-0.80	4.50	-1.00	0.50	5.1800
0.40	3.60	3.20	0.00	2.2600	-1.00	2.90	-1.80	5.00	6.4800
3.20	6.20	-0.60	6.50	4.5400	-1.80	5.10	1.80	0.50	6.7200
-0.60	6.20	-1.90	6.50	6.6700	1.80	7.70	2.70	3.00	12.0100
-1.90	2.50	0.70	4.00	4.1100	2.70	8.50	1.50	0.00	10.7600
0.70	4.90	-1.70	0.00	3.6900	1.50	9.00	1.10	0.50	9.7300
-1.70	1.50	-2.50	0.00	2.9500	1.10	9.00	1.30	0.00	5.9400
-2.50	-1.00	-2.00	0.00	2.2200	1.30	16.10	7.30	0.00	6.2500
-2.00	-0.70	-5.60	0.00	2.7600	7.30	11.20	4.80	0.00	8.6900
-5.60	-1.70	-6.60	0.50	2.3400	4.80	7.90	2.10	0.00	8.4800
-6.60	-2.70	-6.60	0.00	2.0400	2.10	5.60	5.40	0.00	5.3800
-6.60	-3.10	-7.80	0.00	1.7900	5.40	8.30	5.80	0.00	5.9100
-7.80	-3.00	-8.80	0.50	1.8000	5.80	10.30	7.20	0.00	5.0200
-8.80	-4.10	-5.20	0.00	1.5500	7.20	11.50	4.30	0.00	4.9600
-5.20	-2.80	-4.20	0.00	1.7100	4.30	13.90	7.10	0.00	4.3900
-4.20	-0.60	0.00	0.00	1.6800					
0.00	1.90	0.60	0.00	3.7000					
0.60	2.00	-0.60	0.50	4.2000					
-0.60	1.40	-3.90	0.00	3.2400					
-3.90	0.80	-5.90	0.50	3.5700					
-5.90	-2.70	-6.00	0.00	2.5300					
-6.00	-2.30	-4.40	0.00	1.9300					
-4.40	-1.00	-2.30	0.00	1.9500					
-2.30	4.20	3.80	1.50	1.8100					
3.80	5.90	1.30	0.00	3.5300					
1.30	5.70	1.80	0.50	6.9500					
1.80	7.10	-1.00	12.50	14.7800					
-1.00	1.80	-4.00	2.50	8.3100					
-4.00	1.20	-3.80	0.00	4.3300					
-3.80	1.20	-1.20	0.00	3.4900					
-1.20	1.40	0.20	1.50	3.0900					
0.20	3.30	-3.30	1.00	3.0100					
-3.30	-0.40	-3.40	0.40	2.4200					
-3.40	-0.70	-4.20	0.00	2.2600					
-4.20	-0.70	-3.80	9.00	2.1400					
-3.80	2.70	-6.00	0.00	1.9100					
-6.00	3.20	-3.80	0.00	1.8900					
-3.80	3.30	-2.00	0.00	2.1300					
-2.00	1.90	-0.30	0.00	2.0100					
-0.30	1.60	-3.80	2.00	2.4400					
-3.80	0.00	-3.90	0.50	2.3300					
-3.90	3.20	-2.60	6.00	2.9900					
-2.60	3.60	-5.30	1.50	6.1000					
-5.30	-1.30	-5.60	0.00	2.9500					
-5.60	-2.80	-6.10	0.00	2.3300					
-6.10	-3.10	-7.90	0.50	1.9700					
-7.90	-1.80	-5.30	0.00	2.0800					
-5.30	0.30	-5.40	0.00	2.1900					
-5.40	2.00	-6.10	0.00	1.9800					
-6.10	2.30	-2.00	0.00	2.1000					
-2.00	1.10	-1.20	6.00	2.7700					
-1.20	0.90	-0.60	3.00	2.9600					
-0.60	5.70	-4.60	14.50	8.5400					
-4.60	-0.90	-5.20	4.00	5.6800					
-5.20	1.70	1.00	1.00	3.8400					
1.00	3.70	-0.90	2.50	6.5700					
-0.90	5.40	-2.50	6.50	12.3000					
-2.50	1.50	-3.10	0.50	5.1700					
-3.10	0.10	-0.40	7.50	4.7100					
-0.40	1.70	0.10	2.00	7.4400					
0.10	4.90	-1.60	0.50	7.4500					
-1.60	2.50	-2.20	0.00	5.4100					
-2.20	3.60	-0.80	0.00	4.1600					
-0.80	6.70	-1.20	0.00	3.9700					

## Feshie 1979

0.60	8.50	1.40	5.80	3.4414
1.40	12.40	4.30	0.30	18.1238
4.30	11.20	5.30	0.00	22.7239
5.30	9.80	2.50	0.00	19.9601
2.50	13.10	3.10	9.00	14.4791
3.10	9.90	3.40	0.10	18.2343
3.40	7.70	-1.60	0.00	11.8966
-1.60	12.30	0.00	0.00	10.6460
0.00	11.10	7.40	0.10	15.1378
7.40	12.20	3.30	0.00	19.9714
3.30	11.20	2.10	1.70	16.0680
2.10	8.10	3.30	0.20	11.2576
3.30	9.00	1.10	1.30	9.9846
1.10	7.30	2.10	0.80	8.8177
2.10	7.20	2.00	1.60	9.1616
2.00	7.80	3.00	0.20	7.8050
3.00	8.30	-1.60	0.00	6.7498
-1.60	9.40	4.90	0.30	11.6196
4.90	12.80	6.40	0.10	16.8287
6.40	9.60	-0.70	3.10	15.2085
-0.70	4.50	-2.50	0.30	6.6349
-2.50	4.50	-0.50	1.00	4.4765
-0.50	3.60	-2.60	2.60	3.5976
-2.60	4.80	-1.80	0.30	3.0949
-1.80	4.90	-2.00	1.50	2.8016
-2.00	7.00	-0.20	5.60	2.8142
-0.20	8.60	-0.20	0.60	3.8208
-0.20	8.50	-2.40	1.90	4.7519
-2.40	10.20	-1.00	1.10	4.8770
-1.00	8.20	-5.70	0.10	4.4995
-5.70	11.70	5.80	0.40	5.9187
5.80	14.10	6.90	0.50	12.0313
6.90	18.50	8.80	0.00	18.6014
8.80	19.70	11.90	0.00	28.7789
11.90	13.00	6.10	0.80	22.1826
6.10	12.50	1.70	0.00	11.8816
1.70	9.40	4.60	16.50	10.8580
4.60	7.70	2.30	6.80	10.2727
2.30	7.50	0.40	2.40	6.2412
0.40	11.00	4.20	0.00	4.3976
4.20	15.40	5.80	5.50	8.1300
5.80	12.70	4.60	0.10	8.8203
4.60	13.70	-1.00	0.00	8.2287
-1.00	11.00	5.60	5.70	8.2307
5.60	13.30	-1.90	1.20	7.9015
-1.90	13.60	-1.60	3.20	6.0949
-1.60	13.60	2.30	0.00	5.5546
2.30	12.60	2.90	0.40	5.6620
2.90	13.40	5.90	2.50	7.7903
5.90	13.90	8.30	2.40	11.2350
8.30	16.30	7.20	4.80	10.0490
7.20	13.50	2.70	0.00	8.5071
2.70	18.90	-1.10	0.00	7.1400

## Feshie 1980

2.40	8.00	3.00	0.50	3.5582
3.00	7.70	-0.40	4.80	6.5535
-0.40	5.20	1.00	0.40	3.9152
1.00	5.90	1.30	0.00	2.5841
1.30	5.40	1.60	1.10	2.1102
1.60	10.00	-3.50	1.00	4.0520
-3.50	9.70	2.20	0.60	6.9444
2.20	7.40	1.80	0.00	5.3432
1.80	9.00	-0.70	1.20	4.8910
-0.70	11.20	3.90	0.10	5.7269
3.90	12.90	-5.60	0.00	7.6711
-5.60	16.20	-5.30	0.00	8.0318
-5.30	15.50	0.90	0.10	7.0952
0.90	8.00	0.80	0.10	4.6467
0.80	7.40	3.60	0.20	3.0218
3.60	11.00	4.10	0.50	6.3611
4.10	9.40	2.10	0.00	4.7836
2.10	11.90	5.00	0.00	5.6977
5.00	14.80	4.30	0.00	8.0435
4.30	17.40	3.80	0.00	14.0720
3.80	11.90	0.50	0.00	8.0459
0.50	16.60	1.90	0.00	8.8837
1.90	11.60	0.70	1.30	7.7859
0.70	9.60	5.80	0.00	6.9941
5.80	15.20	2.40	0.00	14.7505
2.40	5.60	0.80	0.00	6.5036
0.80	7.80	-5.20	0.00	4.2743
-5.20	8.40	3.10	1.30	4.2606
3.10	10.20	6.00	1.20	6.4700
6.00	12.20	2.60	0.10	7.4004
2.60	11.20	-3.60	0.30	5.2593
-3.60	14.80	-3.50	0.00	5.0809
-3.50	14.30	5.10	0.00	4.6664
5.10	12.10	2.80	4.50	6.0916
2.80	11.30	-0.80	0.00	5.1417
-0.80	10.20	5.20	0.70	5.4184
5.20	10.40	3.00	0.00	6.1041
3.00	14.60	3.50	0.00	5.6551
3.50	14.30	-1.10	0.00	5.9952
-1.10	15.00	2.20	0.00	5.2729
2.20	15.10	2.10	0.00	4.8781
2.10	15.50	3.90	0.00	4.2742
3.90	7.10	2.70	2.10	3.3413
2.70	4.40	-1.50	1.90	2.6459
-1.50	10.50	2.40	0.00	2.2829
2.40	12.50	5.40	0.00	2.7086
5.40	15.30	6.50	0.00	3.1753
6.50	19.80	6.80	0.00	3.8707
6.80	21.60	9.60	0.00	5.1184
9.60	22.30	4.70	0.00	5.1882
4.70	20.80	-1.00	0.00	3.9642
-1.00	22.30	-1.30	0.00	3.3184
-1.30	24.40	-3.80	0.00	2.8603

Feshie 1981

0.30	12.80	5.20	2.10	28.7877
5.20	8.60	2.10	0.60	9.9465
2.10	8.20	-0.40	0.80	3.8600
-0.40	11.40	4.70	0.70	11.9104
4.70	15.30	5.50	0.30	13.4773
5.50	11.80	-3.60	2.00	6.4278
-3.60	11.10	-0.30	2.90	5.3506
-0.30	6.10	-0.80	0.80	4.3775
-0.80	5.60	-2.10	1.90	2.8318
-2.10	3.60	-0.60	1.50	2.1611
-0.60	5.80	0.70	1.10	2.3255
0.70	3.30	-0.10	1.40	1.9361
-0.10	5.60	-0.60	0.30	2.1720
-0.60	6.40	-0.50	3.60	2.4080
-0.50	0.60	-4.30	6.30	1.7759
-4.30	2.80	-2.50	0.20	1.6320
-2.50	3.90	0.50	1.00	1.7063
0.50	8.90	2.50	4.00	13.7785
2.50	13.50	4.10	6.20	18.6407
4.10	8.40	2.40	1.60	6.6773
2.40	11.50	6.60	0.50	8.5774
6.60	11.70	-1.80	1.20	15.8021
-1.80	13.90	-4.80	0.00	5.2361
-4.80	14.20	-4.90	0.00	4.0598
-4.90	15.00	0.70	0.00	3.8789
0.70	13.90	-2.40	0.00	3.2201
-2.40	12.70	-7.60	0.00	3.1723
-7.60	13.80	-6.90	0.00	2.7395
-6.90	15.30	4.20	0.40	2.9645
4.20	8.40	-3.40	0.00	2.5581
-3.40	9.80	2.40	0.00	2.2956
2.40	8.70	3.70	0.00	2.0036
3.70	11.90	5.10	0.00	1.9097
5.10	14.20	5.80	0.00	2.2939
5.80	17.80	2.50	0.10	2.6582

## **APPENDIX B**

Snow survey data collected in the Allt a Mharcaidh catchment during the 1986, 1987 and 1988 melt seasons.

Date 27-2-86

Zone	Area (km <sup>2</sup> )	% cover	WE (mm)	Volume (m <sup>3</sup> )
1	3.05	100	82	250 100
21	1.14	100	77	87 780
23/22	1.20	100	310	372 000
31	0.80	100	458	366 400
33/32	1.05	100	173	181 650
41	0.28	100	162	45 360
42	0.47	100	450	211 500
43	0.42	100	270	117 400
51	0.43	100	135	58 050
52/53	0.18	100	113	20 250
<500m	0.73	100	82	59 860
TOTAL		9.91		1 766 350

Date 4-3-86

Zone	Area (km <sup>2</sup> )	% cover	WE (mm)	Volume (m <sup>3</sup> )
1	3.05	75	57	130 388
21	1.14	60	274	187 416
23/22	1.20	100	158	189 600
31	0.80	100	446	356 800
33/32	1.05	100	162	170 100
41	0.28	100	154	43 120
42	0.47	100	413	193 875
43	0.42	100	275	115 500
51	0.43	100	138	59 125
52/53	0.18	100	110	19 800
<500m	0.73	75	57	31 207
TOTAL		8.51		1 496 931

Date 5-3-86

Zone	Area (km <sup>2</sup> )	% cover	WE (mm)	Volume (m <sup>3</sup> )
1	3.05	100	66	210 300
21	1.14	30	197	67 374
23/22	1.20	100	153	183 600
31	0.80	100	485	388 000
33/32	1.05	100	153	160 650
41	0.28	100	154	43 120
42	0.47	100	413	193 875
43	0.42	100	275	115 500
51	0.43	100	138	59 125
52/53	0.18	100	110	19 800
<500m	0.73	100	66	48 180
TOTAL		9.11		1 480 524

Date 26-3-86

Zone	Area (km <sup>2</sup> )	% cover	WE (mm)	Volume (m <sup>3</sup> )
1	3.05	100	39	118950
21	1.14	90	20	32832
23/22	1.20	100	47	56400
31	0.80	20	161	25760
33/32	1.05	100	102	107100
41	0.28	100	88	24640
42	0.47	100	530	249100
43	0.42	100	279	117180
51	0.43	100	70	30100
52/53	0.18	100	371	66780
<500m	0.73	100	39	28470
TOTAL		9.16		857,312

Date 13-4-86

Zone	Area (km <sup>2</sup> )	% cover	WE (mm)	Volume (m <sup>3</sup> )
1	3.05			
21	1.14			
23/22	1.20	100	81	96600
31	0.80			
33/32	1.05	100	212	241110
41	0.28	100	222	62020
42	0.47	100	735	345450
43	0.42	100	340	142590
51	0.43	100	66	28268
52/53	0.18	100	389	70020
<500m	0.73			
TOTAL		4.2km <sup>2</sup>		986058

Date 25-4-86

Zone	Area (km <sup>2</sup> )	% cover	WE (mm)	Volume (m <sup>3</sup> )
1	3.05			16717
21	1.14	15	98	
23/22	1.20	100	98	117360
31	0.80	40	128	40864
33/32	1.05	100	428	448560
41	0.28	100	468	130956
42	0.47	100	468	219819
43	0.42	100	468	196434
51	0.43	100	98	42140
52/53	0.18	100	98	17640
<500m	0.73			
TOTAL		4.68km <sup>2</sup>		1,230,490

Date 2-5-86

Zone	Area (km <sup>2</sup> )	% cover	WE (mm)	Volume (m <sup>3</sup> )
1	3.05			
21	1.14			
23/22	1.20	33	360	145440
31	0.80			
33/32	1.05	68	360	231120
41	0.28	70	240	38400
42	0.47	50	452	105270
43	0.42	50	452	105270
51	0.43	100	330	141900
52/53	0.18	100	330	59400
<500m	0.73			
TOTAL				826,800

DATE: 23-1-87

<u>SITES</u>	<u>AREA</u>	<u>%COVER</u>	<u>WE(mm)</u>	<u>VOLUME(M3)</u>
1	3.11			
2,3,12,13	2.97			
4	0.56	20	41	46,080
5	0.52			
6,7	0.70	75	50	226,500
8	0.14			
11	1.41			
9	0.43			
<u>10</u>	<u>0.07</u>	<u>100</u>	<u>1440</u>	<u>100,800</u>
<u>TOTAL</u>	<u>9.91</u>	<u>Sca 0.73 km2</u>		<u>373,380</u>

DATE 13-2-87

<u>SITES</u>	<u>AREA</u>	<u>%COVER</u>	<u>WE(mm)</u>	<u>VOLUME(M3)</u>
1	3.11	100	36	111,960
2,3,12,13	2.97	100	40	118,800
4	0.56	100	540	303,480
5	0.52	100	37	19,240
6,7	0.70	100	54	37,960
8	0.14	100	86	12,040
11	1.41	100	60	84,600
9	0.43	100	35	14,910
<u>10</u>	<u>0.07</u>	<u>100</u>	<u>&gt;1700</u>	<u>119,000</u>
<u>TOTAL</u>	<u>9.91</u>			<u>821,990</u>

DATE: 20-2-87

<u>SITES</u>	<u>AREA</u>	<u>%COVER</u>	<u>WE(mm)</u>	<u>VOLUME(M3)</u>
1	3.11	100	36	111,960
2,3,12,13	2.97	100	45	133,650
4	0.56	100	490	275,380
5	0.52	100	52	27,040
6,7	0.70	100	79	55,540
8	0.14	100	111	15,540
11	1.41	100	90	126,900
9	0.43	100	117	49,840
10	0.07	100	>1770	123,900
<b>TOTAL</b>	<b>9.91</b>	<b>100</b>		<b>919,750</b>

DATE 23/26-2-87

<u>SITES</u>	<u>AREA</u>	<u>%COVER</u>	<u>WE(mm)</u>	<u>VOLUME(M3)</u>
1	3.11	100	22	68,420
2,3,12,13	2.97	100	36	99,029
4	0.56	100	540	303,480
5	0.52	100	50	260,000
6,7	0.70	100	83	58,350
8	0.14	100	120	16,800
11	1.41	100	100	141,000
9	0.43	100	88	37,490
10	0.07	100	>2000	140,000
<b>TOTAL</b>	<b>9.91</b>	<b>100</b>		<b>890,569</b>

DATE: 3-3-87

<u>SITES</u>	<u>AREA</u>	<u>%COVER</u>	<u>WE(mm)</u>	<u>VOLUME(M3)</u>
1	3.11			
2,3,12,13	2.97			
4	0.56	90	480	242,780
5	0.52	80	15	6,240
6,7	0.70	100	140	98,480
8	0.14	100	76	10,640
11	1.41	100	13	18,330
9	0.43	100	20	8,520
10	0.07	100	>2000	140,000
<b>TOTAL</b>	<b>9.91</b>	<b>SCA = 3.71 km</b>		<b>524,930</b>

DATE 12-3-87

<u>SITES</u>	<u>AREA</u>	<u>%COVER</u>	<u>WE(mm)</u>	<u>VOLUME(M3)</u>
1	3.11			
2,3,12,13	2.97	40	10	11,880
4	0.56	100	350	196,700
5	0.52	20	6	624
6,7	0.70	85	22	13,150
8	0.14	100	90	12,600
11	1.41	20	6	1,692
9	0.43	80	28	9,540
10	0.07	100	>2000	140,000
<b>TOTAL</b>	<b>9.91</b>	<b>SCA = 3.29 km</b>		<b>386,186</b>

DATE: 19-3-87

<u>SITES</u>	<u>AREA</u>	<u>%COVER</u>	<u>WE(mm)</u>	<u>VOLUME(M3)</u>
1	3.11	100	5	15,550
2,3,12,13	2.97	100	24	71,280
4	0.56	100	160	89,920
5	0.52	100	12	6,240
6,7	0.70	100	41	28,820
8	0.14	100	131	18,340
11	1.41	100	26	36,660
9	0.43	100	70	29,820
10	0.07	100	>2000	140,000
<b>TOTAL</b>	<b>9.91</b>	<b>100</b>		<b>436,630</b>

DATE 24-3-87

<u>SITES</u>	<u>AREA</u>	<u>%COVER</u>	<u>WE(mm)</u>	<u>VOLUME(M3)</u>
1	3.11			
2,3,12,13	2.97	85	24	60,588
4	0.56	100	205	115,210
5	0.52	20	15	1,560
6,7	0.70	100	54	37,962
8	0.14	100	130	18,200
11	1.41	100	26	36,660
9	0.43	70	52	15,500
10	0.07	100	>2000	140,000
<b>TOTAL</b>	<b>9.91</b>	<b>SCA = 4.98 km</b>		<b>425,700</b>

DATE: 31-3-87

<u>SITES</u>	<u>AREA</u>	<u>%COVER</u>	<u>WE(mm)</u>	<u>VOLUME(M3)</u>
1	3.11			
2,3,12,13	2.97	10	22	6,530
4	0.56	95	242	129,200
5	0.52	20	20	2,080
6,7	0.70	95	175	116,870
8	0.14	90	101	12,730
11	1.41	50	10	7,050
9	0.43	70	82	24,450
10	0.07	100	>2000	140,000
<b>TOTAL</b>	<b>9.91</b>	<b>SCA = 2.47 km</b>		<b>438,910</b>

DATE 8-4-87

<u>SITES</u>	<u>AREA</u>	<u>%COVER</u>	<u>WE(mm)</u>	<u>VOLUME(M3)</u>
1	3.11			
2,3,12,13	2.97	100	3	8,910
4	0.56	100	185	103,970
5	0.52	70	5	1,820
6,7	0.70	100	95	66,785
8	0.14	100	140	19,600
11	1.41	30	10	4,230
9	0.43	70	74	22,070
10	0.07	100	>2000	140,000
<b>TOTAL</b>	<b>9.91</b>	<b>SCA = 6.03 km</b>		<b>367,385</b>

**DATE:** 3-2-88

<u>SITES</u>	<u>AREA</u>	<u>%COVER</u>	<u>WE(mm)</u>	<u>VOLUME(M3)</u>
1	3.11	100	158	491,380
2,3,12,13	2.97	100	99	294,030
4	0.56	100	570	320,340
5	0.52	100	150	78,000
6,7	0.70	100	400	281,200
8	0.14	100	574	80,360
11	1.41	100	200	282,000
9	0.43	100	162	69,012
10	0.07	100	>1250	87,500
<b>TOTAL</b>	<b>9.91</b>	<b>SCA 9.91km2</b>		<b>1,454,080</b>

**DATE** 19-3-88

<u>SITES</u>	<u>AREA</u>	<u>%COVER</u>	<u>WE(mm)</u>	<u>VOLUME(M3)</u>
1	3.11			
2,3,12,13	2.97	35	193	258,000
4	0.56	100	244	137,128
5	0.52	70	100	36,400
6,7	0.70	100	500	228,475
8	0.14	100	364	50,960
11	1.41	70	125	123,375
9	0.43	75	127	40,520
10	0.07	100	>1500	>100,000
<b>TOTAL</b>	<b>9.91</b>	<b>SCA 1.19km2</b>		<b>977,775</b>

<u>DATE:</u>	29-3-88			
<u>SITES</u>	<u>AREA</u>	<u>%COVER</u>	<u>WE(mm)</u>	<u>VOLUME(M3)</u>
1	3.11			
2,3,12,13	2.97	20	157	93,258
4	0.56	100	213	119,425
5	0.52	50	4	1,040
6,7	0.70	100	324	227,490
8	0.14	100	334	46,704
11	1.41	100	112	157,356
9	0.43	100	112	47,541
10	0.07	100	>1440	>100,080
<hr/>				
TOTAL	9.91	SCA 9,91km2		784,614
<hr/>				

<u>DATE</u>	13-4-88			
<u>SITES</u>	<u>AREA</u>	<u>%COVER</u>	<u>WE(mm)</u>	<u>VOLUME(M3)</u>
1	3.11			
2,3,12,13	2.97	30	25	22,275
4	0.56	80	144	64,608
5	0.52			
6,7	0.70	100	200	140,600
8	0.14	100	398	55,720
11	1.41			
9	0.43	100	30	12,780
10	0.07	100	>1500	>105,000
<hr/>				
TOTAL	9.91	SCA 2.70km2		400,983
<hr/>				

## **APPENDIX C**

Coding for an early version of TINDEX, on of the models developed in the project. The program was written in standard Fortran 77

```

C
C TEMPERATURE INDEX PROGRAMME TO RUN ON MEAN DAILY MIN AND MAX
C
C TEMPS BASED ON MODEL DEVELOPED BY R.I FERGUSON
C
C CODED BY AMB ON 9 9 88
C UPDATED ON : 3 11 88
C
C .....
C
C INITIALISE
C
C .....
C
C PROGRAM INDEX
C REAL R(10),AB,DT,Q0,Q,V,VP,DD,TMIN(120),TMAX(120),NTMIN(120)
C REAL SRAD(120),PPT(120),WSP(120),FLOW(120),AA(10),M(10),W(10),K
C REAL A2,A1,ATEM(120),NRAD(120),E(10),X(10)
C INTEGER ND,NOPT,ZOPT
C INTEGER HMAX,H1,H2,HMIN,HMET,IOPT,JOPT,KOPT,LOPT
C
C .....
C
C MAIN TASK
C
C .....
C
C PRINT*, 'ENTER INITIAL DISCHARGE AND NUMBER OF DAYS'
C READ*, Q0, ND
C PRINT*, 'ENTER NUMBER OF TEMP LAPSE RATE OPTIMISATION RUNS'
C READ*, NOPT
C PRINT*, 'ENTER', NOPT, ' TRIAL VALUES OF E=TEMPERATURE LAPSE RATE'
C READ*, (E(I), I=1, NOPT)
C PRINT*, 'ENTER NUMBER OF RECESSION COEFF OPTIMISATION RUNS'
C READ*, IOPT
C PRINT*, 'ENTER', IOPT, ' TRIAL VALUES OF R=RECESSION COEFFICIENT'
C READ*, (R(I), I=1, IOPT)
C PRINT*, 'ENTER NUMBER OF INITIAL SNOW AREA OPTIMISATION RUNS'
C READ*, JOPT
C PRINT*, 'ENTER', JOPT, ' TRIAL VALUES OF AA=INITIAL SNOW AREA IN KM2'
C READ*, (AA(I), I=1, JOPT)
C PRINT*, 'ENTER NUMBER OF MELT COEFFICIENT OPTIMISATION RUNS'
C READ*, KOPT
C PRINT*, 'ENTER', KOPT, ' TRIAL VALUES OF M=MELT COEFFICIENT'
C READ*, (M(I), I=1, KOPT)
C PRINT*, 'ENTER NUMBER OF INITIAL PACK WE OPTIMISATION RUNS'
C READ*, LOPT
C PRINT*, 'ENTER', LOPT, ' TRIAL VALUES OF W=INITIAL PACK WE(MM) '
C READ*, (W(I), I=1, LOPT)
C PRINT*, 'ENTER NUMBER OF ALBEDO FACTOR OPTIMISATION RUNS'
C READ*, ZOPT
C PRINT*, 'ENTER', ZOPT, ' TRIAL VALUES OF ALBEDO FACTOR'
C READ*, (X(I), I=1, ZOPT)
C Q-Q0

```

```

PRINT*, 'ENTER BASIN AREA IN KM2'
READ*, AB
READ(14,400) HMAX,H1,H2,HMIN,A2,A1,HMET
400  FORMAT(1X,4I5,2F7.2,I5)
SMIN=100
READ(11,500)
500  FORMAT(1X,' MINTEM MAXTEM NMINTEM AVGTEM INRADN SOLRAD TOTPPN AVGW
& SP AVGFLOW')
DO 5,I=1,ND
READ(11,100) TMIN(I),TMAX(I),NTMIN(I),ATEM(I),NRAD(I),
& SRAD(I),PPT(I),WSP(I),FLOW(I)
100  FORMAT(1X,8F7.1,F7.3)
c    READ(11,100)TMIN(I),TMAX(I),NTMIN(I),PPT(I),FLOW(I)
c100  FORMAT(1X,4F6.2,F8.4)
5  CONTINUE
DO 8,N=1,NOPT
DO 10,I=1,ILOPT
DO 20,J=1,JOPT
DO 30,K=1,KOPT
DO 40,L=1,LOPT
DO 50,Z=1,ZOPT
CALL MODEL(E(N),R(I),AA(J),M(K),W(L),Q0,ND,AB,SE,HMET,
& HMAX,H1,H2,HMIN,A2,A1,TMIN,TMAX,NTMIN,ATEM,NRAD,SRAD,
& PPT,WSP,FLOW,X(Z))
c  & HMAX,H1,H2,HMIN,A2,A1,TMIN,TMAX,NTMIN,PPT,FLOW,X(Z))
IF (SE.GE.SMIN) GO TO 50
BE=E(N)
BR=R(I)
BA=AA(J)
BM=M(K)
BW=W(L)
BX=X(Z)
SMIN=SE
WRITE(*,300)SMIN,BE,BR,BA,BM,BW,BX
300  FORMAT('SMIN,E,R,A,M,W,X ARE ',2F7.4,f7.4,3f7.2,f7.3)
50  CONTINUE
40  CONTINUE
30  CONTINUE
20  CONTINUE
10  CONTINUE
8  CONTINUE
CALL FMODEL(BE,BR,BA,BM,BW,Q0,ND,K,AB,A,HMET,HMAX,H1,H2,HMIN,A2,
C  &A1,TMIN,TMAX,NTMIN,ATEM,NRAD,SRAD,PPT,WSP,FLOW,BX)
&A1,TMIN,TMAX,NTMIN,PPT,FLOW,BX)
PRINT*, 'FINAL AREA OF SNOWPACK IS ',A
C .....
C
C  TERMINATE
C
C .....
C
STOP
END
C .....

```



```

C   HMIN ...../
C   ^ ^           ^ ^
C   0  A1           A2 AB
C
C
C
C   SLOPE CALCULATIONS FOR EACH SECTION OF THE HYPISO CURVE
C
C   S0=(HMAX-H1)/A1
C   S1=(H1-H2)/(A2-A1)
C   S2=(H2-HMIN)/(AB-A2)
C
C   DETERMINATION OF SNOWLINE HEIGHT
C
C   IF(A.GT.A2) THEN
C     HT=H2-S2*(A-A2)
C   ELSEIF (A.GT.A1) THEN
C     HT=H1-S1*(A-A1)
C   ELSEIF (A.GT.0) THEN
C     HT=HMAX-S0*A
C   ENDIF
C   END
C .....
C
C   MODEL FUNCTION
C .....
C
C   FUNCTION MODEL(E,R,AA,M,W,Q0,ND,AB,SE,HMET,HMAX,H1,H2,HMIN,A2,A1,
C   &TMIN,TMAX,NTMIN,ATEM,NRAD,SRAD,PPT,WSP,FLOW,X)
C   &TMIN,TMAX,NTMIN,PPT,FLOW,X)
C   REAL  TMIN(120),TMAX(120),NTMIN(120),ATEM(120),NRAD(120),SRAD(120)
C   REAL  E,R,A,M,W,Q0,AB,K,PPT(120),WSP(120),FLOW(120),ERR,SS,SE
C   REAL  A2,A1,AM,CDD,HHT,EL,PA,ESAT,WINDM,UADJ,WFUN,WETM,TAV(120)
C   INTEGER HMET,HMAX,H1,H2,HMIN
C   INTEGER ND
C   K=2*W/AA
C   CDD=0
C   Q=Q0
C   SS=0
C   A=AA
C   WFUN=0.002
C   DO 15,I=1,ND
C     HHT=1*(HT(A,HMAX,H1,H2,HMIN,A2,A1,AB)-HMET)
C     DT=E*HHT
C     TAV(I)=(TMIN(I)+TMAX(I))/2
C     DT=E*(HT(A,HMAX,H1,H2,HMIN,A2,A1,AB)-HMET)
C     CDD=CDD+DA(TMIN(I),TMAX(I),DT)
C     AM=M-(M-1)*EXP(-X*CDD)
C     IF (PPT(I).LE.1) THEN
C       V=AM*A*DA(TMIN(I),TMAX(I),DT)
C     ELSE
C       V=AM*A*DD(TMIN(I),TMAX(I),NTMIN(I),DT)
C     EL=HHT/100

```

```

PA=1012.4-(11.34*EL)+(0.00745*EL**2.4)
ESAT=2.749*10**8*(exp(-4278.6/(TAV(I)+242.8)))
WINDM=WSP(I)*86.4
UADJ=WINDM*WFUN
WETM=3.67*10**-9*(TAV(I)+273)**4-81.6+0.0125*PPT(I)*TAV(I)
&      +8.5*UADJ*((0.9*ESAT-6.11)+0.00057*PA*TAV(I))
V=WETM*A
IF (V.LE.0) V = 0
ENDIF
VP=(AB-A)*PPT(I)
C
C
c      Y=1-R*(Q**0.5)
Y=1-R*((V+VP)/86.4)**0.5)
Q=Y*Q+(1-Y)*(V+VP)/86.4
c      Q=R*Q+(1-R)*(V+VP)/86.4
C      Q=R*Q+(1-R)*V/86.4
TERM=A**2-2*V/K
IF (TERM.LE.0)TERM=0
A=SQRT(TERM)
ERR=FLOW(I)-Q
SS=SS+ERR**2
15 CONTINUE
SE=SQRT(SS/ND)
END
C .....
C
C      FINAL MODEL RUN FUNCTION
C .....
C
FUNCTION FMODEL(BE,R,BA,BM,BW,Q0,ND,K,AB,A,HMET,HMAX,H1,H2,HMIN,
&A2,A1,TMIN,TMAX,NTMIN,ATEM,NRAD,SRAD,PPT,WSP,FLOW,BX)
c  &A2,A1,TMIN,TMAX,NTMIN,PPT,FLOW,BX)
REAL TMIN(120),TMAX(120),NTMIN(120),ATEM(120),NRAD(120),SRAD(120)
REAL BE,R,BA,BM,BW,Q0,AB,K,PPT(120),WSP(120),FLOW(120),ERR,SS,SE
REAL A1,A2,AM,CDD,hht,el,pa,esat,windm,uadj,wfun,wetm,tav(120)
INTEGER HMET,HMAX,H1,H2,HMIN
INTEGER ND
CDD=0
Q=Q0
A=BA
SS=0
K=2*BW/BA
wfun=0.002
DO 25,I=1,ND
HHT=1*(HT(A,HMAX,H1,H2,HMIN,A2,A1,AB)-HMET)
DT=E*HHT
TAV(I)=(TMIN(I)+TMAX(I))/2
C      DT=BE*(HT(A,HMAX,H1,H2,HMIN,A2,A1,AB)-HMET)
CDD=CDD+DA(TMIN(I),TMAX(I),DT)
AM=BM-(BM-1)*EXP(-BX*CDD)
IF (PPT(I).LE.1) THEN
V=AM*A*DA(TMIN(I),TMAX(I),DT)

```

```

ELSE
  EL=HHT/100
  PA=1012.4-(11.34*EL)+(0.00745*EL**2.4)
  ESAT=2.749*10**8*(exp(-4278.6/(TAV(I)+242.8)))
  WINDM=WSP(I)*86.4
  UADJ=WINDM*WFUN
  WETM=3.67*10**-9*(TAV(I)+273)**4-81.6+0.0125*PPT(I)*TAV(I)
&      +8.5*UADJ*((0.9*ESAT-6.11)+0.00057*PA*TAV(I))
  V=WETM*A
  IF(V.LE.0) V = 0
ENDIF
  VP=(AB-A)*PPT(I)
C      Y=1-R*(Q**0.5)
  Y=1-R*(((V+VP)/86.4)**0.5)
  Q=Y*Q+(1-Y)*(V+VP)/86.4
c      Q=R*Q+(1-R)*(V+VP)/86.4
C      Q=R*Q+(1-R)*V/86.4
  TERM=A**2-2*V/K
  IF (TERM.LE.0)TERM=0
  A=SQRT(TERM)
  ERR=FLOW(I)-Q
  SS=SS+ERR**2
  WRITE(12,200)Q,FLOW(I),CDD,V,PPT(I),WETM
200  FORMAT(2F9.4,4F7.1)
25  CONTINUE
  SE=SQRT(SS/ND)
  WRITE(*,300)SE,BE,BR,BA,BM,BW
300  FORMAT(' SE,E,R,AND A,M AND W ARE ',F6.3,F7.4,4F7.3)
END

```

## APPENDIX D TRACER EXPERIMENTS IN THE MHEARCAIDH

Following the early stages of model development it was decided to carry out tracer experiments during the later stages of the melt season. It was thought useful to have an idea of the travel time of the meltwater through the snowpack so that the different routing methods used in the models could be adjusted, discounted or accepted depending on the results.

Following consultation with the other SWAP workers in the catchment who were studying stream water chemistry it was decided to use lithium chloride as the tracer. This could be detected in very low concentrations meaning that very little salt had to be used. This ensured that by carrying out the work on a snowpatch high in the catchment the concentration of lithium at GS1 would be negligible and would not affect the work of the other parties.

Late in the 1988 melt season a snowpatch was selected for the study on the eastern side of the gully at approximately 850m amsl. The snowpatch measured some 150m wide and 80m from top to bottom, and was drained by a small burn that entered the main gully some 125m below. An automatic liquid sampler (ALS) (Plate D.1) was sited next to the burn some 20m from the base of the snowpack.

Lithium chloride (600g) salt was dissolved in three buckets

of stream water and spread along a shallow trench 10m from the top of the snowpack. The trench was 85m long and the snowpack was between 0.8 and 1.7 m deep along the transect. Samples were collected by both the ALS and by hand, and then taken back to Stirling for analysis.

The lithium concentration in the samples was determined by atomic absorption spectrophotometry (AAS) in the laboratory, previous work prior to the experiments having shown that levels as low as  $0.02\text{mg l}^{-1}$  of lithium could be accurately determined.

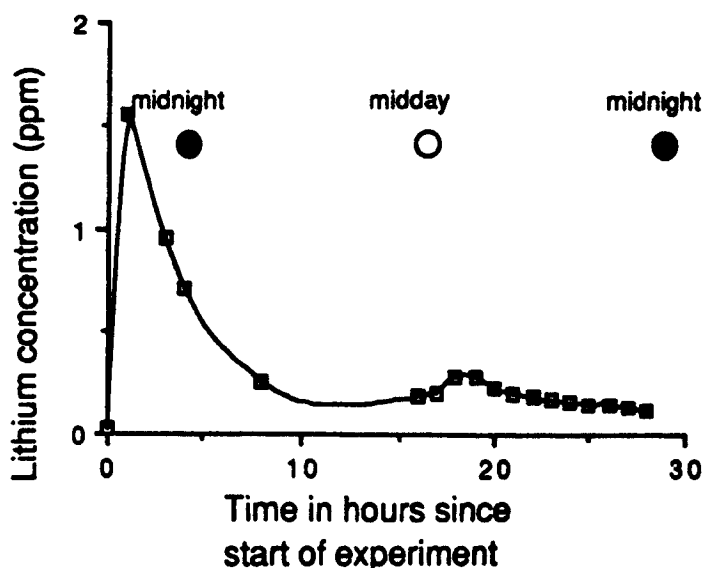


**Figure D.1** Plot of lithium concentrations from the tracing experiments in spring 1988

The results from the AAS analysis are shown in Figure D.1. As the experiment was only successfully completed once it is not possible to draw too many decisions from the results(it was repeated a week later but due to a re-freeze all the ALS bottles cracked before it was possible to retrieve them; the following year the experiment was also

repeated but was disturbed, either by deer or a school party that had been in the catchment, the bottles being spread over a 20m radius). What can be seen, however, is that the meltwater does appear to travel rapidly through a ripe snowpack, the highest concentrations being found in the first hour. It can also be seen that the lithium continues to be in the meltwater the following day, a diurnal cycle being clearly visible.



Plate D.1 The automatic liquid sampler at the base of the snowpatch used for the lithium chloride tracing experiments.

## APPENDIX D

### NOTATION USED IN THE THESIS

All symbols are listed alphabetically for the first chapter that they appear in. Thereafter the same definition applies.

#### Chapter 1

ALPHA	Liquid water retention coefficient	(%)
C	Ferguson's snowpack distribution exponent	
DHF	Archer (1983) melt factor	(mm°C hr <sup>-1</sup> )
LOSS	Input to output loss coefficient	(%)
M	Melt factor	(mm°C hr <sup>-1</sup> )
MD	Depth of melt produced in unit time (water equivalent)	
n	Day number of model run	
ps	Density of snow	(kg m <sup>3-1</sup> )
pw	Density of water	(kg m <sup>3-1</sup> )
Q <sub>e</sub>	Latent heat	
Q <sub>g</sub>	Conducted heat from the ground	
Q <sub>h</sub>	Convective/sensible heat	
Q <sub>ln</sub>	Nett long wave radiation at snow/air boundary	
Q <sub>m</sub>	Energy available for melt	
Q <sub>p</sub>	Heat gained from rainfall	
Q <sub>sn</sub>	Nett short wave radiation at snow/air boundary	
R	Recession coefficient	
RC	Runoff coefficient	
Rd	Daily runoff depth	(m)
T <sub>a</sub>	Air temperature	(°C)
T <sub>b</sub>	Base temperature foe melt to occur	(°C)
T <sub>d</sub>	Number of degree days	(°C day <sup>-1</sup> )
z <sub>o</sub>	Aerodynamic roughness length parameter	(m)

#### Chapter 3

AWS	Automatic weather station	
CWE	Catchment water equivalent	(mm)
MWS	Mountain weather station	
SCA	Snow covered area	(km <sup>2</sup> )
SWE	Snowpack water equivalent	(mm)

## Chapter 4

A	Snow covered area	(km <sup>2</sup> )
AA	Initial snow covered area	(km <sup>2</sup> )
AB	Catchment area	(km <sup>2</sup> )
ALB	Gradually increasing melt factor parameter	
A <sub>n</sub>	Area of snowpack after melt on day n	(km <sup>2</sup> )
ATEM	Average daily temperature	(°C)
A1	Area of catchment above H1	(km <sup>2</sup> )
A2	Area of catchment above H2	(km <sup>2</sup> )
DALT	Altitude difference between HMET and freezing level (m)	
DD	Number of degree days	
DT	Temperature difference between AWS and snowline (°C)	
E	Temperature lapse rate	(°C m <sup>-1</sup> )
FA	Final snow covered area	(km <sup>2</sup> )
FFA	Area of catchment above freezing level	(km <sup>2</sup> )
FL	Altitude of freezing level	(m)
FLOW	Mean daily discharge	(m <sup>3</sup> s <sup>-1</sup> )
HMAX	Maximum altitude of catchment	(m)
HMET	Altitude of meteorological station	(m)
HMIN	Altitude of gauging station	(m)
HT(A)	Hypsometric curve function	
H1	Altitude of upper break of slope on hypsometric curve	
H2	Altitude of lower break of slope on hypsometric curve	
MA	Area of snowpack available for melt	(km <sup>2</sup> )
MFMAX	Maximum melt factor (21 June)	
MFMIN	Minimum melt factor (21 December)	
ND	Number of days over which model is run	
NTMIN	Following day minimum temperature	(°C)
PPT	Total daily precipitation	(mm)
Q	Outflow from catchment	(m <sup>3</sup> s <sup>-1</sup> )
Q <sub>0</sub>	Initial discharge at start of model run	(m <sup>3</sup> s <sup>-1</sup> )
Q <sub>-1</sub>	Previous day's discharge	(m <sup>3</sup> s <sup>-1</sup> )
S	Volume of water stored in catchment	(m <sup>3</sup> )
SD	Standard deviation	
SE	Standard error	
SS	Sum of squares	
SSD	Snowpack slope distribution	
S1, S2, S3	Gradients of hypsometric curve sections	
TMAX	Maximum daily temperature	(°C)
TMIN	Minimum daily temperature	(°C)
V	Volume of total daily melt	(m <sup>3</sup> )
V <sub>n</sub>	Volume of melt produced on day n	

VP	Volume of daily precipitation	(m <sup>3</sup> )
W	Initial SWE over snow covered area	(mm)
Y	Variable non-linear routing coefficient	

### Chapter 5

A(n)	Snow covered area in zone n	(km <sup>2</sup> )
AZ(n)	Area of zone n	(km <sup>2</sup> )
EL	Mean altitude of snowpack	(m)
ESAT	Saturation vapour pressure	
KK(n)	Snowpack slope constant for zone n	
PA	Atmospheric pressure	
SCA(n)	Initial SCA in zone n	(km <sup>2</sup> )
SMAX(n)	Maximum SWE in zone n	(mm)
SMIN(n)	Minimum SWE in zone n	(mm)
SNEW	Depth of fresh snow (water equivalent)	(mm)
STORE	Non-linear store used for routing melt	
TW <sub>(i)</sub>	Total volume of water produced on day i	(m <sup>3</sup> )
UADJ	Mean daily wind function	(mm mb <sup>-1</sup> day <sup>-1</sup> )
WETM	DEpth of melt during rain events	(mm)
WFUN	Mean wind function during rain events	(mm mb <sup>-1</sup> )
WINDM	Total wind movement over one day	(km)